REINFORCED CONCRETE SLAB ELEMENTS UNDER BENDING AND TWISTING MOMENTS

by

SAROSH HASHMAT LODI
BE (CIVIL), MS

Thesis submitted for the Degree of
Doctor of Philosophy
to the Department of Civil and Offshore Engineering,
Heriot-Watt University, Edinburgh

DEPARTMENT OF CIVIL AND OFFSHORE ENGINEERING,
HERIOT-WATT UNIVERSITY, EDINBURGH

December 1997

COPYRIGHT STATEMENT

TABLE OF CONTENTS

LIST OF TABLES

LIST OF FIGURES

ACKNOWLEDGEMENTS

I am grateful to God for giving me the endurance and courage to fulfil this task. I would like to express my appreciation and thanks to my supervisor Prof. I M May who has contributed immensely by encouragement, suggestions, discussion and guidance though out this period.

I would like to thank my brother Dr. Omer H Lodi for his immense moral and timely financial support with out which it would not be possible to carry out this study. I am also grateful to my family in Pakistan for their support and encouragement especially my father Prof. Hashmatullah Lodi and my eldest sister Prof. Ismat Rizwan Lodi for the inspiration. I am also thankful to my wife and children for their endurance and perseverance.

I would also like to express my sincere thanks to Mr. SFA Rafeeqi and Mr. M Almograbi for their support and encouragement. Finally I would like to express my thanks to Ministry of Education, Pakistan and NED University of Engineering and Technology, Pakistan for providing me with this opportunity.

DECLARATION

The work embodied in this thesis is a result of the author's own investigation except where due reference is made. It has been submitted, and is not being concurrently presented in candidature for any other degree.

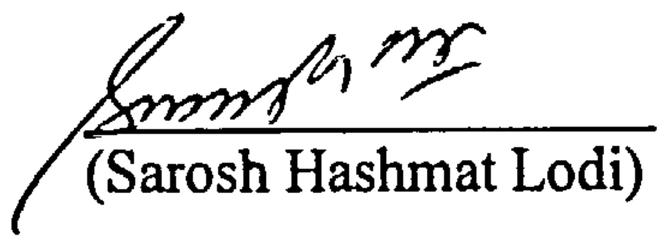

(Sarosh Hashmat Lodi)

DEDICATION

Dedicated to my parents, wife and my children

ABSTRACT

The ultimate strength design of slabs is carried out using the Wood-Armer rules in the UK. These design rules provide optimum reinforcement for the slabs for any given moment field. The rules have been formulated using the normal moment yield criterion. This yield criterion uses Johansen's yield criterion to define the strength of the slab. Johansen's yield criterion has some deficiencies which lead to increasingly unconservative strength predictions for increasing reinforcement ratios and for increasing angle between the principal moments and the reinforcement directions.

There are two facts due to which Johansen's yield criterion over estimates of the ultimate moment capacity of the slab elements. Firstly, in order to determine the moment capacity in a desired direction the ultimate moment capacities m_{xu} and m_{yu} in the reinforcement directions are calculated. The moment transformation is then applied to the uniaxial bending moment capacities which can not predict the actual stress state of the element. The incorrect stress state under estimates the neutral axis depth which leads to over estimation of lever arm and moment capacity. Secondly, the reduction in the compressive strength of concrete due to orthogonal cracking has not been accounted for and thus the actual moment capacity of the slab element is over estimated further.

Owing to the above mentioned facts, not only the moment capacity reduces but in some cases even the mode of failure can change from under reinforced failure as predicted by Johansen's yield criterion, to over reinforced failure specially for higher reinforcement ratios, thus nullifying the chances of moment redistribution.

A computer program has been developed which has the capability of modelling the behaviour of reinforced concrete slabs cross-section using non-linear analysis upto and beyond failure. The computer program has been validated by comparing the analytical results against several experimental studies. The developed software has been used to determine the ultimate moment capacity of isotropic and orthotropic reinforced concrete slab elements under different moment combinations. Numerically generated failure surfaces have been developed in the principal moment field using the program, which confirmed the deficiencies in Johansen's yield criterion.

Guidelines for the analysis and design of slab elements under any set of moments have been proposed.

CHAPTER 1

INTRODUCTION

1.1 BACKGROUND

The developments in the technology, improved construction techniques, increase in the loading requirements etc. have pursued the design engineers to produce economical design and better structural assessment methods. An ever increasing demand for the economical design of structures and better assessment methods have culminated in improved and refined techniques based on a better understanding of material and structural behaviour. However, the need for the improvements in existing design and assessment methodologies is still required and researchers are devising means and ways to fulfil this objective.

Over the recent decades numerous attempts have been made to provide design guidelines for reinforced concrete slabs. Reinforced concrete slabs can be designed using either elastic or plastic methods, both of which require an understanding of material and structural behaviour.

Reinforced concrete slabs are designed and analysed using Wood-Armer rules, strip method and yield line theory. The usual concept on which the design of reinforced concrete slabs has been based, the normal moment yield criterion, is that the moment capacity of the slab in the direction normal to the failure direction must be less than or equal to the applied moments. The capacity of the slab in the normal moment yield criterion has been defined by Johansen's yield criterion. Johansen's yield criterion requires the uniaxial moment capacities in the two orthogonal reinforcement directions transformed in the desired direction using simple stress transformation.

The assessment of the existing reinforced concrete slabs is the a pressing need now-a-days due to the increase in the loading requirements. Methods based on Johansen's yield criterion are currently being used to assess the strength of the slabs.

Johansen's yield criterion has been shown to have over estimated the moment capacity of the slabs with twisting moment in the reinforcement directions. This over estimation increases with the increase in the twisting moment. The unconservatism of the criterion is more significant for slabs with high reinforcement ratios. Thus any design or assessment method based on Johansen's yield criterion can not produce a safe design or adequate assessment for all loading conditions.

1.2 OBJECTIVES

In order to confirm the deficiencies in the normal moment yield criterion a computer program has been written which can predict the non-linear response of reinforced

concrete shell elements subjected to a set of three in-plane forces and three moments, upto and beyond failure. The computer program includes the non-linear behaviour of the concrete and the reinforcement. It performs the analysis of a reinforced concrete cross-section subjected to monotonically increasing loads. The computer program was used to achieve the following objectives.

1. To identify the deficiencies in the normal moment yield criterion.

2. To investigate the causes of deficiencies in the normal moment yield criterion.

3. To either propose a new yield criterion or to define the limit of area of reinforcement and loading pattern for which the normal moment yield criterion can be used.

4. To understand and explain the behaviour of reinforced concrete slab elements under pure twisting.

5. To study the influence of parameters e.g. tension stiffening, compression softening, area of reinforcement, number of integration points etc. on the overall response of reinforced concrete slab elements when subjected to pure twisting.

Even though the computer program is capable of analysing reinforced concrete shell elements, it was used for slab elements subjected to moment triad only. The effects of

membrane forces have not been studied. The design methods for slabs in mixed moment field are derived from Johansen's yield criterion which does not cater for the in-plane membrane forces, therefore, the effect of such forces have not been included in this study.

CHAPTER 2

LITERATURE REVIEW

2.1 INTRODUCTION

In order to design reinforced concrete slab elements under a mixed moment field, methods based on the normal moment yield criterion have normally been used. The normal moment yield criterion requires that at any point in the slab the moment capacity, m_{nu}, in a direction normal to the direction under consideration must be greater than or equal to the applied moment, m_n, in that direction i.e.

$$m_{nu} \geq m_n \qquad 2.1$$

In order to apply the normal moment yield criterion, a criterion is required to define the strength of slab element. A number of attempts have been made to either establish a strength yield criterion or to validate the existing strength formulation.

Because it is intended to study the ultimate strength of slab elements subjected to a mixed moment field using a numerical technique, therefore, this Chapter provides an

overview of the literature pertaining to the yield criteria for reinforced concrete slabs. It also provides a review of the literature for the design procedures for reinforced concrete slabs in mixed moment fields. A review of the literature pertaining to the modelling of concrete and reinforced concrete is also presented in this Chapter as it is intended to develop computer program based on the numerical modelling of the concrete and the reinforcement that can predict the non-linear response of shell elements up to and beyond failure. The positive sign convention used in this study is given in Figure 2.1.

2.2 YIELD CRITERIA

Reinforced concrete slabs can be designed for the ultimate state, for a generalised set of moments using the Wood-Armer rules[1,2]. These design rules provide optimum reinforcement for the slabs. The rules use the yield criterion developed by Johansen[3]. The widely used Johansen's yield criterion has some deficiencies and can provide unconservative strength predictions for certain load combinations. This fact has been pointed out by several researchers[4,5,6,7]. Therefore, the need for an accurate yield criterion to define the strength of reinforced concrete slab elements is of prime importance. An attempt has been made in the following Section to outline the research conducted related to the yield criteria used to define the strength of reinforced concrete slabs.

2.2.1 LITERATURE REVIEW

The pioneering work by Johansen[3] provided a yield criterion that can predict the

strength of the slab in any direction, n, if no in-plane forces act on the cross-section. The work was based on the theory of plasticity. After the translation of this work into English, the proposed yield criterion gained popularity due to its simplicity and ease of use.

The expression proposed by Johansen was,

$$m_{nu} = m_{xu} \cos^2\theta + m_{yu} \sin^2\theta \qquad 2.2$$

where, m_{nu} = capacity of the slab in desired direction n

m_{xu}, m_{yu} = capacity of the slab element in reinforcement directions x and y

The above expression gives the strength of an element and has been used extensively in the normal moment yield criterion, equation 2.1. It was suggested that physical tests should be carried out to confirm the validity of this criterion.

Wood[8] raised several objections to the yield criterion proposed by Johansen[3]. One of the objections raised was that the reinforcement directions were assumed to be the principal moment directions which will not be valid for all loading conditions and twisting moments can exist in the reinforcement directions. It has also been pointed out that at the intersection of top and bottom hinge lines, for slabs with different top and bottom reinforcement, there will be two different Mohr's circles of moments for the same stress state, which can not be possible. The possibility of having two distinct Mohr's circles of moments for same stress state is due to the fact that the transformation was applied to the ultimate moment instead of the stress in the concrete and the reinforcement at

ultimate.

Nielsen[4] derived expressions for the moment carrying capacity of slabs when subjected to uniaxial bending and pure twisting separately, based on assumed models for the constituents i.e. reinforcement and concrete. The reinforcement was assumed to be elastic-plastic capable of carrying axial forces only and concrete was modelled as perfectly plastic in compression, but with no tensile strength. The square strength envelope for concrete in compression was used. It was appreciated that the strength of concrete increases in biaxial compression but as this strength increase causes an insignificant increase in the moment capacity, this effect was ignored. In order to determine the stress resultants, a stress distribution was assumed through the depth of the element using the defined constituent models. The work, however, neglected in-plane forces.

Nielsen[4] proved that the square yield criterion proposed by Johansen[3] for moments can be used for isotropic slabs provided that either the failure is in the reinforcement direction i.e. the twisting moment in the reinforcement direction is zero, or the percentage of reinforcement is low. Nielsen extended the work further for the case of pure twisting i.e. when equal and opposite principal moments were applied at $\pm 45^{o}$ from the reinforcement directions. It was found that for low percentages of reinforcement, when the ratio of the depth of neutral axis to the overall depth is less than or equal to 0.2, the difference between the pure twisting capacity and the uniaxial bending capacity is less than 6%. It was thus concluded that the uniaxial bending and pure twisting capacities of a slab are similar for low reinforcement ratios. But for high reinforcement ratios, the pure twisting capacity will be lower than that the uniaxial

bending capacity. Nielsen pointed out that in the case of pure twisting when the reinforcement is at $\pm 45^{\circ}$ to the principal moment directions, as the depth of the neutral axis increases, the difference between the pure twisting and the bending capacities of the section for isotropic slabs also increases. For an increase in the neutral axis depth at failure it can be implied that either the reinforcement ratio must increase or the compressive strength of concrete decreases. In the case of pure twisting the compressive strength of concrete is always reduced considerably due to compression softening[25] which is discussed in more detail in Section 2.4.5.2. It can thus be concluded that slabs elements under pure twisting with high reinforcement ratios have a smaller moment capacity than the uniaxial bending capacity. The difference between the pure twisting and uniaxial bending capacities arise due to the incorrect lever arm implied using Johansen's yield criterion approach. It was pointed out that this criterion used an intuitive approach and can be termed as 'isotropic' as it assumed that the principal moment and reinforcement directions were the same.

Nielsen[4] extended the work further and proposed a yield criterion for isotropic slabs subjected to combined bending and twisting moments. The proposed yield criterion was based on the principal moments yield criterion. In order to define the capacity of the element in any direction, the uniaxial moment capacity of the element was used. The principal moment criterion in the reinforcement direction x and y was expressed as follows.

$$\frac{1}{2}(m_x+m_y)\pm\sqrt{\frac{1}{4}(m_x-m_y)^2+m_{xy}{}^2}=\pm m_F \qquad 2.3$$

The left hand side of the above equation represent the applied principal moments where m_x, m_y and m_{xy} are the applied bending and twisting moments and the right hand side represents the uniaxial moment capacity, m_F. The above expression can be represented as two cones lying back to back in m_x, m_y and m_{xy} space as shown in Figure 2.2.

Kemp[9] presented an extension of Nielsen's[4] work for orthotropic slabs. The normal moment yield criterion was used but defined in the principal moment field. The strength of the slab was defined using Johansen's yield criterion[3]. Kemp proposed the following equations.

For positive yield:

$$mM_1(\sin^2\phi + \mu\cos^2\phi) + mM_2(\cos^2\phi + \mu\sin^2\phi) - M_1M_2 - \mu m^2 = 0 \qquad 2.4a$$

For negative yield:

$$m'M_1(\sin^2\phi + \eta\cos^2\phi) + m'M_2(\cos^2\phi + \eta\sin^2\phi) - M_1M_2 - \mu m'^2 = 0 \qquad 2.4b$$

where, m, m' = moment capacity per unit length in x direction bottom and top faces respectively

μ, η = degree of orthotropy in y direction bottom and top faces respectively

M_1, M_2= applied principal moments

ϕ = clockwise angle between the reinforcement in x direction and principal moment M_1

The graphical representation of the yield criterion given by equations 2.4 is shown in Figure 2.3. The flow rules associated with the bending of the orthotropic plates, which had not been defined earlier were stated clearly. A discussion was also presented on the possibility of enhancement of moment capacity of the element due to the presence of twisting and tangential moments along the hinge line. However, an analytical solution was not presented to extend the yield criterion due to lack of understanding of this phenomenon.

Morley[10] developed a generalised yield criterion for reinforced slab subjected to six stress resultants, M_x, M_y, M_{xy}, N_x, N_y, N_{xy}, based on the theory of plasticity, where, M_x, M_y, M_{xy} are the moments and N_x, N_y, N_{xy} are the in-plane forces in the x and y directions and the in-plane shear respectively expressed per unit length. This criterion used similar models for the reinforcement and the concrete to those proposed by Nielsen[4]. The resistance offered by the cross-section was based on the assumed models.

Morley[10] presented an upper bound based on the assumption that the concrete had infinite compressive strength. Morley also presented an upper bound solution, which accounted for the finite compressive strength of concrete. The square strength surface for concrete was assumed in compression whereas the tensile strength of concrete was neglected. The reinforcement was assumed to carry axial forces only. It was shown that if the compressive strength was assumed to be infinite, then there was no difference between the two solutions. When the concrete has a finite strength and there are no in-plane forces, the upper bound solution reduces to the criterion proposed by Nielsen[4].

To check the closeness of the two upper bound solutions, Morley[10] also performed numerical experiments. The experiments were conducted on slabs with no in-plane forces and by varying the strength factor, ϕ, where ϕ is defined by

$$\phi = \frac{\sigma_c D}{\sigma_y a} \qquad 2.5$$

where, σ_c = compressive strength of concrete

D = overall depth of the section of slab

σ_y = yield strength of reinforcement

a = thickness of smeared reinforcement layer.

For a given section in which σ_c, σ_y and D are constant, ϕ will vary inversely with an increase in the area of reinforcement. Thirty numerical experiments were performed on slabs with equal top and bottom reinforcement, with the thickness of the smeared layer of reinforcement in the y direction 0.2 times the thickness of the x direction reinforcement, and with $\phi = 10$. The infinite compressive strength criterion was compared with the finite compressive strength criterion, which in turn was compared with Nielsen's[4] lower bound solution. An average of 6.5% lesser strength was obtained for the upper bound solution with finite compressive strength when compared with the infinite strength criterion. Similarly an average of 2.2% lesser strength was obtained for Nielsen's lower bound solution when compared with the upper bound finite strength solution. For another 30 slabs with the same ϕ but no top reinforcement and with a ratio of thickness of the smeared reinforcement layers being 0.3, it was found that the infinite

compressive strength solution over estimated the strength by an average of 2.8% when compared with the finite compressive strength solution. Whereas, the finite compressive strength solution over estimated the strength by 1% when compared with Nielsen's lower bound solution. For the same reinforcement arrangement but $\phi=3$, it was found that infinite compressive strength solution over estimated the strength of the slab by 9.1% on average when compared with the finite compressive strength solution which in turn over estimated the strength by 3.8% with respect to Nielsen's lower bound solution. Hence it was argued that the finite compressive strength solution was sufficiently close to Nielsen's lower bound solution for practical ranges of the reinforcement areas. For more generalised cases with all the six stress resultants acting, Morley performed a few more numerical experiments and compared the two criteria. The numerical results showed acceptable agreement.

Morley[11] tested 30 isotropic slabs with $\cong 0.5\%$ reinforcement. The slabs can be broadly classified according to the type of reinforcement used. In the first series 18 slabs, $1\frac{3}{8}''$ thick and reinforced with $3/32''$ diameter wire, were tested. In the second series 12 slabs, $1\frac{1}{4}''$ thick and reinforced with $3/32''$ diameter welded wire fabric, were tested. Thirteen of the slabs in the first series were rhomboid and were tested under twisting moment with equal and opposite loads applied at the corners, Figure 2.4. This loading arrangement produced moments that were assumed to be constant over the slab area. According to the small deflection theory of thin plates, the moment can be expressed as;

$$M_n = -\frac{b}{2a}P \qquad 2.6a$$

$$M_t = \frac{a}{2b} P \qquad 2.6b$$

such that,

$$\frac{M_n}{M_t} = -\frac{b^2}{a^2} \qquad 2.6c$$

where a and b are the half-length of the diagonals of the rhomboid and P is the applied load. The dimensions of the slabs were set such that the ratios of M_n/M_t were –1, -0.651 and –0.206. The orientation of the reinforcement was 0°, 22.5° and 45° with respect to the principal moment direction. The remaining 5 slabs in this series were rectangular, $36'' \times 26\frac{1}{2}''$, and were subjected to uniaxial bending moment over a span of 24″ by applying uniformly distributed load. The reinforcement was at 0°, 22.5° and 45° with respect to the principal moment direction.

Eight of the slabs in the second series were rhomboid and were tested with values of M_n/M_t of –1 and –0.413 with reinforcement at 0°, 22.5° and 45° with respect to the principal moment directions. The remaining four slabs in this series were rectangular, $36'' \times 26\frac{1}{2}''$, and were subjected to uniaxial bending moment over a span of 24″ by applying uniformly distributed load with the reinforcement placed as described earlier. The ultimate strengths were compared with Johansen's yield criterion[3]. It was concluded that, in general, Johansen's yield criterion predicted the strength accurately but, as the

ratio of M_n/M_t approached -1, Johansen's yield criterion slightly over predicted the ultimate moment capacity. The reason for this over estimation can be attributed to the fact that incorrect lever arm is estimated by Johansen's yield criterion as mentioned by Nielsen[4]. However, the insignificant difference in the moment capacities is due to the low reinforcement ratio provided in the tested slabs. It is worth mentioning that out of 21 rhomboid slabs tested only three slabs were tested in under pure twisting moment with reinforcement at $\pm 45^{o}$ from the principal moment directions with approximately 0.45% reinforcement. To the knowledge of the author, this was the first experimental study conducted to check the validity of Johansen's yield criterion.

Lenshow and Sozen[12] conducted an experimental study on 22 slab elements under constant biaxial, uniaxial and twisting moments. Full details of the experiments are given elsewhere[13], however, a summary of the experimental results are given in Table 2.1. Slabs in C series were tested under equal biaxial bending. Slabs B4, B10, B13, B15, B18 and B19 were tested with zero twisting moment in the reinforcement directions. Slabs B16, B20, B21 and B22 were tested under pure twisting, with the reinforcement placed at $\pm 45^{o}$ with respect to the applied principal moment directions. Two of the slabs in this category, B16 and B20, were isotropically reinforced with reinforcement ratios of $\rho_x = \rho'_x = \rho_y = \rho'_y = 0.84$ and $\rho_x = \rho'_x = \rho_y = \rho'_y = 0.4$ respectively, while the remaining slabs, B21 and B22, were orthotropically reinforced with reinforcement ratios $\rho_x = \rho'_x = 0.82, \rho_y = \rho'_y = 0.18$. The isotropic slab with maximum amount of reinforcement, B16, showed over reinforced behaviour[13] i.e. the concrete crushed prior to the yielding of reinforcement, whereas the slabs with low percentages of reinforcement showed under reinforced response i.e. the reinforcement yielded prior to the crushing of concrete. In the remaining six slabs, the reinforcement was at an angle to the

principal moment directions, thus were tested in a mixed moment field. It is interesting to note that only four of slabs tested had a negative principal moment ratio, of which three had low proportion of reinforcement. The aim of the study was to check the validity of Johansen's yield criterion[3]. The ultimate moment capacities were compared with Johansen's yield criterion and a good agreement was obtained. Lenshow and Sozen developed a graphical representation of the normal moment yield criterion in polar co-ordinates. It was, however, pointed out that for $\rho > 0.125 f'_c/f_y$, the strength predictions using Johansen's yield criterion may not be accurate.

The reason for obtaining good agreement with Johansen's yield criterion is due to the fact that slabs B20, B21 and B22, tested under pure twisting with the reinforcement at $\pm 45^{\circ}$, had a low amount of reinforcement. Only slab B16, which was isotropically reinforced and had a reinforcement ratio of $\cong 0.84\%$, showed over reinforced failure[13]. However, the moment capacity predicted by Johansen's yield criterion[3] for that particular slab was 3% greater than the experimental moment capacity. The higher moment obtained experimentally was due to the loading set up. The two parallel sides of the slab were clamped to the channel section through which the loads were applied. The channel section provided axial restraint, thus inducing an in-plane compressive force, which had enhanced the capacity.

Cardenas[14], in the discussion of Lenshow and Sozen's[12] work, pointed out that the ratios of the principal moments covered in their testing programme were positive except for slabs under twisting moments for which the ratio was –1. It was pointed out further that there can be another two possible ranges of the principal moments ratios i.e. $0<m_1/m_2<1$ and $-1<m_1/m_2<0$. Results of isotropically reinforced slabs tested, one for each of the

above mentioned ranges of the principal moment ratio, were also provided. It was shown that, like the results of the slabs tested by Lenshow and Sozen, these results agreed well with Johansen's yield criterion[3]. However, the exact principal moment ratios used in the tests were not mentioned.

Lenkei[15], in the discussion of Lenshow and Sozen's[12] work, provided experimental results for tests on 45 slabs. The slabs were categorised into three series depending on the degree of orthotropy. Slabs 1-15 had degree of orthotropy $\lambda = 0.936$, whereas, for slabs 16-30 and 31-45 $\lambda = 1.65$ and 2.203-2.46 respectively. The slabs, which were tested under uniaxial bending had reinforcement orientation with respect to the applied moment, of 0^{o}, 22.5^{o}, 45^{o}, $67{,}5^{o}$ and 90^{o}. The results showed good agreement with Johansen's yield criterion[3]. It is important to note that the maximum percentage of the reinforcement was 0.72%.

Prince and Kemp[16] developed an expression to define the strength of reinforced concrete slab elements based on the concept that both concrete and reinforcement will contribute in carrying the in-plane shear due to the twisting moment in addition to carrying axial stresses. The expression was derived using strain compatibility. The developed expression was then used in the normal moment yield criterion instead of Johansen's yield criterion[3]. To validate the developed yield criterion three isotropically reinforced slabs were tested. The results showed good agreement with the developed yield criterion. The loading applied was pure twisting and the reinforcement angles were varied. It was pointed out that during the tests, no visible signs of kinking of reinforcement were observed. It is important to note that only one slab, with the reinforcement at $\pm 45^{o}$ from the principal moment directions, was tested but the

reinforcement ratio was $\cong$ 0.5%.

Holmes and Downham[17] presented an experimental study of 48 slabs orthogonally reinforced with varying proportions of reinforcement and varying orientation of the reinforcement with respect to the edge of the slabs. The slabs were tested either under uniaxial bending or bending and twisting. The intention of this study was to check the validity of the normal moment yield criterion. It was argued that along the hinge line not only the normal moment but twisting and tangential moments also play an important role in the ultimate moment capacity. As the normal moment yield criterion only checks the normal moment it thus assumes that the twisting and the tangential moments do not effect the ultimate moment capacity. It was concluded from the results of the uniaxial tests (for all orientations of the reinforcement) that the shear stiffness of the reinforcement should be taken into account and that the twisting and the tangential moments along the yield line effect the ultimate capacity. However, from the results presented, this effect appeared to be insignificant. The reorientation of cracks under progressively increasing load was also observed.

Cardenas and Sozen[18] tested 19 slabs with different principal moment ratios. Three slabs were test with $m_1/m_2 = 1$, nine with $m_1/m_2 = -0.14$ and the remaining seven with $m_1/m_2 = -0.45$. The percentage of reinforcement was varied from 0.25% to 1% and the degree of orthotropy from 1 to 0.25. The reinforcement orientations were 0°, 22.5°, 45° and 67.5°. Full details of the experiments can be found elsewhere[19]. The results showed good agreement with the normal moment yield criterion.

Jain and Kennedy[20] tested 29 slabs under different principal moment ratios. The slabs

were categorised into five different series depending on the type of loading. Four isotropically reinforced and eight orthotropically reinforced slabs were tested under uniaxial bending. Eight isotropically and six orthotropically reinforced slabs were tested under pure twisting. Three orthotropically reinforced rectangular slabs with reinforcement only at the tension face were tested under uniformly distributed load. The reinforcement orientations used were 0^{o}, 15^{o}, 30^{o} and 45^{o} with respect to the principal moment direction within each category. The results showed good agreement with the normal yield criterion. The isotropically reinforced slab under pure twisting moment with reinforcement at $\pm 45^{o}$ had a reinforcement ratio of $\cong$ 0.7%. The analytical work presented in this paper is the representation of the normal moment yield criterion in the principal moment field. The analytical work was similar to that described by Lenshow and Sozen[12,13].

Rajendran and Morley[21] presented a numerical technique, based on the theory of plasticity, to define a failure surface for a slab element subjected to a generalised set of loading with the six stress resultants, N_x, N_y, N_{xy}, M_x, M_y, M_{xy}. It was argued that the effect of the two stress resultants due to out of plane shear are insignificant and were thus neglected. The square compressive strength envelope was used to model the compressive strength of concrete and the tensile strength was neglected. It was, however, appreciated that the compressive strength of the concrete increases under biaxial compression but the effect of the increase of the compressive strength of concrete on the ultimate moment capacity is not significantly large. The reinforcement was modelled as a smeared layer and was assumed to carry axial stress only. It was proposed that for a given combination of stress resultant, u_i, Yu_i, satisfies the yield criterion where Y defines the length of stress resultant vector, u_i, Figure 2.5. The given

vector u_i defines the direction in the stress resultant space. If the value of Y can be found, the yield surface can be defined completely, Figure 2.5. A numerical procedure was then adopted to obtain the close approximation on Y. An upper bound, λ, on the value of Y was first obtained by assuming a set of plastic strain rates and using the models of the concrete and the reinforcement. The value of λ was then minimised to obtain a close approximation to Y. The proposed numerical technique proved to be efficient and robust. Some comparisons were made between the numerical technique and the expression derived by Morley[10] for concrete with infinite compressive strength. The two techniques agreed well as long as the depth of the concrete compressive stress block was less than 20% of the overall depth in the numerical procedure. However, when the depth of concrete in compression was large, 50% of the overall depth, Morley's expression over predicted the ultimate strength. For the case when the slab was subjected to bending and twisting with no in-plane forces, it was shown that the numerical results agreed well with Johansen's yield criterion[3]. The surface obtained numerically was verified by an experimental study in which the reinforced concrete element has been subjected to in-plane force N_y, in-plane shear N_{xy} and bending moment M_y. Good agreement between the experimental and the numerical results was obtained.

Cookson[22] provided a yield criterion for a slab element subjected to six stress resultants, the three in-plane forces and the three moments based on the theory of plasticity. The strength of concrete in tension was ignored and the compressive strength was modelled with the square strength envelope. The reinforcement was assumed to carry axial forces. The proposed yield criterion when used for a system of stress resultants with no in-plane forces yielded an expression similar to the normal moment yield criterion. It was thus concluded the yield criterion for six stress resultant was an extension of the normal

moment yield criterion.

Marti et al[6] presented the results of an experimental study of nine reinforced concrete square slabs (1700 mm x 1700 mm x 200 mm) with varying amount of reinforcements (0.25% to 1%) subjected to pure twisting. The reinforcement was placed at $\pm 45^{o}$ from the principal moment directions. Six of the tested slabs were isotropic with 0.25%, 0.5% and 1% reinforcement per layer per direction and three slabs were orthotropically reinforced with 0.25% and 1%, 0.5% and 1% and 0.25% and 0.5% reinforcement in each layer top and bottom. This study was the first to prove the unconservatism of Johansen's yield criterion[3]. It was found that yield line approach which uses Johansen's yield criterion can over estimate the strength by two for slab elements with high reinforcement ratios. The experimental results were compared with the American, ACI 318-83[23] and Canadian, CAN3-A23.3-M84[24], codes of practices and it was shown that both the codes over estimated the strength of the slabs and that this over estimation increased with the increase in the reinforcement ratios. The approach adopted by yield line analysis was shown to have deficiencies but the possible reasons for the unconservatism were not discussed.

Khalifa[5] pointed out that for slab elements with no in-plane forces the yield line theory over estimated the strength of the element if significant twisting moment is present in the reinforcement directions even though the correct mechanism was used. This over estimation increases with an increase in the area of reinforcement. It should be remembered that yield line theory use Johansen's yield criterion[3] and thus it would appear that the discrepancy was due to the errors in the yield criterion. Khalifa showed that this over estimation in the moment capacity was mainly due to two reasons. Firstly

due to an over estimation of the lever arm and secondly due to neglecting compression softening[25]. On the basis of the above Khalifa proposed a modification in the yield line theory or modification in the normal moment yield criterion.

It was argued that as the strength of the slab in certain loading conditions is considerably less than the strength predicted by the yield line theory, a modification to yield line theory should be made. The modification can either be made by taking into account the reduction in the moment capacity or by amplification of the applied moment. Determination of the reduced capacity of an element is a cumbersome procedure, as it requires the correct estimation of neutral axis depth or lever arm. But on the other hand the amplification of the applied moment is relatively easier. Thus it was suggested that the applied twisting moment should be amplified and the following modification was proposed to the normal moment yield criterion,

$$(m_{xu} - m_x)(m_{yu} - m_y) \geq (r_k\, m_{xy})^2 \qquad 2.7a$$

$$(m'_{xu} - m_x)(m'_{yu} - m_y) \geq (r_k\, m_{xy})^2 \qquad 2.7b$$

where,

m_{xu}, m_{yu}, m'_{xu} and m'_{yu} = moment capacities of the section in reinforcement directions x and y top and bottom faces respectively

m_x, m_y, m_{xy} = applied bending and twisting moments.

r_k = amplification factor = $\dfrac{m^{Y}_{xyu}}{m^{L}_{xyu}}$

m^{Y}_{xyu} = maximum twisting capacity of the section using yield line

theory

m^{L}_{xyu} = maximum twisting capacity of the section using a lower bound solution

It was suggested that for low percentages of reinforcements r_k should be taken as 1.

Khalifa[5] derived a lower bound solution for the yield criterion. The square strength envelope was used to model the compressive strength of concrete and the tensile strength was neglected. A compressive strength reduction factor of 0.45 was proposed to account for compression softening when the concrete was in the state of compression-tension. The reinforcement was assumed to carry axial forces only. In the lower bound solution, the depth of the element was divided into three zones. It is worth mentioning here that if the two compressive stress blocks of unequal depths lie on the same face of the section, then both the stresses will taken as the uniaxial compressive strength, whereas in the concrete in the region below the smaller stress block, the concrete will be in compression-tension and thus the compressive strength of the concrete will be greatly reduced. This approximation in estimating the strength of concrete will lead to an over estimation of the moment capacity of the section.

Marti and Kong[7] provided an extensive analytical study for orthogonally reinforced concrete slab elements subjected to pure twisting. Expressions were derived for the ultimate moment capacity of slab sections under pure twisting using linear elastic, parabolic and perfectly plastic responses of concrete in compression. The tensile strength of the concrete was neglected. The effect of compression softening[25] was also included in the proposed analytical models. Reinforcement was modelled as a linear

elastic-plastic material. The analytical work was verified by the experimental data obtained by Marti et al[6]. A comparison was made between the moment capacities calculated using the normal moment yield criterion and analytical expressions presented in the study using perfect plastic models for the constituents. It was shown that the normal moment yield criterion over estimated the moment capacity when the section has a high percentage of reinforcement. It was pointed out that this discrepancy is due to the incorrect depth of neutral axis calculated using normal moment yield criterion approach. It was suggested that when designing a section for twisting moment an appropriate modification should be made to account for the reduction of moment capacity. The work was, however, restricted to the case of pure twisting moment only. The models proposed do not provide the analysis of the section for the entire loading history but provide solutions at cracking and at the ultimate load level. Once again the actual root cause of over estimation of the moment capacity under pure twisting in the normal moment yield criterion i.e. Johansen's yield criterion[3] was not identified.

2.2.2 SUMMARY

In the light of the above discussion of the literature regarding the yield criteria, the following important work has been summarised to draw conclusions.

Nielsen[4] pointed out that the uniaxial moment capacity of a slab is approximately the same as that of pure twisting moment capacity for slabs with low reinforcement ratios. Therefore, the square yield surface developed by Johansen[3] can be used. But as the area of reinforcement increases the difference between the two capacities also increases.

Morley[11] and Lenshow and Sozen[12] carried out experiments to check the validity of Johansen's yield criterion[3] and found that Johansen's yield criterion provides good estimates for strength for all loading conditions. However, both Morley, and Lenshow and Sozen indicated that for certain conditions the strength predictions using Johansen's yield criterion would be inaccurate. Morley indicated that as the ratio M_n/M_t approaches –1, Johansen's yield criterion slightly over estimates the moment capacity. Similarly Lenshow and Sozen proposed that as $\rho > 0.125 f'_c/f_y$, the strength predictions by Johansen's yield criterion were different from the experimentally obtained moment capacities for slabs under pure twisting.

Marti et al[6] were the first ones to confirm the deficiency in the normal moment yield criterion experimentally. Marti and Kong[7] pointed out analytically that under pure twisting when the ratio of two principal moments is -1, and the reinforcement is at $\pm 45^{\circ}$ with respect to the principal moment directions the moment capacity calculated using Johansen's yield criterion[3] can be as high as twice of the actual moment capacity for high reinforcement ratios, ($\geq 1\%$).

Khalifa[5] was the first one to include the effect of compression softening[25] for slabs with twisting moment in the reinforcement direction. Khalifa pointed out that the normal moment yield criterion has deficiencies and it can over estimate the moment capacity of the slab if significant twisting moment is present in the reinforcement directions.

In the light of the summary presented above it can be concluded that the normal moment yield criterion over estimates the moment capacity of reinforced concrete slabs with increasing reinforcement ratio and with increasing angle between the reinforcement and

principal moment directions, if the ratio of the principal moments is negative. The reason for the over estimation by the normal moment yield criterion is that it uses Johansen's yield criterion[3] to predict the strength of the slab elements. Johansen's yield criterion assumes that the orthogonal sets of reinforcements were always in the principal directions, thus as the twisting moment in the reinforcement directions increases, the over estimation of the strength also increases.

2.3 DESIGN METHODOLOGIES

The design of slab elements in mixed moment fields has been an area of research for several decades. A number of attempts have been made to provide design guidelines for slab elements with combined bending and twisting moments[1,2,4,26]. The following section summarises the design procedures.

2.3.1 LITERATURE REVIEW

Hillerborg[26] presented a procedure for the design of reinforcement in concrete slabs in mixed moment fields with no in-plane forces. The design procedure adopted the normal moment yield criterion approach. The applied bending and twisting moments, Figure 2.1, were transformed into a direction normal to the direction of failure and the difference between the moment capacity and the applied moments was then minimised. The capacity of the section was defined by Johansen's yield criterion[3]. In order to have a safe design the capacity of the slab in any direction must be greater than or equal to the applied loads, thus

$$m_{nu} \geq m_n \qquad 2.8$$

where, m_{nu} = capacity of the section normal to the failure direction

m_n = applied moments transformed in the failure direction

if the moment capacity, m_{nu} is defined by,

$$m_{nu} = m_{xu}\cos^2\theta + m_{yu}\sin^2\theta \qquad 2.9$$

and the applied moments, m_n, transformed normal to the failure direction are,

$$m_n = m_x\cos^2\theta + m_y\sin^2\theta + 2m_{xy}\sin\theta\cos\theta \qquad 2.10$$

where, θ is the direction of failure, then

$$m_{xu}\cos^2\theta + m_{yu}\sin^2\theta = m_x\cos^2\theta + m_y\sin^2\theta + 2m_{xy}\sin\theta\cos\theta \qquad 2.11$$

Dividing equation 2.11 by $\cos^2\theta$ and introducing

$$\tan\theta = k \qquad 2.12$$

to obtain the following formulation.

$$f(k) = m_{xu} + k^2 m_{yu} - m_x - k^2 m_y - 2km_{xy} \geq 0 \qquad 2.13$$

The greater the value of f(k), greater will be the margin of safety. The most critical direction, k_1, can, therefore, be obtained by finding the minimum for f(k) the values of m and m_u.

$$\frac{df(k)}{dk} = 2k_1 m_{yu} - 2k_1 m_y - 2m_{xy} = 0 \qquad 2.14$$

and,

$$\frac{df^2(k)}{dk^2} = 2 m_{yu} - 2m_y \geq 0 \qquad 2.15$$

From equation 2.14, the value of m_y can be obtained.

$$m_{yu} = m_y + \frac{1}{k_1}|m_{xy}| \qquad 2.16$$

From equations 2.14 and 2.15 following condition can also be obtained.

$$\frac{m_{xy}}{k_1} \geq 0 \qquad 2.17$$

Similarly the expressions for the design moments in x and y directions both for negative and positive moments can be obtained which are

For positive moments, Figure 2.1

$$m_{xu} = m_x + k_1 |m_{xy}| \qquad 2.18a$$

$$m_{yu} = m_y + \frac{1}{k_1} |m_{xy}| \qquad 2.18b$$

For negative moments, Figure 2.1

$$m_{xu} = m_x - k_2 |m_{xy}| \qquad 2.19a$$

$$m_{yu} = m_y + -\frac{1}{k_2} |m_{xy}| \qquad 2.19b$$

where, m_x, m_y, m_{xy} = applied bending and twisting moments

m_{xu},m_{yu} = design moments in the orthogonal reinforcement directions

k_1, k_2 = arbitrary positive factors

The value of factor k_1 and k_2 must be chosen from the following condition.

$$m^{\bullet}_x \, m^{\bullet}_y \geq 0 \qquad 2.20$$

For economic reasons the values of k_1 and k_2 must be close to 1.

It was also pointed out the best reinforcement pattern would be to place the reinforcement in the principal tensile stress directions, which may not be practical because it would mean, in most cases, reinforcement changing direction continuously.

Johansen's yield criterion[3] has been used to define the strength of the slab. Because this yield criterion over estimates the strength under certain loading conditions as described in Section 2.2.2, the design guidelines do not always produce a safe design.

Nielsen[4] independently adopted the same approach as Hillerborg[26] and proposed the same equations. It was stated that "it appears that the problem of designing reinforcement has now been reduced to a problem of pure bending". However, Johansen's yield criterion[3] is used in this design procedure which over estimates the strength of the slab, Section 2.2.2, hence the design carried out using the procedure outlined by Nielsen does not always produce a safe design.

Morley[27] outlined a procedure that can be used for the design of reinforcement for slabs based on the theory of plasticity. It was assumed that the reinforcement is closely spaced relative to the dimensions of the slab, thus an equivalent continuous plate, assumed to carry axial stress in the direction of the reinforcement, can replace the bars. Hence the area of reinforcement required can be expressed in terms of the minimum volume of the steel plate. The problem of determining the minimum volume was dealt with separately for slabs with and without membrane forces. For a slab of given thickness with no membrane forces, if the lever arm was assumed to be the same in both directions and the concrete was assumed to have infinite compressive strength and no tensile strength, the required thickness, a_i, of the plate to carry a principal moment, M_i, will be,

$$a_i = \frac{|M_i|}{\sigma_y d} \qquad 2.21$$

where, σ_y = yield strength of the reinforcement

d_l = lever arm

thus the total volume of the steel plate, V_s, can be obtained by integration over the surface area of the slab, A,

$$V_s = \int_A (a_1 + a_2)\, dA = \frac{1}{\sigma_y d_l} V \qquad 2.22$$

The above expression for determining the minimum reinforcement reduces to that of determining the minimum moment volume, V. Using the lower bound theorem of the limit analysis, sufficient conditions for minimum moment volume can be obtained by considering a virtual displacement, w, of the slab, normal to its plane.

i.e. $$\int pwdA = \int \{M_x k_x + M_y k_y + M_{xy} k_{xy}\}\, dA \qquad 2.23$$

where, M_x, M_y and M_{xy} are the applied bending and twisting moments, k_x, k_y and k_{xy} are the corresponding curvatures and p is the load per unit area.. Transforming the moment and the curvatures to the principal directions leads to the following expression for minimum volume of reinforcement, V_{sm}.

$$V_{sm} = \frac{1}{k_p \sigma_y d} \int pwdA \qquad 2.24$$

where, $k_p = |k_1| = |k_2|$ = principal curvature

The above expression was used for slabs with different shape and boundary conditions to obtain the minimum volume of reinforcement. Morley[27] further extended the work by taking into account the finite strength of concrete.

Using the approach adopted by Hillerborg[26], Wood[1] derived rules to determine the area of reinforcement for slab elements under mixed moment fields. The work was based on normal moment yield criterion i.e. the moment capacity of the section must be greater than or equal to the applied moments in the direction normal to the yield line. The moment capacity of the section was defined using Johansen's[3] yield criterion. The applied moments were transformed in the direction normal to the failure direction and then the difference between the capacity and the applied moments was minimised using the concept that in the failure direction the curve representing the strength must be tangential to the applied moments curve. This approach not only provides optimum reinforcement but also ensures that the capacity of the slab is always greater than the applied moment in any direction other than the failure direction. Wood has also shown that the factors k_1 and k_2 in equations 2.18 and 2.19 are 1, i.e. the failure direction is 45° except for certain conditions, if the optimum reinforcement is desired. Therefore, equations 2.18 and 2.19 can be written as follow.

For the positive moment, Figure 2.1

$$m^{\bullet}_x = m_x + |m_{xy}| \qquad 2.25a$$

$$m^{*}_{y} = m_{y} + |m_{xy}| \qquad 2.25b$$

if $m^{*}_{x} < 0$ then,

$$m^{*}_{x} = 0 \qquad 2.25c$$

$$m^{*}_{y} = m_{y} + \frac{|m_{xy}^{2}|}{m_{x}} \qquad 2.25d$$

similarly if $m^{*}_{y} < 0$ then

$$m^{*}_{y} = 0 \qquad 2.25e$$

$$m^{*}_{x} = m_{x} + \frac{|m_{xy}^{2}|}{m_{y}} \qquad 2.25f$$

For the negative moment, Figure 2.1

$$m^{*}_{x} = m_{x} - |m_{xy}| \qquad 2.26a$$

$$m^{*}_{y} = m_{y} - |m_{xy}| \qquad 2.26b$$

if $m^{*}_{x} > 0$ then

$$m^{*}_{x} = 0 \qquad 2.26c$$

$$m^{*}_{y} = m_{y} - \frac{|m_{xy}^{2}|}{m_{x}} \qquad 2.26d$$

similarly if $m^{*}_{y} > 0$ then

$$m^{*}_{y} = 0 \qquad 2.26e$$

$$m^{*}_{x} = m_{x} - \frac{|m_{xy}^{2}|}{m_{y}} \qquad 2.26f$$

where, m^{*}_{x}, m^{*}_{y} = design moments in reinforcement directions x and y respectively

m_x, m_y, m_{xy} = applied bending and twisting moments

Equations 2.25c – 2.25f and 2.26c – 2.26f represent the conditions when the failure is not at 45° i.e. factors k_1 and k_2 are not equal to 1.

Armer[2] extended the equations proposed by Wood[1] to cover the placement of reinforcement in non orthogonal directions. The equations are known as the Wood-Armer rules. The Wood-Armer rules use Johansen's[3] yield criterion and thus do not always produce safe design.

Morley[28] extended the work described earlier[27] for slab elements subjected to bending and twisting moments with skew reinforcement. Using the normal moment yield criterion, the expressions for the moment capacity were first obtained for concrete with infinite compressive strength and zero tensile strength. The volume of the reinforcement

as a proportion of the volume of the slab was obtained using the approach discussed in reference 27. An allowance for the finite compressive strength of the concrete has also been included.

Morley[29] provided a design technique, based on the theory of plasticity, for reinforced concrete slab elements subjected to six stress resultants i.e. three in-plane forces and three moments. It was assumed that the concrete had infinite compressive strength and zero tensile strength. The method was based on the concept that, at failure, in a rigid plastic material, if the rate of energy dissipation per unit volume is constant, the volume of the material, which is yielding, must be minimum. This concept was applied to reinforced concrete and it was shown that if the difference between the energy dissipation rate of concrete and reinforcement was constant, then the area of the reinforcement will be minimum. It was then argued that since the rate of energy dissipation in the concrete was very small compared with the rate of energy dissipation in the reinforcement, it can be neglected. This assumption simplified the problem to a condition of constant magnitude of energy since the reinforcement is provided in form of small diameter bars capably of resisting uniaxial stresses. It was further assumed that the amount of reinforcement was such as to ensure yielding. Using this approach, expressions to determine the area of reinforcement were developed for two skew directions for the top and bottom faces of the slab element. The expressions developed for the four sets of the reinforcement included the effect of the three in-plane forces. The expressions were then compared with previous work. It was found that these expressions reduce to the expressions developed by Nielsen[32] for the design for in-plane forces and the expressions developed by Wood[1] for the design for moments. However, it was stated that the method is based on strain rates, which vary through the depth of the

element and are not known beforehand, thus the proposed technique requires an iterative computer program. Solutions can be obtained for a few cases by hand calculation.

Clark[30] discussed the deficiencies in the normal moment yield criterion. It was pointed out that one of the main deficiencies in the normal moment yield criterion is the incorrect estimation of the lever arm. A discussion is provided in Section 6.3, Chapter 6, to highlight the problem of over estimation of lever arm for an element subjected to pure twisting. Clark proposed an algorithm for the determination of the correct moment capacity of the section, which depends on the determination of the correct lever arm. Expressions were developed to determine the correct lever arm. The value of the lever arm depends on the depth of the neutral axis. The correct depth of the neutral axis can only be determined by taking into account the high tensile strains in the principal directions due to the difference of the angle between the principal strain and reinforcement directions. The high tensile strains were not taken into account when determining the depth of the neutral axis. Thus the algorithm does not provide the correct lever arm. Furthermore, the proposed algorithm was iterative and is not suitable for hand calculations.

Gulvanessian[31] in an attempt to develope a method for the design of reinforced concrete slabs elements subjected to three in-plane forces and three moments used a sandwich model. The expressions developed by Nielsen[32] for the design for in-plane forces and by Wood[1] and Armer[2] for the design for moments were used. It was proposed that the contribution of each set of the reinforcement can be determined by equilibrium. Then the reinforcement on each face in each direction can be designed using expressions developed by Nielsen. Gulvanessian extended the work to accommodate skew

reinforcements.

Gupta and Sen[33] proposed two methods for the design of reinforced concrete slab elements subjected to a moment triad with no in-plane forces. The first method termed the Principal of Minimum Resistance Method (PMR), determines the reinforcement required in two orthogonal directions and the method is exactly the same as that proposed earlier by Wood[1]. The second method termed the Three Equivalent Moment Method (TEM), required reinforcement in three directions and was based on transformation of the applied moments into three pre-set reinforcement directions. From a comparison of the two methods it was concluded that the TEM method can save up to 40% of reinforcement with respect to the PMR method. However, provision of three layers of reinforcement on each face of the slab does not seems practical.

Morley and Gulvanessian[34] proposed a design method for slab elements subjected to a combination of three in-plane forces and three moments. The design method was based on equations developed by Nielsen[32] and Clark[35] and used a filled sandwich model. The slab element was divided into two reinforced outer layers separated by an un-reinforced concrete filling, Figure 2.6. The thickness of the outer layers of the sandwich was taken as twice the distance between the centroid of the reinforcement and the nearest concrete edge. The un-reinforced concrete filling was divided further into five stress zones. Immediately inside the bottom outer layer was a zone with compressive stress, f_c, in all directions. Inside this zone was a layer with zero and f_c as the principal tensile and compressive stresses. There were two similar zones inside the top outer layer. The fifth (central) zone of the filling was assumed to carry no stress. The square failure surface was used to model the ultimate compressive strength of concrete and the tensile strength

was neglected. The response in compression was modelled as linear elastic-plastic. The reinforcement was assumed to carry longitudinal forces only. Computer programs were written to carry out design for a given loading and known material and section properties. It was pointed out that the proposed sandwich model is not suitable if the diameter of the reinforcing bar is of significant proportion of the thickness of the slab.

Gupta[36] proposed an iterative procedure for the design of reinforced concrete elements subjected to six stress resultant i.e. three in-plane forces and three moments. In the proposed procedure the unknown depth of the neutral axis and the failure directions were first assumed. The principal stresses in concrete were then calculated. The stresses were then transformed into the reinforcement directions and equilibrium conditions were then applied. Thus a better estimate of the depth of neutral axis was obtained. The new depth of neutral axis was then used to recalculate the stresses and failure direction until convergence was achieved. Since this a cumbersome technique it is not suitable for hand calculation.

Khalifa[5] proposed modifications in the design procedure developed by others[26,1,2]. The modified design rules are,

$$m_{xu} \geq m_x + kr_k|m_{xy}| \qquad 2.27a$$

$$m_{yu} \geq m_y + \frac{1}{k} r_k|m_{xy}| \qquad 2.27b$$

$$m'_{xu} \geq -m_x + kr_k|m_{xy}| \qquad 2.27c$$

$$m'_{yu} \geq -m_y + \frac{1}{k} r_k |m_{xy}| \qquad 2.27d$$

where, m_x, m_y, m_{xy} = applied bending and twisting moments

m_{xu}, m_{yu} = positive design moment for section in x and y directions.

m'_{xu}, m'_{yu} = negative design moment for section in x and y directions.

k = $\tan\theta$

θ = failure direction

r_k = amplification factor

The approach adopted by Khalifa in the proposed design rules is not only unorthodox but non-scientific as the amplification is applied to the applied loading.

Lourenco and Figueiras[37,38] in their studies used the technique proposed by Gupta[36] and have coded it into a finite element program for the design of reinforced concrete shell elements. Comparisons were made with different experimental studies and good results were obtained.

2.3.2 DISCUSSION

The design methods based on the normal moment yield criterion, discussed earlier[1,2,4,5,26,33], adopt the approach in which the applied moments were transformed in a direction normal to the failure direction first and then the difference between the moment capacity and the applied moments was minimised. Johansen's yield criterion[3]

was used to define the moment capacity of the section in the failure direction. The transformation of the moment capacities in the reinforcement directions into a desired direction does not account for the actual stress state of the element and, therefore, can not predict the neutral axis depth correctly and thus over estimates the lever arm. The incorrect estimation of lever arm in turn produces higher moment capacity, which eventually produces unsafe design under certain loading conditions.

For a section with no twisting moments, there is no interaction between the orthogonal sets of reinforcement and the principal moment and reinforcement directions coincide. Design carried out for such an element using the concept of transformation of moment capacities in the failure direction will be safe, efficient and economical. As the twisting moment increases, the interaction between the orthogonal sets of reinforcement increases, and so does the angle between the principal moments and reinforcement directions, the design concept in which the moment capacities are transformed, can not cater for different angle between the principal moments and reinforcement directions thus produce unsafe design. As the twisting moment increases, and hence the angle between the reinforcement and principal moment directions increases the design rules based on transformation of moment capacities will produce more unsafe and inefficient design.

2.4 MATERIAL MODELS

The object of the present work was to study the behaviour of reinforced concrete slab elements subjected to generalised set of moments. A computer program, described in

Chapter 4, that can predict the non-linear response shell elements has been written. The numerical representation of the concrete properties is one of the most important aspects of a realistic analysis. The behaviour of concrete in a biaxial stress state is complex due to its orthotropic nature, its non-linear behaviour in compression and the occurrence of cracking. In order to model concrete numerically, an understanding of the constitutive material model is necessary. An attempt has been made in the following paragraphs to identify the different approaches used to model the mechanical properties of concrete.

Due to the complex behaviour of concrete, special emphasis have been given to its constitutive models. Generally, three different theories have been employed to model the mechanical properties of concrete viz.

1. Models based on theory of elasticity
2. Models based on theory of plasticity
3. Endochronic models

A detailed discussion of these approaches has been given in references 39, 40. In the following sections, the basic concepts and the limitations of these approaches have been discussed briefly.

2.4.1 MODELS BASED ON THEORY OF ELASTICITY

Two different approaches have been employed in the formulation of non-linear elasticity based constitutive models. The two approaches are, total and incremental stress-strain formulations. In the total stress-strain models, the stress state is assumed to be uniquely

expressed as a function of strain. This type of formulation is reversible and loading path independent and thus cannot be used to model unloading regimes. In spite of this shortcoming, the total stress-strain models have been used, mainly because of their simplicity, to predict the non-linear behaviour of concrete under biaxial and triaxial stress states.

The incremental, hypoelastic, stress-strain models are used to describe the behaviour of materials in which the stress state depends on the current strain state and the stress path followed to reach that state. In the hypoelastic material model, the stress and strain incremental vectors are linearly related through the tangential material stiffness matrix $\underline{D}_T$ as:

$$\underline{d\sigma} = \underline{D}_T \underline{d\varepsilon} \qquad 2.28$$

where $\underline{d\sigma}$ and $\underline{d\varepsilon}$ are the stress and the strain increment vectors respectively. This type of formulation is incrementally reversible and path dependent and, therefore, provides a good representation of concrete behaviour under non-monotonic and non-proportional loading regimes. A number of incremental models have been developed for isotropic, orthotropic stress-strain relationships under biaxial and triaxial stress states[41,42,43,44,45].

In the present study, the work has been limited to the behaviour of reinforced concrete slab elements under monotonic loading without any unloading. Total stress-strain models based on theory of elasticity have been used, due to their simplicity and

reasonable accuracy and have been described in Chapter 3.

2.4.2 MODELS BASED ON THEORY OF PLASTICITY

In-elastic deformations in concrete occur if it is stressed beyond the limit of elasticity and upon unloading only a proportion of the total strain can be recovered. Therefore, the total strain in concrete may be separated into recoverable and irrecoverable components. The recoverable part is treated within the framework of elasticity, while the irrecoverable part can be treated on the basis of the theory of plasticity.

In the incremental theory of plasticity, the total strain increment vector, $\underline{d}\,\varepsilon$, is assumed to be the sum of the elastic, $\underline{d}\,\varepsilon^{e}$, and plastic, $\underline{d}\,\varepsilon^{p}$, components. In addition to the strain decomposition, three other fundamental assumptions are required to formulate the constitutive relations for a work hardening material. They are:

1. The shape of initial yield surface and subsequent loading surfaces.

2. The formulation of a suitable hardening rule that describes the evolution of subsequent loading surfaces.

3. The formulation of an appropriate flow rule that specifies the stress-strain relation in plastic range.

The initial yield surface is required to mark the stress level at the onset of plastic deformations. It can be expressed as:

$$f(\underline{\sigma}) = k \qquad 2.29$$

where f is some function of stress and k is a parameter to be defined experimentally. When a work hardening material is stressed beyond the elastic limit i.e. beyond the initial yield surface, a new yield surface, called the loading surface is developed. This loading surface will change its configuration at any stage of plastic deformation and it may be expressed in terms of plastic strain, $\underline{\varepsilon}^p$, and a hardening parameter, h, as:

$$f = f(\underline{\sigma}, \underline{\varepsilon}, h) \qquad 2.30$$

For condition when $f < 0$, material is within the limit of elasticity and when $f = 0$, yield has occurred.

The evolution of subsequent loading surfaces during plastic deformation is described by specifying an appropriate hardening rule. Three types of hardening rules are frequently used in connection with the strain hardening plasticity models viz. isotropic, kinematic and mixed plasticity rules. In isotropic hardening models, the subsequent loading surfaces are a uniform expansion of the original yield surface. The kinematic hardening rule assumes that the subsequent loading surfaces preserve the shape and orientation of the initial yield surface during plastic flow but they translate in the stress space as rigid bodies. In the mixed hardening rule, the loading surface experiences a translation and a uniform expansion in all directions[39,46].

In order to establish the stress-strain relation in the plastic range, the concept of a plastic-potential function, $g(\underset{\sim}{\sigma})$, is introduced[39]. The plastic strain increment vector is assumed to be proportional to the stress gradients of the plastic potential function, so that

$$d\underset{\sim}{\varepsilon}^{p} = d\lambda \frac{dg(\underset{\sim}{\sigma})}{d\underset{\sim}{\sigma}} \qquad 2.31$$

where, $d\lambda$ is a positive scalar factor of proportionality. Equation 2.31 is termed as flow rule since it governs the plastic flow after yielding. The gradient of the potential surface, $dg(\underset{\sim}{\sigma}) / d\underset{\sim}{\sigma}$, defines the direction of the plastic strain increment vector and the length is determined by the factor, $d\lambda$. When the current surface and the plastic potential coincide, $f(\underset{\sim}{\sigma}) \equiv g(\underset{\sim}{\sigma})$, equation 2.31 becomes,

$$d\underset{\sim}{\varepsilon}^{p} = d\lambda \frac{df(\underset{\sim}{\sigma})}{d\underset{\sim}{\sigma}} \qquad 2.32$$

This relationship is known as the associated flow rule, because it is connected with the loading surface. It is also called the normality condition since $df(\underset{\sim}{\sigma}) / d\underset{\sim}{\sigma}$ represents a vector directed normal to the current loading surface at the stress point under consideration.

Plasticity based models have been extensively used to describe the behaviour of concrete[47,48, 49,50,51]. In general models based on theory of plasticity assume an elastic

plastic hardening behaviour of concrete up to the ultimate strength followed by a rigid plastic response until the crushing surface is reached. After crushing, the concrete is assumed to lose completely its resistance against further deformation. Since decreasing of all stress components is impossible for strictly plastic behaviour satisfying Ducker's stability postulate[52], such models are not capable of representing degradation of stiffness and softening due to unstable fracturing of the material.

More refined approaches based on plastic-fracturing theory have been developed and used in modelling the post failure, softening, response of concrete[53,54,55]. The fracturing phenomena are better described in terms of loading surfaces that depend on strains rather then stresses since micro-fracturing can lead to a decrease in stress at constant strain. Therefore, two loading surfaces are required in the plastic-fracturing theory to account for the strain hardening behaviour. In addition to strain decomposition, the stress increment is also decomposed into an elastic stress increment and a fracture stress decrement.

2.4.3 ENDOCHRONIC MODELS

The endochronic theory of viscoplasticity was originally proposed by Valanis[56] and has been applied to predict the mechanical response of metals under complex strain histories. The first application to geo-materials and concrete as well as the first compressive endochronic constitutive equation was developed by Bazant and Bhat[57]. Unlike the elasticity and the plasticity models, the endochronic formulation is incrementally non-linear. The basic concept underlying the theory is that of intrinsic time. Intrinsic time is a non-decreasing scalar variable that depends on the increments of

strains as well as time[58]. Although the theory is capable of modelling many complex phenomena, the early endochronic formulation was subjected to serious criticisms concerning uniqueness of response, stability and energy dissipation during load cycles[59,60]. These criticisms were eliminated when Bazant[61] introduced the concepts of loading surfaces and jump-kinematic hardening to give the theory features similar to that of the theory of plasticity. Valanis[62] refined the intrinsic time in terms of plastic strain and showed that the various versions of classical plasticity theories represent particular cases of endochronic formulation.

Constitutive models based on endochronic theory, are relatively difficult to use due to the complexity of the mathematics involved and thus total elasticity based models have been given preference over plasticity and endochronic models in the present study.

2.4.4 REVIEW OF MODELS FOR PLAIN CONCRETE UNDER BIAXIAL STRESS

A number of attempts have been made to explain and quantify the ultimate stress state of plain concrete under biaxial stresses. The work carried out is outlined in this Section.

Kupfer et al[63] provide a brief summary of the work conducted up to 1969 and also described tests to investigate the failure surface. Concrete plates, 7.9 in x 7.9 in x 2 in, were made with three different types of concrete to give uniaxial compressive strengths of 2700, 4450 and 8350 psi. These plates were tested under biaxial compression, compression-tension and biaxial tension. Within each biaxial stress combination four different stress ratios of σ_1/σ_2 were chosen and six specimens were tested for each type of concrete and each stress ratio. Specially designed loading equipment was used. A

constant strain rate was chosen such that the maximum load was obtained after approximately 20 minutes. The stress and strain in the concrete in the three principal directions were recorded. It was concluded that when loaded with equal biaxial compressive stress an increase in strength of 27% was achieved as compared to the uniaxial strength of concrete in compression. Empirical expressions to define the strength and corresponding strain under different biaxial stress states were given.

Liu et al[64] proposed a stress-strain equation to predict the response of concrete under compression with any stress ratio taking into account the Poisson's ratio effect. Based on the earlier experimental data[65], expressions for peak stress, corresponding strain and a simplified failure envelope in biaxial compression were proposed. The work was, however, limited to the biaxial compression-compression state.

Kupfer and Gerstle[66] proposed a failure surface based on tests carried out earlier for the full range of biaxial loading. They proposed also expressions for ultimate stress, bulk modulus and shear modulus.

Tasuji et al[67] tested concrete plates of 5 in x 5 in x ½ in under different biaxial stress combinations. For the compression-compression region stress ratios of 0, 0.2, 0.5 and 1.0, for the tension-compression -0.05, -0.1 and -0.25 and for the tension-tension 0, 1.0 and 2.0 were used. The specimens with uniaxial and biaxial compression were applied with a constant stress rate of 390 psi/min and 140 psi/min for tests in tension. Only one type of concrete was used with an average uniaxial compressive strength of 4827 psi and an average tensile strength of 418 psi. Expressions to determine ultimate strengths were also proposed.

Rosmtad, Taylor and Herrmann[68] developed an isotropic stress-strain model for concrete under biaxial loading. Instead of utilising one continuous curve to represent degradation of concrete, the model used four regions, depending on the stress ratios, to represent the degradation of concrete. In these regions the material properties were altered to match the degradation of concrete caused by the increased stresses. Within each region the modulus of elasticity and Poisson's ratio were kept constant.

Tasuji et al[69] extended the earlier work[67] and modified the proposed expressions for the ultimate strength and the corresponding strain for concrete under different biaxial stress states. They compared the proposed model with the existing models[64,66,67] and the experimental data of others[66] and concluded that their model was a better representation of ultimate stress state, Figure 2.7. The proposed model is discussed in more detail in Chapter 3.

Ganaba[70] identified that Tasuji et al's[69] model has some deficiencies due to the empirical nature of the developed expressions. It was found that there was a discontinuity in the biaxial compression stress state when equal compressive stress were applied in the two orthogonal directions. The strain corresponding to the peak compressive stresses were found to be different if the compressive strength of concrete was other than 23.5 MPa. Therefore, Ganaba using the experimental data of Tasuji et al modified the expressions for the strains corresponding to the peak stresses.

2.4.5 REVIEW OF THE MATERIAL MODELS FOR REINFORCED CONCRETE

The response of reinforced concrete under different biaxial stress states is of vital importance in predicting the overall response of reinforced concrete elements. Phenomena like tension stiffening and compression softening must be modelled adequately to study the response of reinforced concrete. For over two decades attempts have been made to model the response of reinforced concrete under different state of stresses. The following Sections provides an overview of the work done to model such phenomena.

2.4.5.1 Models for Tension Stiffening

When loaded in tension, reinforced concrete does not fail to carry load beyond first cracking like plain concrete, but it still carries stress and offers stiffness because of the uncracked concrete between the cracks. This phenomenon is called tension stiffening. It has been recognised that tension stiffening results from crack formation and bond slip between reinforcing bars and surrounding concrete[71], Figure 2.8. It affects the service behaviour of reinforced concrete members by significantly increasing the stiffness of the reinforced concrete element in the post cracking range as compared with the element in which tension stiffening is not considered. A review of the work to quantity and model tension stiffening has been discussed in this Section.

Clark and Speirs[72] tested 14 beams and 9 slabs under two point loading with various steel areas and bar arrangements. It was concluded that the tension stiffening can be

calculated on the basis of an average tensile stress expressed as a fraction of the tensile strength of concrete acting over an effective area of concrete surrounding the bars in the tension zone. The values of the average tensile stress and the effective zones over which tension stiffening acts were proposed for beams and slabs separately.

Gilbert and Warner[73] used a layered discrete element method to investigate the behaviour of reinforced concrete slabs under short term loading. Various models to define tension stiffening were compared. Instead of proposing a post cracking response of concrete to model tension stiffening modifications in the stress-strain curve of the reinforcement were proposed. Hence the concrete was assumed to carry zero stress after cracking.

Clark and Cranston[74] extended the experimental work on reinforced concrete slabs[72] and presented a formulation to quantify tension stiffening. It was argued that tension stiffening should only be used in a region around the reinforcement and is dependent on the size and spacing of the reinforcing bars.

Carreira and Chu[75] used experimental data from several studies and proposed a complete stress-strain response for reinforced concrete in tension, which takes into account tension stiffening. They used a continuous function to represent the stress-strain curve in tension for reinforced concrete with a degree of non-linearity varying from 1.45 to 2.25. They further concluded that the tension stiffening depended on crack propagation, formation of external and internal cracks around and along the bar, the strength of the concrete, the shape and size of the test specimen and shrinkage.

Fifteen 1:3.33 scale model longitudinal strips of reinforced concrete voided slabs were tested by Oduyemi and Clark[76] under four point loading to study the effect of tension stiffening. A simplified procedure was proposed to determine the tension stiffening response of solid and voided slabs.

Link et al[77] derived a tension stiffening relation for generally oriented cracks. As the cracks are not usually normal to the reinforcement, tension stiffening was quantified by using an equivalent steel ratio normal to the crack orientation, taking into consideration possible yielding of one or more layers of reinforcement at a crack. They proposed a two stage full response of reinforced concrete in tension. The relationship consisted of a linear ascending branch up to cracking followed by a non-linear descending curve up to the yielding of steel. The model was implemented into a finite element program and was then compared with the tests conducted by Vecchio and Collins[25] and good agreement was found with the experiments.

Gupta and Maestrini[78] proposed an analytical model of tension stiffening phenomenon in cracked reinforced concrete. It was assumed that the bond stress-slip relationship is bilinear and remains linear throughout the bar in the initial stages of cracking. At the later stages the bond stress-slip relationship becomes constant. The experimental results of others[86] were used to compare the analytical model.

Prakhya and Morley[79] presented expressions to quantify tension stiffening in reinforced concrete based on the experimental work conducted by others[72,80,81,82,83]. The tensile response was modelled as a linear ascending branch up to cracking followed by descending non-linear branch. It was argued that tension stiffening depends on

parameters such as bar diameter, reinforcement spacing and cover and thus the proposed tension stiffening model included the effect of these parameters. It was also emphasised that all the layers of concrete in tension do not follow the same tension stiffening curve but for simplicity only one stress-strain curve for the concrete was used. Comparison of the model with the experimental data[72,80-83] showed good agreement.

An analytical model of tension stiffness of a reinforced concrete panel in-plane stress state has been developed based on the bond slip mechanism by Wu et al[84]. A fourth rank stress reduction tensor was defined in terms of crack strain and the reinforcement tensor was defined in terms of the stress increase in the reinforcement resulting from the stiffness of the reinforcement. Another stress reduction tensor for plastic strain was also defined and the coupling relation between these tensors was considered in a general constitutive equation. The general constitutive equations for the composite material, made up of reinforcement and concrete, were developed for a two dimensional stress field, with multiple crack orientations using these tensors. This study was limited to proportional monotonic loading without unloading and reloading. The crack shear stiffness from the aggregate interlock was also considered to be negligible. The proposed model gave good agreement with several experimental studies[25,85,86,87].

Belarbi and Hsu[88] conducted tests on 17 reinforced concrete panels loaded in uniaxial tension. The panels were 55 in. square with thickness of 7 in. The reinforcing steel was placed in two layers adjacent to the two surfaces of the panel in two orthogonal directions. A tensile load was applied to the sets of reinforcement placed in one direction. Various percentages of main reinforcement (0.54% to 2.1%) were arranged in the direction in which the load was applied and a constant reinforcement ratio of 0.54%

was used in the orthogonal direction. The tensile strains in the concrete were measured by placing LVDTs on both the faces while strains in the reinforcement were also measured using electrical strain gauges installed on the bars at various locations. Based on the experimental results analytical relationships were derived for stress-strain curves for concrete and steel. It was proposed that the tensile response of concrete can be modelled by a linear ascending branch up to cracking followed by an exponential descending branch. It was argued that the reinforcing steel embedded in concrete does not show a distinct yield point on the stress-strain curve of the reinforcement. It was also showed that the yield stress of the embedded reinforcement reduces when compared with the yield stress of a bare bar due to the difference of strains in the embedded reinforcement at the cracks and in between the cracks. An analytical model for embedded reinforcing steel in tension was also proposed.

Pitt[89] successfully adopted an approach usually employed in composite laminates to model tension stiffening in reinforced concrete members. The tension zone was sub divided into two regions. In the region close to the reinforcement, full tension stiffening was applied whereas, in the remaining of the tension region only tensile strength was used.

Choi and Cheung[90] presented an analytical model with special emphasis on the final cracking point, which was defined as the point after which further cracks cannot occur in a member. It was argued that tension stiffening depends on the transfer length, average crack spacing and the distribution of the concrete stress. The transfer length was defined as the distance between the crack to the point on the reinforcement where the strain in the crack and the reinforcement becomes equal. The expressions to evaluate the

effect of these parameters were obtained by solving a differential equation based on the bond action between the concrete and the reinforcement. The model was then further extended to the case where the cracks are not orthogonal to the reinforcement. The model was validated by implementing it in a finite element computer program and comparing the analytical results with experimental studies[25, 86].

Hsu and Zhang[91] extended the work described in reference 88 and compared three different models that can be employed for concrete and steel in uniaxial tension. The first model assumed no tensile strength for concrete and a perfect elastic-plastic response of steel. This model over estimated the deformation. The second model used a linear ascending branch up to cracking followed by exponential descending branch to model the response of concrete in tension and a perfect elastic-plastic response of steel. This model correctly predicted the deformation but resulted in an increase in the yield strength of the reinforcement. The third model, which can be termed as the accurate model, used the same response of concrete in tension as that for the second model but a modified response of steel. The modified response was assumed to be perfectly elastic up to a modified yield stress, which was lower than the actual yield stress. Beyond yielding the steel was assumed to be strain hardening but with a very small slope. This model best fitted to the experimental results.

Wollrab et al[92] studied tension stiffening by testing 23 reinforced concrete specimens in uniaxial tension. Three main parameters the reinforcement ratio, bar spacing and concrete strength were studied. It was found that the cracking strength increased with an increase in the spacing of the reinforcement but that tension stiffening was independent of reinforcement ratio. It was also found that the slip between the concrete and the

reinforcement was higher for high strength concrete. It was argued that the larger bond slip can be attributed to the more brittle behaviour of high strength of concrete.

Abrishami and Mitchell[93] tested several reinforced concrete specimens in uniaxial tension with reinforcement of different diameters and different concrete strengths to study the effect of splitting cracks on tension stiffening. Tensile load was applied to a single reinforcing bar embedded in concrete. Two different types of cracking, splitting and transverse were observed. It was found under progressively increasing loads, the region in which splitting cracks appear increases. Thus splitting cracks influence the post cracking behaviour of reinforced concrete. A tension stiffening model based on equilibrium and compatibility was developed that takes splitting cracks into account. It was found that concrete cover to reinforcing bar diameter ratio, c/d_b, is a good measure to define the extent of longitudinal splitting cracks.

Ouyang et al[94] presented the results of an experimental study on reinforced concrete specimens subjected to uniaxial tension. Eighteen reinforced concrete specimens were tested with different reinforcement ratios and concrete strength. A model was developed that can predict concrete and reinforcement strains and stresses in cracked reinforced concrete. The model was based on a fracture mechanics approach. The model was then compared with the experimental results and good agreement was obtained.

2.4.5.2 Models for Compression Softening

Reinforced concrete structures are often subjected to a compression-tension stress state. It has been shown that the compressive strength of concrete is significantly reduced due

to orthogonal cracking. A number of attempts have been made to study this phenomenon and in the following an overview is provided.

Harder[95] tested nine isotropically and nine orthotropically reinforced concrete slabs elements under pure twisting to quantify the effect of compression softening due to the orthogonal cracking. Based on equilibrium and compatibility an algorithm was proposed to quantify the softening of the compressive strength of concrete. It was found that on average the compressive strength was 55% of the uniaxial compressive strength in the tested specimens.

At the University of Toronto[25] 30 square reinforced concrete elements have been tested loaded by in-plane stresses. These tests were carried out in a specially designed test rig. The intention was to use the tests to develop a better understanding of behaviour of reinforced concrete. The panels had varying amounts of reinforcement in the two orthogonal directions. Different combinations of in-plane loads were applied to the specimens. It was observed that the compressive strength of concrete was significantly reduced compared to the uniaxial compressive strength as the tensile strain in the orthogonal direction increased. A model was proposed to define the stress-strain response of the concrete in the presence of orthogonal cracking. It was proposed that both the peak compressive stress and the corresponding strain should be reduced by the same amount and the reduction factor was dependent on the ratio of principal tensile and compressive strains.

Cervenka[96] proposed an analytical model to define the compressive response of concrete softened by the orthogonal cracking. It was proposed that the reduction factor was a

function of the tensile strain only and that it should be applied to the peak compressive stress. The model was compared with the experimental results of four panels in reference 25 and good agreement was obtained.

Vecchio and Collins[97] proposed a modified model for compression softening, which was an improvement on that proposed in reference 25. A strength reduction factor was proposed to model the softened response of concrete due to orthogonal cracking. The reduction factor, which was applied to the compressive strength only, was a function of the ratio of the principal tensile and the strain corresponding to the maximum uniaxial compressive strength of concrete. The model was compared with the experimental results for the reinforced concrete panels[25] and good agreement was obtained.

Hsu[98] provided a brief history of the development of the models for compression softening of concrete. A model was proposed for compression softening based on equilibrium and compatibility. The proposed softening coefficient was a function of principal compressive and tensile strains. In order to model the softened response of concrete the softening coefficient should be applied to both the uniaxial compressive strength and the corresponding strain. The reduction factor was, however, similar to the softening coefficient proposed in reference 25.

Vecchio and Collins[99] provide an excellent review of compression softening models. Based on 116 specimens tested at the University of Toronto two different models were proposed for compression softening. Two different parabolic curves were used to define the stress-strain response of softened concrete and it was found that the equation proposed by Theronfeldt et al[100] predicted a better response than that of Hognestad[101]

and hence used. The two proposed models were termed Model A and Model B. For Model A, a reduction factor was applied to the uniaxial compressive strength and corresponding strain of concrete to model the softened response. The reduction factor was found to be a function of the principal tensile and compressive strains and the uniaxial compressive strength of concrete. Model A has been adopted to model the softened compressive strength in this study and is discussed in more detail in Section 3.2.2, Chapter 3. Model B was shown to be slightly less accurate than Model A. A slightly different softening coefficient was proposed in Model B. However, the softening coefficient in Model B was also a function of ratio of principal tensile and compressive strains but was applied to the uniaxial compressive strength of the concrete only. The two models were compared with the other models[25,97,102,103,104,105] and it was found that both models predicted the softening of concrete better than the others, however, Model A gave better response than Model B.

Belarbi and Hsu[106] tested 22 reinforced concrete panels 55 in. square and 7 in. thick. Tensile load was applied in one direction and compressive load was applied in the orthogonal direction. The amount of reinforcement placed in the direction of tensile load was kept constant whereas, the amount of reinforcement in the compressive load direction was varied. An analytical model was proposed based on equilibrium of forces and compatibility of strains in the concrete and the reinforcement. It was proposed that a reduction factor should be applied to the uniaxial compressive strength of concrete to model compression softening. The model was then compared with the experimental results and was found to fit the experimental data.

Thienel and Shah[107] tested 56 orthogonally reinforced concrete specimens of several

sizes under in-plane compression-tension in the reinforcement directions. The study investigated the effects of concrete strength, lateral tensile loading, reinforcement ratio, reinforcing bar spacing and panel height on the strain-softening behaviour, final crack formulation, compressive strength and strain at ultimate. Since the reinforcement in the tensile loading direction was low, the applied tensile load was also limited, thus the effect of softening due to orthogonal tensile strain could not be quantified. However, a reduction in the compressive strength was observed.

References

1 Wood, RH, The reinforcement of slabs in accordance with a predetermined field of moments, Concrete, London, vol. 2, February 1968, pp 69-76.

2 Armer GST, Discussion on 'The reinforcement of slabs in accordance with a predetermined field of moments', Concrete, London, vol. 8, August 1968, pp 319-321.

3 Johansen, KW, Brudlinieteorier, Gjellerup, Copenhagen, Denmark 1943, English edition: Yield line theory, Cement and Concrete Association, London 1962, 181p.

4 Nielsen, MP, Limit analysis of reinforced concrete slabs, Acta Polytechnica Scandiniavica, Ci 26, Copenhagen, Denmark, 1964, 167p.

5 Khalifa, JU, Limit analysis of reinforced concrete shell elements, PhD Thesis, Department of Civil Engineering, University of Toronto, May 1986. 222 p.

6 Marti, P, Leesti, P, Khalifa, WU, Torsion tests on reinforced concrete slab elements, Jnl. of St. Eng., ASCE, vol. 113, no. 5, May 1987, pp 994-1010.

7 Marti, P and Kong, K, Response of reinforced concrete slab elements to torsion, Jnl. of St. Eng., ASCE, vol. 113, no. 5, May 1987, pp 976-993.

8 Wood, RH, Plastic and elastic design of slabs and plates, First edition, Thames and Hudson, London, 1961, 344 p.

9 Kemp, KO, The yield criteria for orthotropic reinforced concrete slabs, Int. Jnl. of Mech. Sci., vol. 7, no. 11, November 1965, pp 737-746.

10 Morley, CT, On the yield criteria of an orthogonally reinforced concrete slab element, Jnl. of the Mech. and Phy. of Solids, vol. 14, no. 1, January 1966, pp 33-47.

11 Morley, CT, Experiments on the yield criterion of isotropic reinforced concrete slabs, ACI Jnl., Proceedings, vol. 64, no. 1, January 1967, pp 40-45.

12 Lenshow, R, Sozen, MA, A yield criterion for reinforced concrete slabs, ACI Jnl., Proceedings vol. 64, no. 5, May 1967, pp 266-273.

13 Lenshow, R and Sozen, MA, A yield criterion for reinforced concrete under biaxial moment and forces, Civil Engineering Studies Structural Research Series No. 311, University of Illinois, July 1966, 527 p.

14 Cardenas, A, Discussion on 'A yield criterion for reinforced concrete slabs, ACI Jnl., Proceeding , vol. 64, no. 11, November 1967, pp 783-784.

15 Lenkei, Peter, Discussion on 'A yield criterion for reinforced concrete slabs, ACI Jnl., Proceeding , vol. 64, no. 11, November 1967, pp 786-789.

16 Prince, MR and Kemp KO, A new approach to the yield criterion for isotropically reinforced concrete slabs, Magazine of Concrete Research, vol. 20, no. 62, March 1968, pp 13-20.

17 Holmes, M and Downham, RJ, An experimental investigation into the yield criterion for reinforced concrete slabs, Structures, Solid Mechanic and Engineering Design: Proceedings of the Civil Engineering Material Conference, University of Southampton, April 1969, vol. 2, pp 1321-1331.

18 Cardenas, AE, and Sozen , MA, Flexural yield capacity of slabs, ACI Jnl. Proceedings, vol. 70, no. 2, February 1973, pp 124-126.

19 Cardenas, AE, and Sozen, MA, Strength and behavior of isotropically and nonisotropically reinforced concrete slabs subjected to combination of flexural and torsional moments, Civil Engineering Series No. 336, Department of Civil Engineering, University of Illinois, May 1968, 250 p.

20 Jain, SC, Kennedy, JB, Yield criteria for reinforced concrete slabs, Jnl. of St. Eng., ASCE, vol. 100, ST3, March 1974, pp 631-644.

21 Rajendran ,S and Morley, CT, A general yield criteria for reinforced concrete slab elements, Magazine of Concrete Research, vol. 26, no. 89, December 1974, pp 213-220.

22 Cookson, PJ, A general yield criterion for orthogonally reinforced concrete slab elements, Plasticity of Reinforced Concrete, Final Report, IABSE Colloquium, Copenhagen 1979, pp 43-50.

23 ACI 318-83, Building code requirements for reinforced concrete, American Concrete Institute, Detroit, Mich. 1983.

24 CAN3-A23.3-M84, Design of concrete structures for buildings, Canadian Standard Association, Rexdale, Ontario, 1984.

25 Vecchio, F and Collins, MP, The response of reinforced concrete panels to in-plane shear and normal stress, Publication No. 82-03, Department of Civil Eng., University of Toronto, March 1982, 332 p.

26 Hillerborg, A, Reinforcement for slabs and shells designed according to the theory of elasticity, Betong 1953, vol. 38, no. 2, pp 101-109. Translated by GN Gibson, Graston, Building Research Station, January 1962, 7 p, Library communication no. 1081.

27 Morley, CT, The minimum reinforcement of concrete slabs, Int. Jnl. of Mech. Sci., vol. 8, no. 4, April 1966, pp 305-319.

28 Morley, CT, Skew reinforcement of concrete slabs against bending and torsional moment, Proceedings of Institution of Civil Engineers, vol. 42, January 1969, pp 57-74.

29 Morley, CT, Optimum reinforcement of concrete slab elements against combination of moments and membrane forces, Magazine of Concrete Research,

vol. 22, no. 72, September 1970, pp 155-162.

30 Clark LA, Test on slab elements and skew slab bridges designed in accordance with the factored elastic moment field, Cement and Concrete Association, Technical Report No. 42.474, September 1972, 47p.

31 Gulvanessian, H, The reinforcement of concrete slabs and girders subjected to flexure and in-plane stresses, Proceedings of Institution of Civil Engineers, Part 2, Research and Theory, vol. 55, September 1973, pp 671.

32 Nielsen, MP, Yield conditions for the reinforced concrete shells in the membrane state, Proceedings of IASS Symposium on Non-classical Shell Problems, Warsaw, 1963, North-Holland publishing company, Amsterdam 1964, pp 1030-1040.

33 Gupta, AK and Sen, S, Design of flexural reinforcement in concrete slabs, Jnl. of St. Div., Proceedings of ASCE, vol. 103, ST4, April 1977, pp 793-804.

34 Morley, CT and Gulvanessian, H, Optimum reinforcement for concrete slab elements, Proceedings of Institution of Civil Engineers, Part 2, Research and Theory, vol. 63, June 1977, pp 441-454.

35 Clark, LA, The provision of tension and compression reinforcement to resist in-plane forces, Magazine of Concrete, vol. 28, no. 94, March 1976, pp 3-12.

36 Gupta, AK, Combined membrane and flexural reinforcement in plates and shells, Jnl. of St. Eng., ASCE, vol. 112, no. 3, March 1986, pp 550-557.

37 Lourenco, PB and Figueiras, JA, Automatic design of reinforcement in concrete plates and shells, Engineering Computations, vol. 10, December 1993, pp 519-541.

38 Lourenco, PB and Figueiras, JA, Solution for the design of reinforced concrete plates and shells, Jnl. of St. Eng., ASCE, May 1995, pp 815-823.

39 Chen, WF, Plasticity in reinforced concrete, McGraw-Hill, 1982.

40 Chen, WF and Saleeb, AF, Constitutive equations for engineering materials, vol. 1, Elasticity and modelling, 1981, vol. 2, Plasticity and modelling, 1982, John Willey and Sons, New York.

41 Gerstle, KH, Simple formulation of biaxial concrete behaviour, ACI Jnl., vol. 78, no. 1, September 1981, pp 62-68.

42 Drawin, D and Pecknold, DA, Analysis of RC shear panels under cyclic loading, Jnl. of St. Div., ASCE, vol. 102, ST2, February 1976, pp 355-369.

43 Drawin, D and Pecknold, DA, Non-linear biaxial stress-strain law for concrete, Jnl. of Eng. Mech. Div., ASCE, vol. 103, EM2, April 1977, pp 229-241.

44 Elwi, AA and Murray, DW, A 3D hypoelastic concrete constitutive relationship, Jnl. of Eng. Mech. Div., ASCE, vol. 105, EM4, August 1979, pp 623-641.

45 Bathe, KJ and Sundberg, JA, Computational modelling of reinforced concrete structures (Chapter 4), edited by Hinton, E and Owen, R, Pineridge Press, Swansea, 1986, pp 101-121.

46 Owen, DRJ and Hinton, E, Finite elements in plasticity, theory and application, Pineridge Press, Swansea, 1980.

47 Buyukozturk, O, Non-linear analysis of reinforced concrete structures, Computer and Structures, vol. 7, 1977, pp 149-159.

48 Chen, ACT and Chen, WF, Constitutive relations for concrete, Jnl. of Eng. Mech., ASCE, vol. 101, EM4, August 1975, pp 465-581.

49 Owen, DJR and Figrueiras, JA, Ultimate load analysis of reinforced concrete plate and shell including geometric non-linear effects, Finite element software for plates and shells, Edited by Hinton, E and Owen, DRJ, Pineridge, Press, Swansea, 1984.

50 Imbabi, MS and Cope, RJ, An equivalent elasto-plastic constitutive model for biaxially loaded concrete, Proceeding of Inter. Conference on Computer Aided Analysis and Design of Concrete Structures, edited by Damjanic et al., vol. 1, Split, Yugoslavia, September 1984, pp 275-288.

51 Cervera, M and Hinton, E, Computational modelling of reinforced concrete structures (Chapter 12), edited by Hinton, E and Owen, R, Pineridge Press, Swansea, 1986, pp 327-370.

52 Drucker, DC, A more fundamental approach to plastic stress-strain relations, Proceeding of 1st US National Congress on Applied Mechanics, 1951, pp 487-491.

53 Bazant, ZP and Kim, SS, Plastic-fracturing theory for concrete,, Jnl. of Eng. Mech., ASCE, vol. 105, June 1979, pp 407-428 with errata in vol. 106.

54 Hsieh, SS, Ting EC and Chen, WF, A plastic-fracture model for concrete Jnl. of Solids and St., vol. 18, no. 3, 1982, pp 181-197.

55 Glemberg, R and Samuelsson, A, A general constitutive model for concrete structures, Proceedings of Inter. Conference on Computer Aided Analysis and Design Structures, edited by Damjanic et al., vol. 1, Split, Yugoslavia, September 1984, pp 119-132.

56 Valanis, KC, A theory of viscoplasticity without a yield surface- theory and application, Archives of Mechanics, vol. 23, no. 4, 1971, pp 517-551.

57 Bazant, ZP and Bhat, P, Endochronic theory of inelasticity and failure of concrete, Jnl. of Eng. Mech. Div., ASCE, vol. 102, EM4, August 1976, pp 701-722.

58 Reddy, DV and Gopal, KR, Computational modelling of reinforced concrete structures (Chapter 6), edited by Hinton, E and Owen, R, Pineridge Press,

Swansea, 1986, pp 154-188.

59 Sandler, IS, On the uniqueness and stability of endochronic theories of material behaviour, Jnl. of Appl. Mech., vol. 45, no. 2, June 1978, pp 263-266.

60 Rivlin, RS, Some comments on the endochronic theory of plasticity, Int. Jnl. of Solids and St. Vol. 17, 1981, pp 231-248.

61 Bazant, ZP, Endochronic inelasticity and incremental plasticity, Int. Jnl. of Solids and St., vol. 14, 1978, pp 691-714.

62 Valanis, KC, Fundamental consequences of a new intrinsic time measure-plasticity as a limit of the endochronic theory, Archives of Mech., vol. 32, no. 1, 1980, pp 171-191.

63 Kupfer, HB, Hilsdrof, HK and Rusch, H, Behaviour of concrete under biaxial stress, Jnl. of ACI Proceeding, vol. 66, no. 8, August 1969, pp 656-666.

64 Liu, TCY, Nilson, AH, and Slate, FO, Biaxial stress-strain relationship for concrete, Jnl. of St Div., Proceeding ASCE, vol. 98, ST5, May 1972, pp 1025-1034.

65 Liu, TCY, Stress-strain response and fracture of concrete in uniaxial and biaxial compression, Research Report No. 339, Department of Structural Engineering, Cornell University, New York, February 1971.

66 Kupfer, HB and Gerstle, KH, Behaviour of concrete under biaxial stresses, Jnl. of Eng. Mech., ASCE, vol. 99, EM4, August 1973, pp 853-866.

67 Tasuji, ME, Slate, FO and Nilson AH, Stress-strain response and fracture of concrete in biaxial loading, Jnl. of ACI, Proceeding, vol. 75, no. 7, July 1978, pp 306-312.

68 Rosmtad, KM, Taylor, MA and Herrmann LR, Numerical biaxial characterzation for concrete, Jnl. of Egg Mech. Div., Proceeding ASCE, vol. 100, EM5, pp 935-948.

69 Tasuji, ME, Nilson AH and Slate, FO Biaxial stress-strain relationships for concrete, Magazine of Concrete Research, vol. 31, no. 109, December 1979, pp 217-224.

70 Ganaba, TH, Nonlinear finite element analysis of plates and slabs, PhD Thesis, University of Warwick, August 1985, 215 p.

71 Goto, Y, Cracks formed in concrete around deformed tension deformed bars, ACI Jnl. Proceedings, vol. 668, no. 4, 1971, pp 244-251.

72 Clark, LA and Speris, DM, Tension stiffening of reinforced concrete beams under short term load, Cement and Concrete Association, London, Technical report No. 42.521, July 1978, 20 p.

73 Gilbert, RI and Warner, RF, Tension stiffening in reinforced concrete slabs, Jnl. of St Div., ASCE Proceedings, vol. 4, ST12, December 1978, pp 1885-1900.

74 Clark, LA and Cranston, WB, The influence of bar spacing on tension stiffening in reinforced concrete slabs, Proceeding of the international conference on concrete slabs, Advances in Slabs Technology, Dundee, April 1979, pp 118-128.

75 Cerreira, DJ and Chu, KH, Stress-strain relationship for concrete in tension, Jnl. of ACI, Proceeding, vol. 83, Jan-Feb. 1986, pp 21-28.

76 Oduymi, TOS and Clark, LA, Tension stiffening in longitudinal sections of circular voided concrete slabs, Proceeding of Institution of Civil Engineers, Part 2, no. 83, December 1987, pp 861-874.

77 Link, RA, Elwi, AE and Scanlon, A, Biaxial tension stiffening due to generally oriented reinforcing layers, Jnl. of Eng. Mech., vol. 115, no. 8, August 1989, pp 1647-1662.

78 Gupta, AK and Maestrini, SR, Tension stiffness model for reinforced concrete bars, Jnl. of St. Eng., vol. 116, no. 3, Mar 1990, pp 769-790.

79 Prakhya, GKV and Morley, CT, Tension-stiffening and moment-curvature relations of reinforced concrete elements, ACI St. Jnl., vol. 87, no. 5, Oct-Nov. 1990, pp 597-605.

80 Kishek, MA, Tension stiffening and cracked widths in reinforced concrete beams and slab elements, PhD Thesis, Cambridge University, 1983, 233 p.

81 Williams, A, Tension on large reinforced concrete elements subjected to direct tension, Technical Report No. 42.562, Cement and Concrete Association, London, 1986, 58 p.

82 Bach, C and Graf, O, Tests on reinforced concrete beams for obtaining moment curvature relationships, Bulletin No. 38, Deutscher Ausschuss für Eisenbeton, Berlin 1917, pp 38-41.

83 Sakai, K and Kukuta, Y, Moment-curvature relationships of reinforced concrete members subjected to combined bending and axial force, ACI Jnl. Proceedings, vol. 77, no. 3, May-June 1980, pp 189-194.

84 Wu, Z, Yoshikawa, H and Tanabe, T, Tension stiffness model for cracked concrete, Jnl. of St Eng., vol. 117, no. 3, March 1991 pp 715-732.

85 Oesterle, RG and Russell, HG, Shear transfer in large scale reinforced concrete containment elements, NUREG/CR-1374, Construction Technology, Laboratories, April 1980.

86 Rizkalla, SH and Hwang, LS, crack prediction for members in uniaxial tension, ACI Jnl., vol. 81, no. 6, 1984, pp 572-579.

87 Yamamoto, Y, Study of bond stress of reinforcements, cracking and restoring

characteristics of embedded tension bars, Taisei Technical Report 6, Technical Research Institute, Taisei Corp., 1973, pp 151-193.

88 Belarbi, A and Hsu, TTC, Constitutive laws of concrete in tension and reinforcing bars stiffened by concrete, ACI St Jnl., vol. 91, no. 4, July-Aug 1995, pp 463-474.

89 Pitt, DC, Composite laminate modelling of reinforced concrete elements, M.Sc. Thesis, Heriot-Watt University/ Ecole Polytechnique Federale DeLausanne, September 1995, 77p.

90 Choi, CK and Cheung, SH, Tension stiffening model for planar reinforced concrete members, Computers and Structures, vol. 59, no. 1, January 1996, pp 179-190.

91 Hsu, TTC and Zhang, LX, Tension stiffening in reinforced concrete membrane elements, ACI St Jnl., vol. 93, no. 1, Jan-Feb 1996, pp 108-115.

92 Wollrab, E, Kulkarni, SM, Ouyang, C and Shah, SP, Response of reinforced concrete panels under uniaxial tension, ACI St. Jnl., vol., 93, no. 6, Nov-Dec. 1996, pp 648-657.

93 Abrishami, HH and Mitchell, D, Influence of splitting cracks on tension stiffening, ACI St. Jnl., vol. 93, no. 6, Nov-Dec. 1996, pp 703-710.

94 Ouyang, C, Wollrab, E, Kulkarni, SM and Shah, SP, Prediction of cracking response of reinforced concrete tensile members, Jnl. of St. Eng., ASCE, vol. 123, no. 1, January 1997, pp 70-77.

95 Harder, NA, Strength of the concrete in the shear zone of a reinforced concrete cross section, Experiments with plates loaded in tension, Instituttet for Bygningsteknik, Aalborg, Report No. 7901, August 1979, 49p.

96 Cervenka, V, Constitutive model for cracked reinforced concrete , ACI St. Jnl., vol. 82, no. 6, Nov-Dec. 1985, pp 877-882.

97 Vecchio, FJ and Collins, MP, The modified compression-filed theory for reinforced concrete elements subjected to shear, ACI St Jnl., vol. 83, no. 2, Mar-Apr. 1986, pp 219-231.

98 Hsu, TTC, Softened truss model theory for shear and torsion, ACI St Jnl., vol. 85, no. 6, Nov-Dec. 1988, pp 624-635.

99 Vecchio, FJ and Collins, MP, Compression response of cracked reinforced concrete, Jnl. of St Eng., vol. 119, no. 12, December 1993, pp 3590-3610.

100 Thorenfeldt, E, Tomaszewicz, A and Jensen, JJ, Mechanical properties of high strength concrete and application in design, Proceeding, Symposium of High Strength Concrete, Stavanger, Norway, Tapar, Trondheim 1987.

101 Hognestad, E, Hanson, NW and McHenry, D, Concrete stress distribution in ultimate strength design, Jnl. of ACI, vol. 52, no. 6, December 1955, pp 445-

479.

102 Belarbi, A and Hsu, TTC, Constitutive laws of reinforced concrete in biaxial compression-tension, Research Report UHCEE 91-2, University of Houston, USA, 1991.

103 Kollegger, J and Melhorn, G, Experimentelle Untersuchungen zur Bestimmung der Druckfestigkeit des gerissnen bej einer Querzugbeanspruchung, Report 413, Deutscher Ausschuss F ü r Stahlbeton, Berlin Germany, 1990.

104 Miyahara, T, Kawakami, T and Meakawa, K, Nonlinear behavior of cracked reinforced concrete plate element under uniaxial compression, Concrete Library International, Japan Society of Civil Engineers, JSCE, vol. 11, 1988, pp 306-319.

105 Shirai, S and Noguchi, H, Compressive deterioration of cracked concrete, Proceedings of ASCE St. Congress 1989, Design, Analysis and Testing, ASCE, New York, 1989, pp 1-10.

106 Belarbi, A and Hsu, TTC, Constitutive laws of softened concrete in biaxial tension-compression, ACI St Jnl., vol. 92, no. 5, Sept-Oct 1995, pp 562-573.

107 Thienel, KC and Shah, SP, Postpeak behavior of laterally reinforced concrete panels in compression-tension, ACI St Jnl., vol. 93, no. 6, Nov-Dec. 1996, pp 685-695.

Table 2.1: Details of slabs tested by Lenshow and Sozen.

Mark	f'_c	f_y	Depth	Direction and spacing of reinforcement Top/Bottom				M_{exp}	M_{comp}	Type of load
				Ang_1	s_1/s'_1	Ang_2	s_2/s'_2			B = biaxial bending, U = uniaxial bending, T = torsion
	ksi	ksi	in	deg	in	deg	in	in-k/in	in-k/in	
C1	6.61	50.0	4.12	0	1.50/ -	90	1.375/ -	5.75	5.69/5.73	B
C2	4.58	50.0	4.12	0	1.50/ -	90	1.375/ -	6.10	5.63/5.66	B
C3	2.70	50.0	4.12	0	1.50/ -	90	1.375/ -	5.80	5.50/5.50	B
B4	4.74	50.0	4.15	0	1.50/ -	90	1.375/ -	5.85	5.68	U
B7	5.15	50.0	4.14	-45	1.50/ -	45	1.375/ -	5.85	5.76	U
B8	3.70	50.0	4.18	-22.5	1.50/ -	67.5	1.375/ -	6.08	5.75	U
B9	3.82	50.0	4.23	-45	3.00/ -	45	1.375/ -	4.45	4.00	U
B10	4.92	50.0	4.14	90	1.50/ -	0	1.375/ -	6.10	5.77	U
B11	4.80	50.0	4.12	-22.5	1.50/ -	67.5	2.75/ -	5.35	5.08	U
B12	5.17	47.6	4.12	-22.5	3.00/ -	67.5	1.375/ -	3.82	3.75	U
B13	4.24	47.9	4.01	90	1.50/1.375	0	1.375/1.5	5.96	5.42	U
B15	5.26	47.9	4.09	-45	1.50/1.375	45	1.375/1.5	5.33	5.78	T
B16	4.73	48.3	4.04	90	1.375/1.375	0	1.50/1.50	5.43	5.58	T
B17	5.53	50.8	4.03	-22.5	1.50/1.50	67.5	1.375/1.375	5.88	5.98	T
B18	5.04	56.1	4.08	-45	1.50/1.50	45	1.375/1.375	6.61	6.41	T
B19	5.35	53.1	4.06	-45	3.00/3.00	45	2.75/2.75	3.35	3.23	T
B20	5.49	51.8	4.04	90	3.00/3.00	0	2.75/2.75	3.42	3.34	T
B21	5.18	47.8	4.03	90	1.50/1.50	0	5.50/5.50	3.00	3.00	T
B22	5.46	53.8	4.06	90	1.50/1.50	0	5.50/5.50	3.51	3.40	T
C23	5.96	50.0	4.20	0	3.00/ -	90	2.75/ -	3.20	2.80	B
C24	5.12	50.0	4.20	0	3.00/ -	90	2.75/ -	3.27	3.07	B
C25	4.31	50.0	4.20	0	3.00/ -	90	2.75/ -	3.38	3.06	B

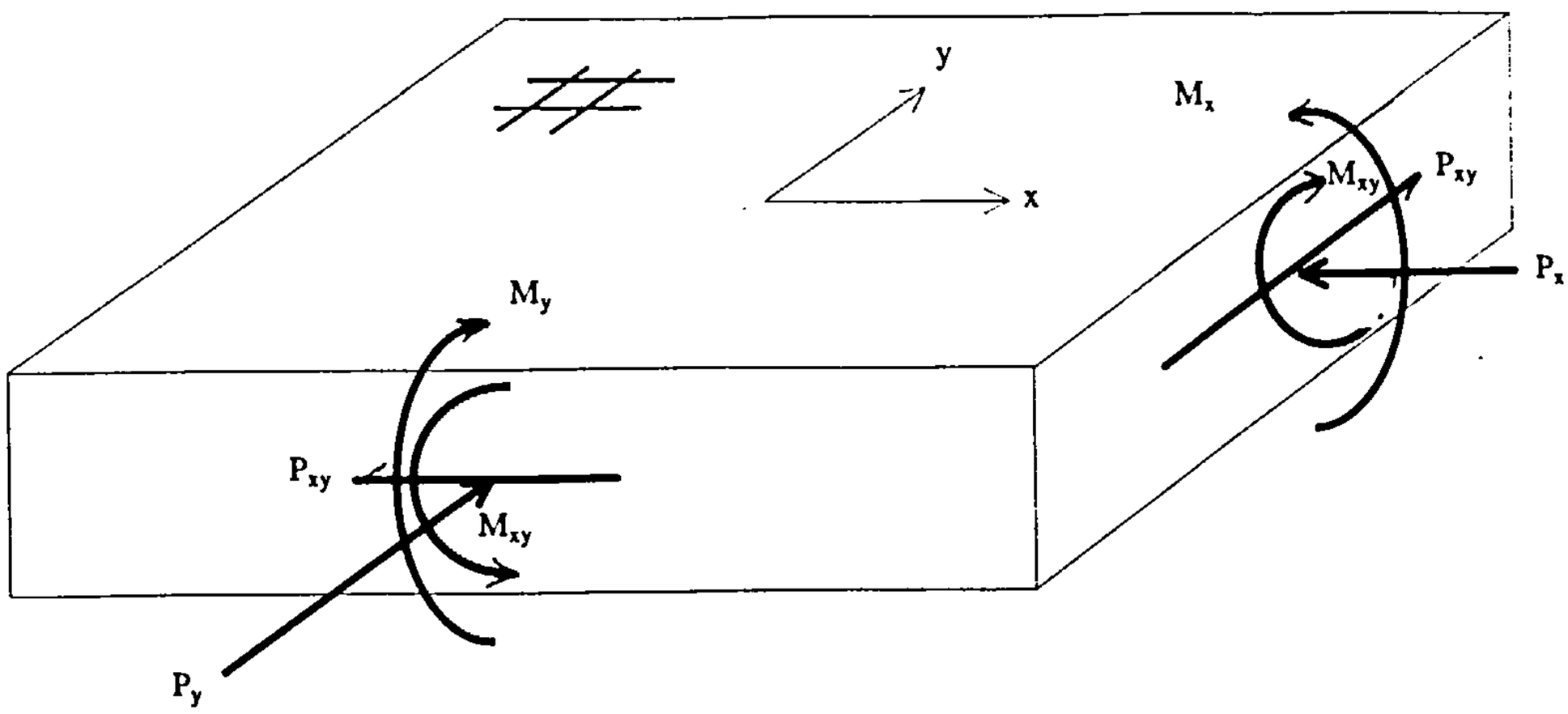

Fig 2.1: Slab element with positive applied loading

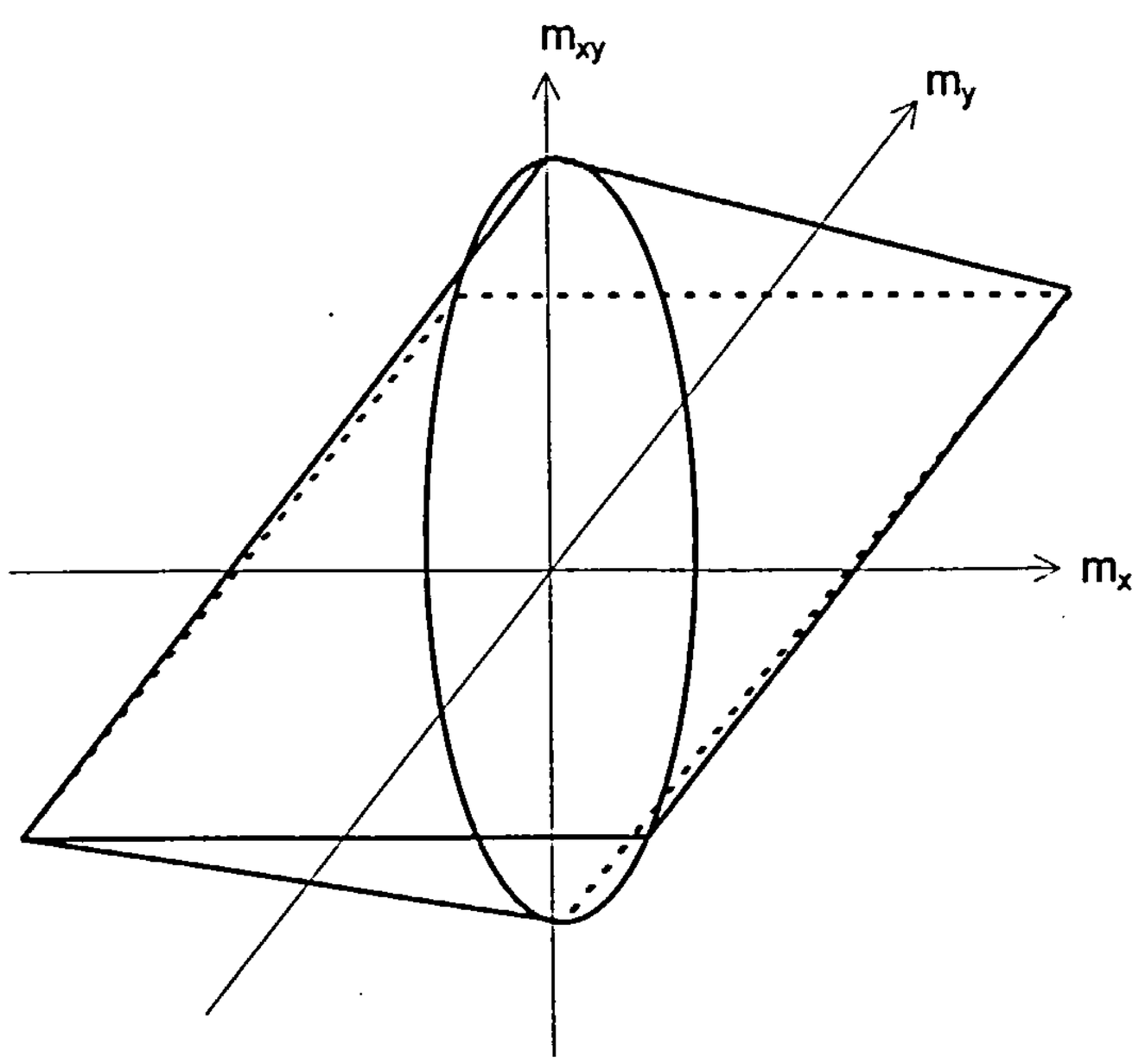

Figure 2.2: Normal moment yield criterion in m_x, m_y and m_{xy} space

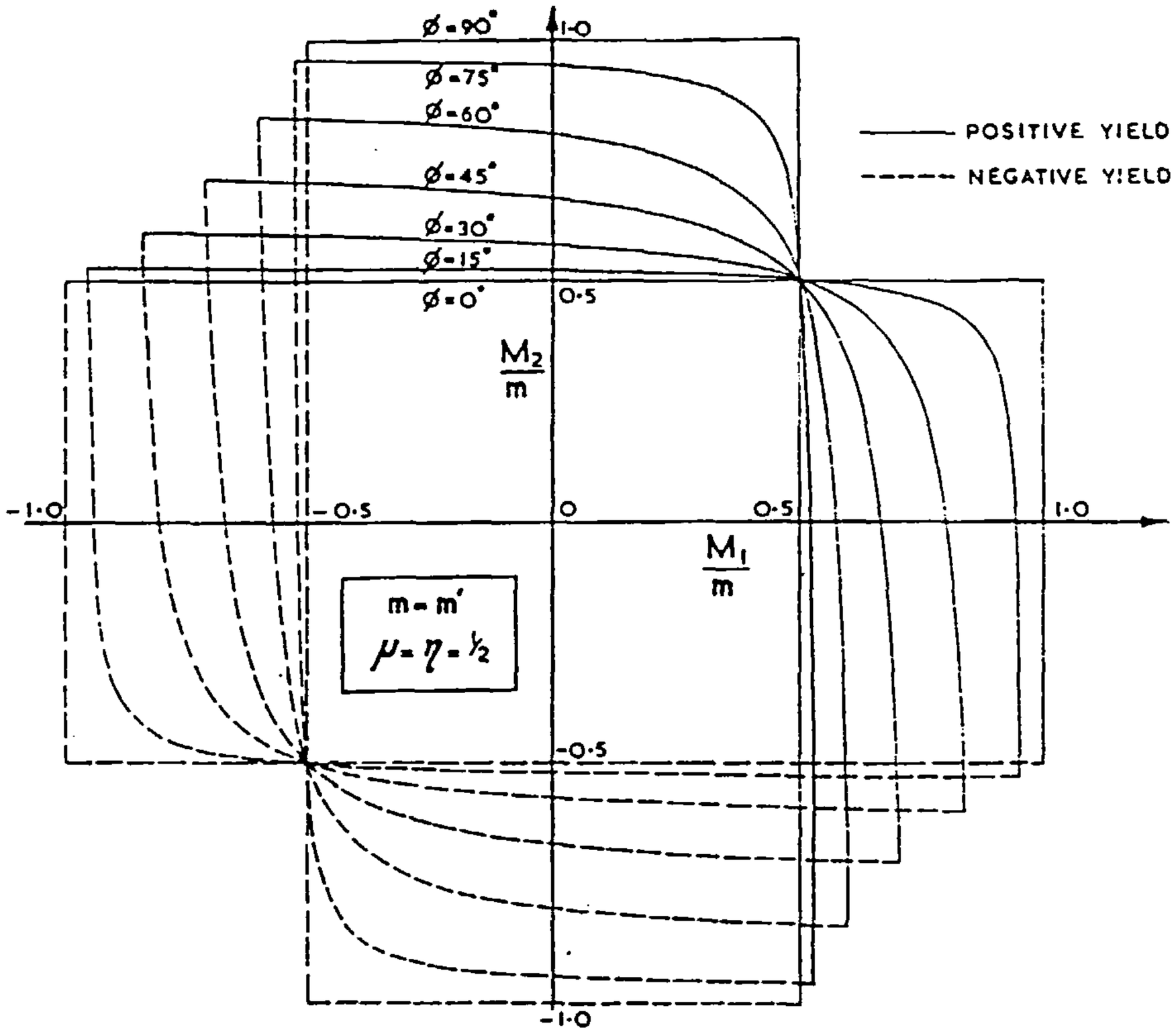

Figure 2.3: Graphical representation of the normal moment yield criterion in the principal moment field for an orthotropic slab [Kemp[9]]

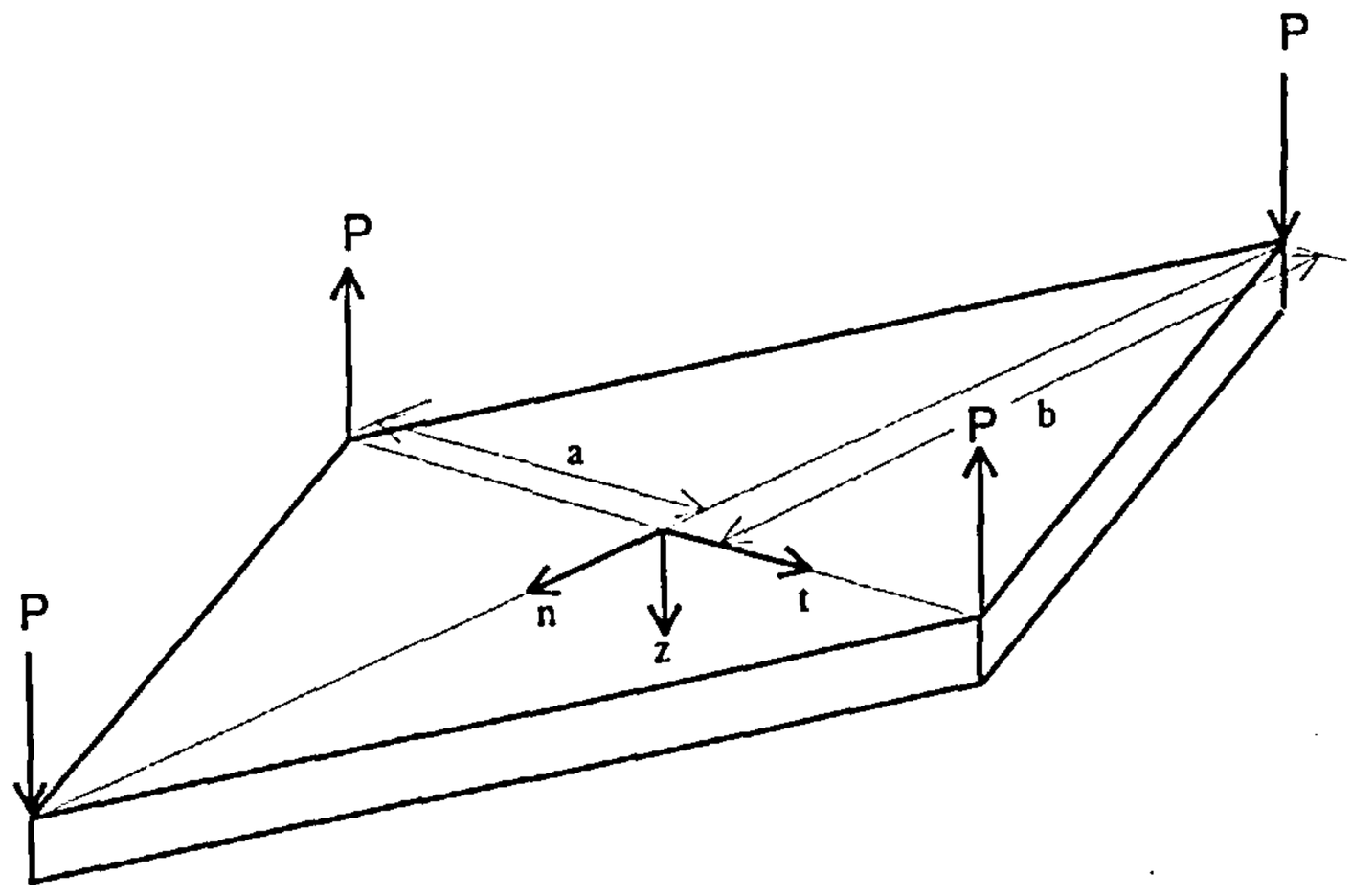

Figure 2.4: Loading arrangement in Morley's[11] tests

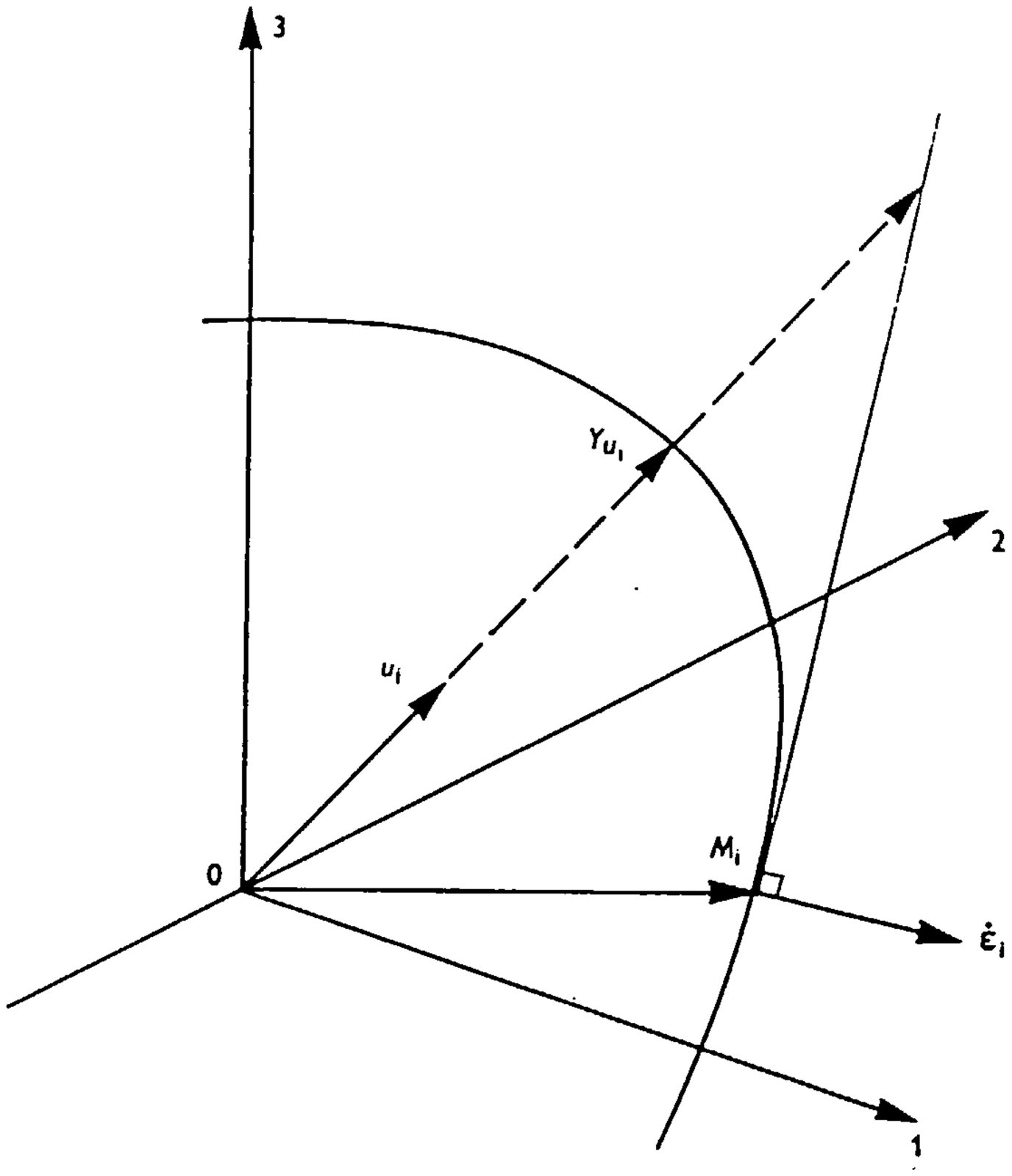

Figure 2.5: Schematic representation of yield surface [Rajendran and Morley[21]]

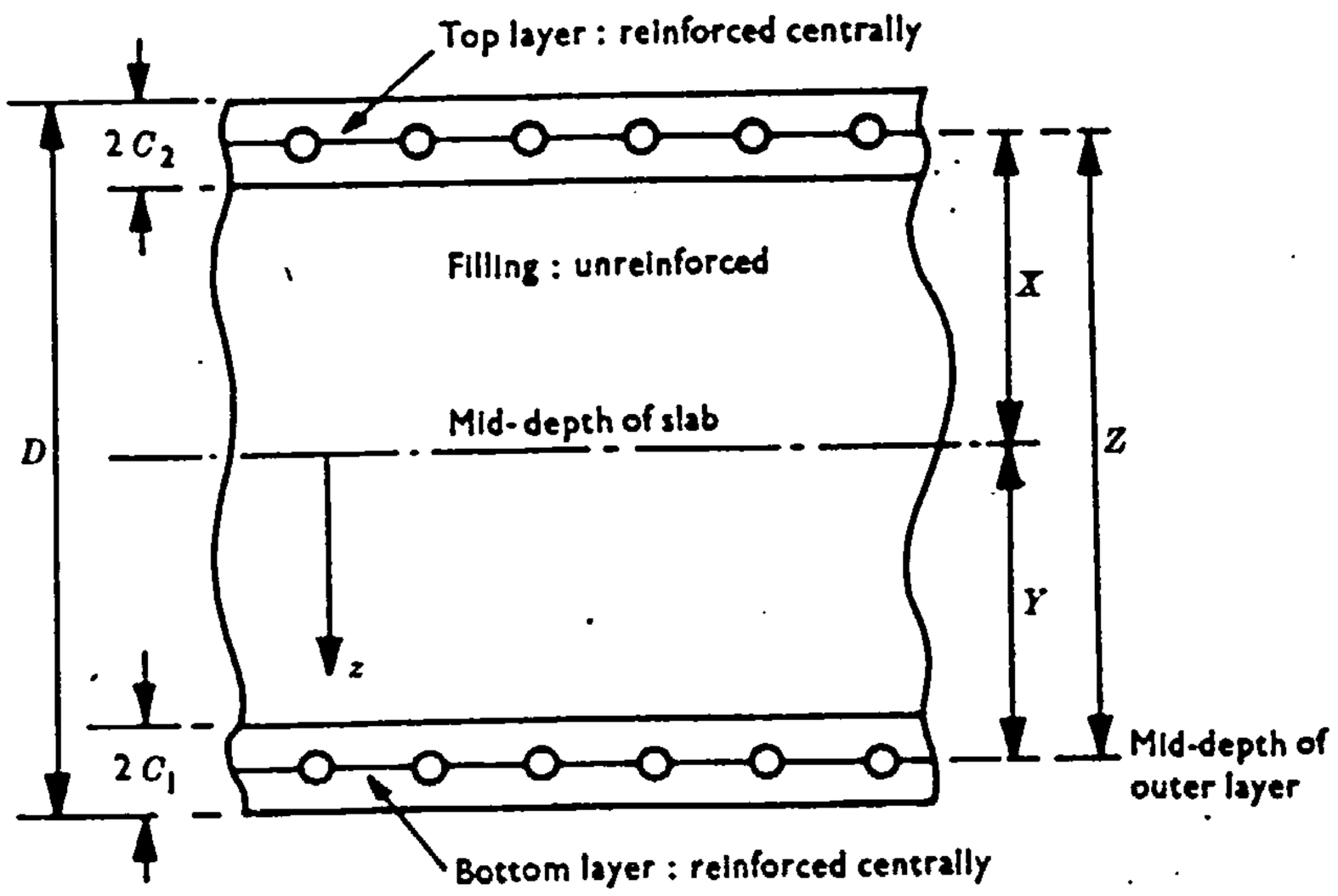

Figure 2.6: Filled sandwich model [Morley and Gulvanessian[34]]

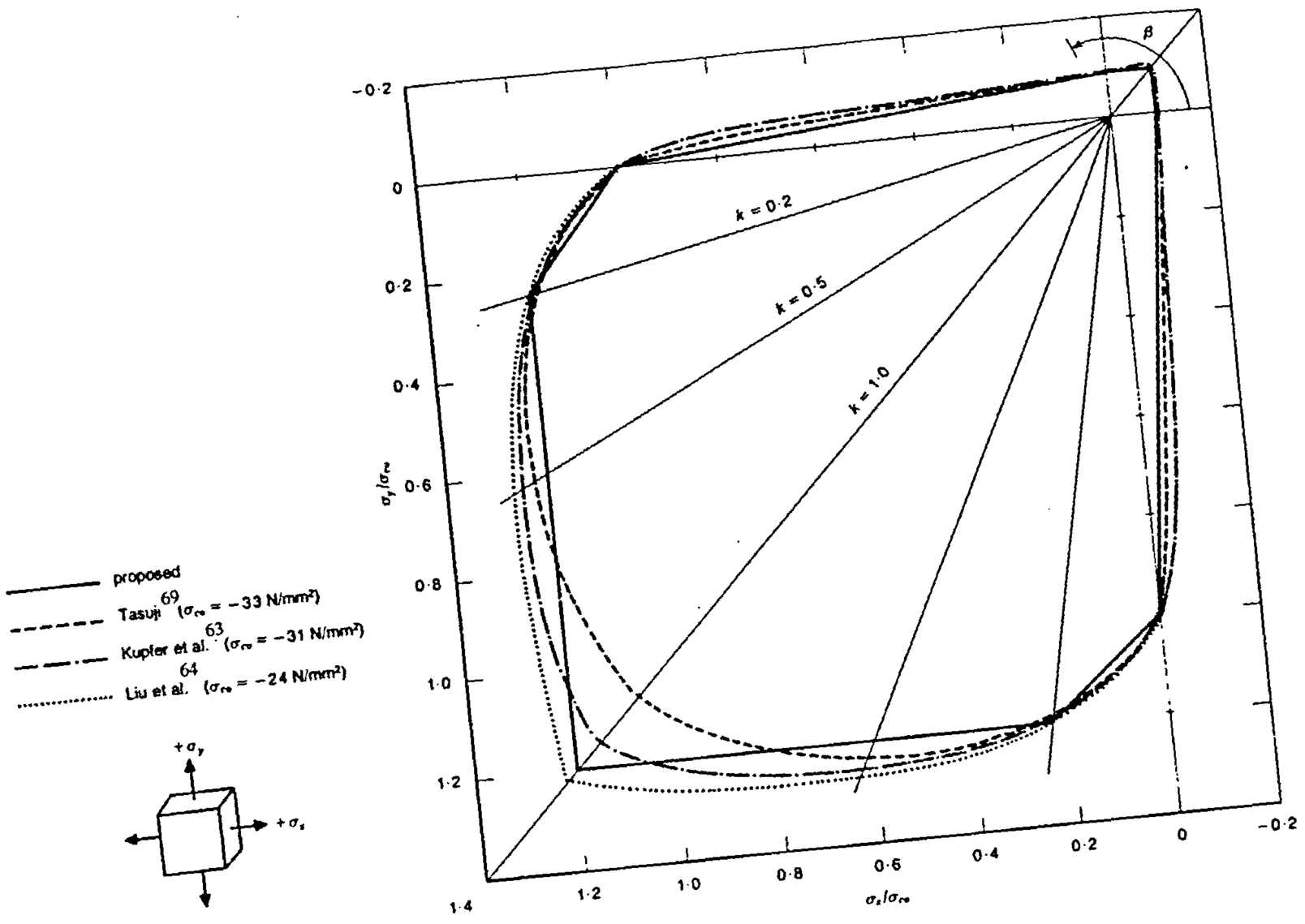

Figure 2.7 Comparison of models representing the ultimate biaxial stress state of concrete [Tasuji et al[69]]

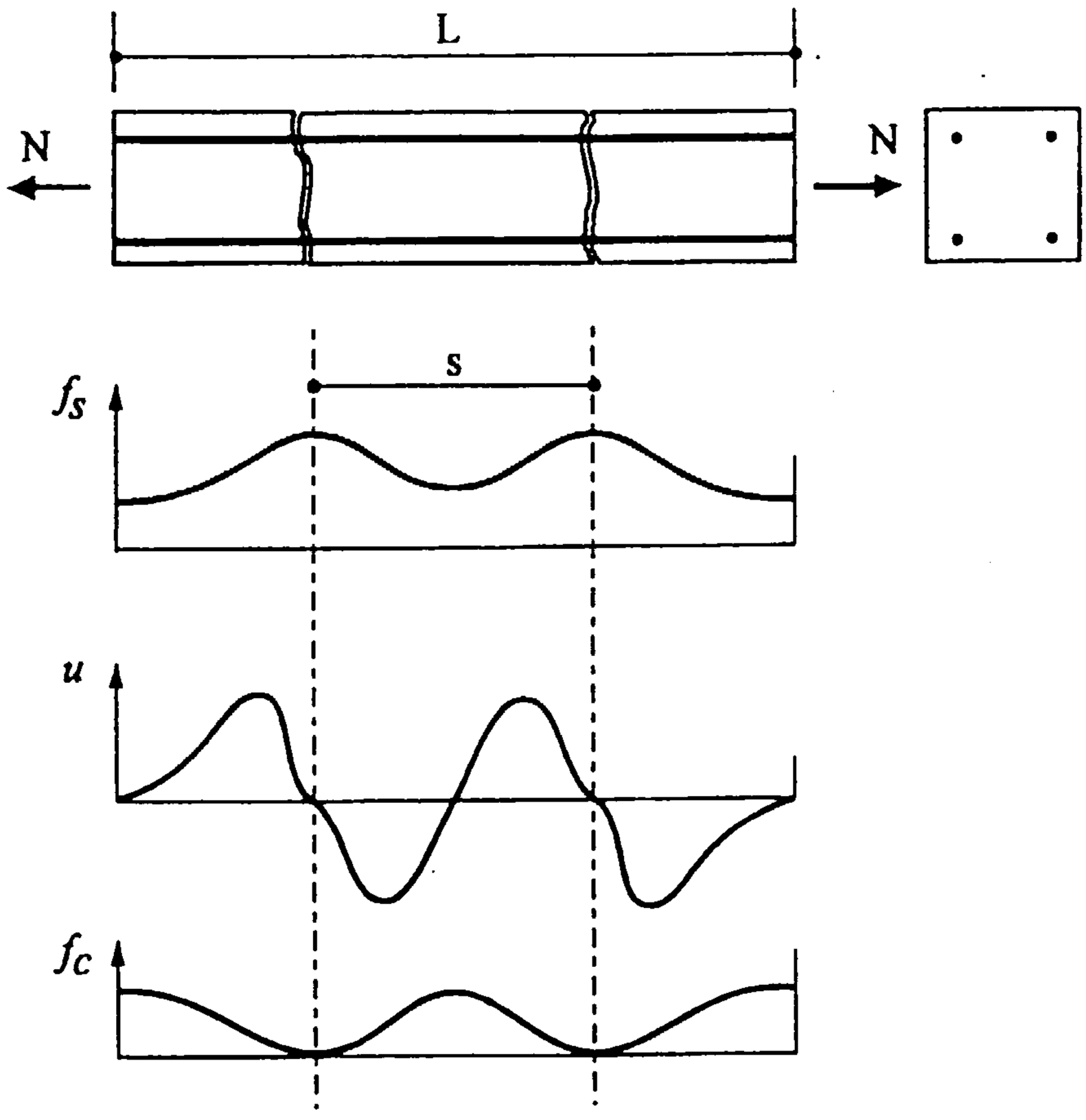

Figure 2.8: Distribution of steel stress, bond stress and concrete stress in tension specimen [Abrishami and Mitchell[93]]

CHAPTER 3

NUMERICAL MODELLING OF THE MATERIAL PROPERTIES

3.1 INTRODUCTION

In order to study the behaviour of reinforced concrete slab elements subjected to any combination of bending and twisting moments and in-plane forces numerically, adequate numerical models of the mechanical properties of concrete, reinforcement and reinforced concrete are essential. This Chapter describes such models.

A new model is proposed to represent the ultimate stress state of concrete under biaxial compression. A new technique which has usually been used in composite laminates is also presented to model tension stiffening.

3.2 MATERIAL MODEL USED IN THE ANALYSIS

Total stress-strain non-linear models based on the theory of elasticity have been used through out the analysis. The total stress-strain models are load path independent and can not be employed to model un-loading, non-monotonic or cyclic loading.

However, the total stress-strain models are reasonably accurate for increasing loads. Since in the present study the work is limited to progressively increasing monotonic loading these models have been adopted.

Perfect bond between the concrete and the reinforcement has been assumed through out the entire loading regime.

3.2.1 MODELLING OF CONCRETE

Concrete is an orthotropic material. The response and the strength of concrete under biaxial stress depends on the nature of the applied stresses. The ultimate strength of concrete can be categorised into three biaxial stress states viz. compression-compression, compression-tension and tension-tension.

3.2.1.1 Response in compression-compression

The response of concrete in compression in principal direction has been modelled by a parabola to the peak stress[1] followed by a linear falling branch. The stress at which concrete was assumed to crush was taken as $0.85\sigma_p$, Figure 3.1. The concrete has been assumed to crush and carry zero stress beyond the crushing strain, ε_{cu}, which corresponds to a stress of $0.85\sigma_p$ on the linear falling branch. The formulations used are

For $\varepsilon_i \leq \varepsilon_{pi}$ (upto peak stress)

$$\sigma_i = \frac{\sigma_{pi}}{\varepsilon_{pi}} \varepsilon_{ei} \left(2 - \frac{\varepsilon_i}{\varepsilon_{pi}}\right) \qquad 3.1a$$

For $\varepsilon_i > \varepsilon_{pi}$ (post peak stress)

$$\sigma_i = \sigma_{pi} - \frac{0.85\,\sigma_{pi}}{\varepsilon_{cu} - \varepsilon_{pi}} (\varepsilon_i - \varepsilon_{pi}) \qquad 3.1b$$

where, σ_i = stress in principal direction i

ε_i = strain in principal direction i

σ_{pi} = peak stress in principal direction i

ε_{pi} = strain corresponding to peak stress in principal direction i

ε_{cu} = crushing strain

In order to determine the stresses for given strains, the peak compressive stress and corresponding strain must be known. It was intended to adopt the simplified failure envelope developed by Tasuji et al[2] later modified by Ganaba[3]. However, numerical problems were encountered and so a new model has been developed. Because this model is based on that of Tasuji et al it is necessary to describe Tasuji et al's model together with the modifications made by Ganaba.

Tasuji et al's[2] model represents the ultimate strength of concrete under different biaxial states of stress based on the assumption that concrete is an orthotropic

material. The relationship, originally developed by Liu[4], used, both in compression and tension to find the principal stresses, σ_1 and σ_2, was

$$\sigma_1 = \frac{\varepsilon_1 E_c}{(1-\nu k)[1+(\frac{1}{1-\nu k}\frac{E_c}{E_s} - 2)(\frac{\varepsilon_1}{\varepsilon_{p1}})+(\frac{\varepsilon_1}{\varepsilon_{p1}})^2]} \qquad 3.2a$$

$$\sigma_2 = \frac{\varepsilon_2 E_c}{(1-\frac{\nu}{k})[1+(\frac{1}{1-\frac{\nu}{k}}\frac{E_c}{E_s} - 2)(\frac{\varepsilon_2}{\varepsilon_{p2}})+(\frac{\varepsilon_2}{\varepsilon_{p2}})^2]} \qquad 3.2b$$

where, σ_1, σ_2 = stress in principal directions 1 and 2

$\varepsilon_1, \varepsilon_2$ = strain in principal directions 1 and 2

E_c = initial tangent modulus

E_s = secant modulus at peak stress = $\frac{\sigma_{p1}}{\varepsilon_{p1}}$ or $\frac{\sigma_{p2}}{\varepsilon_{p2}}$

$\sigma_{p1}, \sigma_{p2}, \varepsilon_{p1}, \varepsilon_{p2}$ = peak stress and corresponding strain in principal directions 1,2

k = stress ratio = $\frac{\sigma_2}{\sigma_1}$, where $\sigma_2 \geq \sigma_1$ algebraically.

ν = Poisson's ratio

The strength envelope proposed by Tasuji et al[2] is shown in Figure 3.2. To determine the peak stresses and corresponding strains in the two principal directions, equations were derived using a least squares fit to experimental data. The equations are given below for the stress ratios, k.

For $0 \leq k \leq 0.2$

$$\sigma_{p1} = f'_c(1+\frac{k}{1.2-k}) \qquad 3.3a$$

For $0.2 \leq k \leq 1.0$

$$\sigma_{p1} = 1.2 f'_c \qquad 3.3b$$

For $0 \leq k \leq 1.0$

$$\sigma_{p2} = k \sigma_{p1} \qquad 3.3c$$

$$\varepsilon_{p1} = 2500 \times 10^{-6} \qquad 3.4a$$

$$\varepsilon_{p2} = (760 + 74.0 \sigma_{p2}) \times 10^{-6} \qquad 3.4b$$

where, σ_{p1}, σ_{p2} = peak stresses in principal direction 1-1 and 2-2 respectively

ε_{p1}, ε_{p1} = strain corresponding to the peak stresses in principal directions 1-1 and 2-2 respectively

Under equal biaxial stresses when k=1, the strains corresponding to the peak stresses should be the same in both principal directions, thus $\varepsilon_{p1} = \varepsilon_{p2}$. On examination of equation 3.4, it can be seen that the strains corresponding to peak stresses can only be the same in both principal directions for concrete of compressive strength of 23.5 MPa. This problem was identified and rectified by Ganaba[3] as discussed in Section 2.4.4, Chapter 2. The strength envelope was not changed but modifications were made to equations for the strains corresponding to the peak stresses. Ganaba also non-

dimensionalised the equation for the peak stresses and corresponding strains. The modified expressions for the strains corresponding to the peak stresses are

For $0 \leq k \leq 1.0$

$$\varepsilon_{p1} = \varepsilon_c \qquad 3.5a$$

where, ε_c is the strain corresponding to the uniaxial compressive strength of concrete.

For $0 \leq k \leq 0.5$

$$\varepsilon_{p2} = \varepsilon_c \left(-0.3040 + 0.9768 \frac{\sigma_{p2}}{f'_c}\right) \qquad 3.5b$$

For $0.5 \leq k \leq 1.0$

$$\varepsilon_{p2} = \varepsilon_c \left(-0.4385 + 1.1985 \frac{\sigma_{p2}}{f'_c}\right) \qquad 3.5c$$

where, f'_c is the uniaxial compressive strength of concrete.

3.2.1.1.1 Deficiencies in the Model

Two deficiencies were identified in the model proposed by Tasuji et al[2] and Ganaba[3] which were the cause of the numerical problems encountered. The deficiencies were

(i) the stress-strain curve defined by equation 3.2 stiffens up in the minor principal stress direction. The stiffening up the curve increases with the decrease in the stress ratio;

(ii) the strain becomes tensile for a stress ratio less than the Poisson's ratio.

Figure 3.3 shows the stress-strain curves for Ganaba's model[3] using equation 3.2 and the stress-strains curves for the proposed model using equation 3.1, which is presented later in Section 3.2.1.1.2, in the minor principal stress direction. The deficiency of stiffening up of the curve in the minor direction is evident from Figure 3.3. For any stress ratio, 1/k, the curve representing Ganaba's model have a lesser slope initially but the curve stiffens up as the strain increases. The stiffening up of the curve is associated with the type of the function used to define the stress-strain curve. The function used was

$$\sigma_i = \frac{A + B\varepsilon E}{(1 - \nu k)(1 + C\varepsilon + D\varepsilon^2)} \qquad 3.6$$

constants A, B, C and D were obtained using the following boundary conditions.

$$\sigma = 0 \qquad \text{at } \varepsilon = 0 \qquad 3.7a$$

$$\frac{d\sigma}{d\varepsilon} = \frac{E_c}{1 - \nu k} \quad \text{at } \varepsilon = 0 \qquad 3.7b$$

$$\sigma = \sigma_{pi} \qquad \text{at } \varepsilon = \varepsilon_{pi} \tag{3.7c}$$

$$\frac{d\sigma}{d\varepsilon} = 0 \qquad \text{at } \varepsilon = \varepsilon_{pi} \tag{3.7d}$$

By substituting the values of the constants A, B, C and D in equation 3.6, the final form of equation 3.2 was obtained. Due to the type of the basic function, the slope of equation decreases with the increase in strain, but it increases to a certain value of strain and then starts to reduce, Figure 3.4. It can be seen from Figure 3.4 that as the stress ratio, 1/k, increases the slope becomes flatter. Hence lesser the value of 1/k, more stiffening of the curve.

The second deficiency i.e. the change of strain corresponding to peak stress from being compressive to tensile for stress ratio greater than Poisson's ratio is due to the empirical nature of equation 3.5b. If the value of σ_{p2} in equation 3.5b is replaced by $1.2 f'_c k$ by using equations 3.3c and 3.3b, it can be seen that for any stress ratio less than 0.259 the strain corresponding to the peak stress will be tensile, whereas the Poisson's ratio of concrete varies from 0.15 to 0.22[5]. For a tensile strain and compressive stress if 1/k is greater than Poisson's ratio equation 3.2 becomes invalid as it adopts an unrealistic shape, Figure 3.5 and hence cannot be used to define the stress-strain response of concrete.

The deficiencies discussed above lead to the development of a new model for the ultimate stress state in biaxial stress state.

3.2.1.1.2 Model for compression-compression

The model developed to determine the ultimate stresses for biaxial compression stress state is a non-linear isotropic elastic model. Modified strains, to take into account the Poisson's ratio effect at any stress level, as proposed by Cope[5] are used. The Poisson's ratio was assumed to be constant through out an analysis for the compression-compression stress state. The modified strains are given by

$$\begin{Bmatrix} \varepsilon_{e1} \\ \varepsilon_{e2} \end{Bmatrix} = \frac{1}{1-\nu^2} \begin{bmatrix} 1 & \nu \\ \nu & 1 \end{bmatrix} \begin{Bmatrix} \varepsilon_1 \\ \varepsilon_2 \end{Bmatrix} \qquad 3.8$$

where, ε_{e1} and ε_{e2} are the modified elastic strains which account for the Poisson's ratio effect and ε_1 and ε_2 are the real strains in principal directions 1-1 and 2-2 respectively.

The strength envelope proposed by Tasuji et al[2] has been used but the strains corresponding to peak stresses have been changed. The expressions for the strains corresponding to the peak stresses has been obtained by rearranging equation 3.8.

$$\begin{Bmatrix} \varepsilon_{p1} \\ \varepsilon_{p2} \end{Bmatrix} = \begin{bmatrix} 1 & -\nu \\ -\nu & 1 \end{bmatrix} \begin{Bmatrix} \varepsilon_{ep1} \\ k\varepsilon_{ep1} \end{Bmatrix} \qquad 3.9$$

where ε_{p1} and ε_{p2} are the real measured strains corresponding to peak stresses in principal directions 1-1 and 2-2 respectively for any stress ratio k and ε_{ep1} is the modified strain corresponding to peak stress in principal direction 1-1. Since the

model is based on the theory of elasticity the peak stress and the corresponding strain in the minor principal direction will be proportional to the peak stress and corresponding strain in the major principal direction, Figure 3.6. The above expression yields a relationship between the modified and the real measured strains corresponding to peak stresses.

$$\varepsilon_{ep1} = \frac{\varepsilon_{p1}}{1 - \nu k} \qquad 3.10$$

since, $$\varepsilon_{ep2} = k\,\varepsilon_{ep1} \qquad 3.11$$

where, ε_{ep2} is the modified strain corresponding to the peak stress in principal direction 2-2.

Substituting the value of ε_{ep1} from equation 3.10 into equation 3.11 to obtain,

$$\varepsilon_{ep2} = \frac{k\varepsilon_{p1}}{(1 - \nu k)} \qquad 3.12$$

Letting,

$$c = \frac{\sigma_{p1}}{f'_c} \qquad 3.13$$

where f'_c is the uniaxial compressive strength of concrete. The peak stress in principal direction 1-1, equation 3.1, will be,

$$\sigma_{p1} = c f'_c = E_s \varepsilon_{ep1} \left(2 - \frac{\varepsilon_{ep1}}{\varepsilon_{ep1}}\right) = E_s \varepsilon_{ep1} \qquad 3.14$$

where E_s = secant modulus at peak stress = $\dfrac{f'_c}{\varepsilon_p}$

ε_p = strain corresponding to the uniaxial compressive strength of concrete

or,
$$\frac{\varepsilon_{ep1}}{c} = \frac{f'_c}{E_s} \qquad 3.15$$

Substituting the value of E_s into equation 3.15 and simplifying to obtain the expression for strain corresponding to the peak stress in the principal direction 1-1.

$$\varepsilon_{ep1} = c\, \varepsilon_p \qquad 3.16$$

Using equation 3.11, the modified strain corresponding to peak stress in principal direction 2-2 will then be,

$$\varepsilon_{ep2} = k\, c\, \varepsilon_p \qquad 3.17$$

Equations 3.16 and 3.17 are the expressions representing the strains corresponding to the peak stresses in the major and the minor principal stress direction. Figure 3.7 shows the comparison between the experimental strains corresponding to the peak stresses[6] with the developed model, equation 3.16 and 3.17, and the model by Ganaba[3], equation 3.5.

The expression for c varies with the stress ratio, k. The expressions for the peak stresses and corresponding strains are summarised as follows for the various stress ratios,

For $0 \leq k \leq 0.2$

$$\sigma_{p1} = (1 + \frac{k}{1.2 - k}) f'_c \qquad 3.18a$$

$$\varepsilon_{cp1} = c\, \varepsilon_p = (1 + \frac{k}{1.2 - k}) \varepsilon_p \qquad 3.19a$$

For $0.2 \leq k \leq 1.0$

$$\sigma_{p1} = 1.2\, f'_c \qquad 3.18b$$

$$\varepsilon_{cp1} = 1.2\, \varepsilon_p \qquad 3.19b$$

For $0 \leq k \leq 1.0$

$$\sigma_{p2} = k\sigma_{p1} \qquad 3.18c$$

$$\varepsilon_{cp2} = k\, c\, \varepsilon_p \qquad 3.19c$$

The predication of the proposed model have been compared with the experimental results of Tasuji[6] and Kupfer et al[7]. Kupfer et al tested concrete under uniaxial compression, equal biaxial compression and a stress ratio of 0.52. Tasuji conducted experiments when the stress ratios were 0, 0.2, 0.5 and 1. The comparisons between the experimental results and the results obtained from the model were found to be good and are shown in Figures 3.8 to 3.14.

3.2.1.2 Response in compression-tension

It has been established that the compressive strength and stiffness of concrete is affected significantly by tensile strain orthogonal to the principal compressive stress direction[8,9,10].

On the basis of discussion provided in Section 2.4.5.2, the compressive response of concrete under compression-tension stress state has been modelled using Model A proposed by Vecchio and Collins[10]. The model consists of three distinct stages, an ascending parabolic branch, a constant stress region and a linear falling branch, Figure 3.15. Equation 3.1a has been used to predict the ascending part of the compressive response to ensure compatibility with the compression-compression stress state.

Model A is based on a statistical analysis of the data. The softening has been incorporated through a softening factor, β, which is given by

$$\beta = \frac{1}{1 + K_c K_f} \qquad 3.20$$

where

$$K_c = 0.35 \left(- \frac{\varepsilon_1}{\varepsilon_2} - 0.28 \right)^{0.8} \geq 1.0, \quad \varepsilon_1 \leq \varepsilon_y \qquad 3.21$$

$$K_f = 0.1825 \sqrt{f'c} \geq 1.0 \qquad 3.22$$

where $\varepsilon_1, \varepsilon_2, \varepsilon_y$ are the principal tensile strain, the principal compressive strain and the yield strain of the reinforcement in tension respectively. The softening factor, β, is applied to both the uniaxial compressive strength and the corresponding strain to obtain the softened response.

For the falling branch equation 3.1b is used. The maximum stress and corresponding strain of concrete in compression when in a state of compression-tension are summarised below.

For region I, $(\varepsilon_1 \leq \beta \varepsilon_p)$

$$\sigma_{p1} = \beta f'_c \qquad 3.23a$$

$$\varepsilon_{p1} = \beta \varepsilon_o \qquad 3.24b$$

For region II, $(\varepsilon_p \leq \varepsilon_1 \leq \varepsilon_p)$

$$\sigma_{p1} = \beta f'_c \qquad 3.23b$$

$$\varepsilon_{p1} = \beta \varepsilon_o \text{ to } \varepsilon_o \qquad 3.24b$$

For region III, $(\varepsilon_p \geq \varepsilon_1 \geq \varepsilon_{cu})$

$$\sigma_{p1} = \beta f'_c \qquad 3.23c$$

$$\varepsilon_{p1} = \varepsilon_o \text{ to } \varepsilon_{cu} \qquad 3.24c$$

The tensile response of concrete under compression-tension stress state has been modelled as a linear elastic material prior to cracking as expressed below. This approach has been generally adopted to model pre-cracked tensile response of concrete[8,11,12].

$$\sigma_2 = E_c \varepsilon_2 \qquad 3.25a$$

After cracking occurs the response has been modelled by a linear descending branch which ends at the yielding of the reinforcement[8], $\xi \varepsilon_t$. The strain at which tension

stiffening ends has been defined in terms of the cracking strain, ε_t. The post cracking response is usually termed as tension stiffening and plays a significant role in the overall response of reinforced concrete. This effect becomes evident after cracking and it influences the response prior to the yielding of reinforcement. Researchers have adopted several concepts to model this property of concrete[13,14,15,16,17,18]. The governing equation used in this study to model tension stiffening is given below.

$$\sigma_2 = \alpha\,[\sigma_{p2} - \frac{\sigma_{p2}}{(\xi-1)\varepsilon_{cp2}}]\,(\varepsilon_{c2} - \varepsilon_{cp2}) \qquad 3.25b$$

where α is a factor defining the discontinuity between the pre and post cracking response. For $\alpha = 1$ there is no discontinuity and for $\alpha = 0$ there is no tension stiffening.

The tensile response has been modelled using two different approaches. The first approach has been adopted from the modelling of tensile response in composite laminates[19]. The second approach, however, is the more usual way of modelling tensile response for reinforced concrete in which there is a discontinuity between the pre-cracking and the post cracking response. The discontinuity can be modelled using the factor α.

In the first approach the tension zone was divided into two regions, Figure 3.16a. The first region was the concrete around the reinforcement. It was assumed that due to the bond between concrete and steel, the concrete would contribute in tension both prior to and after cracking. In this region the tensile response was given by equations 3.25a

and 3.25b with $\alpha = 1$, Figure 3.16b. The remaining concrete was the second region in which it was assumed that, after cracking, the stress in the concrete will be zero, hence only the ascending part, equation 3.25a, was used, Figure 3.16c.

The thickness of the first zone, the concrete around the reinforcement, depends on the bond properties, spacing of the reinforcement, diameter of the reinforcement and thickness of the section[19,20,21].

The tensile response of concrete in the second approach has been modelled assuming that the entire tension zone contribute towards the post cracking response. The level of discontinuity defined by α was varied between 0.4 and 1 depending on the thickness of the element, spacing of the reinforcement and diameter of the reinforcement, Figure 3.17.

In order to determine the cracking stress and strain the model proposed by Tasuji et al[2] has been used. The expressions used are

$$\sigma_{p2} = f'_c\left(1 + \frac{k}{1+ks}\right) \qquad 3.26$$

where, $s = f'_c / f_t$ = ratio of the uniaxial compressive strength to uniaxial tensile strength.

$$\varepsilon_{cp2} = \frac{\sigma_{p2}}{E_c} \qquad 3.27$$

After cracking Poisson's ratio was assumed to be zero.

3.2.1.3 Response in tension-tension

Under biaxial tension the principal stresses have little effect on each other and thus the ultimate stress state can be modelled by a square failure surface[2]. The cracking strain will, however, be different from the uniaxial cracking strain due to the Poisson's ratio effect, hence the cracking strains have been modified to account for this effect using equation 3.8. The expressions for ultimate biaxial tension stress state are

$$\sigma_{p1} = \sigma_{p2} = f_t \qquad 3.28$$

$$\varepsilon_{ep1} = \varepsilon_{ep2} = \frac{f_t}{E_c} \qquad 3.29$$

The response of concrete in biaxial tensile stress state has been modelled using the same approaches as for the tensile response in compression-tension stress state. The Poisson's ratio has been assumed to be zero after cracking.

3.2.2 MODELLING OF THE REINFORCEMENT

The reinforcement has been assumed to be elastic up to yielding and then perfectly plastic up to infinity both in compression and tension, Figure 3.18. The reinforcement

has been assumed to carry axial stresses only. In case of unloading, the reinforced has been assumed to follow the same path as that for loading. This is a deficiency in the reinforcement model. The post ultimate response of under reinforced elements may not be reliable as an stiff response will be predicted. However, the post ultimate response of the over reinforced elements will not be affected as the reinforcement remains elastic and the loading and unloading paths will be the same.

3.3 PROCEDURE ADOPTED TO DETERMINE STRESSES

Six material properties for concrete are required in order to construct the stress-strain relationship. These six properties are the uniaxial compressive strength, f'_c, the corresponding strain, ε_o, Poisson's ratio, ν, the uniaxial tensile strength, f_t, the corresponding cracking strain, ε_t, and the crushing strain, ε_{cu}. All six material properties of concrete can be determined experimentally. The procedure adopted for the evaluation of the stresses in the concrete at any particular load increment is summarised as follows.

1. The principal strains, ε_i, and the angle between the Cartesian and the principal directions, θ, are determined from

$$\varepsilon_{1,2} = \frac{\varepsilon_x + \varepsilon_y}{2} \pm \sqrt{\left(\frac{\varepsilon_x - \varepsilon_y}{2}\right)^2 + \left(\frac{\gamma_{xy}}{2}\right)^2} \qquad 3.30$$

and $$\theta=\frac{1}{2}\tan^{-1}\left(\frac{\gamma_{xy}}{\varepsilon_x-\varepsilon_y}\right) \qquad 3.31$$

2. An initial estimate for the stress ratio, k_{ini}, for the first load increment is made by using the linear elastic relationship between the principal stress and strain.

$$k_{ini}=\frac{\sigma_2}{\sigma_1}=\frac{\varepsilon_2+\nu\varepsilon_1}{\varepsilon_1+\nu\varepsilon_2} \qquad 3.32$$

For subsequent load increments a value of stress ratio, k, from previously converged load increment is used.

3. The modified strains are determined, equation 3.8.

4. For the given stress ratio, the peak stresses, σ_{pi}, and the corresponding modified strains, ε_{epi}, are calculated using equations 3.18 and 3.19 or 3.23 and 3.24 or 3.28 and 3.29.

5. The principal stresses, σ_i, are determined using equations 3.1 and 3.25.

6. The stress ratio, k, is recalculated using the principal stresses.

7. Steps 4-6 are repeated to until the stress ratio, k, becomes acceptably small (1% difference between two successive iterations).

8. The principal stresses are then resolved into the Cartesian direction using the following relationship.

$$\begin{Bmatrix}\sigma_x\\ \sigma_y\\ \tau_{xy}\end{Bmatrix}=\begin{bmatrix}\cos^2\theta & \sin^2\theta & 2\sin\theta\cos\theta\\ \sin^2\theta & \cos^2\theta & -2\sin\theta\cos\theta\\ -\sin\theta\cos\theta & \sin\theta\cos\theta & \cos^2\theta-\sin^2\theta\end{bmatrix}\begin{Bmatrix}\varepsilon_1\\ \varepsilon_2\\ 0\end{Bmatrix} \qquad 3.33$$

In order to determine the stress in the reinforcement, the Cartesian strains at the level of the reinforcement, $\varepsilon_{rx},\varepsilon_{ry}$, are first determined. The stress in the reinforcement is then determined using the following expressions.

Stress prior to yielding:

$$\sigma_{rx}=E\varepsilon_{rx} \qquad 3.34a$$

$$\sigma_{ry}=E\varepsilon_{ry} \qquad 3.35a$$

Stress after yielding:

$$\sigma_{rx}=E\varepsilon_{y} \qquad 3.34b$$

$$\sigma_{ry}=E\varepsilon_{y} \qquad 3.35b$$

where, σ_{rx},σ_{ry} = stress in the reinforcement in x and y direction respectively

$\varepsilon_{rx},\varepsilon_{ry}$ = strain at the level of the reinforcement in x and y direction

respectively

ε_y = yield strain of the reinforcement

E = modulus of elasticity of the reinforcement.

References

1 Hognestad, E, Hanson, NW and McHenry, D, Concrete stress distribution in ultimate strength design, Jnl. of ACI, vol. 52, no. 6, December 1955, pp 445-479.

2 Tasuji, EM, Nilson, AH and Slate, FO, Biaxial stress-strain relationship for concrete, Magazine of Concrete Research, vol. 31, no. 109, December 1979, pp 217-224.

3 Ganaba, TH, Nonlinear finite element analysis of plates and slabs, PhD Thesis, University of Warwick, August 1985, pp 77-81.

4 Liu, TCY, Nilson, AH and Slate, FO, Biaxial stress-strain relationship for concrete, Proceedings ASCE, vol. 98, ST5, May 1972, pp 1025-1034.

5 Cope, RJ, Computational Modelling of Reinforced Concrete Structure (Chapter 1), edited by Hinton, E and Owen, R, Pineridge Press, 1986, pp 3-43.

6 Tasuji, ME, The behavior of plain concrete subjected to biaxial stress, Research Report No. 360, Department of Civil Engineering, Cornell University, New York, March 1976, 171 p.

7 Kupfer, H, Hilsdorf, HK and Rusch, H, Behavior of concrete under biaxial stresses, Jnl. of ACI, Proceedings, vol. 66, no. 8, August 1969, pp 656-666.

8 Vecchio F, and Collins MP, The response of reinforced concrete panels to in-plane shear and normal stress, Publication No. 82-03, Department of Civil Eng. University of Toronto, Canada, March 1982, 332 p.

9 Pang, XBD and Hsu, TTC, Behavior of reinforced concrete membrane elements in shear, ACI St. Jnl., vol. 92, no. 6, Nov-Dec. 1995, pp 665-679.

10 Vecchio, FJ, and Collins, MP, Compression response of cracked reinforced concrete, Jnl. of St. Eng., ASCE, vol. 119, no. 12, December 1993, pp 3590-3610.

11 Wu, Z, Yoshikawa, H and Tanabe, T, Tension stiffness model for cracked concrete, Jnl. of St. Eng., ASCE, vol. 117, no. 3, March 1991, pp 715-732.

12 Choi, CK and Cheung, SH, Tension stiffening model for planar reinforced concrete members, Computers and Structures, vol. 59, no. 1, January 1996, pp 179-190.

13 Clark, LA and Speirs, DM, Tension stiffening of reinforced concrete beams under short term load, Technical Report No. 42.521, Cement and Concrete Association, London, July 1978.

14 Gilbert, RI and Warner, RF, Tension stiffening in reinforced concrete slabs, Jnl. of St. Div., ASCE , Proceedings, vol. 4, ST12, December 1978, pp 1885-1900.

15 Cerreira, DJ and Chu, KH, Stress-strain relationship for concrete in tension, Jnl. of ACI, Proceeding, vol. 83, Jan-Feb. 1986, pp 21-28.

16 Oduymi, TOS and Clark, LA, Tension stiffening in longitudinal sections of circular voided concrete slabs, Proceedings of Institution of Civil Engineers, Part 2, no. 83, December 1987, pp 861-874.

17 Link, RA, Elwi, AE and Scanlon, A, Biaxial tension stiffening due to generally oriented reinforcing layers, Jnl. of Eng. Mech., vol. 115, no. 8, August 1989, pp 1647-1662.

18 Hsu, TTC and Zhang, LX, Tension stiffening in reinforced concrete membrane elements, ACI St. Jnl., vol. 93, no. 1, Jan-Feb. 1996, pp 108-115.

19 Pitt, DC, Composite laminate modelling of reinforced concrete elements, M.Sc. Thesis, Heriot-Watt University/ Ecole Polytechnique Federale De Lausanne, September 1995, 77 p.

20 Clark, LA and Cranston, WB, The influence of spacing on tension stiffening in reinforced concrete slabs, Advances in Concrete Slab Technology, Proceeding of the International Conference on Concrete Slabs, Dundee, April 1979, pp 118-128.

21 Prakhya, GKV, Two-zone model for reinforced concrete elements, Proceeding, Conference on Continuum Mechanics and its Applications, Vancouver, June 1988, pp 257-266.

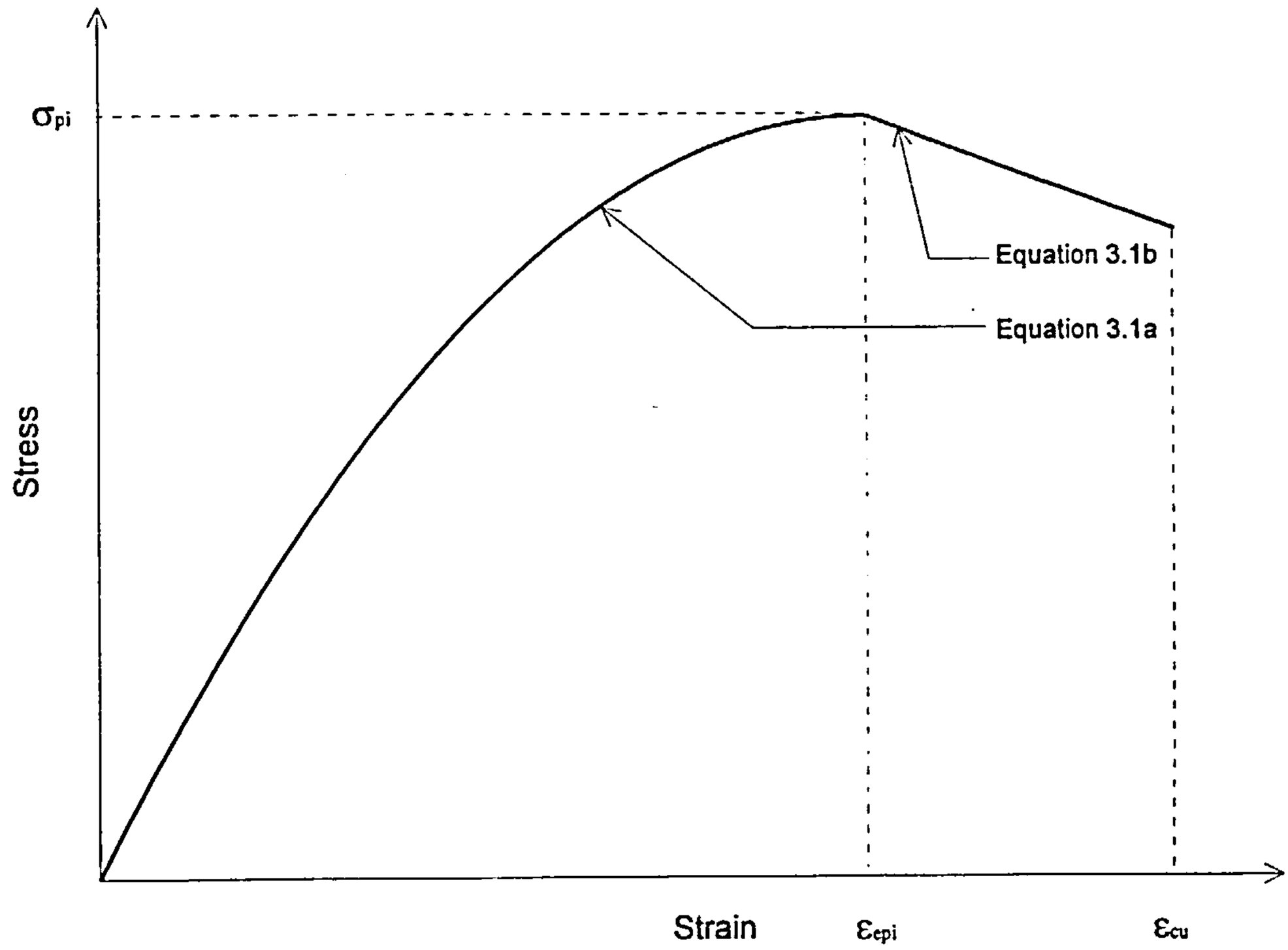

Figure 3.1: Stress-strain response of concrete in compression

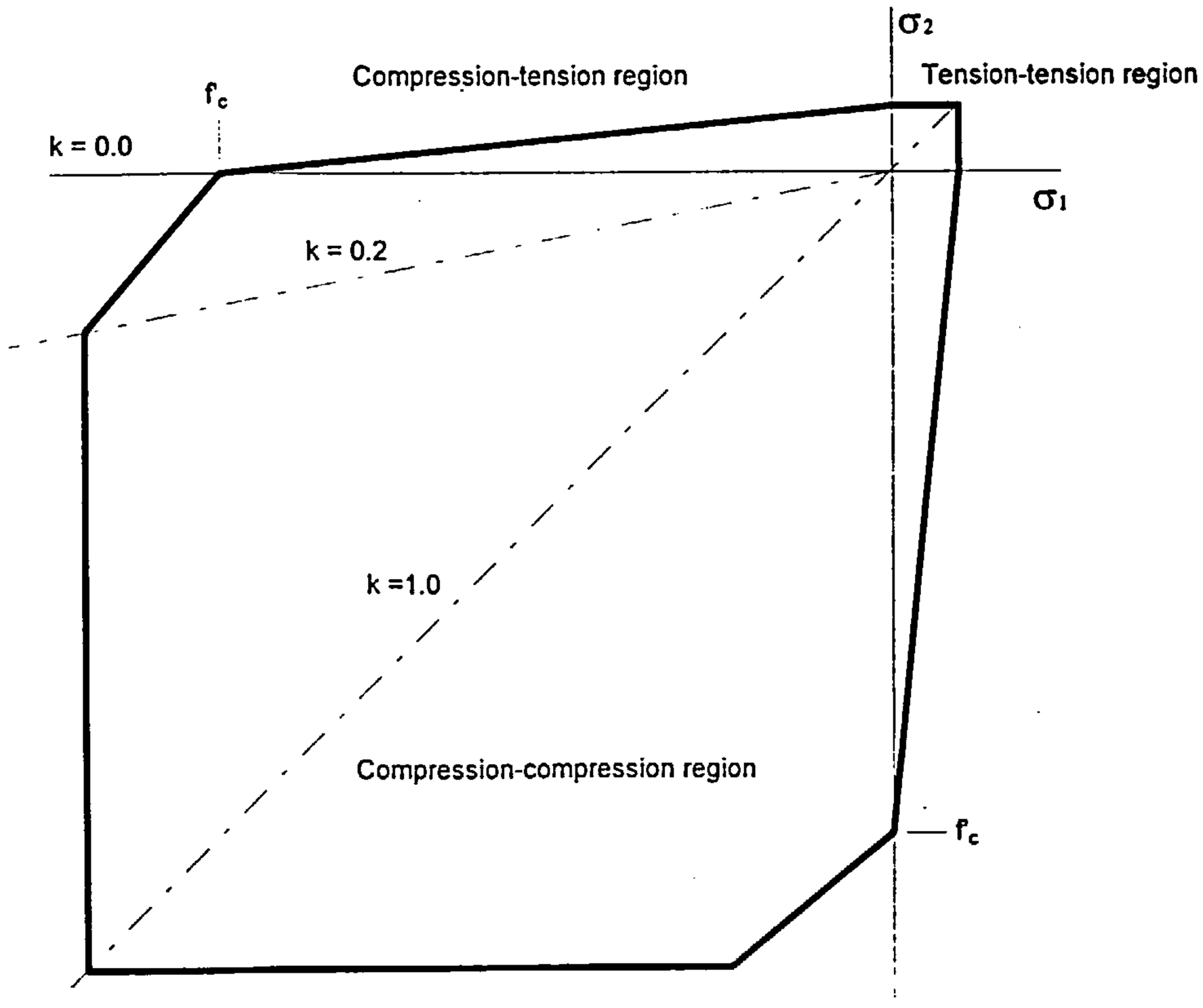

Figure 3.2: Biaxial strength envelope used in the present study

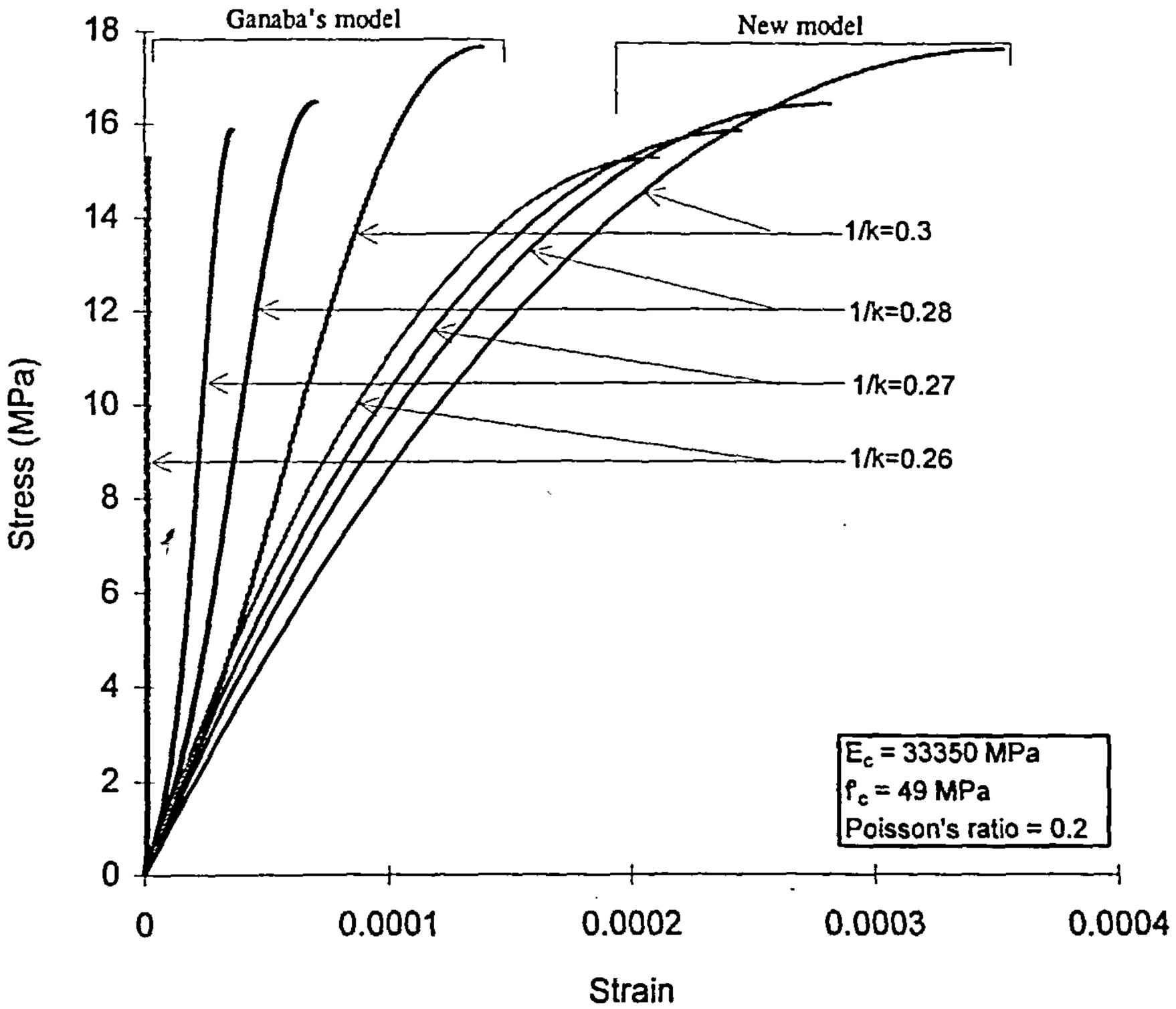

Figure 3.3: Stress-strain response of concrete in minor principal direction using Ganaba's[3] model with equation 3.2 and new model

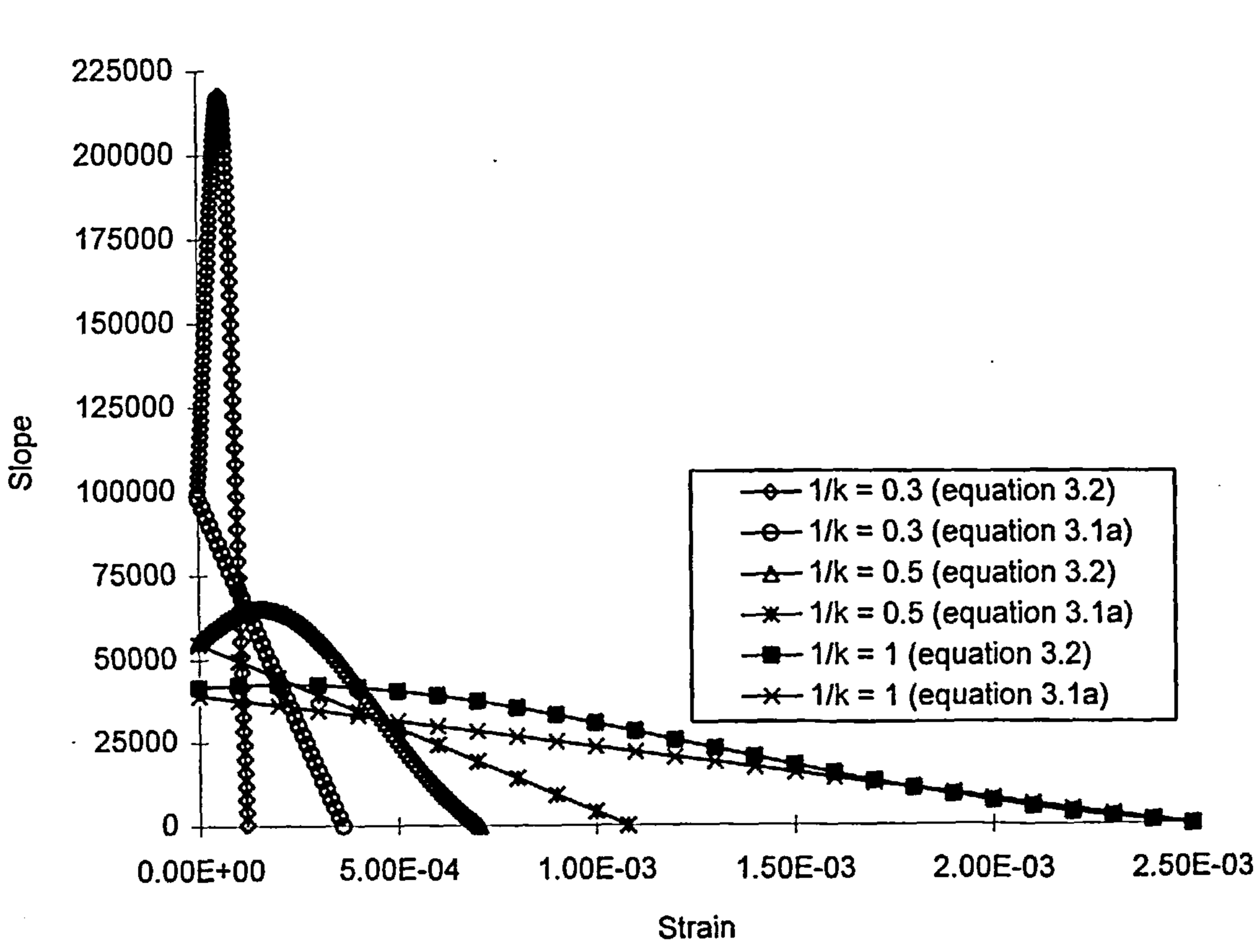

Figure 3.4: Variation of slopes of equation 3.1a and 3.2 in the minor principal stress direction

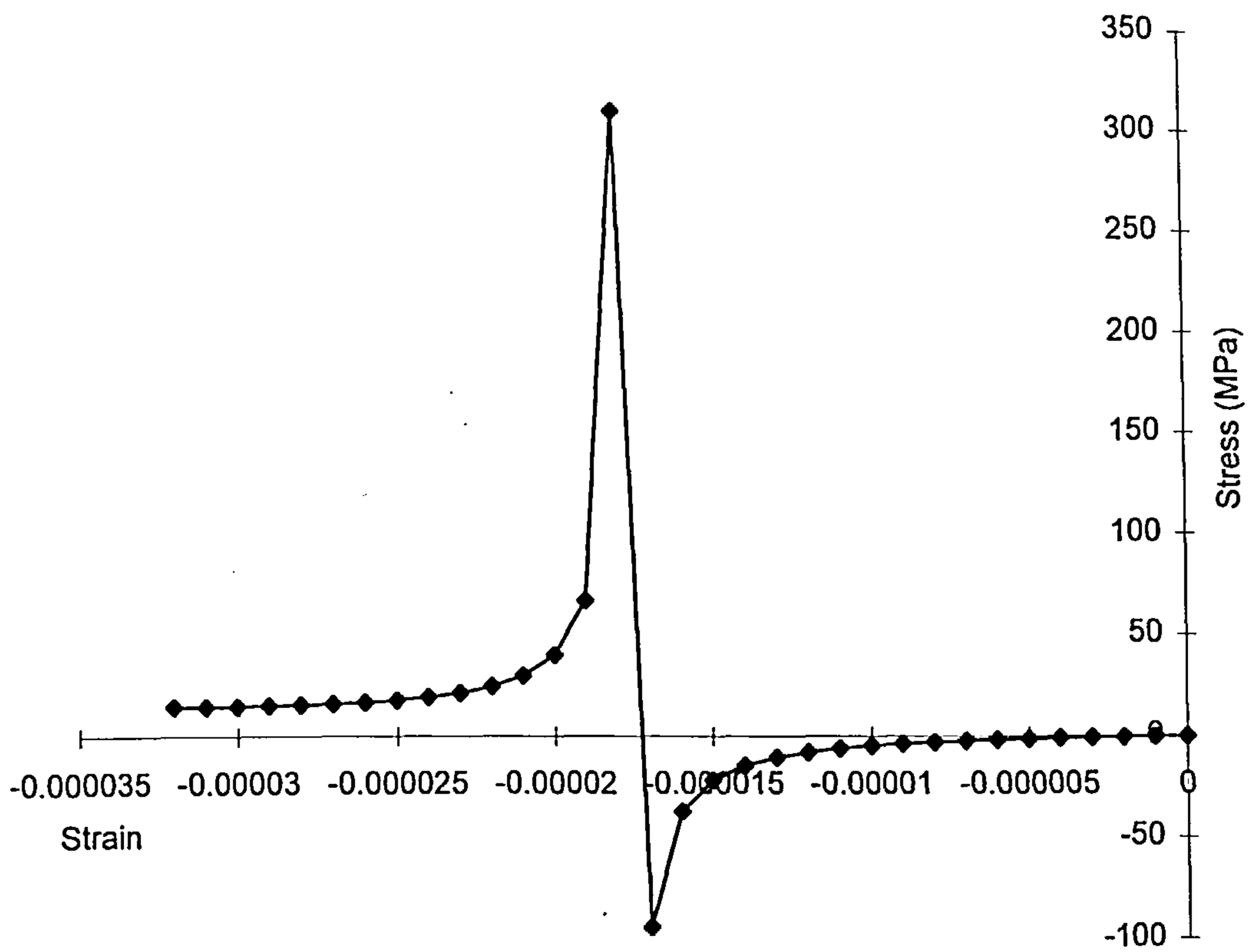

Figure 3.5 Stress strain response in the minor stress direction for 1/k = 0.25 using Ganaba's[3] model and equation 3.2

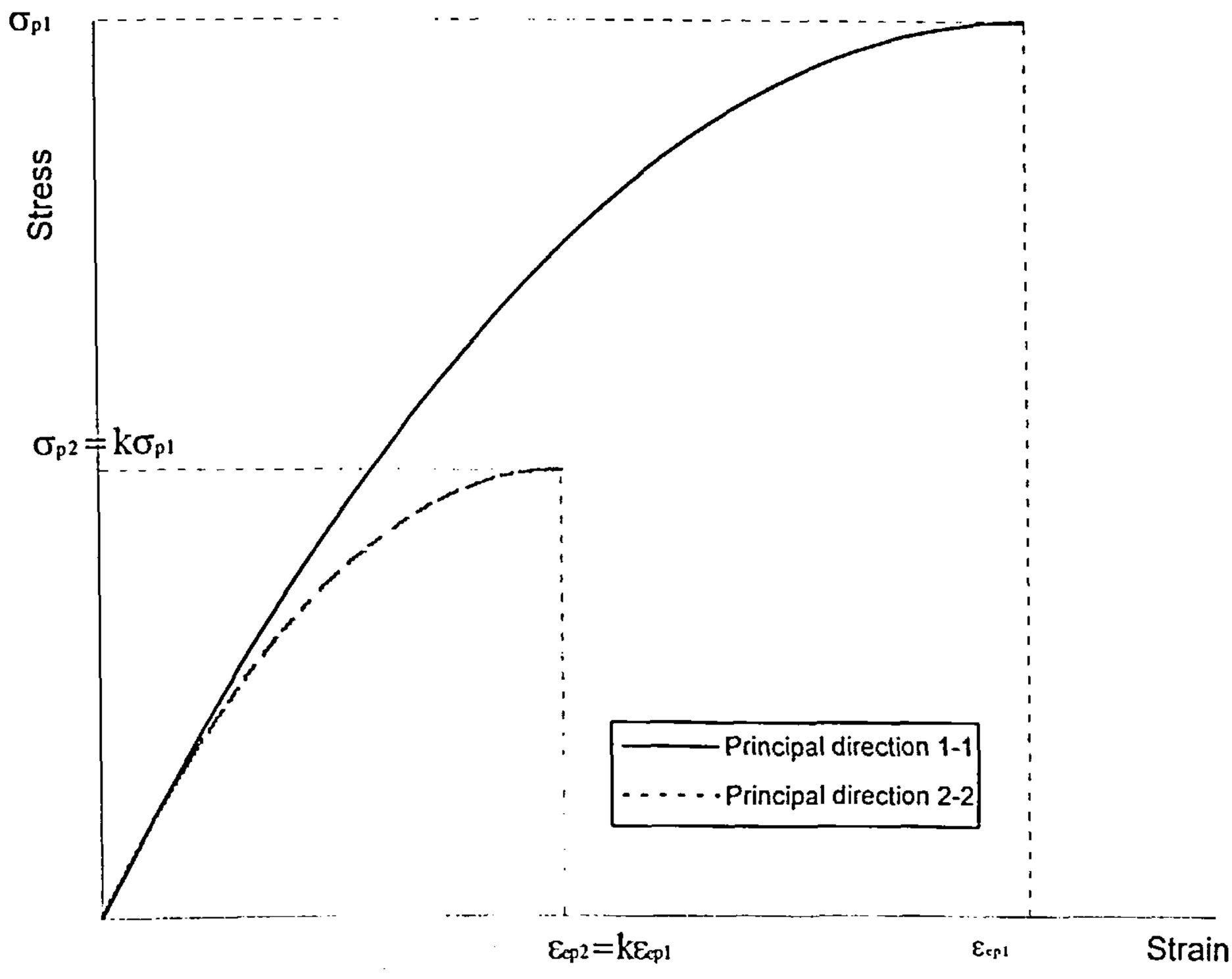

Figure 3.6: The peak compressive stresses and corresponding strains in both the principal directions are proportional to each other

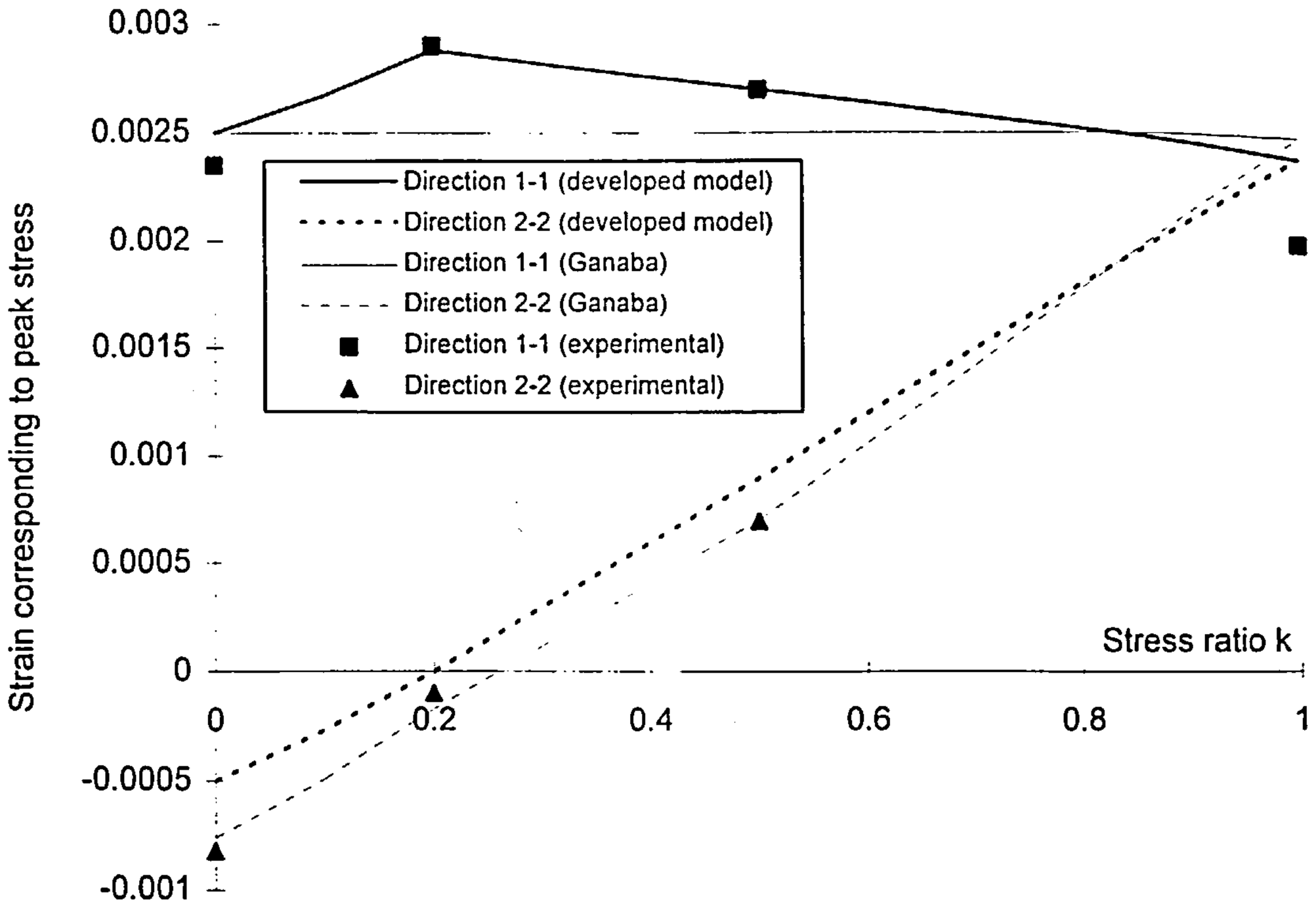

Figure 3.7: Comparison of strains corresponding to peak stresses with the experimental[6] data and Ganaba's[3] model

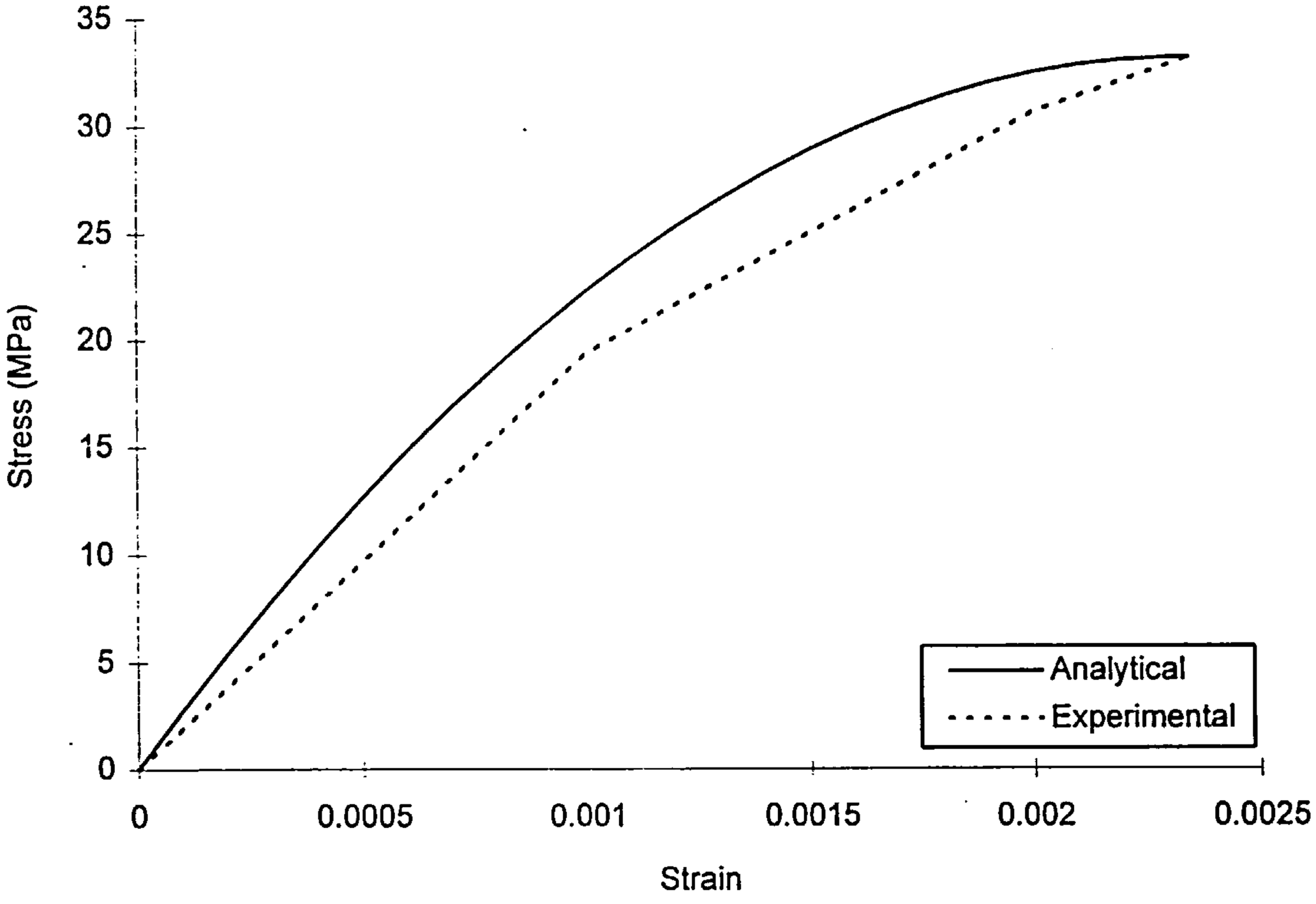

Figure 3.8: Comparison of stress-strain relationship with the experimental data[6] (k=0)

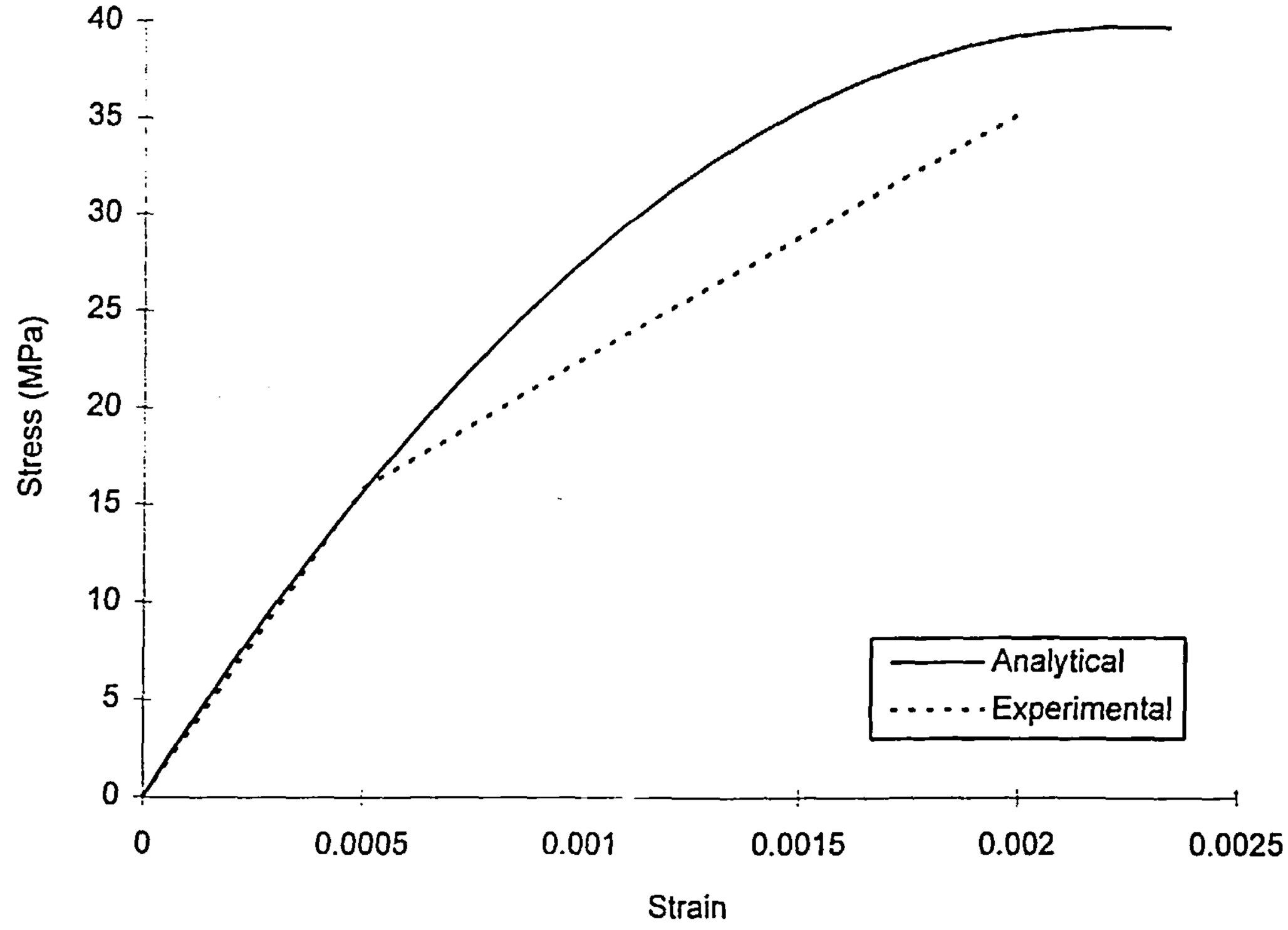

Figure 3.9: Comparison of stress-strain relationship with the experimental data[6] (k=1)

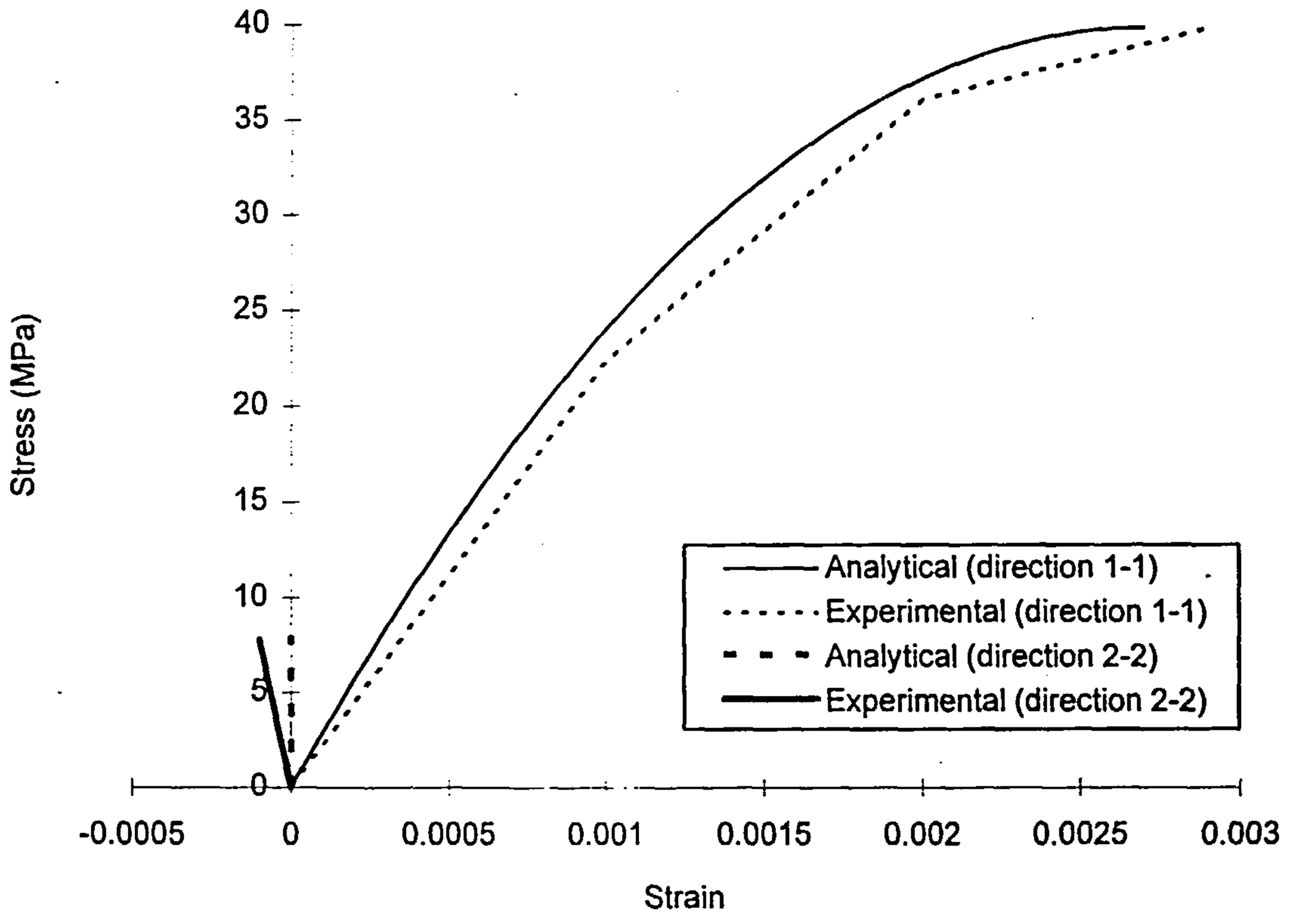

Figure 3.10: Comparison of stress-strain relationship with the experimental data[6] (k=0.2)

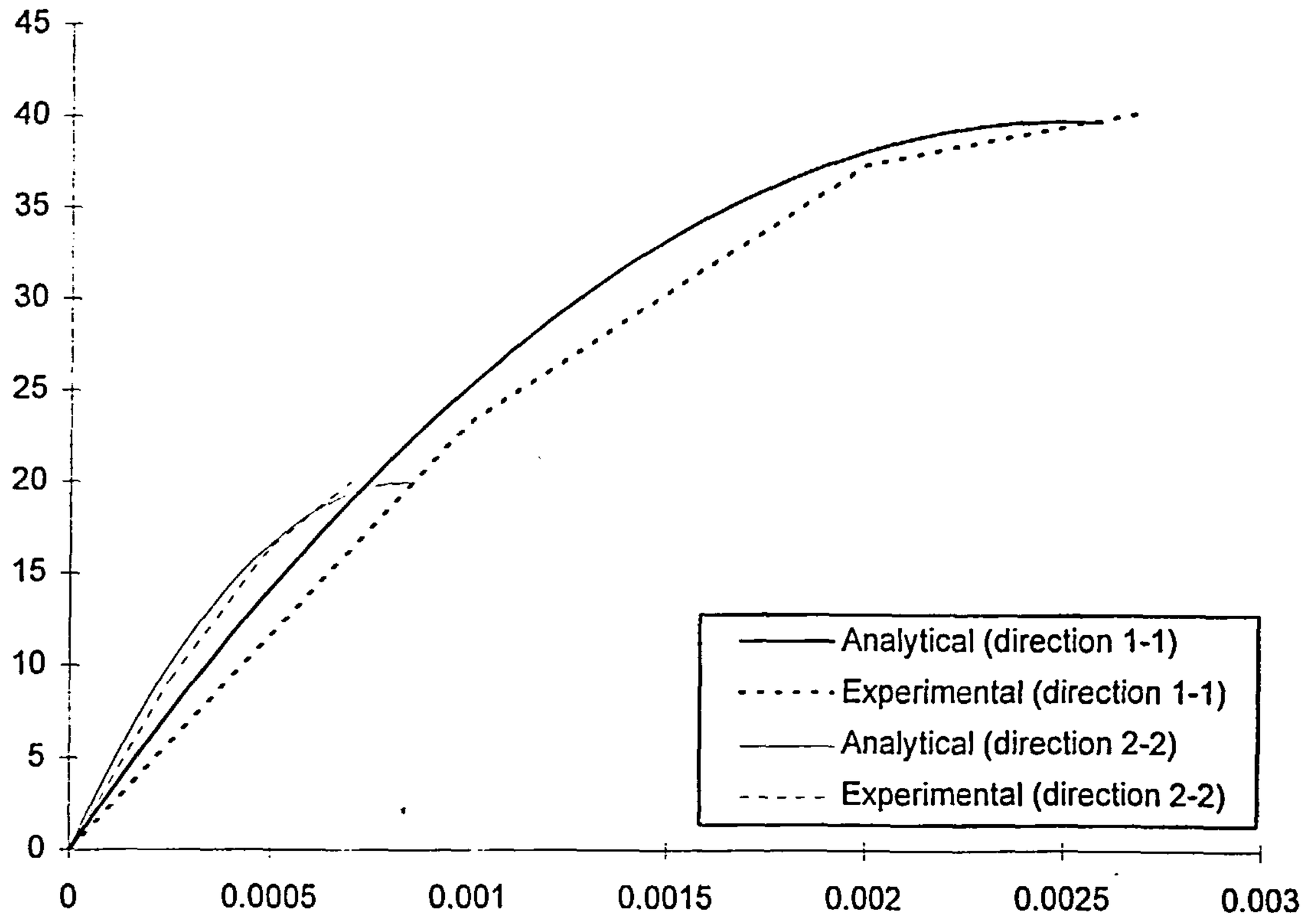

Figure 3.11: Comparison of stress-strain relationship with the experimental data[6] (k=0.5)

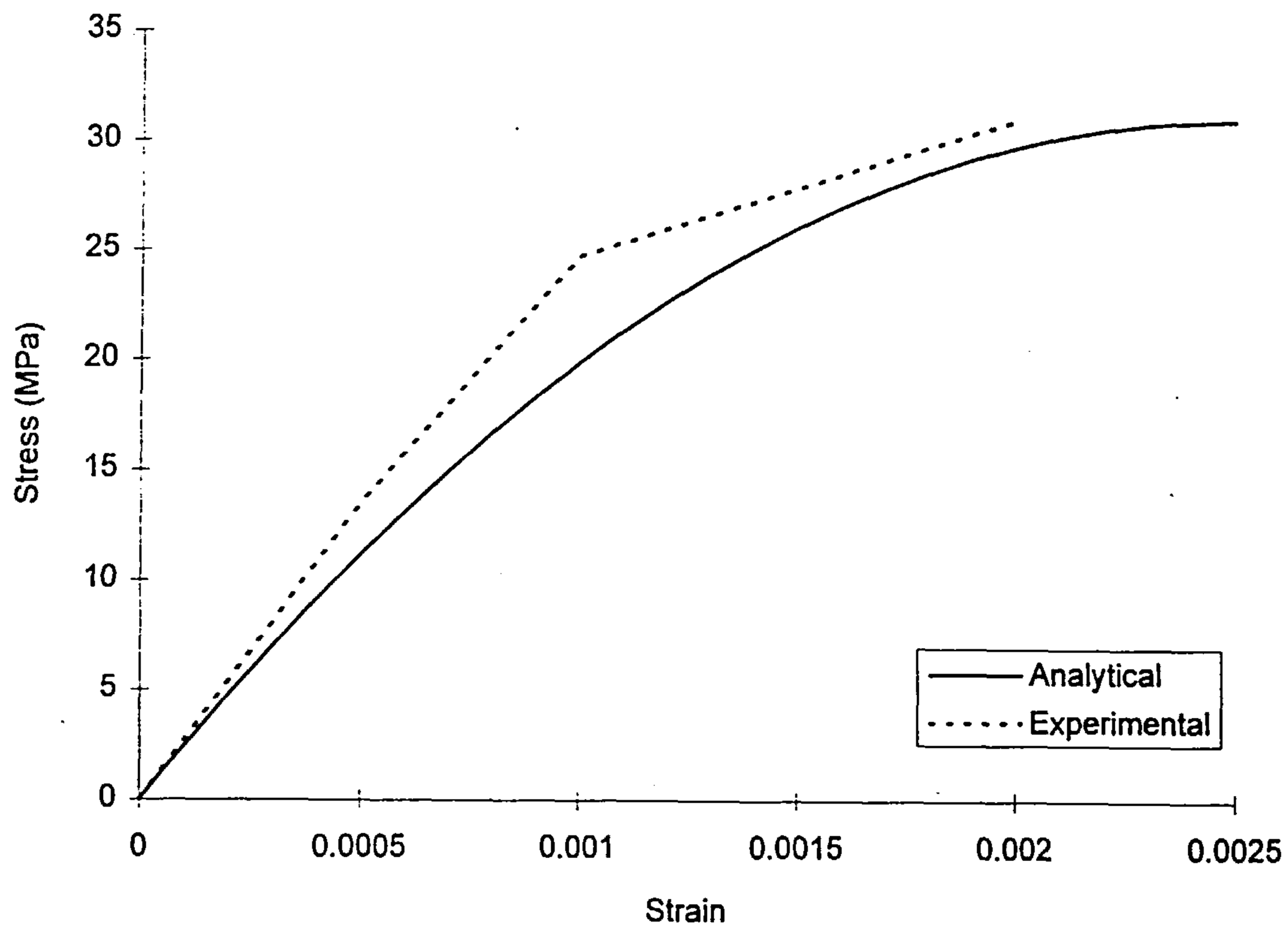

Figure 3.12: Comparison of stress-strain relationship with the experimental data[7] (k=0)

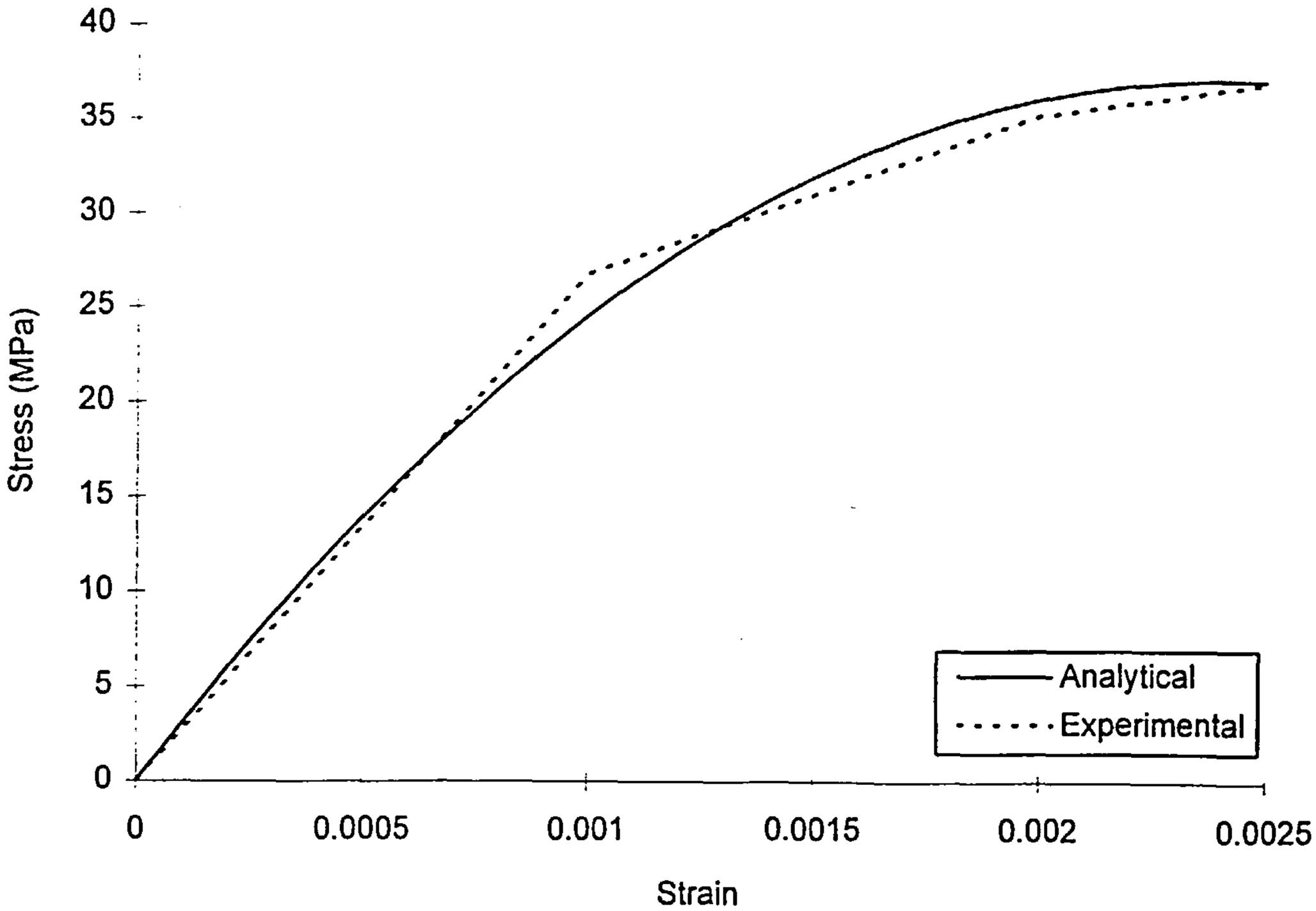

Figure 3.13: Comparison of stress-strain relationship with the experimental data[7] (k=1)

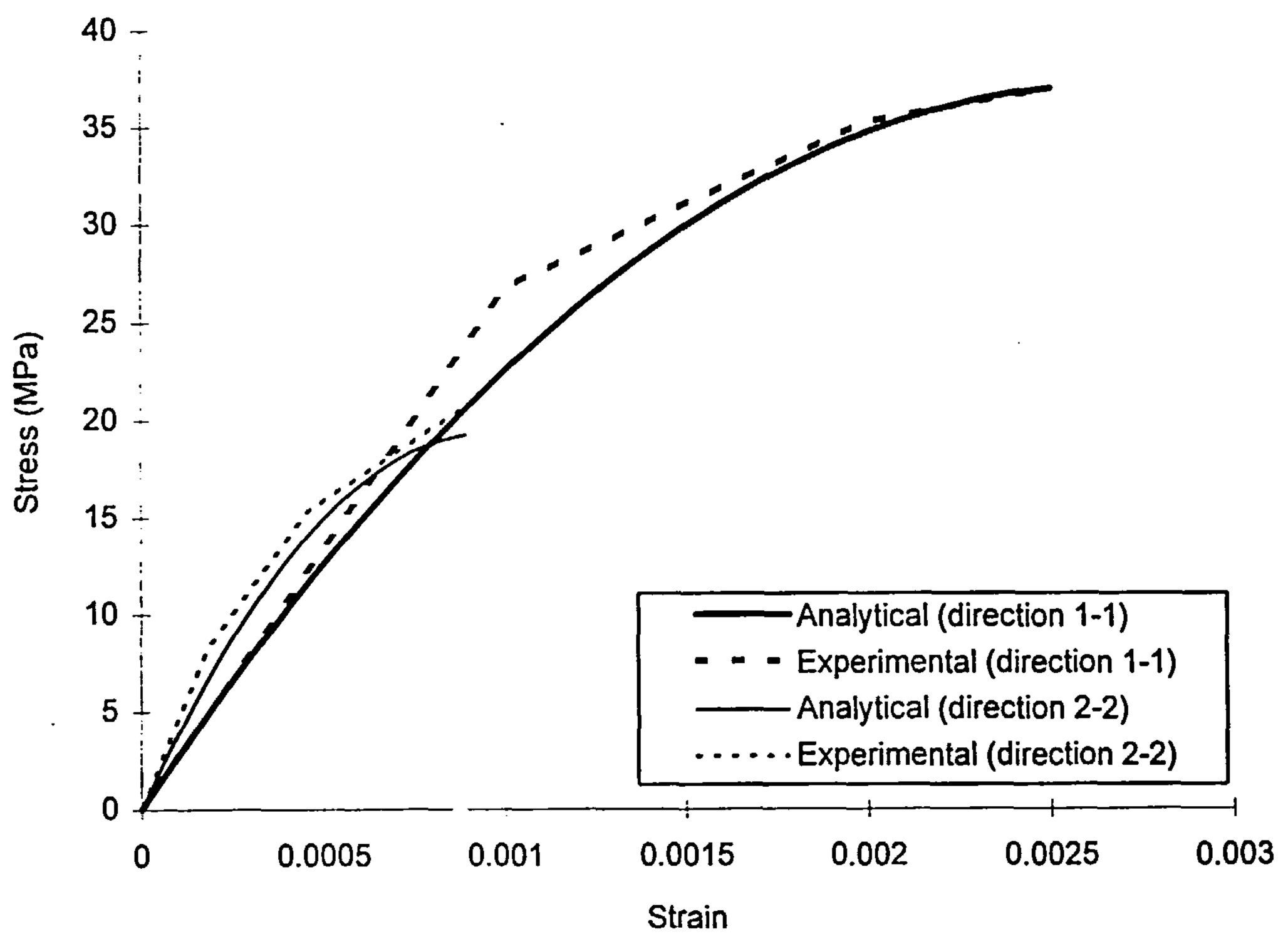

Figure 3.14: Comparison of stress-strain relationship with the experimental data[7] (k=0.52)

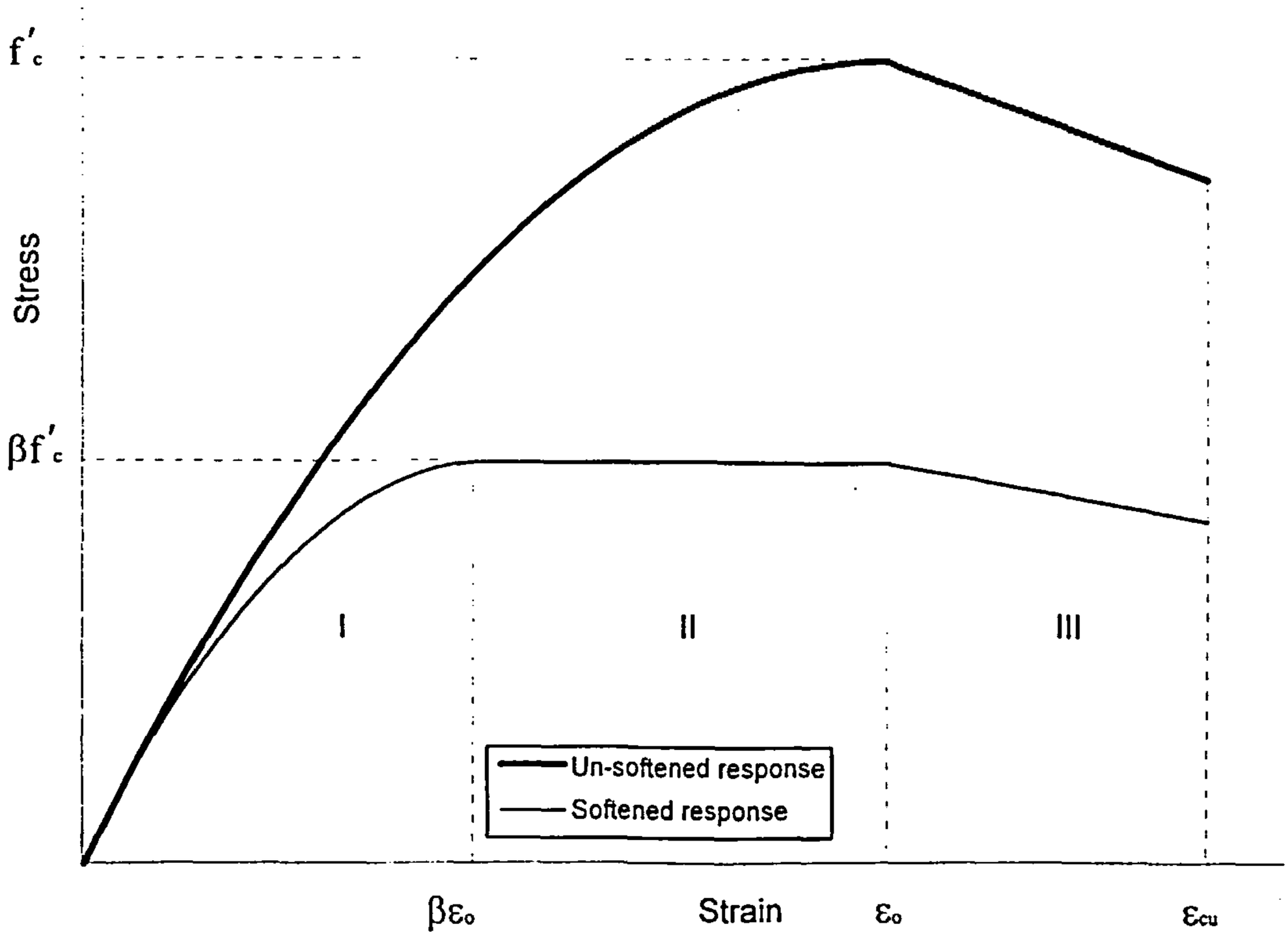

Figure 3.15: Softened response of concrete under biaxial compression-tension

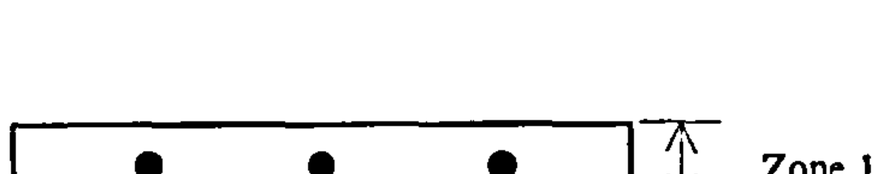

(a)

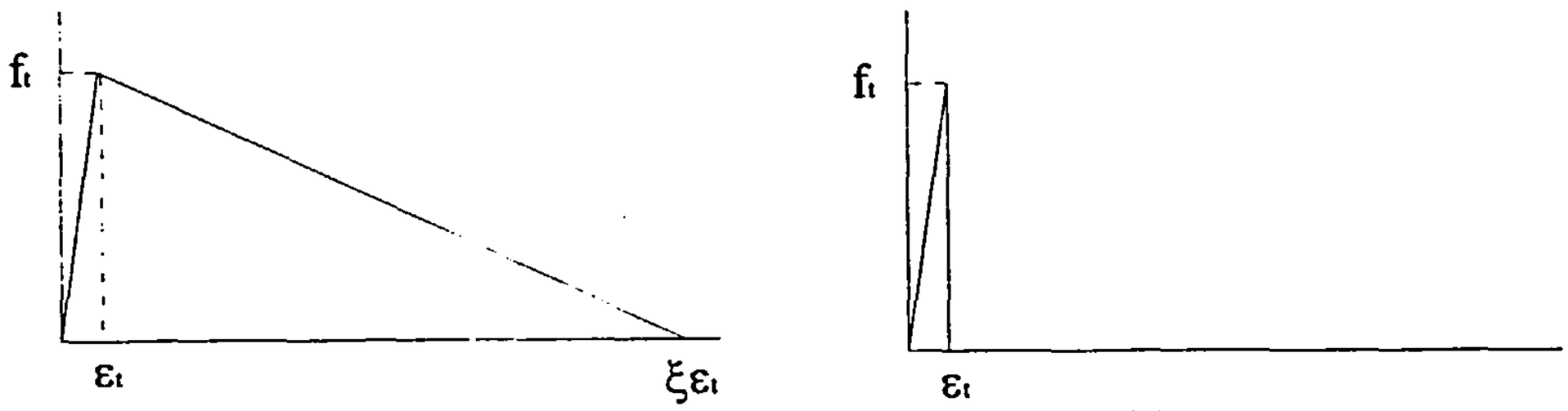

(b) (c)

Figure 3.16: Modelling of tensile response of concrete using regions in tension zone (a) section of slab with zones (b) tensile response for zone 1 (c) tensile response for zone 2

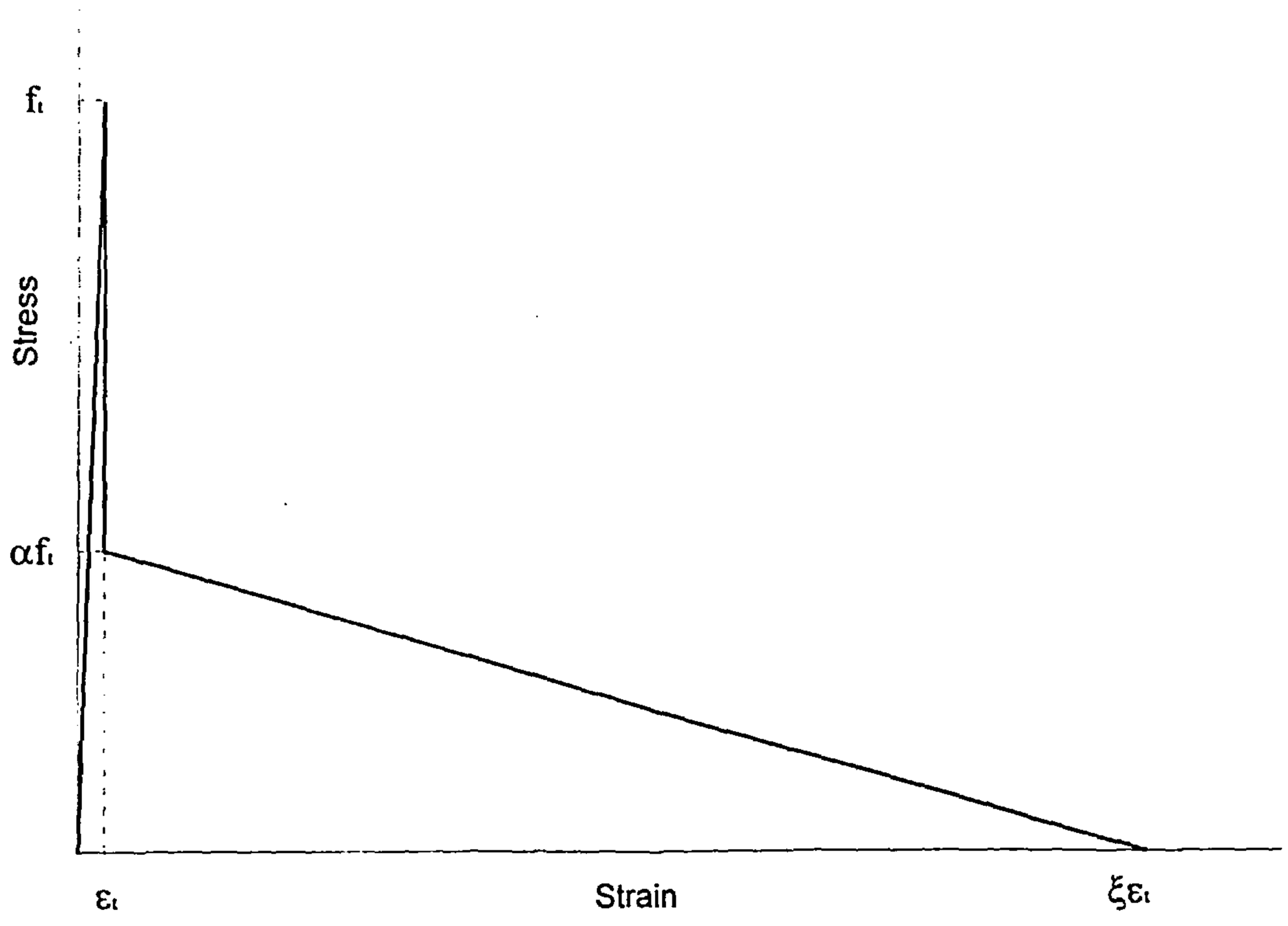

Figure 3.17: Stress-strain response of concrete in tension

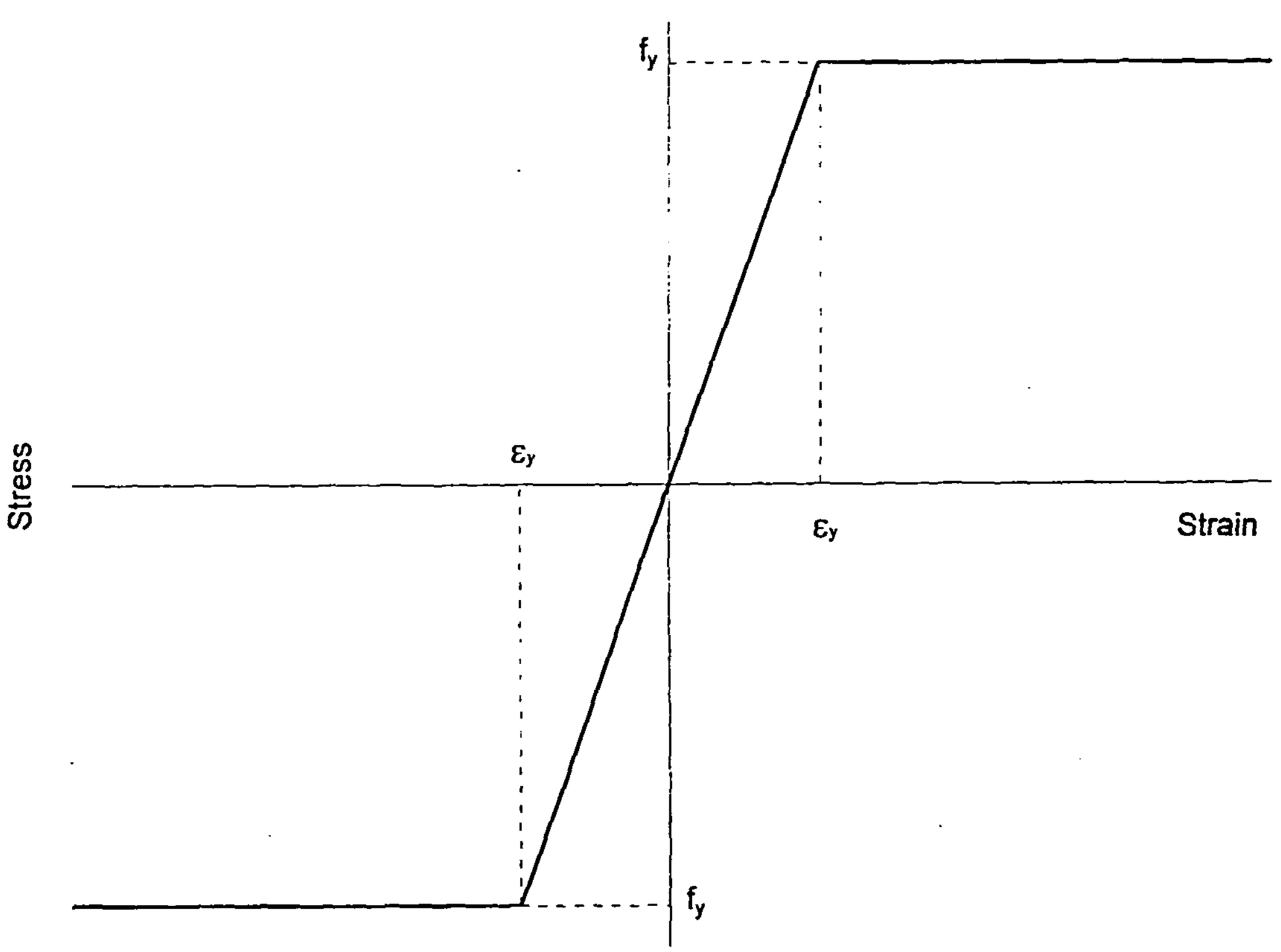

Figure 3.18: Model for the reinforcement

CHAPTER 4

NON-LINEAR ANALYSIS

4.1 INTRODUCTION

One of the objectives of this study was to understand the non-linear behaviour of reinforced concrete slab elements subjected to any combination of moments. In order to achieve this objective a computer program has been written that can predict the response of reinforced concrete shell elements, using the material models described in Chapter 3, subjected to any combination of loading, Figure 4.1,

$$\{F\} = [P_x \quad P_y \quad P_{xy} \quad M_x \quad M_y \quad M_{xy}]^T \qquad 4.1$$

and with the corresponding strains at the centre line of the cross-section,

$$\{\varepsilon_{CL}\} = [\varepsilon_x \quad \varepsilon_y \quad \gamma_{xy} \quad \phi_x \quad \phi_y \quad \phi_{xy}]^T \qquad 4.2$$

up to and beyond failure. The non-linear response of reinforced concrete elements is associated with the non-linear behaviour of concrete under tension, compression and the yielding of the reinforcement.

The non-linear behaviour of concrete in tension is dominated by cracking as the material under goes increasing stress[1]. These cracks produce discontinuities in the structure, which can be either modelled using the discrete crack approach or the smeared crack approach. In the discrete crack approach each crack has to be modelled separately which is the most realistic technique to represent cracking. However, this approach introduces gaps which have to be covered by re-meshing in finite element analysis[1]. One of the problems associated with discrete crack models is that either the crack location needs to be known before finite element meshing is carried or re-meshing has to be carried out when cracks appear using some criterion. Either of the methods can be used but this makes discrete crack modelling difficult and expensive. In the smeared crack approach instead of treating individual cracks separately, the cracks are averaged out or 'smeared-out' over the length of the specimen and the corresponding strains and stresses are termed as average strains and average stresses[1,2,3].

There are two ways of dealing with the directions of the cracks in the smeared crack model described above viz. the rotating crack model and the fixed crack model. In the rotating cracking model, the principal strain and stress directions are assumed to coincide and the cracks are assumed to be orthogonal to the principal tensile stress direction, thus the cracks are allowed to rotate through the depth of the element[1,4], as the principal stress directions rotate. This model could be termed as "un-physical"[5],

because of the fundamental assumption that the cracks' directions are allowed to rotate. This model, however, has been successfully used in numerous finite element analyses[1,6,7] and in developing constitutive models[8,9,10]. The other model is the fixed crack model[1,4,7], in which once the element has cracked, the direction of the crack is assumed to be fixed under further increases in load, by fixing the crack's direction, it can significantly over estimate collapse loads[5].

In the present study the cracks were assumed to be smeared over a finite length and allowed to rotate through the depth under increasing loads.

To solve non-linear problems, normally incremental iterative solution techniques have to be used. In the present work the Modified Newton Raphson with a displacement control procedure has been used.

This chapter describes the non-linear solution technique used, adopted solution algorithm and the techniques associated with numerical integration.

4.2 SOLUTION TECHNIQUES FOR NON-LINEAR PROBLEMS

There are several techniques which can be use to solve the non-linear problems e.g. Direct Iteration, Newton Raphson, Modified Newton Raphson and Incremental Newton Raphson (pure and mixed) methods have been among the techniques[1,11,12] usually used. However, the Newton Raphson and Modified Newton Raphson methods have been among the more popular non-linear solution techniques.

4.2.1 NEWTON RAPHSON METHOD

The Newton Raphson Method can be used for solving any number of non-linear equations. For a system of two equations the Newton Raphson Method is as follows. Let two equations be,

$$f(x_1, x_2)=0 \qquad 4.3a$$

$$g(x_1, x_2)=0 \qquad 4.3b$$

suppose (x_1^k, x_2^k) is an estimate of the root. The method seeks corrections Δx_1 and Δx_2 on x_1 and x_2 so that the corrected values will be

$$x_1^{k+1} = x_1^k + \Delta x_1 \qquad 4.4a$$

and $$x_2^{k+1} = x_2^k + \Delta x_2 \qquad 4.4b$$

for which

$$f(x_1^{k+1}, x_2^{k+2}) = 0 \qquad 4.5a$$

and, $$g(x_1^{k+1}, x_2^{k+2}) = 0 \qquad 4.5b$$

Using Taylor's expansion, equation 4.5 can be expanded as,

$$f(x_1^{k+1},x_2^{k+1})=f(x_1^k,x_2^k)+(x_1^{k+1}-x_1^k)\frac{\partial f(x_1^k,x_2^k)}{\partial x_1}+(x_2^{k+1}-x_2^k)\frac{\partial f(x_1^k,x_2^k)}{\partial x_2}+\ldots=0 \qquad 4.6a$$

$$g(x_1^{k+1},x_2^{k+1})=g(x_1^{k},x_2^{k})+(x_1^{k+1}-x_1^{k})\frac{\partial g(x_1^{k},x_2^{k})}{\partial x_1}+(x_2^{k+1}-x_2^{k})\frac{\partial g(x_1^{k},x_2^{k})}{\partial x_2}+\ldots=0$$

4.6b

Neglecting the higher derivatives and rearranging equation 4.6 gives,

$$-f(x_1^{k+1},x_2^{k+1}) = (x_1^{k+1}-x_1^{k})\frac{\partial f(x_1^{k},x_2^{k})}{\partial x_1} + (x_2^{k+1}-x_2^{k})\frac{\partial f(x_1^{k},x_2^{k})}{\partial x_2} \qquad 4.7a$$

$$-g(x_1^{k+1},x_2^{k+1}) = (x_1^{k+1}-x_1^{k})\frac{\partial g(x_1^{k},x_2^{k})}{\partial x_1} + (x_2^{k+1}-x_2^{k})\frac{\partial g(x_1^{k},x_2^{k})}{\partial x_2} \qquad 4.7b$$

equations 4.7 can be re-written as,

$$-f = \Delta x_1\frac{\partial f}{\partial x_1} + \Delta x_2\frac{\partial f}{\partial x_2} \qquad 4.7c$$

$$-g = \Delta x_1\frac{\partial g}{\partial x_1} + \Delta x_2\frac{\partial g}{\partial x_2} \qquad 4.7d$$

or in matrix form as,

$$\begin{Bmatrix}-f\\-g\end{Bmatrix}=\begin{bmatrix}\frac{\partial f}{\partial x_1} & \frac{\partial f}{\partial x_2}\\ \frac{\partial g}{\partial x_1} & \frac{\partial g}{\partial x_2}\end{bmatrix}\begin{Bmatrix}\Delta x_1\\ \Delta x_2\end{Bmatrix} \qquad 4.8$$

Using the above expression a system of n simultaneous non-linear equations can thus be solved for Δx_1 and Δx_2.

The above equation 4.8 can be use for structural analysis by solving the following governing equation.

$$\{F\}=[k]\{\Delta\} \qquad 4.9a$$

where {F} is the load vector, [k] is the stiffness matrix of the structure and {Δ} is the displacement vector. Similarly the following governing equation can be used to solve the non-linear stress-strain equations.

$$\{F\}=[k]\{\varepsilon_{CL}\} \qquad 4.9b$$

$\{\varepsilon_{CL}\}$ is the strain vector at the centre line of the cross-section of the element and [k] is the tangent stiffness matrix which has to be updated for every iteration as it is the derivative or the slope of the stress-strain curve as shown in Figure 4.2.

4.2.2 MODIFIED NEWTON RAPHSON METHOD

For large systems of equations, calculating the derivatives to form the tangent stiffness matrix,[k], for each iteration can be every expensive. In the Modified Newton Raphson Method usually, the terms of the [k] matrix have to be calculated only once and can be the initial tangent stiffness. This method has proved to be efficient and is less expensive[12]. This solution technique has been based on the concept that the non-linear response can be approximated by a series of linear solutions. The governing equation to be solved will be the same as equation 4.9 but the linear elastic matrix will be replaced by the initial tangent stiffness matrix.

4.2.3 APPLICATION OF THE MODIFIED NEWTON RAPHSON METHOD

The Modified Newton Raphson Method can be employed to solve the non-linear stress-strain equation using equation 4.9b. For any combination of direct strains in the x and y directions, ε_x, ε_y and the shear strain, γ_{xy}, and curvatures in the x and y directions, ϕ_x, ϕ_y and the twisting curvature, ϕ_{xy}, at the centre of the cross-section, the linear elastic forces, {F}, can be calculated using equation 4.9b if the initial tangent stiffness, [k], is known. For the given strains ε_x, ε_y and γ_{xy} and curvatures ϕ_x, ϕ_y and ϕ_{xy}, the resistance offered by the material, $\{F_{cap}\}$, can be calculated using the actual constitutive models for the concrete and the reinforcement. The error forces are the difference of linear elastic forces from equation 4.9b and the resistive forces from the actual constitutive models, $\{F_{cap}\}$, thus

$$\{F_{err}\} = \{F\} - \{F_{cap}\} \qquad 4.10$$

A strain vector, $\{\varepsilon_{err}\}$, corresponding to the error forces can be calculated from the following expression.

$$\{\varepsilon_{err}\} = [k]^{-1} \{F_{err}\} \qquad 4.11$$

A better estimate of strain vector at the centre line of the cross-section is calculated using

$$\{\varepsilon_{new}\} = \{\varepsilon_{CL}\} + \{\varepsilon_{err}\} \qquad 4.12$$

From the better estimate of strain, $\{\varepsilon_{new}\}$, a better estimate of the resistive forces offered by reinforced concrete element, $\{F_{new}\}$, is then calculated using the following expression.

$$\{F_{new}\} = \{F\} + \{F_{err}\} \qquad 4.13$$

A new set of error forces, $\{F_{err}\}$, is then calculated by using $\{F_{new}\}$ in equation 4.10 instead of {F}. This procedure, equations 4.10 to 4.13, is repeated until the error forces became acceptably small as shown in Figure 4.3.

4.3 SOLUTION ALGORITHM

Load control and displacement control techniques can be used to solve non-linear problems. Load control is not suitable for following the post ultimate falling branch responses, whereas, displacement control can easily do so and has proved to be suitable and efficient. The displacement control solution algorithm developed by Batoz and Bhatt[13] and implemented by May et al[12] has been used.

The governing equation 4.9 can be written in the form

$$\{\varepsilon_{CL}\} = [k]^{-1} \lambda \{f\} \qquad 4.14$$

where $\{\varepsilon_{CL}\}$ = strain vector at the centre line of cross-section

λ = load factor

$\{f\}$ = normalised load vector

A prescribed displacement is applied to one of the degrees of freedom. The equations were then solved for the, (n-1), unknown displacements and the load factor, λ. The actual algorithm used is summarised as follows,

1. The displacements, $\{\varepsilon^n{}_{CL}\}$, corresponding to the normalised load can be calculated using the following relationship.

$$\{\varepsilon^n{}_{CL}\}=[k]^{-1}\{f\} \qquad 4.15$$

2. An initial estimate of the load factor, λ, can then be made using the applied known displacement,

$$\lambda=\frac{\varepsilon_k}{\varepsilon^n{}_k} \qquad 4.16$$

where ε_k = known displacement at the k^{th} position of the strain vector

and $\varepsilon^n{}_k$ = known of displacement for the normalised load vector at the k^{th} position, equation 4.15.

3. The first estimate for the strain vector at the centre line of the cross-section is given by,

$$\{\varepsilon_{CL}\} = \lambda \{\varepsilon^{n}{}_{CL}\} \qquad 4.17$$

4. The corresponding set of internal forces {F} can be determined using the constitutive models for the concrete and the reinforcement.

5. A set of residual or error forces, {R}, can be then calculated such that,

$$\{R\} = \lambda \{f\} - \{F\} \qquad 4.18$$

6. From the set of known error forces, {R}, the corresponding strain vector can be determined.

$$\{\varepsilon_{err}\} = [k]^{-1} \{R\} \qquad 4.19$$

7. As the displacement at the k^{th} position of the strain vector is known, there should be no change in the displacement at this position. This can be expressed as

$$\varepsilon_{err_k} + \lambda_{err}\, \varepsilon^{n}{}_{k} = 0 \qquad 4.20a$$

or,
$$\lambda_{err} = -\frac{\varepsilon_{err_k}}{\varepsilon^{n}{}_{k}} \qquad 4.20b$$

where, ε_{err_k} = strain corresponding to the error forces at the k^{th} position of the strain vector

8. A better estimate for the load factor can be obtained from

$$\lambda = \lambda + \lambda_{err} \qquad 4.21$$

9. A better estimate of the strain vector at the centre line can be then obtained using the following expression.

$$\{\varepsilon_{CL}\} = \{\varepsilon_{CL}\} + \{\varepsilon_{err}\} + \lambda_{err}\{f\} \qquad 4.22$$

Steps 4 to 8 were then repeated until {R} becomes acceptably small.

4.4 CONVERGENCE CRITERIA

Ideally the error forces should be reduced to zero. In non-linear analysis it is both time consuming and can also be difficult, if not impossible, to reduce the error forces to zero. It then becomes essential to use a convergence criterion. Normally in non-linear finite element analyses[11,12] energy or work done has been used as a convergence criterion. A pre-set tolerance limit is then used to check whether the convergence has been achieved or not.

In the present study two convergence criteria have been used. The first convergence criterion was based on the absolute values of the error forces and the second criterion was based on an energy norm.

For the first convergence criterion a realistic convergence tolerance limit was set for the error forces and moments through trial and error. This limit vector is shown below.

$$|\{F_{err}\}| \leq \{ERROR\} \qquad 4.23$$

This convergence criterion may not be generalised as it is not dimensionless and the limit on the magnitude of the error forces may vary from one analysis to another.

Two different {ERROR} vectors were used in the analysis for the elements under bending and twisting moments and elements under in-plane forces. The reason for using two different set of convergence limit was that the element tested under in-plane forces were of comparatively smaller depth than the element tested under bending and twisting moment. Thinner elements required smaller tolerance limits than the thicker elements. Hence the following convergence criterion was used for elements under bending and twisting moments,

$$\{ERROR\} = \{10 \quad 10 \quad 10 \quad 100 \quad 100 \quad 100\}^T \qquad 4.24a$$

similarly for elements under in-plane forces following criterion was used.

$$\{ERROR\} = \{1 \quad 1 \quad 1 \quad 10 \quad 10 \quad 10\}^T \qquad 4.24b$$

The error forces and the moments were in N/mm and N mm/mm respectively.

It is relatively difficult to satisfy the convergence criterion based the magnitude of the error forces than the usual energy based criteria, as it requires to satisfy all six stress resultants to be acceptably small independently at the same time. On the other hand, the magnitude of acceptably small error forces can vary from analysis, equation 4.24. Hence due to the limitations of the convergence criterion based on error forces, a convergence criterion based on energy norm has also been used which is

$$E_{cov} = \frac{\{F\}\{\varepsilon_{CL}\}^T - \lambda\{f\}\{\varepsilon_{CL}\}^T}{\lambda\{f\}\{\varepsilon_{CL}\}^T} \qquad 4.25$$

A value, of E_{cov} of 0.001 has been used in the analysis. The difference between the analysis the using either of the convergence criterion was insignificant.

4.5 CALCULATION OF INTERNAL FORCES

To determine the internal forces the assumption that plane sections remain plane before and after bending has been made. The procedure adopted to determine the internal forces is that the section is divided into number of slices through out the depth, Figure

4.4. Given the curvatures and strains at the centre of the section, the strains at the centre of each slice can be calculated using,

$$\varepsilon_{n_x} = \phi_x h_n + \varepsilon_{CL_x} \qquad 4.26a$$

$$\varepsilon_{n_y} = \phi_y h_n + \varepsilon_{CL_y} \qquad 4.26b$$

$$\gamma_{n_{xy}} = 2\phi_{xy} h_n + \gamma_{CL_{xy}} \qquad 4.26c$$

Given the strains $\varepsilon_{n_x}, \varepsilon_{n_y}$ and $\gamma_{n_{xy}}$, then, for concrete, the principal strains are calculated and the principal stresses are determined using the relevant constitutive model, Section 3.3, Chapter 3. The principal stresses are then transformed back to the global x and y axes and $\sigma_{n_x}, \sigma_{n_y}$ and $\tau_{n_{xy}}$ are obtained. The procedure is carried out for each slice. The contribution of the reinforcement is determined using the strain at the level of the reinforcement and the constitutive model for steel. The axial force and moment on the cross-section is then determined by assuming the contribution of each slice and using the following expressions.

$$P_x = \sum \sigma_{n_x} t_n + P_{rx} \qquad 4.27a$$

$$P_y = \sum \sigma_{n_y} t_n + P_{ry} \qquad 4.27b$$

$$P_{xy} = \sum \tau_{n_{xy}} t_n \qquad 4.27c$$

and

$$M_x = \sum \sigma_{n_x} t_n h_n + M_{rx} \qquad 4.28a$$

$$M_y = \sum \sigma_{n_x} t_n h_n + M_{ry} \qquad 4.28b$$

$$M_{xy} = \sum \tau_{n_{xy}} t_n h_n \qquad 4.28c$$

where the summation is carried out over all the slices.

M_{rx} and M_{ry} are the moments due to the reinforcements in x and y directions respectively. P_{rx} and P_{ry} are the axial forces due to the reinforcement in x and y directions respectively.

The flow chart for the program is given in Figure 4.5.

References

1 Kotsovos, MD and Pavlovic MN, Structural concrete- Finite-element analysis for limit state design (Chapter 2), First edition, Thomas Telford, London, 1995, pp 164-174.

2 Cope, RJ, Nonlinear analysis of concrete slabs (Chapter 1), edited by Hinton, E and Owen, R, Pineridge Press, Swansea, 1986, pp 3-43.

3 de-Brost, R, Computational aspects of smeared crack analysis (Chapter 2), edited by Hinton, E and Owen, R, Pineridge Press, Swansea, 1986, pp 44-83.

4 Bangash, MYH, Concrete and concrete structures: Numerical modelling and applications (Chapter II), First edition, Elsevier Applied Science, Essex, 1989, pp 74.

5 Crisfield, M and Wills, J, Numerical comparisons involving different 'concrete models', Computational mechanics of concrete structures-advances and applications, Proceeding of IABSE Colloquium, Delft 1987, pp 177-187.

6 Hu, HT and Schnobrich, WC, Non-linear analysis of cracked reinforced concrete, ACI St. Jnl., vol. 87, no. 2, Mar-Apr. 1990, pp 199-207.

7 Al-Shaarbaf, IAS, Three-dimensional non-linear finite element analysis of reinforced concrete beams in torsion, PhD Thesis, University of Bradford, 1990, pp 70-126.

8 Hsu, TTC, Towards a unified nomenclature for reinforced-concrete theory, Jnl. of St. Div., ASCE, vol. 122, no. 3, March 1996, pp 275-283.

9 Vecchio, FJ, Collins, MP, The response of reinforced concrete to in-plane shear and normal stresses, Publication No. 82-03, Department of Civil Engineering, University of Toronto, March 1982, 332 p.

10 Vecchio, FJ and Collins, MP, The modified compression-field theory for reinforced concrete elements subjected to shear, ACI St. Jnl., Mar-Apr. 1986, pp 219-231.

11 May, IM, Naji, JH and Ganaba, TH, Displacement control for non linear analysis of reinforced concrete structures, Engineering Computations, vol. 5, no. 4, December 1988, pp 266-273.

12 Ma, SYA and May, IM, The Newton Raphson method used in the non linear analysis of reinforced concrete structures, Computers and Structures, vol. 24, no. 2, 1986, pp 177-185.

13 Batoz, J and Bhatt, G, Incremental displacement algorithms for non linear problems, Int. Jnl. of Num. Meth. Eng., vol. 14, no. 8, August 1979, pp 1262-1266.

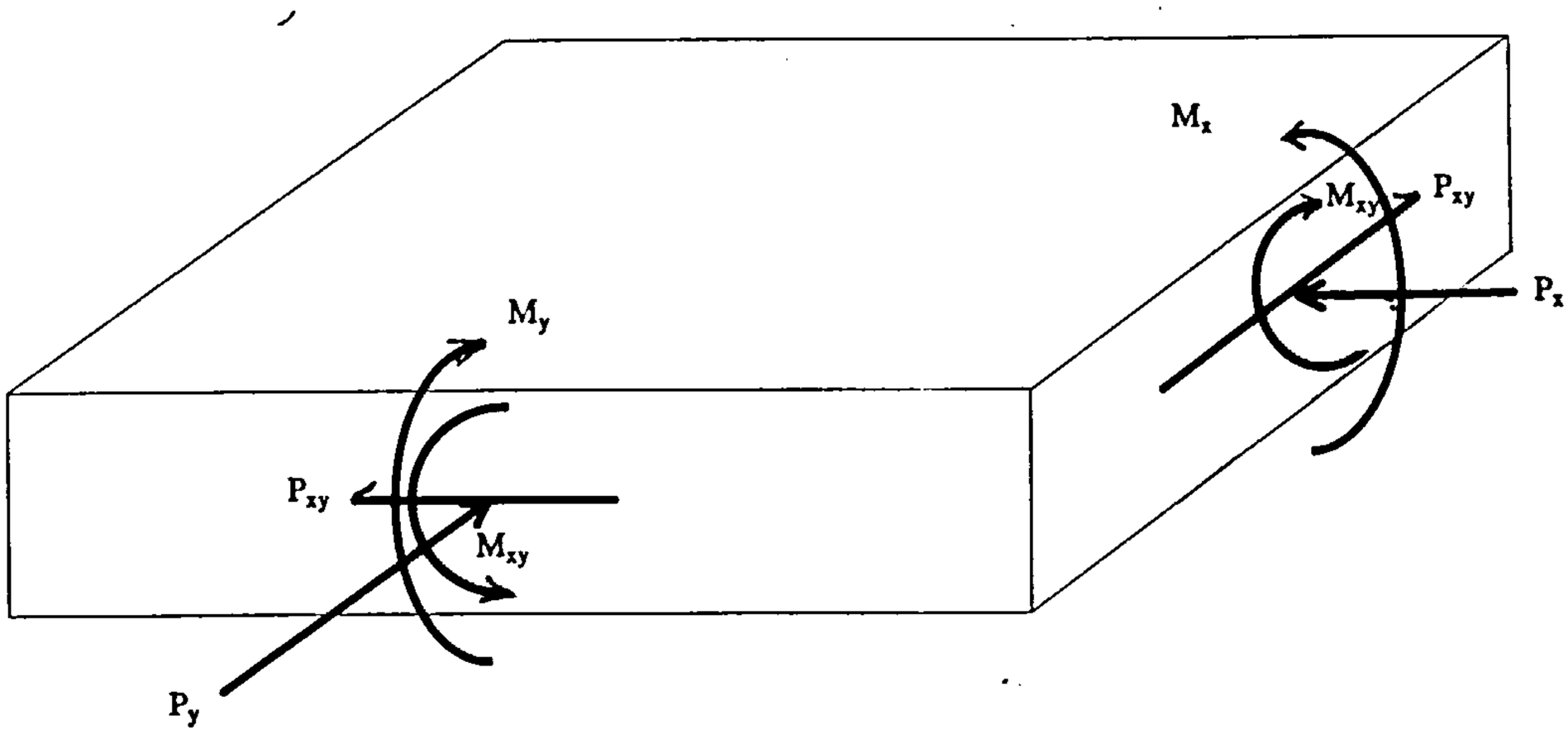

Fig 4.1: Slab element and applied loading

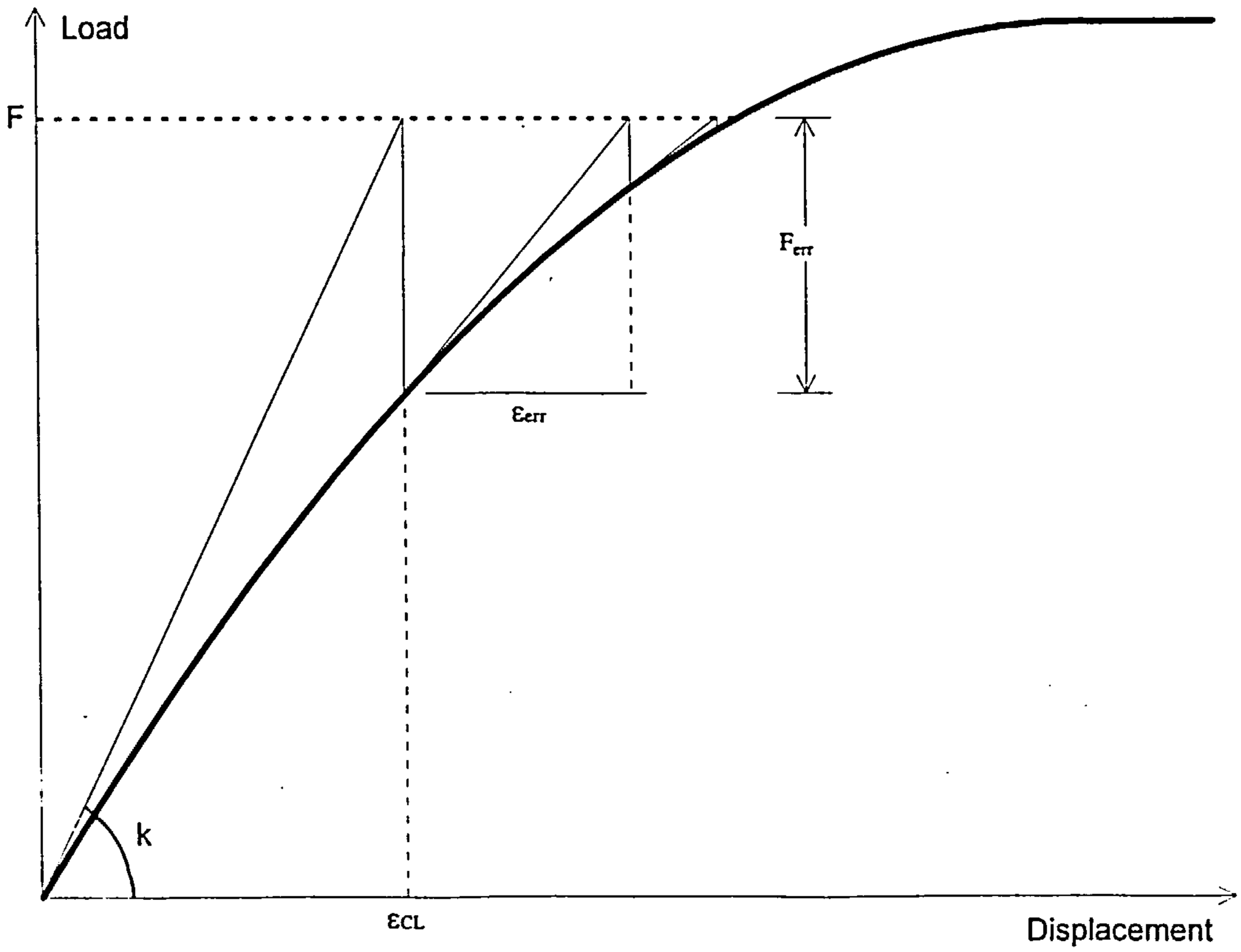

Figure 4.2: Newton Raphson Method

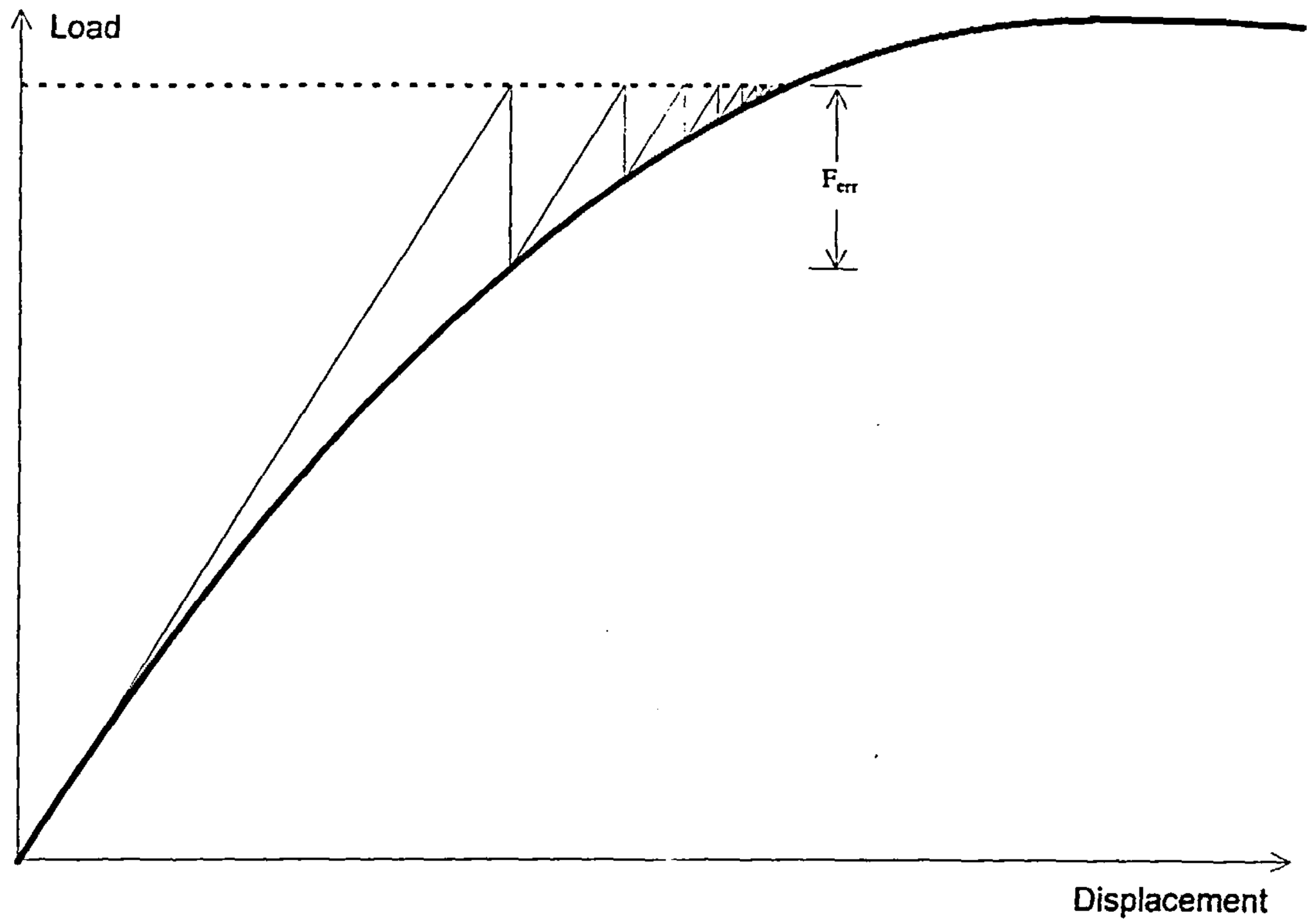

Figure 4.3: Modified Newton Raphson Method

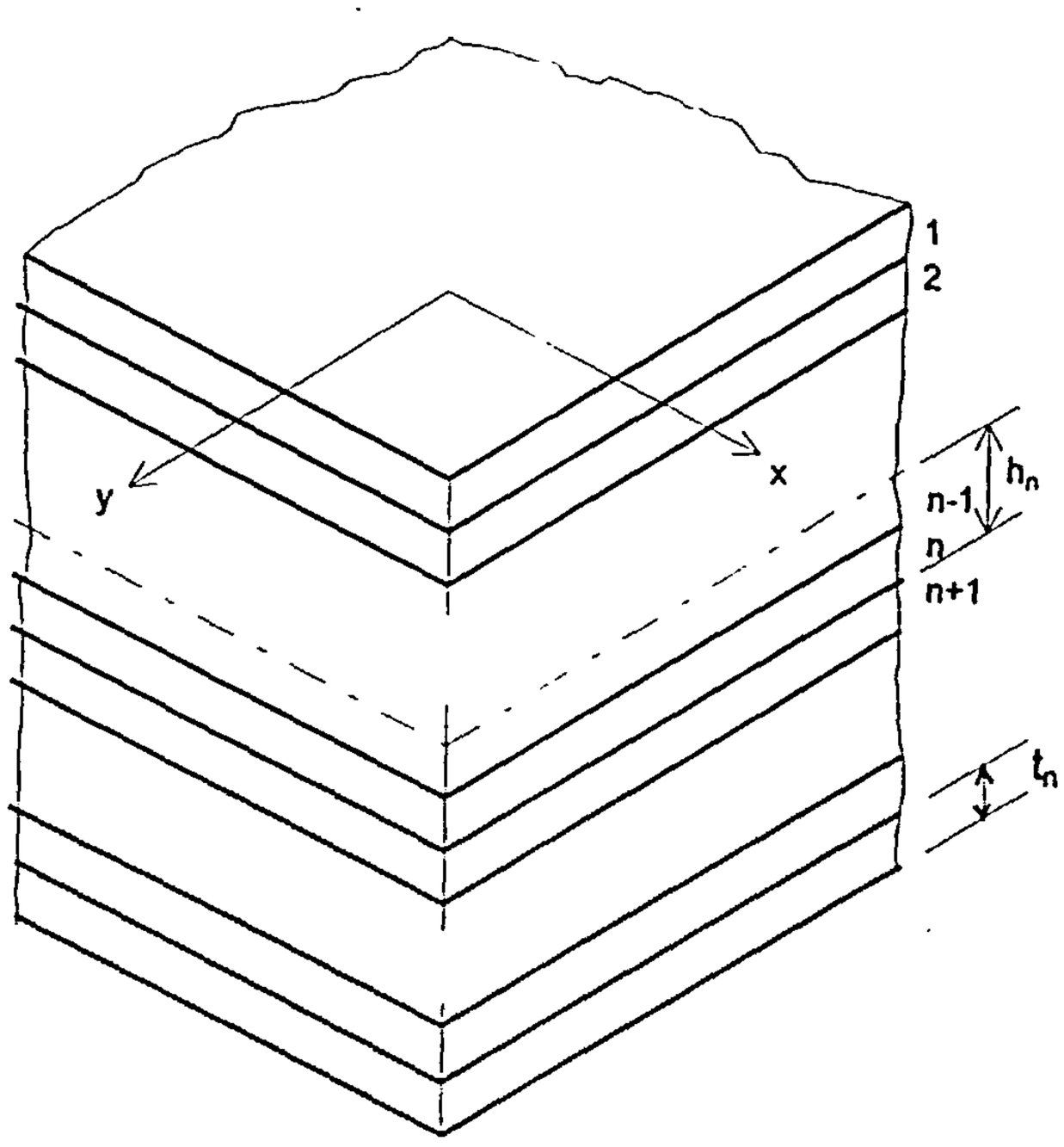

Figure 4.4: Division of slab element into slices

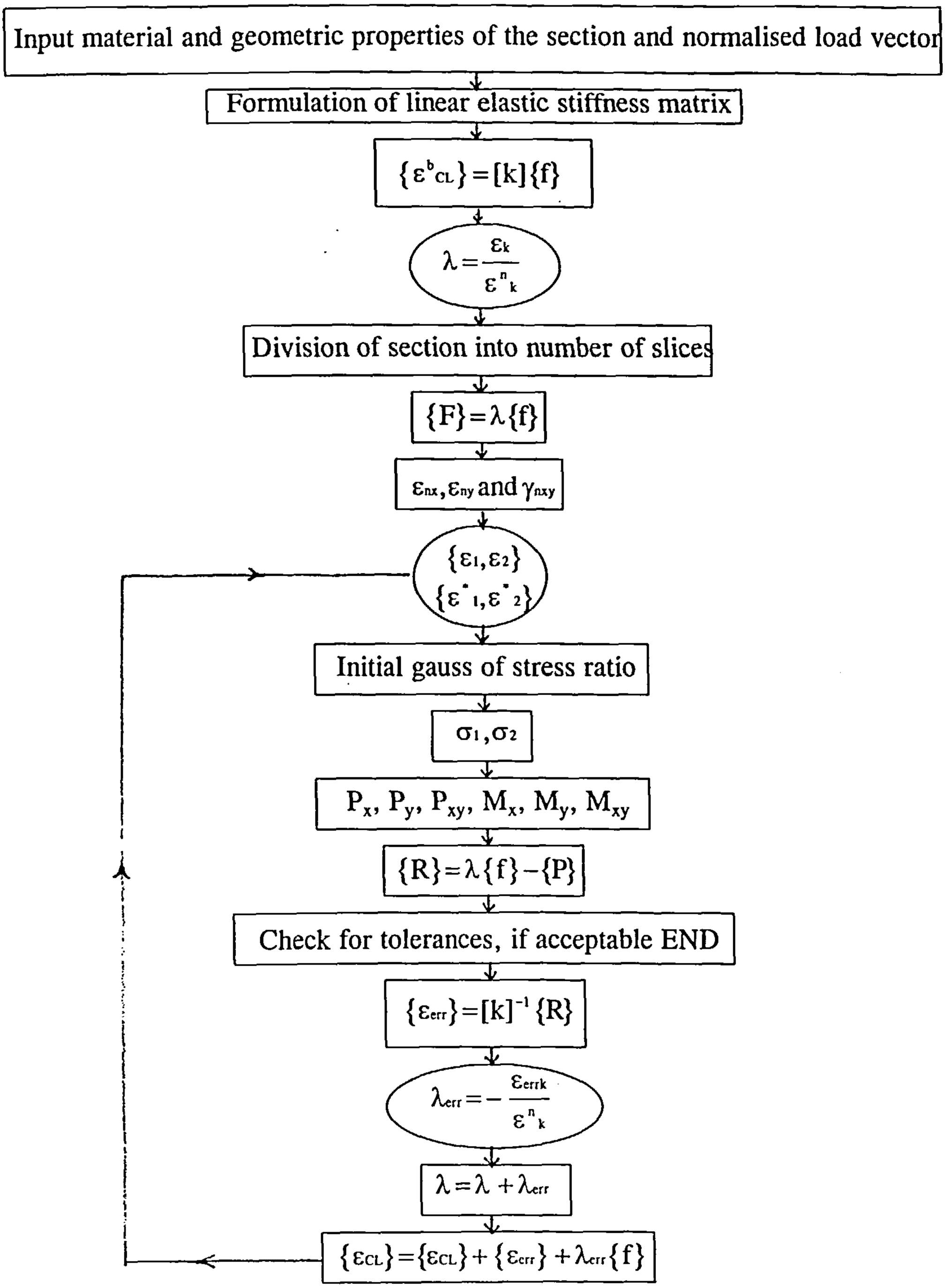

Figure 4.5: Flow diagram of the computer program

CHAPTER 5

VALIDATION OF THE ADOPTED SOLUTION TECHNIQUE

5.1 INTRODUCTION

A computer program has been developed that can predict the non-linear response of reinforced concrete shell elements and has been described in Chapter 4. The non-linear models for concrete, reinforcement and reinforced concrete used in the program have been described in Chapter 3. The software has been validated by comparing the analytical results from the program with those from several experimental works.

This Chapter, apart from dealing with the validation of the program, describes the effect of number of points through the depth of the element at which the strains and the stresses are calculated on the overall response. This Chapter also describes the behaviour of elements under in-plane shear and twisting moment, prior to cracking, at the post-cracking and at the post ultimate load stages. The effect of the parameters such as tension stiffening, compression softening and the amount of reinforcement are also studied.

5.2 VALIDATION OF SOFTWARE

In order to validate the developed software several experimental studies were chosen. The first three sets of experimental works were conducted at the University of Toronto by Vecchio and Collins[1], Bhide and Collins[2] and Kirschner and Collins[3] respectively. The fourth set of data was chosen from the experiments carried out at the University of Manchester by Samad[4] and the fifth set of work, also carried out at the University of Toronto, was conducted by Marti et al[5].

5.2.1 IN-PLANE TESTS, VECCHIO AND COLLINS[1]

An extensive experimental study was carried out at the University of Toronto to study the behaviour of reinforced concrete panels under in-plane forces. A specially designed rig, capable of applying in-plane shear, axial compression and axial tension or any combination was used. In all, thirty reinforced concrete panels (890 mm x 890 mm x 70 mm) were tested under different loading conditions and with varying amounts of reinforcement. The details of the loading conditions have been discussed in Section 2.4.5.2, Chapter 2. It was only possible to analyse the twenty eight out of the thirty panels that were loaded monotonically. Table 5.1 shows the material and section properties and the loading regime of five of the panels and Figures 5.1 to 5.5 show the comparison between the experimental and analytical results. A reasonably good agreement was obtained between the experimental and the analytical results, through out the loading regime.

Table 5.2 shows the comparison between the experimental and the analytical results at the ultimate load for twenty eight and a good agreement has been obtained.

5.2.2 IN-PLANE TESTS, BHIDE AND COLLINS[2]

Thirty four reinforced concrete panels (890 mm x 890 mm x 70 mm) were tested at the University of Toronto using the same testing rig as used by Vecchio and Collins[1], Section 5.2.1, by Bhide and Collins[2]. In this study all but two of the concrete panels were reinforced in one direction only. Five panels were tested in pure in-plane shear, eight in uniaxial tension, sixteen in uniaxial tension with monotonic in-plane shear and the rest under non-monotonic loading.

Three panels were analysed using the program. The material and section properties and the loading history for these panels are given in Table 5.3. For panels PB 12 and PB 18, that were subjected to in-plane shear, it was observed from the tests that the cracks first formed at 45° from the reinforcement direction but further cracks formed turning quickly to a direction which was smaller than 45°. For panel PB 10 it was observed that the cracks appeared in the directions predicted by assuming uncracked elastic behaviour but that the additional cracks formed near the ultimate load stage which were closer to the reinforcement direction. As a rotating crack model has been adopted in the analysis, it was not possible with this analysis to maintain the actual crack directions after first cracking as the load increased due to the uni-directional distribution of the reinforcement. The cracks turned much more rapidly in the failure

direction than predicted by the analysis, Figure 5.6. Therefore, it was not possible to predict the post cracking response accurately. However, good agreement between the experimental and the analytical results was obtained upto first cracking. This is shown in Figures 5.6 to 5.9. It was also observed that the panels exhibited a long plateau after cracking which was not predicted by the analysis. This is due to the aggregate interlock and dowel action. The comparison between the experimental and analytical cracking loads is also given in Table 5.3. The program under estimated the cracking strength by 4.54% with a standard deviation of $\pm 2.46\%$.

5.2.3 IN-PLANE TESTS, KIRSCHNER AND COLLINS[3]

A shell element tester was designed and used by Kirschner and Collins[3] at the University of Toronto. This test rig was capable of testing shell elements subjected to either in-plane forces and moments or combinations of in-plane forces and moments. Six reinforced concrete panels (1625 mm x 1625 mm x 285 mm) were tested under different load combinations by Kirschner and Collins. Two out of six panels were made out of light weight aggregates. The remaining four elements were made of normal weight aggregates. In the panels made of normal weight aggregates the reinforcement was placed in two orthogonal directions, skewed at $\pm 45^{o}$ angle with respect to the edge of the panel. The panels were subjected to in-plane shear, uniaxial bending and a combination of monotonic in-plane shear and uniaxial bending with respect to the direction of the reinforcement. The details of the loading and properties of the four panels are given in Table 5.4 along with the comparison between the experimental and the analytical ultimate loads. Figures 5.10 to 5.14 show the

comparison between analytical and experimental results and good agreement was obtained throughout the loading regime.

5.2.4 BENDING AND TWISTING TESTS, UNIVERSITY OF MANCHESTER[4]

Thirteen slab elements (1600 mm x 1600 mm x 150 mm) were tested under different combinations of biaxial bending and twisting moments. A specially designed testing rig capable of applying any combination of uniform bending and twisting moments to the slab was used. The slabs were placed vertically in the rig and uniform moments were applied through an arrangement of 20 loading arms[4]. Surface strains, deflections and loads were recorded. The summary of the nine slab elements for which reliable experimental data was obtained is given in Table 5.5 along with the comparison of the experimental and the analytical ultimate moments. Comparisons of the experimental and analytical results for six typical slab elements are given in Figures 5.15 to 5.20. It can be seen that there is a good agreement between the experimental and the analytical results throughout the loading upto the ultimate load level. However, for slab element 12 which was tested under pure torsion there was a significant difference between the experimental and the analytical results after cracking. It was suspected, that a small axial restraint may have been introduced while applying the loads. The twisting moment was applied only at the four corners using 4 jacks whereas the remaining 16 jacks were assumed to be idle. The assumed idle jacks may have introduced an axial restraint while the slab was being loaded by the twisting moment. To investigate this, slab element 12 was then analysed with a very small degree of axial force. Tensile forces of $\cong 3\%$ of the axial tensile capacity, in magnitude were applied in the both the

reinforcement directions. A better comparison between the experimental and the analytical results was then obtained as shown in Figure 5.21.

5.2.5 PURE TWISTING TESTS, MARTI, LEESTI AND KHALIFA[5]

Nine slabs (1700 mm x 1700 mm x 200 mm) were tested at the University of Toronto under pure torsion with varying amounts of reinforcement in the two orthogonal directions. A summary of the material and section properties is given in Table 5.6 along with the comparison between the experimental and analytical ultimate moments.

The loading arrangement to apply torsion was that the three corners of the slab were on supports, restrained against translation in the vertical direction but free to rotate. A downward load was applied to the fourth corner. This set-up led to a loading condition in which two sets of equal and opposite vertical forces were applied at the two corners as shown in Figure 5.22. It was assumed that this type of loading would produce uniform twisting through out the slab.

The analysis of the slabs using the program showed good agreement between the experimental and the analytical results. Six typical slabs are shown in Figures 5.23 to 5.28. Slabs 2 and 4, shown in Figures 5.23 and 5.24, however, failed abruptly and prematurely due to brittle corner failure prior to reaching the ultimate load. It was mentioned by Marti et al[5] that in slabs 2 and 4 corner failure occurred close to the ultimate load.

5.3 EFFECT OF NUMBER OF INTEGRATION POINTS

Numerical integration has been employed in this study, Section 4.5, Chapter 4, to determine the internal resistance offered by the reinforced concrete element. In order to determine the resistive concrete forces, a number of points have been selected at which the strains and corresponding stresses have been calculated. These points are termed integration points. The greater the number of integration points, the more accurate the analysis, but an increase in the number of integration means an increase in the computation time. Thus an optimum number of integration points are of vital importance.

The elements under in-plane shear or any other in-plane load have a constant state of stress across the depth, therefore, the number of integration points does not increase the accuracy of the analysis in such loading cases. However, elements subjected to any type of moments have a continuously changing state of strains and stresses through the depth. The optimum number of integration points under such loading conditions are of significant importance specially for elements with lesser area of reinforcement. The element with smaller area of reinforcement will have smaller depth of neutral axis. Therefore, less integration points will be available to calculate the compressive resistance offered by concrete which can significantly affect the moment capacity of the element.

In order to study the effect of number of integration points for reinforced concrete elements subjected to pure twisting moment, slab 1 of reference 5 was used. Slab 1 was isotropically reinforced with 0.25% reinforcement at top and bottom faces in x and y directions. The reason of selecting slab 1 was due to the least area of reinforcement among the slabs testing in the study. The slab 1 will have smallest depth of neutral axis which means least number of integration points in compression region of concrete and hence the effect on the moment capacity can be significant.

The number of integration points used was 10, 25, 50, 75, 100 through the depth of the element. Figure 5.29 shows the response of the slab with the above mentioned integration points. It can be observed from Figure 5.29 that with 10 integration points correct cracking moment was not predicted, however, the ultimate moment capacity was $\cong$ 2% less than that with 100 integration points.

Figure 5.30 shows the principal concrete stress distribution through the depth at same twisting curvature i.e. 8×10^{-5} 1/mm. As the number of integration points was increased, the concrete stresses were more accurately predicted numerically, especially in the region around the neutral axis. But approximation in the stress distribution through the depth due to the lesser number of integration points does not significantly affect either the ultimate moment capacity or the overall response. It can, therefore, be concluded that about 10 to 25 integration points can be used. However, 100 integration points have been used through out the study to avoid any unforeseen problem.

5.4 BEHAVIOUR OF ELEMENTS UNDER IN-PLANE SHEAR AND TWISTING MOMENT

After validating the program, the influence of various parameters such as tension stiffening, compression softening and area of reinforcement on slab elements subjected to pure in-plane shear and pure twisting were studied. The reason for selecting these loading conditions was that the behaviour of reinforced concrete elements is well understood under uniaxial or biaxial bending without any twisting moment or axial in-plane loads without any in-plane shear since the principal strain directions coincide with the reinforcement directions in such loading conditions. But as the twisting moment or in-plane shear increases in the reinforcement, the angle between the principal strain and the reinforcement directions also increases. Prior to cracking elements subjected to pure in-plane shear or pure twisting moment have maximum angle of $\pm 45^{o}$ between the principal strain and the reinforcement directions and no direct load acts in the reinforcement. The concrete will be in a state of compression-tension in the principal stress directions. This can significantly reduce the compressive strength of concrete, Section 3.2.1.2, Chapter 3.

In order to further explain the effect of differences mentioned in the preceding paragraph the behaviour of the reinforced concrete elements under in-plane shear and pure twisting will be described.

5.4.1 PRE-CRACKING RESPONSE

In an element which has orthogonal reinforcement and which is subjected to either in-plane shear or twisting moment, the reinforcement is unstressed prior to cracking, if the reinforcement is assumed to carry axial stresses only. Prior to cracking the principal axes are at $\pm 45^{o}$ with respect to the direction of the reinforcement, as shown in Mohr's circle of strains, Figure 5.31.

5.4.2 POST CRACKING RESPONSE

For an isotropically reinforced element subjected to in-plane shear, after cracking, the angles between the reinforcement and the principal strain directions remain at $\pm 45^{o}$. However, because after cracking the concrete can carry little or no tensile stress, then to satisfy equilibrium the reinforcement has to be in tension. Mohr's circles of strain after cracking under increasing load are shown in Figure 5.32 where compressive strain is taken as positive.

At any load stage, an isotropically reinforced element subjected to pure twisting behaves in a similar fashion to an isotropically reinforced element under in-plane shear. The strains, however, in the principal directions vary linearly through out the depth whereas, the principal strains are constant through out the depth for in-plane shear. Hence the strain state under in-plane shear at a particular load stage represents a point on the strain profile of an element under pure twisting.

In an orthotropically reinforced element subjected to in-plane shear, after cracking, the reinforcement carries tension and in addition the principal strain directions also change from $\pm 45^{o}$, Figure 5.33. The crack direction moves towards the direction of stronger reinforcement. A similar response also occurs in orthotropically reinforced elements under pure twisting at the level of the reinforcement i.e. both the top and the bottom sets reinforcement remain in tension in x and y directions.

The maximum compressive stress that concrete can carry while under compression-tension stress state has been modelled by constant stress between $\beta\varepsilon_o$ and ε_o, Figure 3.15, Chapter 3. If the failure of the element is due to crushing of concrete prior to yielding of the reinforcement i.e. over reinforced failure, the response is dictated by the compression model of the concrete. Therefore, the flat top model of concrete should be evident from the response under in-plane shear in case of an over reinforced failure which is evident from Figures 5.1 to 5.5 and 5.11.

In the case of pure twisting, under progressively increasing load, the principal curvatures increase and the depths of the neutral axes reduce. The increase in the principal curvatures increases the strains on the extreme fibres of concrete. The strains can be such that either the reinforcement yields in tension prior to the crushing of concrete in compression or vice versa. If the reinforcement yields first, ductile behaviour will be exhibited as shown in Figures 5.24, 5.26 and 5.27, but if the concrete crushes prior to the yielding of the reinforcement, the element will show a brittle response as shown in Figures 5.23, 5.25 and 5.28.

Marti et al[6] found that if the ratio $\rho\frac{f_y}{f_c} > \frac{1}{4}$, the element exhibits as an over reinforced response, where ρ is the amount of steel ratio, f_y is the yield strength of the reinforcement and f_c is the softened compressive strength of concrete. For the slabs tested by Marti et al[5] it has been observed that for an isotropic element that if the area of steel is greater than about 0.5 mm^2/mm per layer in each direction, the element exhibits over reinforced behaviour. The over reinforced response at such a low reinforcement level is due to two facts. Firstly, that the four sets of the reinforcement are at an angle from the principal strain directions, the strain in the reinforcement will be less that the principal tensile strain whereas, the concrete will be subjected to principal compressive strain. Therefore, the direct tensile strain in the reinforcement will be less than the yield strain but the principal compressive strain in the concrete will be large enough to cause crushing. Secondly, the compressive strength of concrete will be significantly reduced due to the compression softening[18], Section 3.2.1.2, Chapter 3, causing an increase in the depth of compressive stress block.

5.4.3 POST ULTIMATE RESPONSE

In the post ultimate range, concrete in compression has been modelled by a straight falling line between the strain corresponding to peak stress, ε_o, and crushing strain, ε_{cu}, Figure 3.15. Beyond the crushing strain the concrete has been assumed to carry zero stress. The effect of this model on the behaviour of the reinforced concrete slab elements is that after the concrete crushes, any further increase in curvature causes the neutral axis to move towards the centre of the element in order to achieve equilibrium, Figure 5.34. As the neutral axis moves towards the centre of the

element, the strain at the level of reinforcement reduces and the reinforcement begins to unload. The unloading of the reinforcement follows the same path as that for loading due the type of models adopted in this study, Section 3.2.2, Chapter 3.

5.5 RESPONSE UNDER INFLUENCING PARAMETERS

In order to study the influence of various parameters on the overall response of reinforced concrete slab elements under in-plane shear and pure twisting moment a number of studies were carried out. The parameters considered were tension stiffening, compression softening and the amount of area of steel to study their effects on the overall behaviour of slab elements.

5.5.1 EFFECT OF TENSION STIFFENING:

Tension stiffening is used to model complex stress state of concrete in tension after cracking. It can be defined as an alternative way of modelling two properties of reinforced concrete viz. the tensile strength of concrete in between the cracks and the bond between the concrete and the reinforcement. Several approaches have been adopted by researchers to model tension stiffening of reinforced concrete[7,8,9,10,11,12]. Tension stiffening plays a significant role in the overall response of reinforced concrete. The effect of tension stiffening becomes evident after cracking and influences the response prior to the yielding of reinforcement. The effect of tension stiffening is more significant in elements with a smaller area of reinforcement. In such

elements the depth of neutral axis is small, thus the overall response is dictated by the tensile response of the concrete and the reinforcement.

Two different approaches have been employed in this study to model tension stiffening and have been discussed in detail in Section 3.2.1.2, Chapter 3. The first approach has been used to model the tensile response in composite laminates[13] but has been adopted for reinforced concrete. The second approach has been more commonly used in reinforced concrete to model tension stiffening.

To study the influence of tension stiffening on the overall response of the element two parameters were varied as mentioned below.

1. Thickness of the region of concrete around reinforcement in the first approach or the level of discontinuity in the second approach, Figures 5.35 and 5.36.

2. Principal tensile strain at which the tension stiffening ends.

The thickness of the region of concrete around reinforcement or the level of discontinuity represents the influence of the same property i.e. how the tensile resistance of concrete decays away from the reinforcement. The thickness of the concrete region around the reinforcement, Figure 5.35 was taken as 20 mm, 25 mm, 30 mm and 35 mm. The level of discontinuity, Figure 5.36, was taken as 0.25 f_t, 0.4 f_t, 0.75 f_t and f_t.

The tensile strain at which tension stiffening ends, should coincide with the yielding of the reinforcement. Since the reinforcement and the principal strain directions do not coincide it is difficult to match the principal tensile strain in concrete with the yield strain of the reinforcement especially for orthotropically reinforced elements. However, the second parameter used to study the effect of tension stiffening was the magnitude of principal tensile strain expressed as a proportion of the cracking strain at which the tension stiffening must end i.e. the length of the falling branch, $\xi\varepsilon_i$. To study the effect the length of the falling branch of tension stiffening curve, several models were adopted as shown in Figure 5.37.

5.5.1.1 Response in In-plane Shear

To study the effect of tension stiffening on in-plane shear, using the variation of parameters described above panel PV 27 from reference 1 has been used. Figure 5.38 shows a comparison of the results of the analyses, for different thickness of the zone with respect to tension stiffening, with the experimental results. It is evident from the Figure 5.38 that when the zone is equal to the full thickness of the element i.e. 70 mm, the agreement with the experimental results is best. Hence the full thickness of the concrete has been used for all the analyses of elements under in-plane loads. The tensile response of concrete while using the full thickness is analogous to model 1 of Figure 5.36 in which there is no discontinuity in the tensile response at the level of cracking. It can be further observed from Figure 5.38 that, after cracking, as the thickness of the tension zone decreases the response becomes less stiff. This is

because the tensile resistance offered by the concrete becomes less, thus for a given load, larger tensile force i.e. larger area of tension stiffening is required. This leads to higher strains and hence the less stiff response.

Figure 5.39 shows the comparison of the experimental results with the tension stiffening models of varying lengths of falling branch. Once again it is obvious from the Figure 5.39 that as the length of the tail decreases, the response, as expected becomes less stiff. This less stiff response is due to the reason given in the preceding paragraph. Too long a falling branch can effect the ultimate load capacity, therefore, tension stiffening must end prior to the ultimate load, if the failure has been initiated by the yielding of steel. This can be observed in the responses using a length of the tail greater than $30\varepsilon_t$ and affected the ultimate load significantly. It can also be observed that when the tension stiffening ends, the response becomes similar for all the models.

5.5.1.2 Response in Pure Torsion

The tensile resistance of concrete plays a significant role in the post cracking response of an element when subjected to pure twisting moment in a similar fashion as discussed in Section 5.5.1.1. However, as the curvature increases due to the increase in loads, the tensile resistance offered by the concrete decreases. Due to the increase in the curvature the compression resistance increases and the moment of resistance increases. With the increase in the curvature the depth of the neutral axis reduces, thus increasing the lever arm. This phenomena is elaborated through Figure 5.40.

To study the effect of tension stiffening in the case of pure twisting moments, slab 9 of reference 5 has been used.

The two tension stiffening models as described earlier have been used. The thickness of the concrete region around the reinforcement in which tension stiffening occurs has been kept same for the top and the bottom reinforcement and was varied from 30 mm to 60 mm. Figure 5.41 shows the response of slab 9^5 using different thickness of concrete region around the reinforcement in the tension stiffening model. It is evident from the Figure 5.41 that the response is significantly affected by varying the thickness of the around the concrete in the post cracking response. The response after cracking becomes less stiff as the depth of the tension zone decreases. Figure 5.42 shows the principal stress distribution in concrete at the same level of twisting curvature, using different thickness of concrete region around the reinforcement. As the thickness of the concrete region increases the neutral axis moves towards the centre of the element, which decreases the lever arm but on the other hand the amount of tensile force increases significantly. The decrease in the lever arm is not as significant as the increase in the tensile resistance of concrete and hence, a higher moment of resistance has been achieved. This leads to a stiffer response.

The effect of the length of the falling branch, $\xi\varepsilon_t$, was also studied by varying $\xi\varepsilon_t$ from $20\varepsilon_t$ to $100\varepsilon_t$. Figure 5.43 shows the effect of the length of the falling branch. A similar pattern has been observed as in case of in-plane shear, Section 5.5.1.1, that the model having the longest tail showed a stiffer response. This stiff response once

again is due to the reason given in the preceding paragraph for the stiffer response due to the increase in the tension stiffening zone. Since the failure slab 9^5 was due to the crushing of the concrete not by the yielding of the steel, therefore, $100\varepsilon_t$ has been adopted in the final analysis to match the principal tensile strain in concrete with the yielding of the reinforcement.

From the discussion in the preceding paragraphs, it can be concluded that tension stiffening is a complex phenomena that effects the post cracking response of reinforced concrete elements significantly. It was found[7,14] to be dependent on the bond properties, spacing of reinforcement, diameter of reinforcing steel and thickness of the element. The contribution of concrete in tension decays as the integration point moves away from the reinforcement. An attempt have been made in the present study to model this decaying phenomena by dividing the tension zone into two part. It was found the zone of influence in which tension stiffening is effective is about 35 mm for both the loading conditions i.e. in-plane shear and pure twisting moment. The ideal way to model the tensile response of concrete would be to include the bond properties of the concrete and the reinforcement and to models these properties. However, the practical approach to model tension stiffening would be to divide the tension region of concrete into two zones and model tensile response separately for both the zones as adopted in this study.

5.5.2 EFFECT OF COMPRESSION SOFTENING

A reinforced concrete element when subjected to a state of compressive stress and tensile strain in the two principal directions, the strength as well as stiffness in compression reduces drastically. Extensive experimental and analytical work has been done by the researchers[15,16,17,18,19] to quantify this property of reinforced concrete.

As mentioned in Section 3.2.1.2, Chapter 3, model A, Vecchio and Collins[18] has been used in the present study. The softening parameter, β, proposed in the reference 18 is a function of the compressive strength and the ratio of principal tensile to principal compressive strains. The compressive strength of concrete has no effect on β if the strength is less than 30 MPa. But as the strength increases over and above 30 MPa, the value of β reduces, Figure 5.44. The ratio of the principal tensile to principal compressive strains, $\varepsilon_1 / \varepsilon_2$, also significantly affects β if $\varepsilon_1 / \varepsilon_2 > 4$ and β decreases exponentially with an increase in $\varepsilon_1 / \varepsilon_2$. But if $\varepsilon_1 / \varepsilon_2 \leq 4$, β remains constant.

It was observed during this study that in case of pure twisting the adopted model over estimated the softening phenomena. The reason of this over estimation of softening may be due to the fact that the model was developed for in-plane loading conditions. Under in-plane loading the state of stress and strain are uniform through the depth of the element. Cracks thus developed pass all the way through the depth of the element. The compression orthogonal to the crack direction is carried by the concrete in between the cracks. These compression struts are isolated from each other and may be

too slender for the compressive load they carry as their width is restricted by the spacing of the cracks. The compression strut may crush as well as buckle due to its slenderness, thus reducing the compressive strength and stiffness of the concrete.

In the case of pure twisting moment, the strain and the stress state are not uniform across the depth. In one principal direction the state of stress varies from compression at the top face to tension at the bottom face and vice versa in the other principal direction. The depth of cracks are thus restricted to the tension zone only. The compression in the orthogonal direction is then carried by the cracked concrete. These compression struts are not isolated from each other but they are held in place due to the compression above or below the neutral axes, Figure 5.45. Thus the softening will be less than calculated on the basis of in-plane loading.

To study the effect of variation of β in case of pure twisting, once again slab 9 from reference 5 was used. The softening parameter, β, was varied from the value calculated from the model[18], Section 3.2.1.2, Chapter 3, to a value which was 20% higher than calculated from the model. Figure 5.46 shows the comparison of the results using different values of β with the experimental results. The response in which the value of β calculated from the model was used showed an ultimate strength 15% lower than the experimental ultimate strength, whereas, the model with 10% and 20% higher values of β showed an ultimate strengths 8% and 2% lower than the actual ultimate strength. Thus the value of β increased by 20% exhibited a reasonable estimate of actual softening and was used through out the study. The effect of variation of compressive strength on the overall response is effectively same as the

variation of the value of β. In the over reinforced slab elements the compressive strength plays a significant role and the post cracking response is significantly affected by the compressive strength, Figure 5.46.

5.5.3 EFFECT OF AREA OF STEEL

The area of reinforcement plays a significant role in the overall response of reinforced concrete elements subjected to any combination of loading. The effect of the area of reinforcement on the behaviour of elements subjected to either in-plane shear or pure twisting moment has been mentioned in Section 5.5.1.

5.5.3.1 Response in In-plane Shear

In order to study the effect of the area of reinforcement on reinforced concrete under in-plane shear, panel PV 27 from reference 1 has been selected. The area of steel in one direction was kept constant (the same as in the original experiment) and the reinforcement ratio was varied from 0.893% to 0.1% of the overall depth of the element, in the other direction. The details of the areas of steel used in the study are given in Table 5.7. The response of the element with different amounts of reinforcement are shown in Figure 5.47.

The reinforcement does not contribute prior to cracking as discussed in Section 5.4.1 in such loading as can be observed from Figure 5.47. In the post cracking region, the response of the element is stiffer if an increased area of steel is provided. The stiffer

response is mainly due to the fact that at a given strain an element can resist more tensile force.

5.5.3.2 Response in Pure Torsion

In order to investigate the effect of the area of steel for a slab element loaded with pure twisting moment, slab 9 from reference 5 has been analysed for six different combinations of area of steel. Table 5.8 gives the details for the areas of reinforcement used in these analyses. Figure 5.48 shows the response of the slab element with different amounts of steel.

The area of reinforcement has no effect to cracking in the case of pure twisting and this is evident from the pre-cracking responses for all the cases shown in Figure 5.48. This fact has been discussed in Section 5.4.1.

Increasing area of reinforcement increases the ultimate moment capacity of the element, as expected. Increasing the amount of steel can also change the mode of failure of the slab element. For case 1 which has the maximum area of steel (1% in each direction), the slab element fails due to crushing of concrete rather than the yielding, whereas for 1% reinforcement ratio, the slab element with no twisting moment would fail due to the yielding of the reinforcement.

The ductility decreases with the increase in the amount of steel owing to the fact that the reinforcement is less stressed with the increase in the area of steel. For cases 2-6

the element fails due to yielding of steel, however, as expected ductility decreases as the reinforcement ration increases. The decrease in ductility thus reduces the ability for moment redistribution. For case 1 the element behaves as an over reinforced section with no possibility of moment redistribution.

References

1 Vecchio, F and Collins, MP, The response of reinforced concrete panels to in-plane shear and normal stress, Publication No. 82-03, Department of Civil Engineering, University of Toronto, March 1982, 332 p.

2 Bhide, SB and Collins, MP, Reinforced concrete elements in shear and tension, Publication No, 87-02, Department of Civil Engineering, University of Toronto, January 1987, 147 p.

3 Kirschner, U and Collins, MP, Investigating the behaviour of reinforced concrete shell elements, Publication No. 86-09, Department of Civil Engineering, University of Toronto, September 1986, 83 p.

4 Samad, AAA, The response of reinforced concrete slabs subjected to biaxial bending and twisting moments, PhD Thesis, University of Manchester, June 1994, 354 p.

5 Marti, P, Leesti, P and Khalifa, WU, Torsion test on reinforced concrete slab elements, Jnl. of St. Eng., ASCE, vol. 113, no. 5, May 1987, pp 994-1010.

6 Marti, P, Kong, K, Response of reinforced concrete slab elements to torsion, Jnl. of St. Eng., ASCE, vol. 113, no. 5, May 1987, pp 976-993.

7 Clark, LA and Speris, DM, Tension stiffening of reinforced concrete beams under short term load, Technical Report No. 42.521, Cement and Concrete Association, London, July 1978.

8 Gilbert, RI and Warner, RF, Tension stiffening in reinforced concrete slabs, Jnl. of St. Div., ASCE Proceedings, vol. 4, no. ST12, December 1978, pp 1885-1900.

9 Cerreira, DJ and Chu, KH, Stress-strain relationship for concrete in tension, Jnl. of ACI, Proceeding, vol. 83, no. 1, Jan-Feb. 1986, pp 21-28.

10 Oduymi, TOS and Clark, LA, Tension stiffening in longitudinal sections of circular voided concrete slabs, Proceeding of Institution of Civil Engineers, Part 2, no. 83, December 1987, pp 861-874.

11 Link, RA, Elwi, AE and Scanlon, A, Biaxial tension stiffening due to generally oriented reinforcing layers, Jnl. of Eng. Mech., ASCE, vol. 115, no. 8, August 1989, pp 1647-1662.

12 Hsu, TTC and Zhang, LX, Tension stiffening in reinforced concrete membrane elements, ACI St. Jnl., vol. 93, no. 1, Jan-Feb. 1996, pp 108-115.

13 Pitt, DC, Composite laminate modelling of reinforced concrete elements, M.Sc. Thesis, Heriot-Watt University/ Ecole Polytechnique Federale De Lausanne, September 1995, 77 p.

14 Clark, LA and Cranston, WB, The influence of spacing on tension stiffening in reinforced concrete slabs, Advances in Concrete Slab Technology, Proceedings of the International Conference on Concrete Slabs, Dundee, April 1979, pp 118-128.

15 Cervenka, V, Constitutive model for cracked reinforced concrete, ACI St. Jnl., vol. 82, no. 6, Nov-Dec. 1985, pp 877-882.

16 Vecchio, FJ and Collins, MP, The modified compression-filed theory for reinforced concrete elements subjected to shear, ACI St. Jnl., vol. 83, no. 2, Mar-Apr. 1986, pp 219-231.

17 Hsu, TTC, Softened truss model theory for shear and torsion, ACI St. Jnl., vol. 85, no. 6, Nov-Dec. 1988, pp 624-635.

18 Vecchio, FJ and Collins, MP, Compression response of cracked reinforced concrete, Jnl. of St. Eng., ASCE, vol. 119, no. 12, December, 1993, pp 3590-3610.

19 Belarbi, A and Hsu, TTC, Constitutive laws of softened concrete in biaxial tension-compression, ACI St. Jnl., vol. 92, no. 5, Sept-Oct. 1995, pp 562-573.

Table 5.1: Section and material properties and loading ratios of Vecchio and Collins[1] panels.

No	$F_x:F_y:F_{xy}$	A_{sx} (mm²/mm)	A'_{sx} (mm²/mm)	A_{sy} (mm²/mm)	A'_{sy} (mm²/mm)	f'_c (MPa)	f_t (MPa)
PV 22	0:0:1	0.625	0.625	0.532	0.532	19.6	2.42
PV 26	0:0:1	0.625	0.625	0.355	0.355	21.3	2.00
PV 27	0:0:1	0.625	0.625	0.625	0.625	20.5	2.04
PV 24	0.83:0.83:1	0.625	0.625	0.625	0.625	23.8	4.97
PV 28	-0.32:-0.32:1	0.625	0.625	0.625	0.625	19.0	1.66

Table 5.2: Comparison at ultimate load.

No	$F_x:F_y:F_{xy}$	V_{exp} (N/mm)	V_{ana} (N/mm)	Difference (%)
PV1	0:0:1	561.4*	582.8	3.80
PV2	0:0:1	81.2*	76.1	-6.27
PV3	0:0:1	214.9*	329.1	53.13
PV4	0:0:1	202.3	200.8	-0.75
PV5	0:0:1	296.8*	503.4	69.60
PV6	0:0:1	318.5	336.5	5.65
PV7	0:0:1	476.7*	572.9	20.18
PV8	0:0:1	466.9*	521.5	11.69
PV9	0:0:1	261.8	234.0	-10.60
PV10	0:0:1	277.9	290.6	4.56
PV11	0:0:1	249.2	255.5	2.51
PV12	0:0:1	219.1	201.5	-8.02
PV13	0:0:1	140.7	153.0	8.74
PV14	0:0:1	366.8*	394.8	7.63
PV16	0:0:1	149.8	142.1	-5.1
PV18	0:0:1	212.8	196.3	-7.74
PV19	0:0:1	276.5	276.6	0.02
PV20	0:0:1	298.2	314.5	5.47
PV21	0:0:1	352.1	378.9	7.61
PV22	0:0:1	424.9	386.4	-9.05
PV23	0.39:0.39:1	620.9	492.4	-20.69
PV24	0.83:0.83:1	555.8	445.3	-19.89
PV25	0.69:0.69:1	638.4	443.4	-30.54
PV26	0:0:1	378.7	399.9	5.59
PV27	0:0:1	444.5	393.5	-11.48
PV28	-0.32:-0.32:1	406.1	350.0	-13.78
			Average	2.39
			St. dev.	20.83

* premature failure

Table 5.3: Section and material properties and loading ratios of Bhide and Collins[2] panels.

No	F_x:F_y:F_{xy}	A_{sx} (mm^2/mm)	A'_{sx} (mm^2/mm)	A_{sy} (mm^2/mm)	A'_{sy} (mm^2/mm)	f'_c (MPa)	f_t (MPa)	V_{exp} (N/mm)	V_{exp} (N/mm)	Diff (%)
PB 12	0:0:1	76	76	0	0	23.1	1.33	95.76	89.13	-6.92
PB 18	0:0:1	154	154	0	0	25.3	1.62	115.4	109.94	-4.70
PB 10	-5.9:0:1	76	76	0	0	24.0	0.31	39.41	38.62	-2.00
									Avg	-4.54
									St. dev	2.46

Table 5.4: Section and material properties and loading ratios of Kirschner and Collins[3] panels.

No	F_{xy}:M_x	A_{sx} (mm^2/mm)	c_x (mm)	A'_{sx} (mm^2/mm)	c'_x (mm)	A_{sy} (mm^2/mm)	c_y (mm)	A'_{sy} (mm^2/mm)	c'_y (mm)	f'_c (MPa)	f_t (MPa)	V_{exp} (N/mm)	V_{ana} (N/mm)	Diff (%)
SE1	1:0	417.5	21	417.5	21	139.4	43	139.4	43	42.5	4.4	1927	2019.17	4.81
SE5	1:0	417.5	21	417.5	21	417.5	43	417.5	43	25.9	2.4	547000	509111.5	-6.93
SE3	0:1	417.5	21	417.5	21	139.4	43	139.4	43	46.1	4.4	961	883.53	-8.06
SE4	1:500	417.5	21	417.5	21	139.4	43	139.4	43	42.2	4.4	2307	1898.98	-17.89
													Avg	-6.79
													St. dev	9.21

Table 5.5: Section and material properties and loading ratios for slabs tested at the University of Manchester[4].

No	M_x:M_y:M_{xy}	A_{sx} (mm^2/mm)	c_x (mm)	A'_{sx} (mm^2/mm)	c'_x (mm)	A_{sy} (mm^2/mm)	c_y (mm)	A'_{sy} (mm^2/mm)	c'_y (mm)	f'_c (MPa)	f_t (MPa)	M_{exp} (kN-m/m)	M_{ana} (kN-m/m)	Diff (%)
4	1:1:0	1.413	25	-	-	1.413	40	-	-	46	3.5	79	83.07	5.15
5	0:1:0	1.413	40	-	-	1.413	25	-	-	48	4.2	81	94.55	16.72
7	-1:1:0	-	-	1.413	25	1.413	25	-	-	40	3.9	83	88.45	6.57
8	0.5:1:0	1.413	40	-	-	1.413	24	-	-	45	4.0	86	95.70	11.27
9	0:1:0	1.413	38	-	-	1.413	25	-	-	52	4.0	86	95.12	10.60
10	1:1:0	0.707	41	-	-	1.413	28	-	-	47	3.3	43	42.95	-0.11
11	1:1:0	0.707	41	-	-	0.707	28	-	-	46	3.9	40	42.91	7.28
12	0:0:1	1.413	40	1.413	25	1.413	40	1.413	25	50	5.0	45	57.03	26.73
13	1:1:0.25	1.413	40	1.413	25	1.413	40	1.413	25	49	4.2	62.5	69.79	11.66
													Avg	10.65
													St. dev	7.68

Table 5.6: Section and material properties of Marti et al[5] slabs.

No	A_{sx} (mm^2/mm)	c_x (mm)	A'_{sx} (mm^2/mm)	c'_x (mm)	A_{sy} (mm^2/mm)	c_y (mm)	A'_{sy} (mm^2/mm)	c'_y (mm)	f'_c (MPa)	f_t (MPa)	M_{exp} (kN-m/m)	M_{ana} (kN-m/m)	Diff (%)
1	0.5	16	0.5	16	0.5	27	0.5	27	46.7	3.69	44.4*	48.41	9.03
2	1.0	16	1.0	16	1.0	27	1.0	27	36.2	3.72	69.5*	73.19	5.31
3	2.0	18	2.0	18	2.0	34	2.0	34	37.5	3.35	93.8*	85.59	-8.75
4	1.0	16	1.0	16	0.5	27	0.5	27	44.7	4.63	50.8*	61.72	21.5
5	2.0	18	2.0	18	0.5	32	0.5	32	35.6	3.38	60.6*	59.16	-2.38
6	2.0	18	2.0	18	1.0	34	1.0	34	23.3	2.74	63.6	56.28	-11.5
7	0.5	16	0.5	16	0.5	27	0.5	27	44.4	4.39	42.5	42.76	0.61
8	2.0	18	2.0	18	0.5	32	0.5	32	49.1	4.51	64.8	64.09	-1.10
9	2.0	18	2.0	18	2.0	34	2.0	34	44.4	3.90	101.5	99.37	-2.10
												Avg	1.17
												St. dev	9.87

* premature corner failure

Table 5.7: Reinforcement ratios used for parametric study for in-plane shear.

Case No	ρ_{sx} (%)	ρ'_{sx} (%)	ρ_{sy} (%)	ρ'_{sy} (%)
1	0.893	0.893	0.893	0.893
2	0.893	0.893	0.75	0.75
3	0.893	0.893	0.5	0.5
4	0.893	0.893	0.25	0.25
5	0.893	0.893	0.1	0.1

Table 5.8: Reinforcement ratios used for parametric study for twisting moment.

Case No	ρ_{sx} (%)	ρ'_{sx} (%)	ρ_{sy} (%)	ρ'_{sy} (%)
1	1	1	1	1
2	1	1	0.5	0.5
3	1	1	0.25	0.25
4	0.5	0.5	0.5	0.5
5	0.5	0.5	0.25	0.25
6	0.25	0.25	0.25	0.25

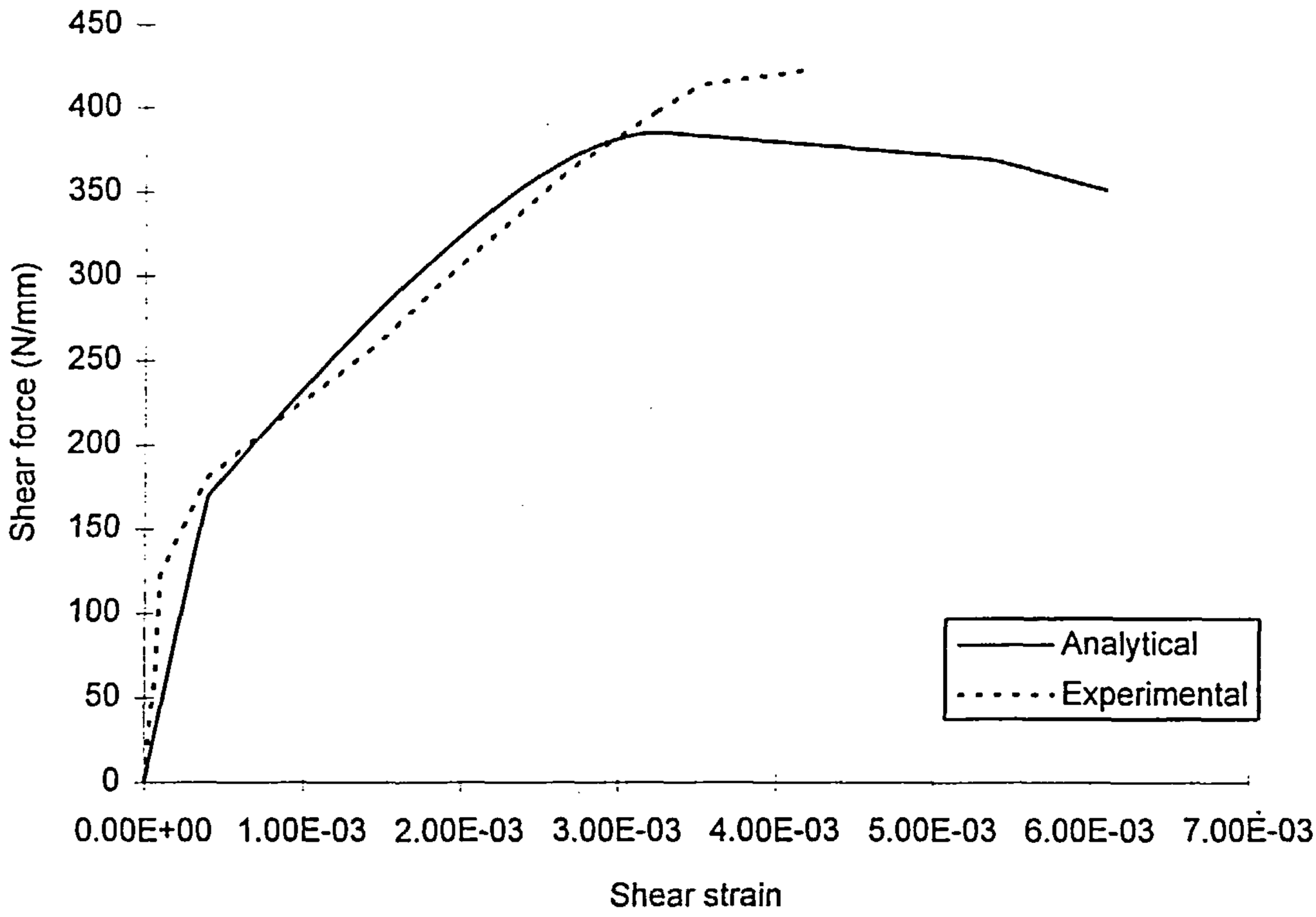

Figure 5.1: Comparison of experimental and analytical results of PV 22

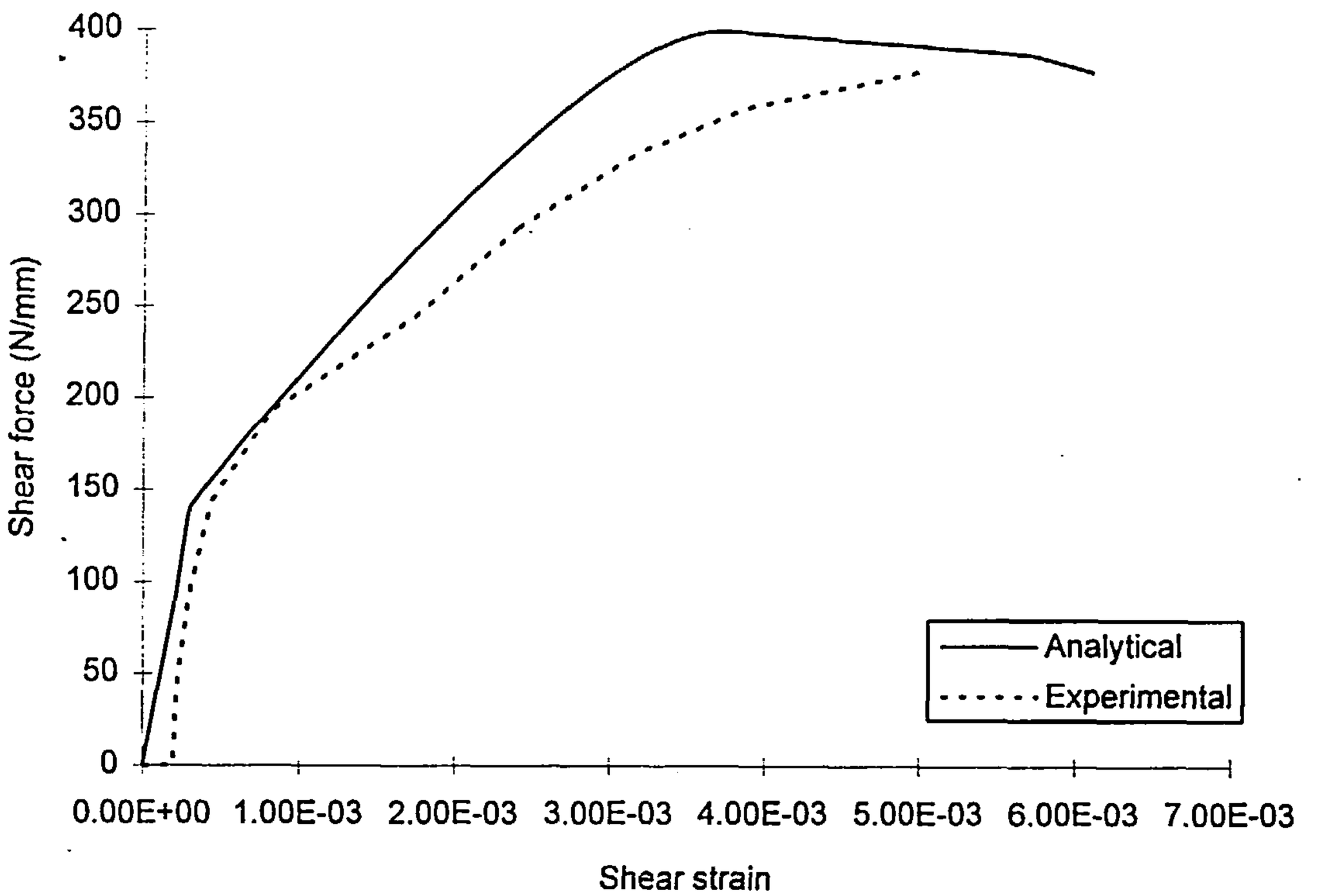

Figure 5.2: Comparison of experimental and analytical results of PV 26

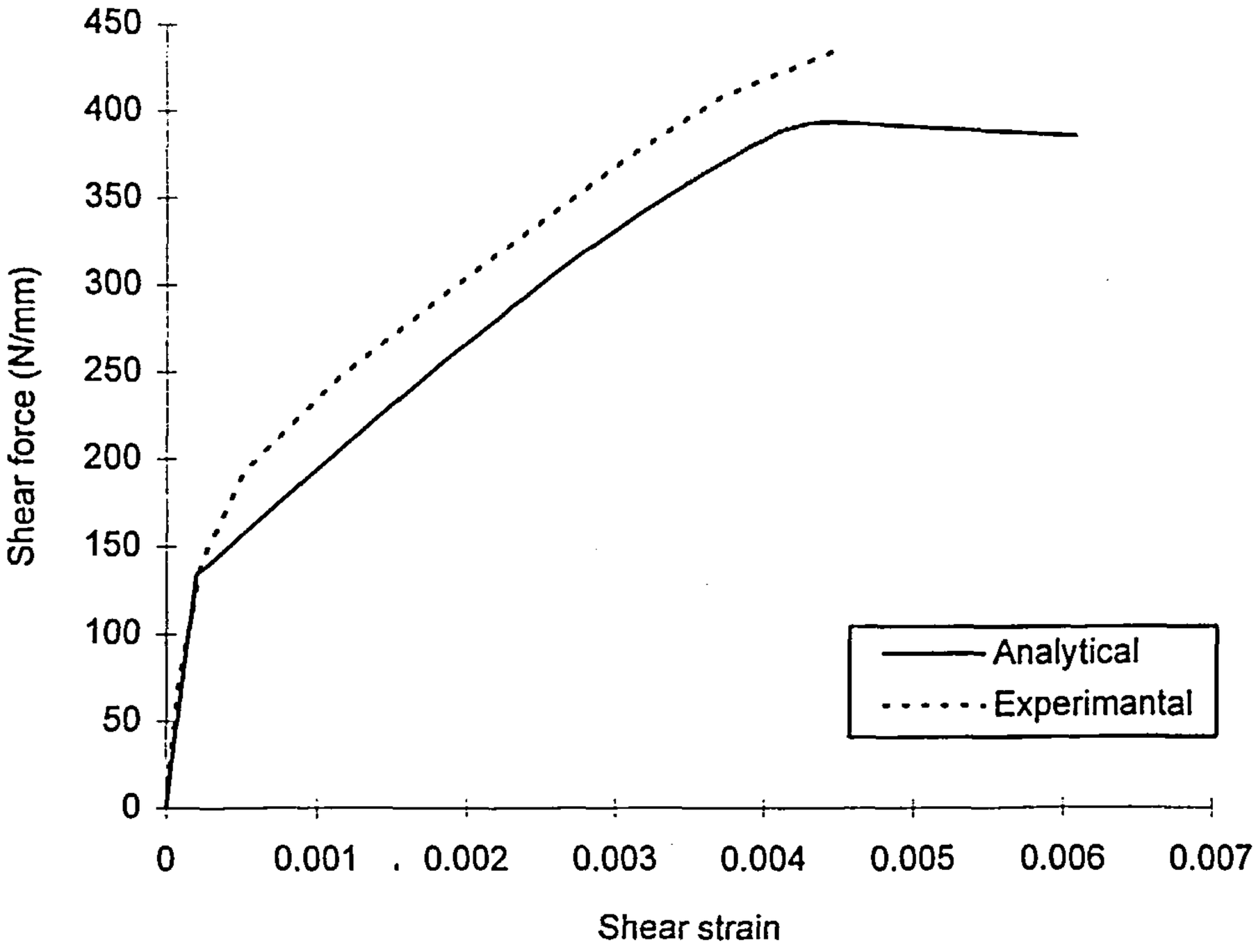

Figure 5.3: Comprison of experimental and analytical results of PV 27

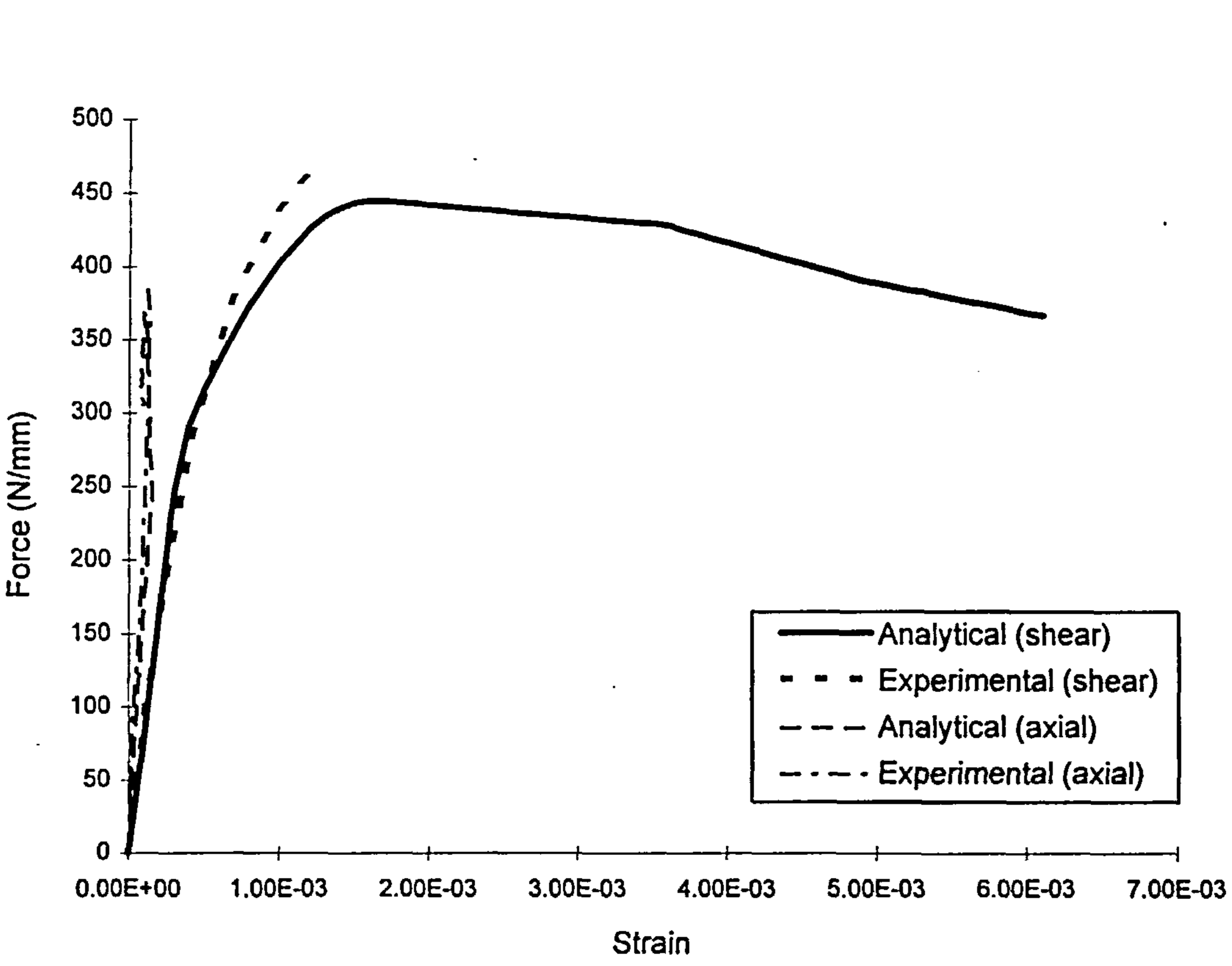

Figure 5.4: Comparison of experimental and analytical results of PV 24

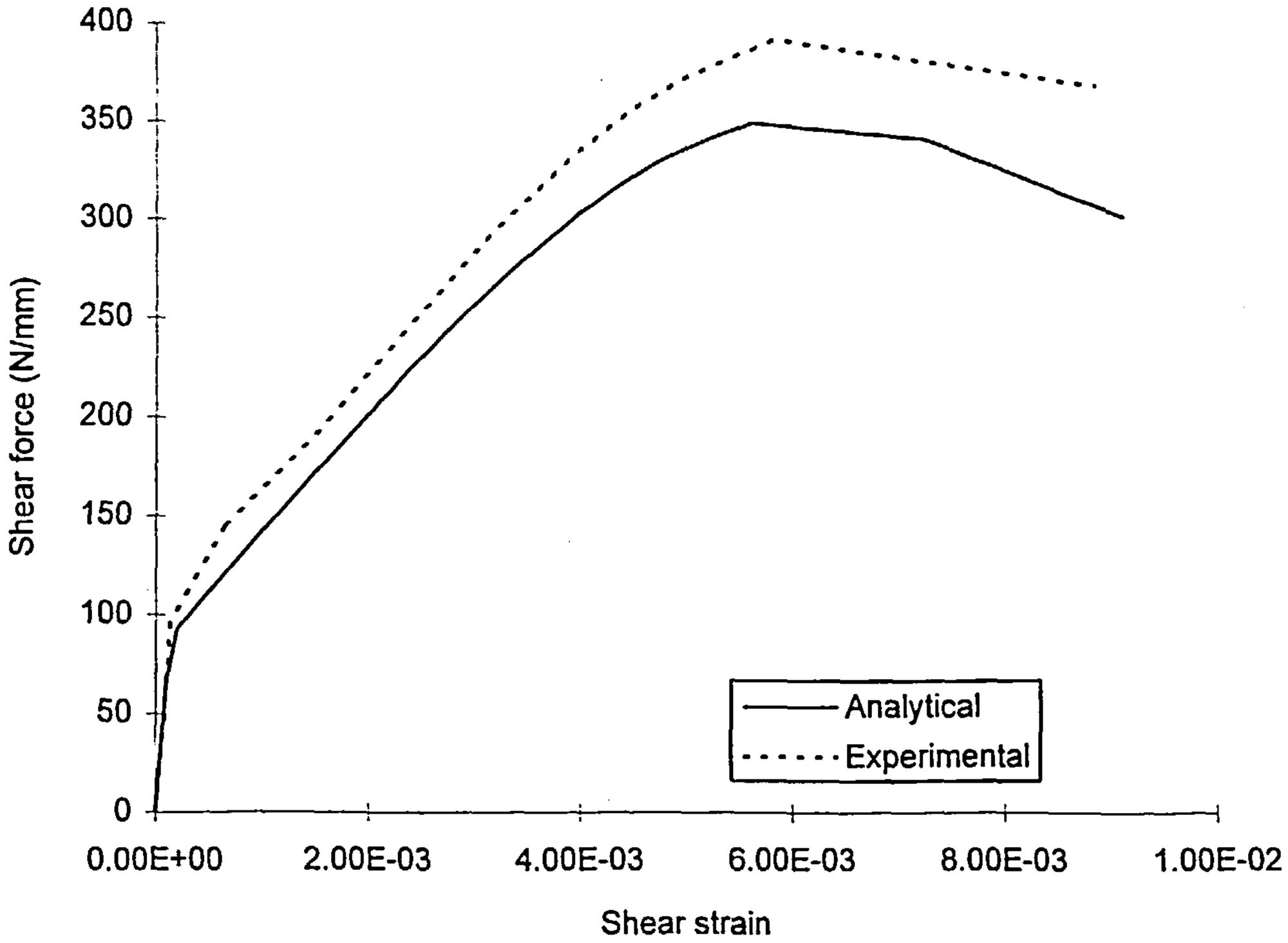

Figure 5.5: Comparison of experimental and analytical results of PV 28

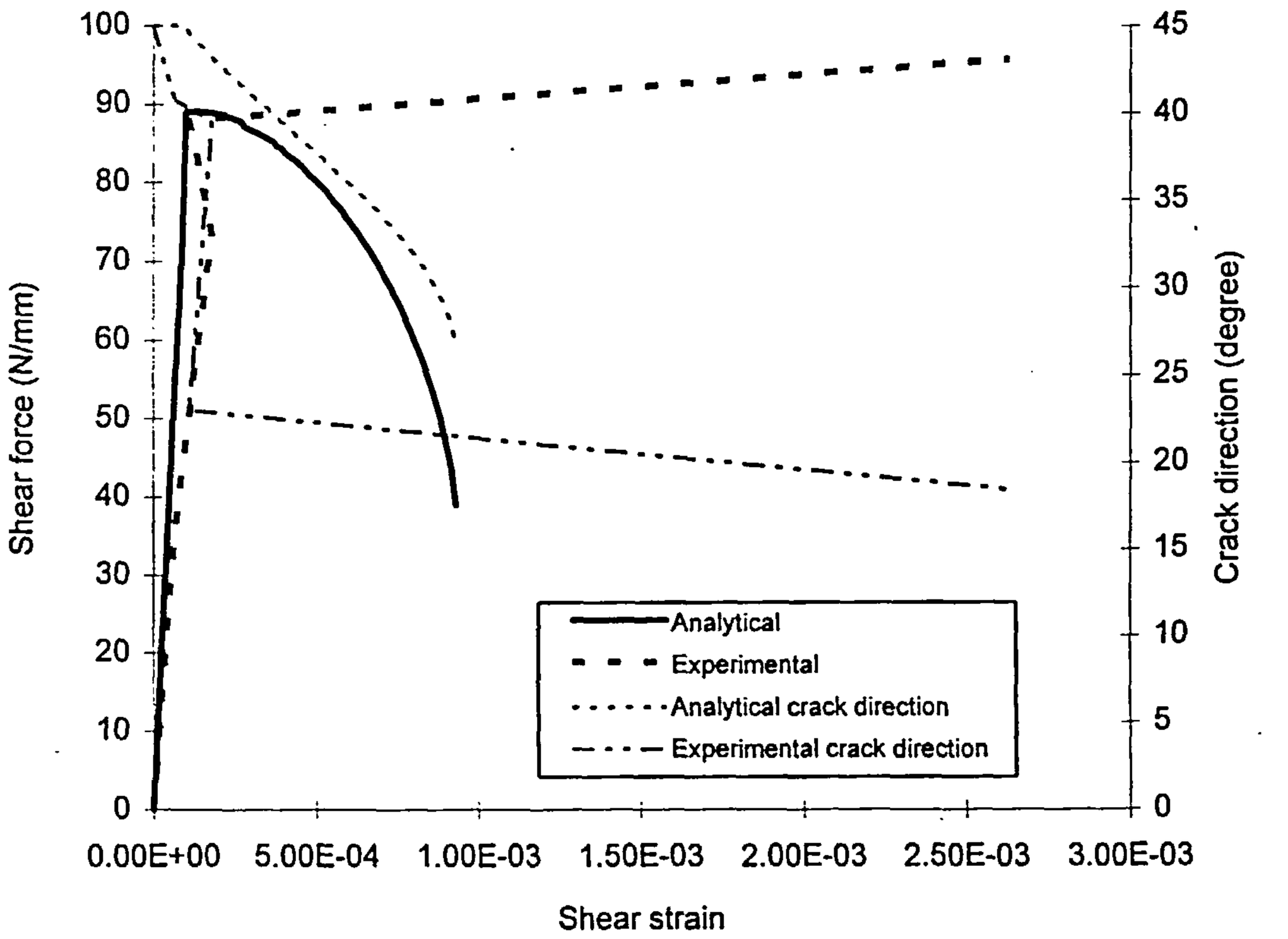

Figure 5.6: Comparison of experimental and analytical results of PB 12

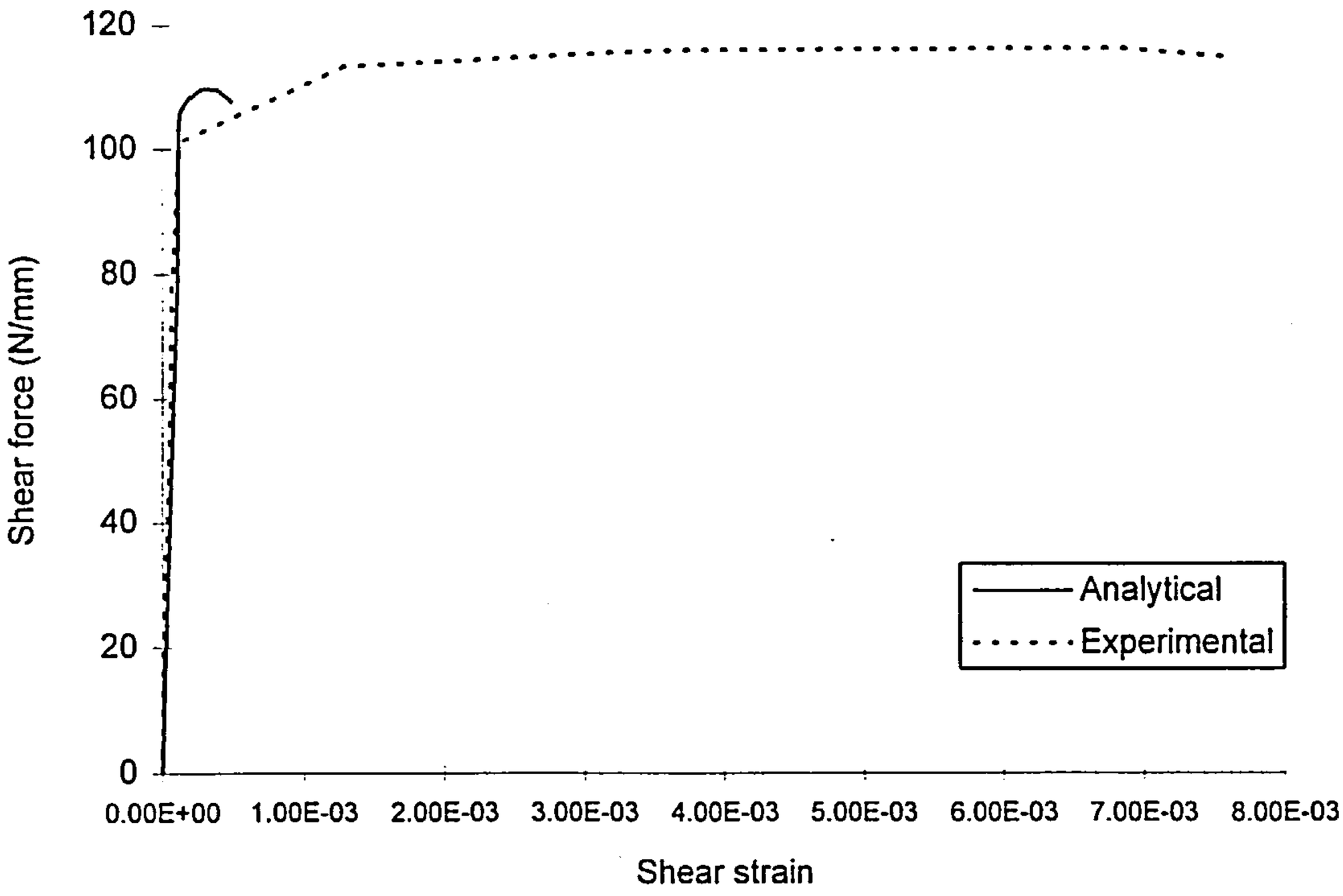

Figure 5.7: Comparison of experimental and analytical results of PB 18

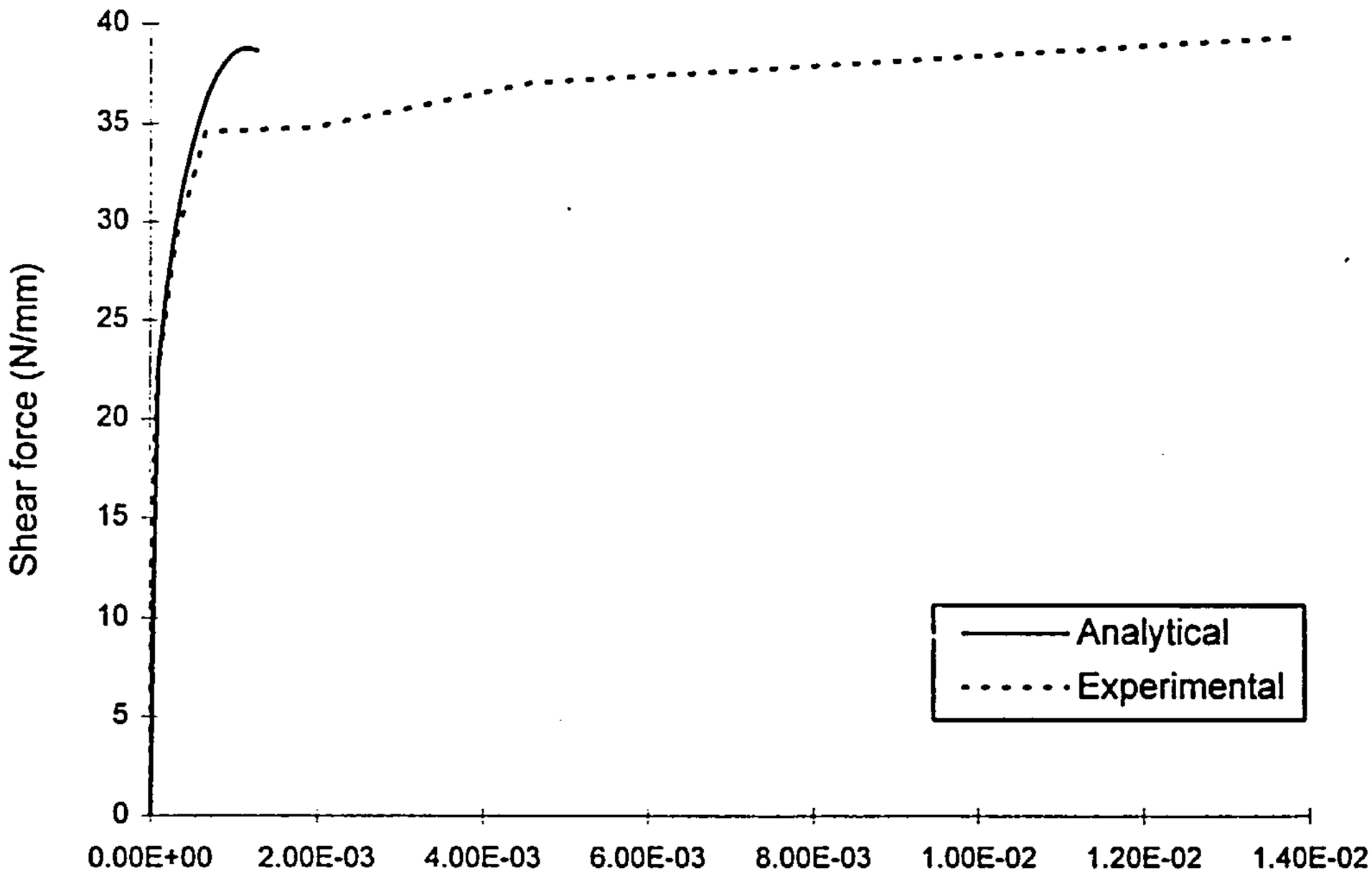

Figure 5.8: Comparison of experimental and analytical results of PB 10

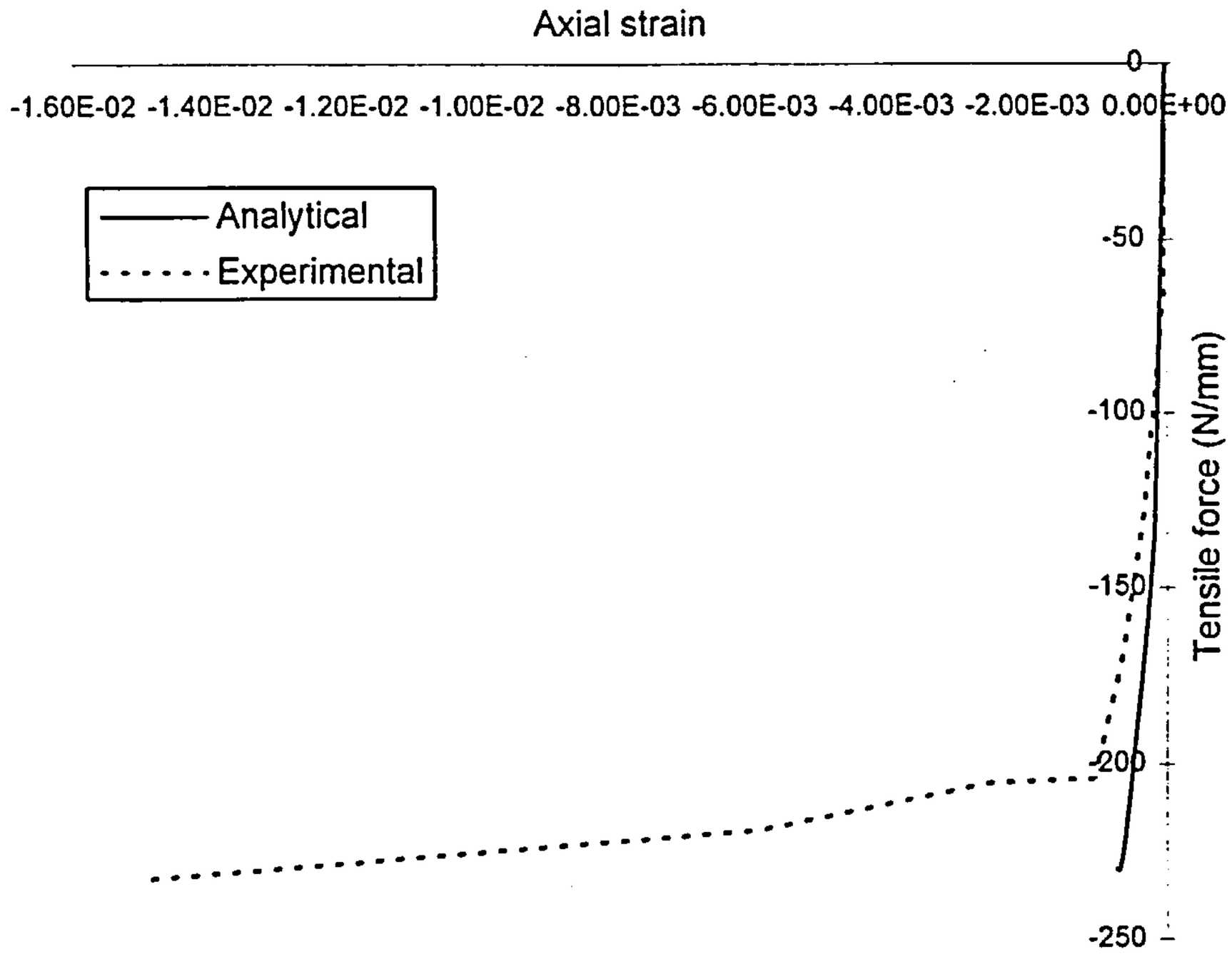

Figure 5.9: Comparison of experimental and analytical results of PB 10

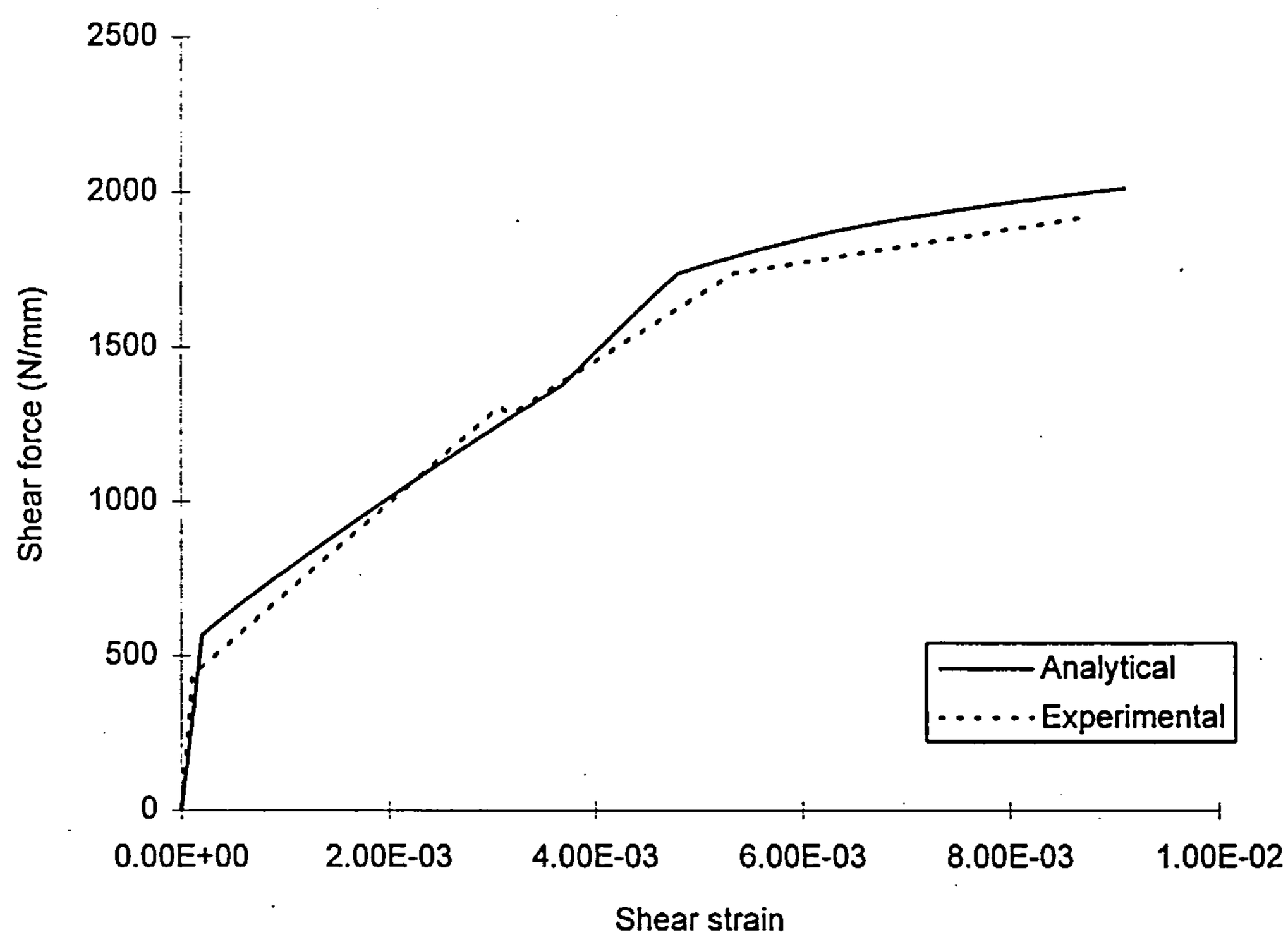

Figure 5.10: Comparison of experimental and analytical results of SE 1

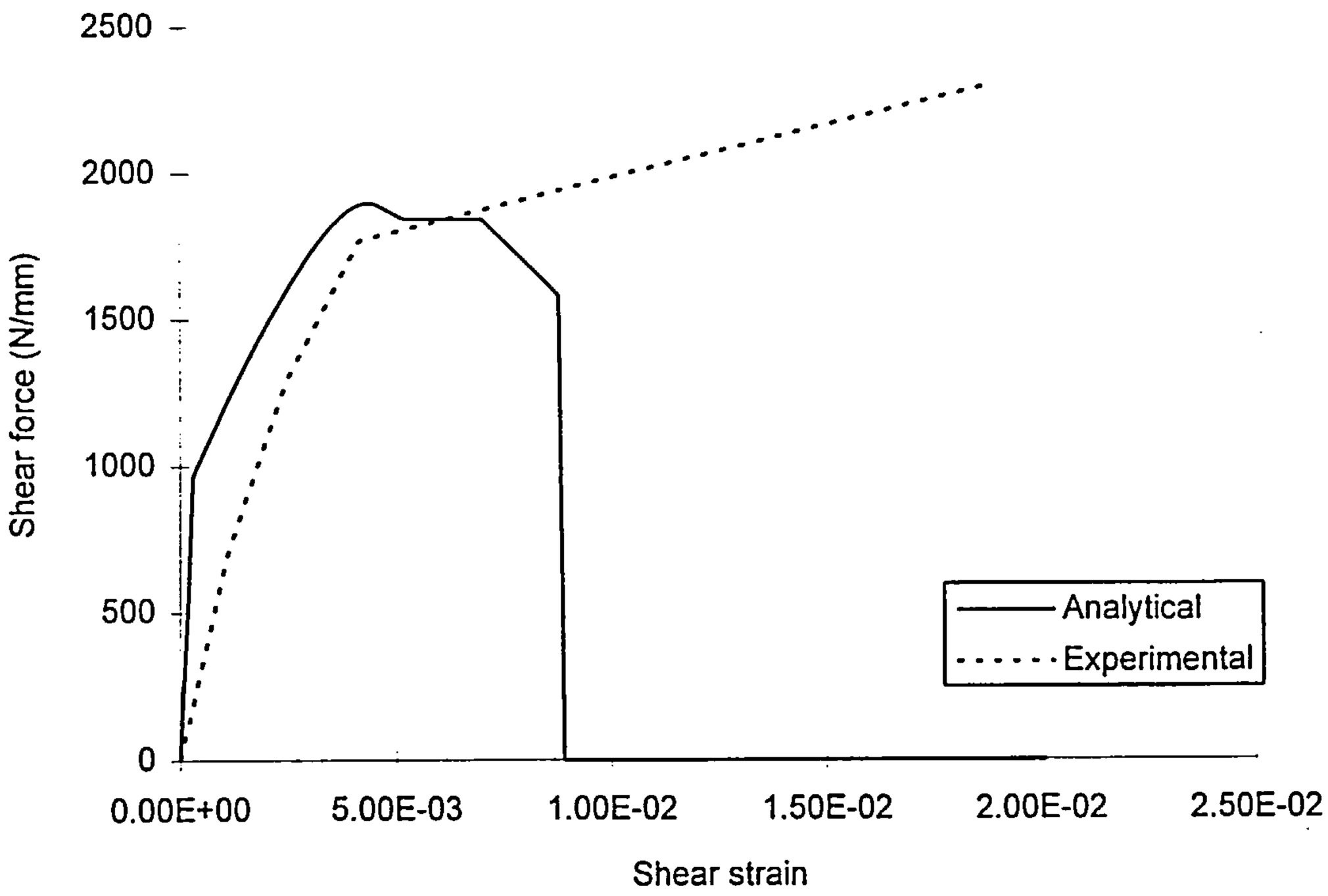

Figure 5.11: Comparison of experimental and analytical results of SE 5

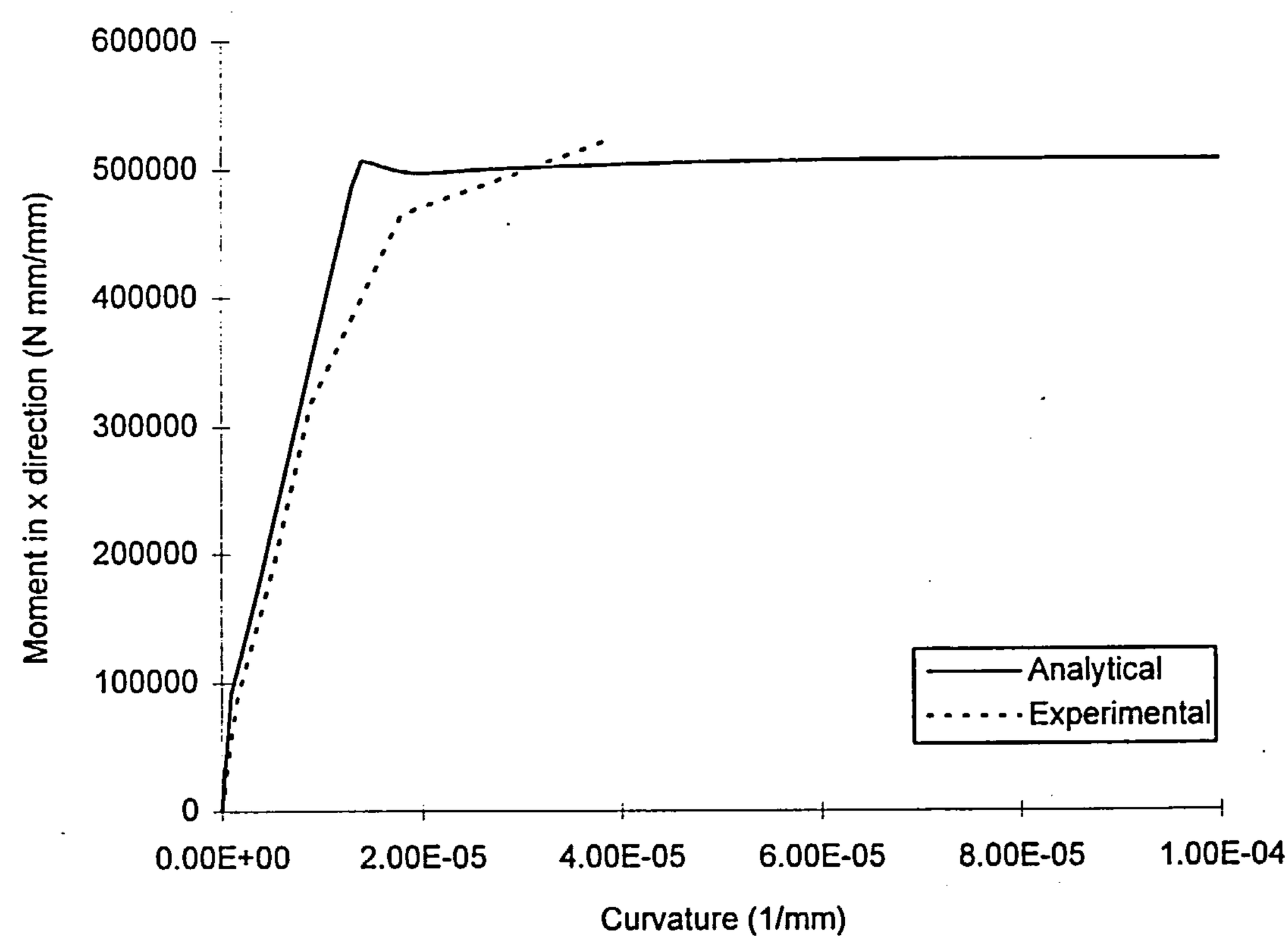

Figure 5.12: Comparison of experimental and analytical results of SE 3

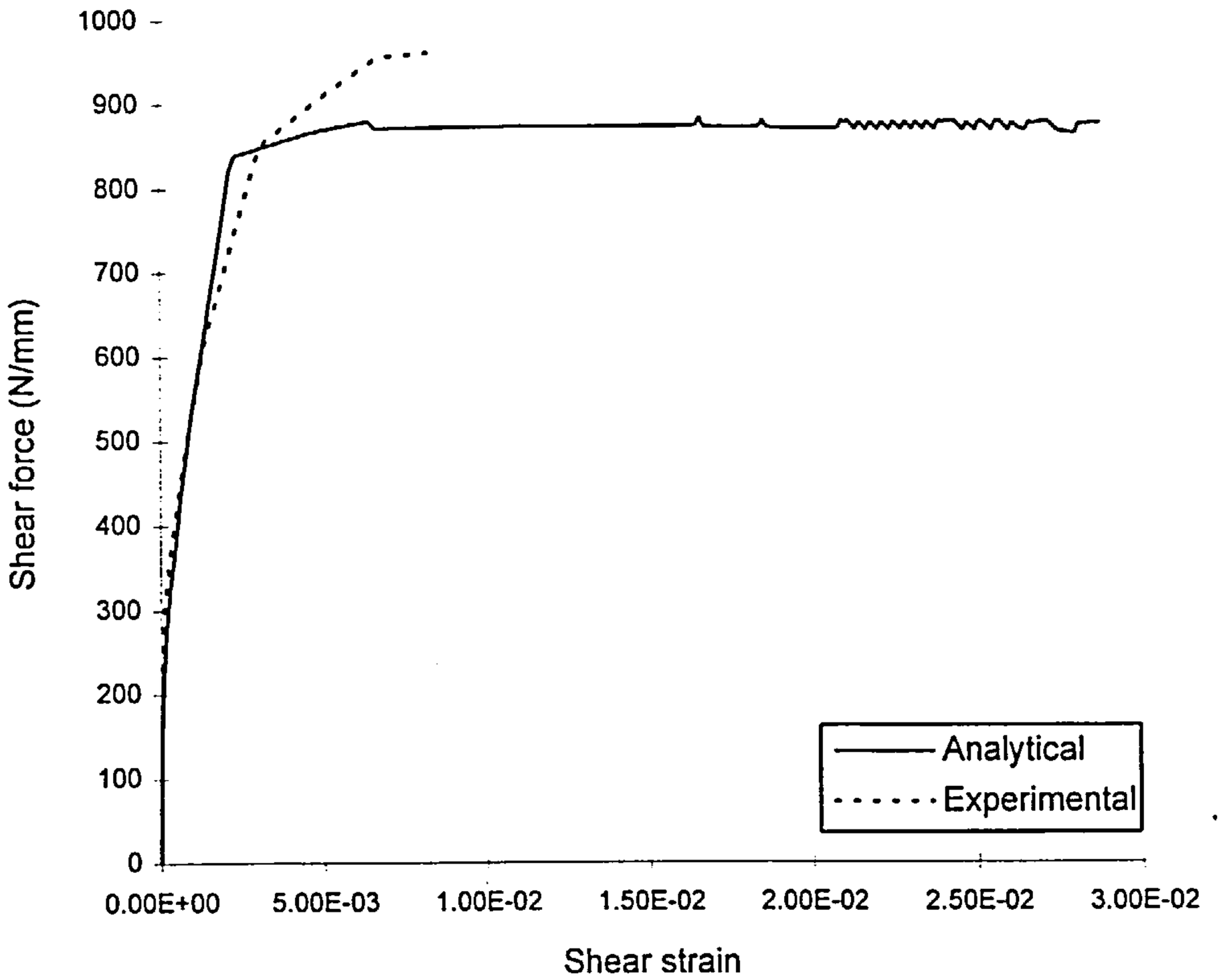

Figure 5.13: Comparison of experimental and analytical results of SE 4

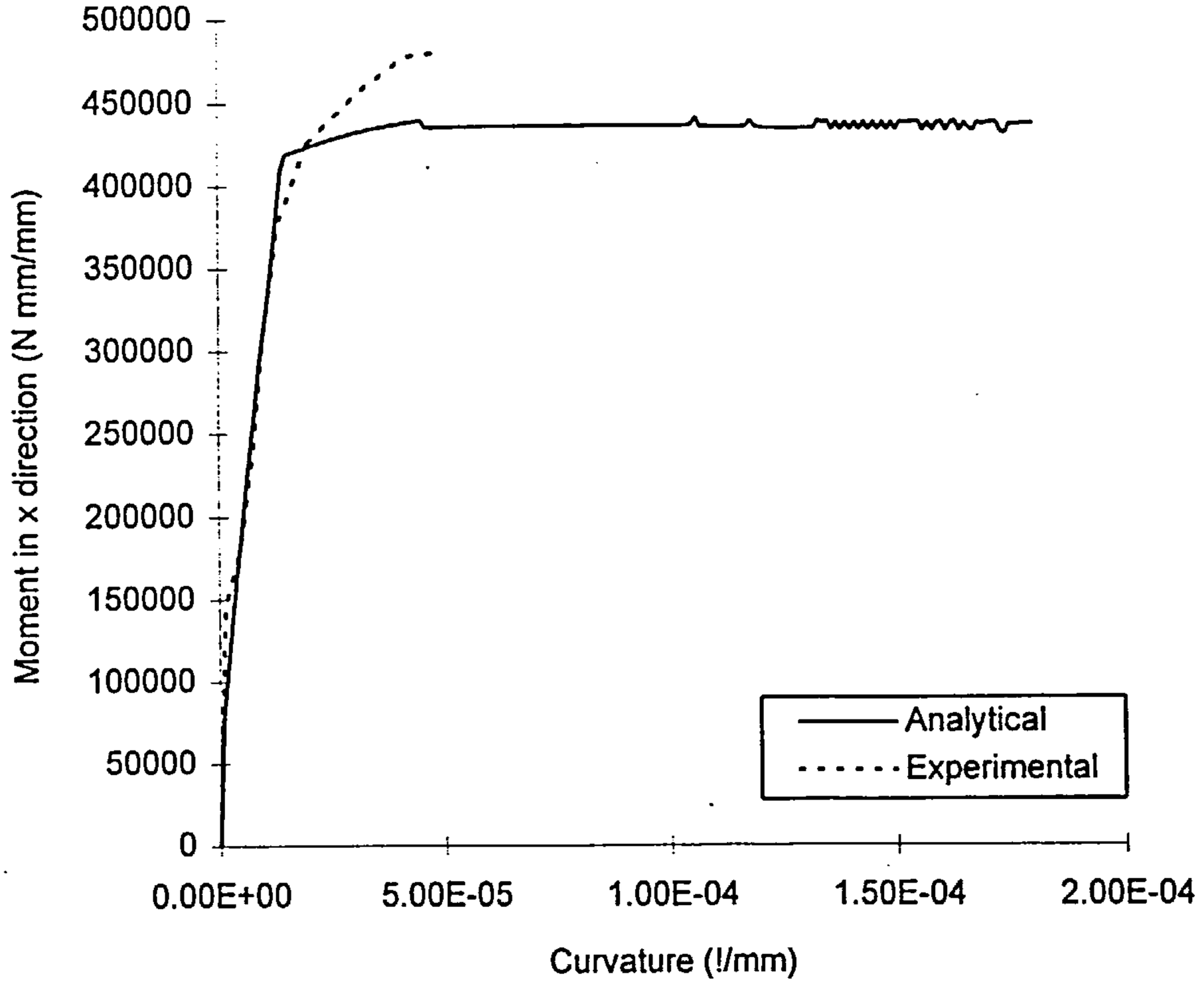

Figure 5.14: Comparison of experimental and analytical results of SE 4

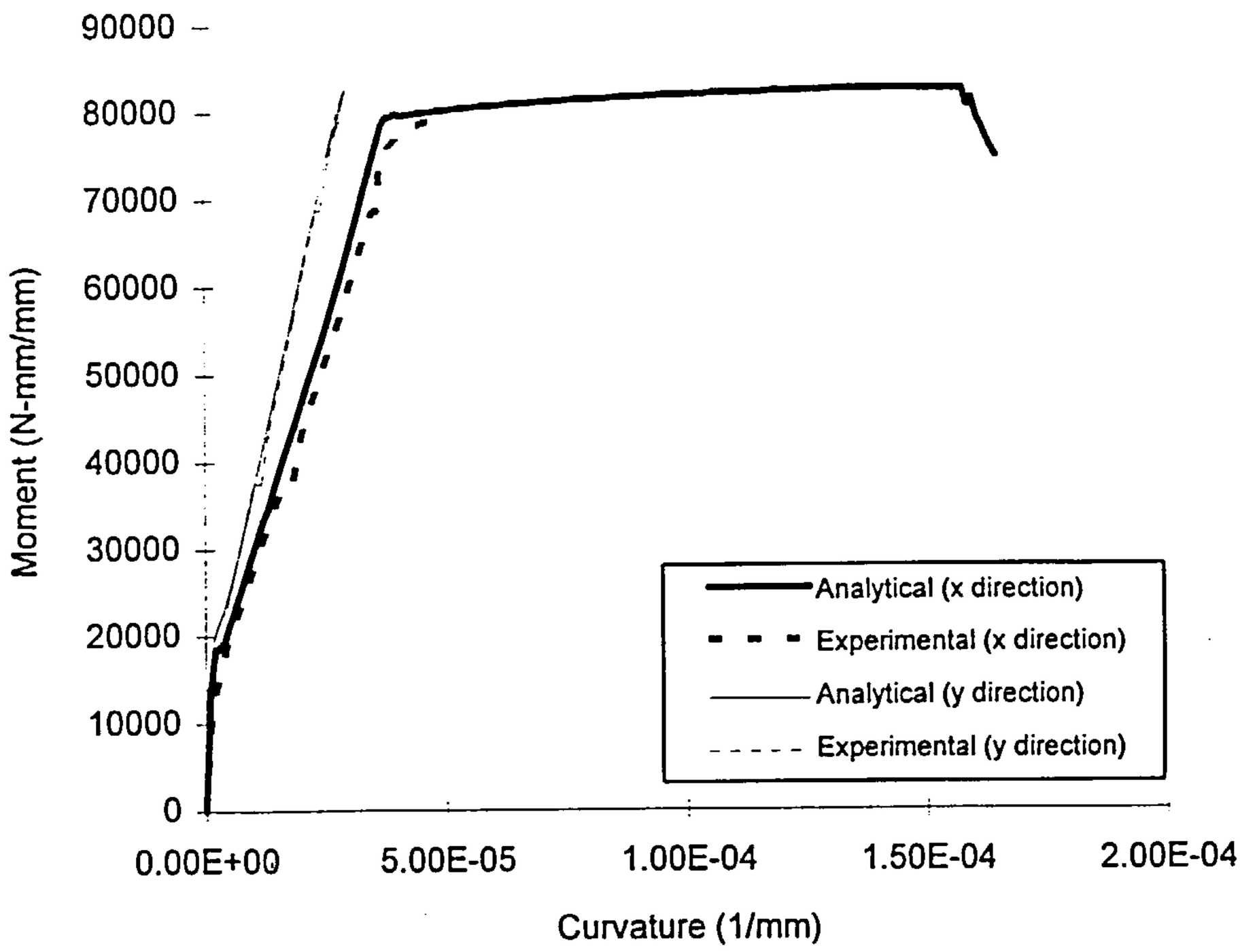

Figure 5.15: Comparison of experimental and analytical results of Samad's slab 4

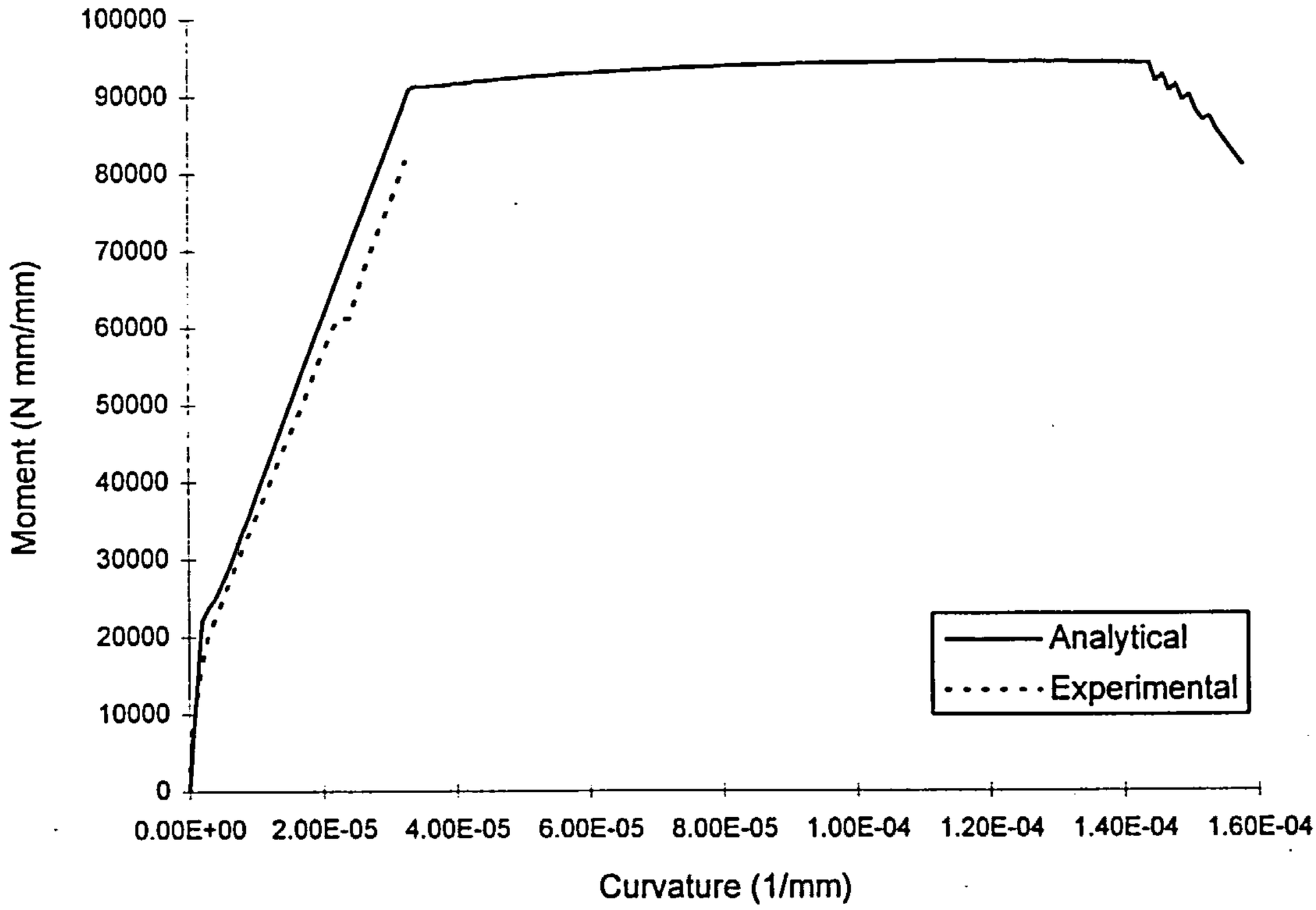

Figure 5.16: Comparison of experimental and analytical results of Samad's slab 5

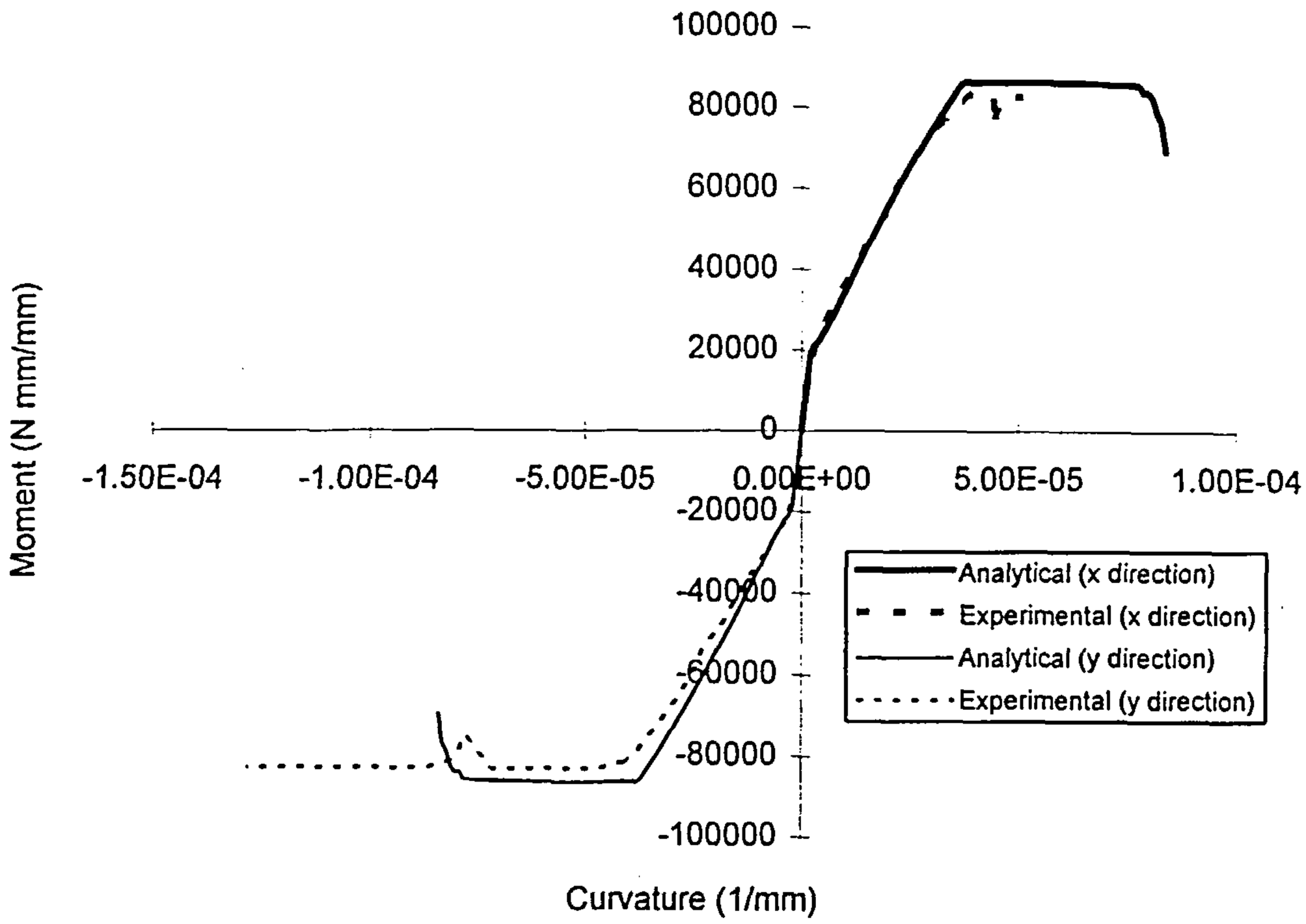

Figure 5.17: Comparison of experimental and analytical results of Samad's slab 7

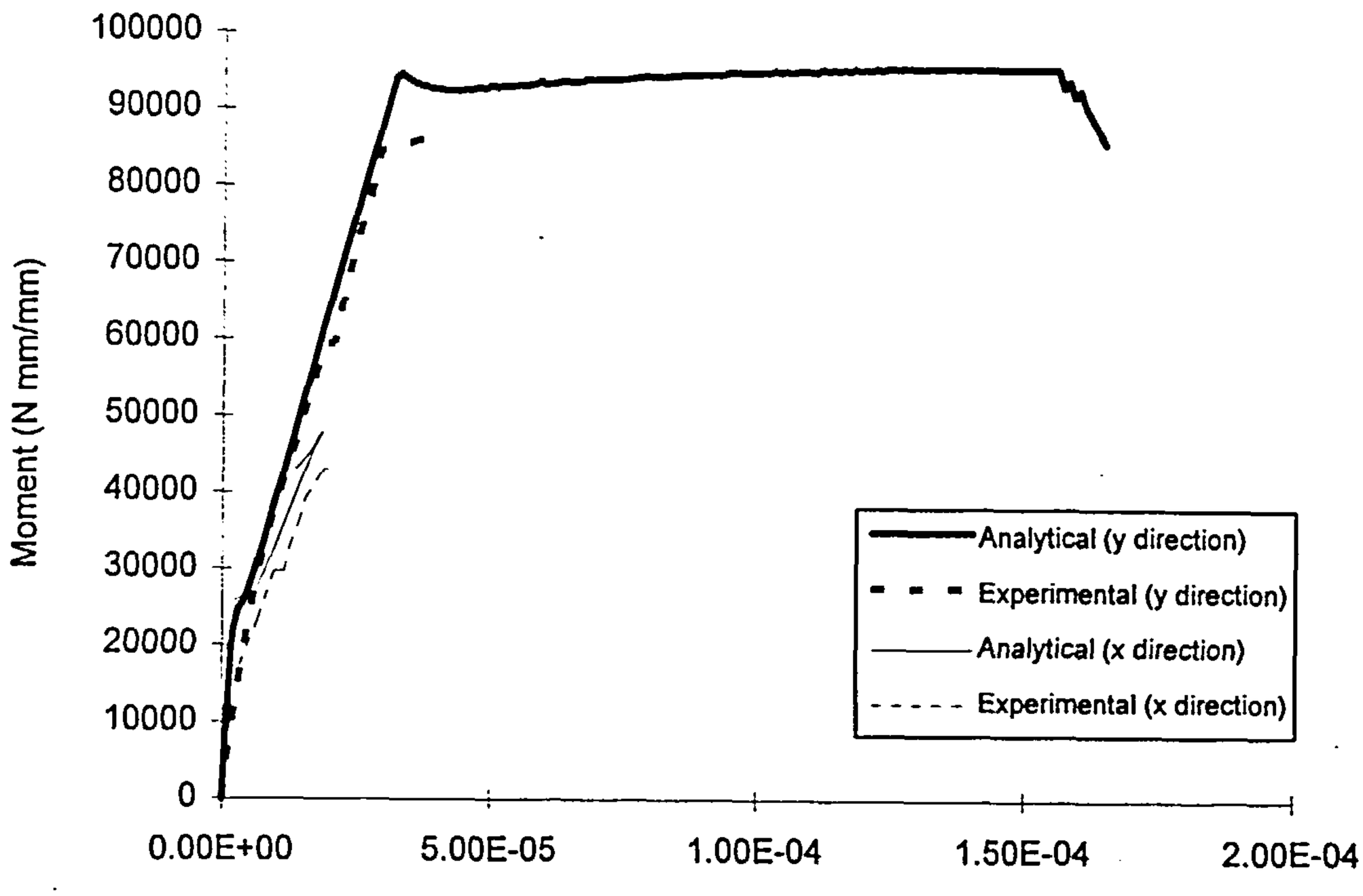

Figure 5.18: Comparison of experimental and analytical results of Samad's slab 8

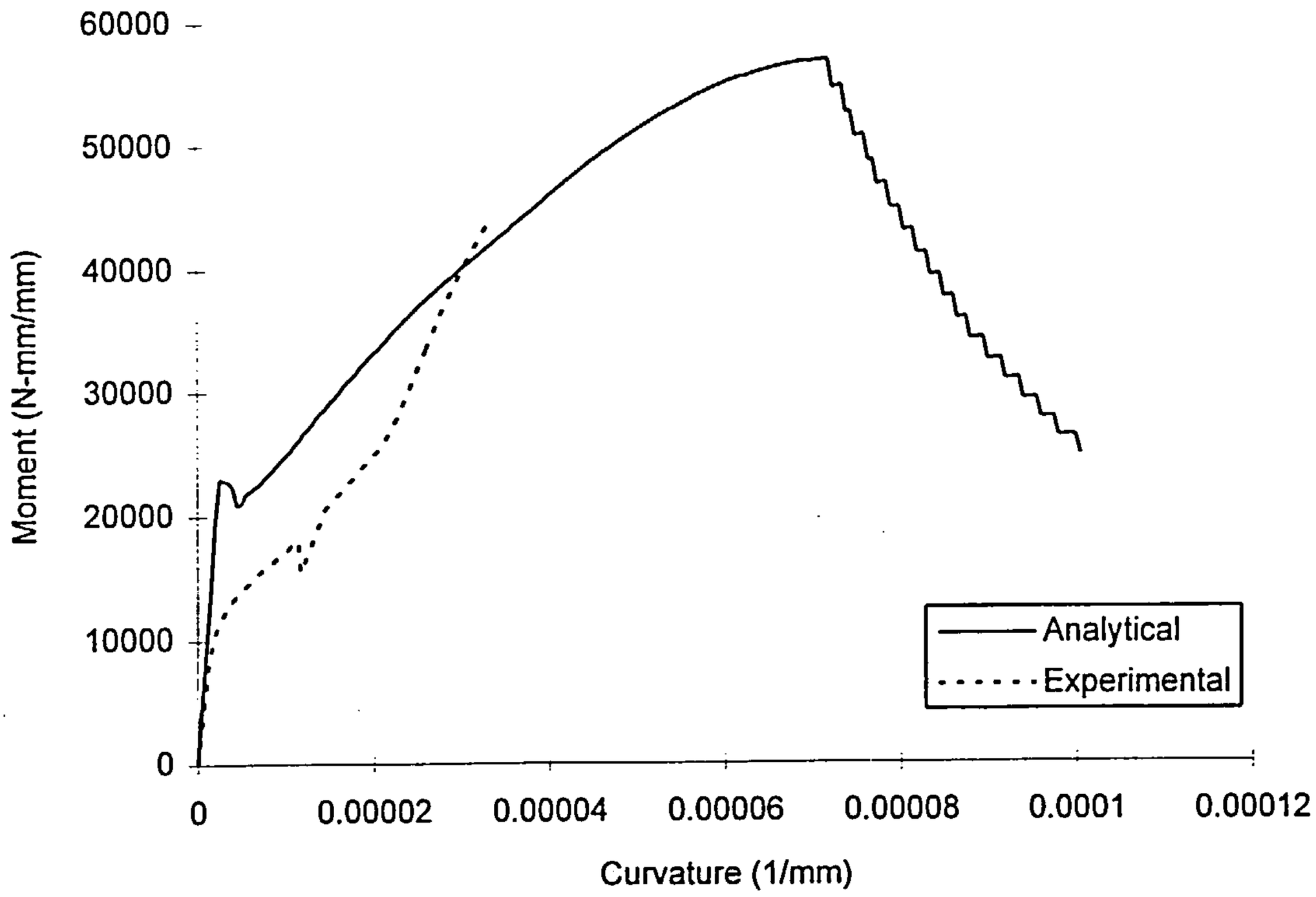

Figure 5.19: Comparison of experimental and analytical results of Samad's slab 12

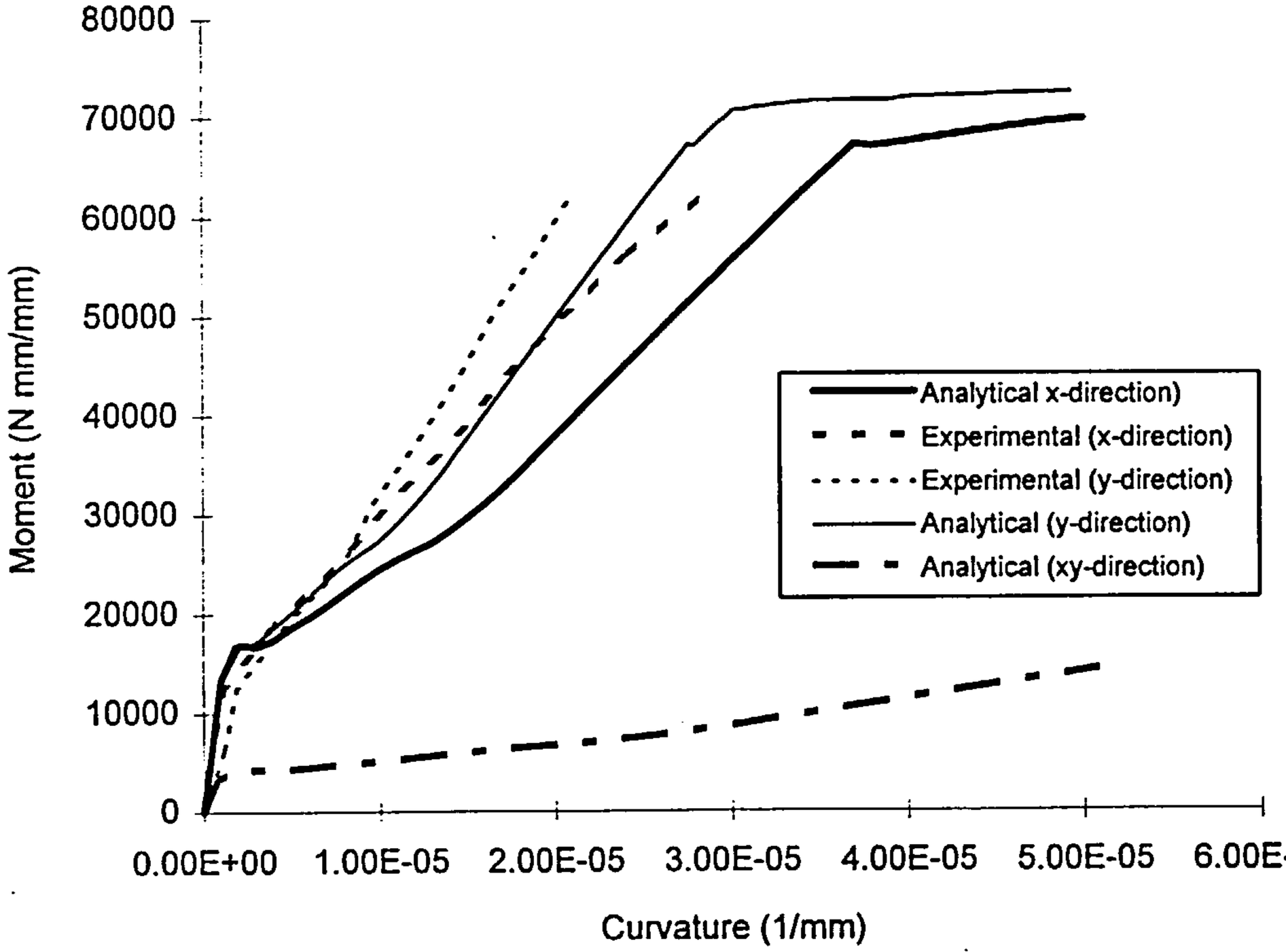

Figure 5.20: Comparison of experimental and analytical results of Samad's slab 13

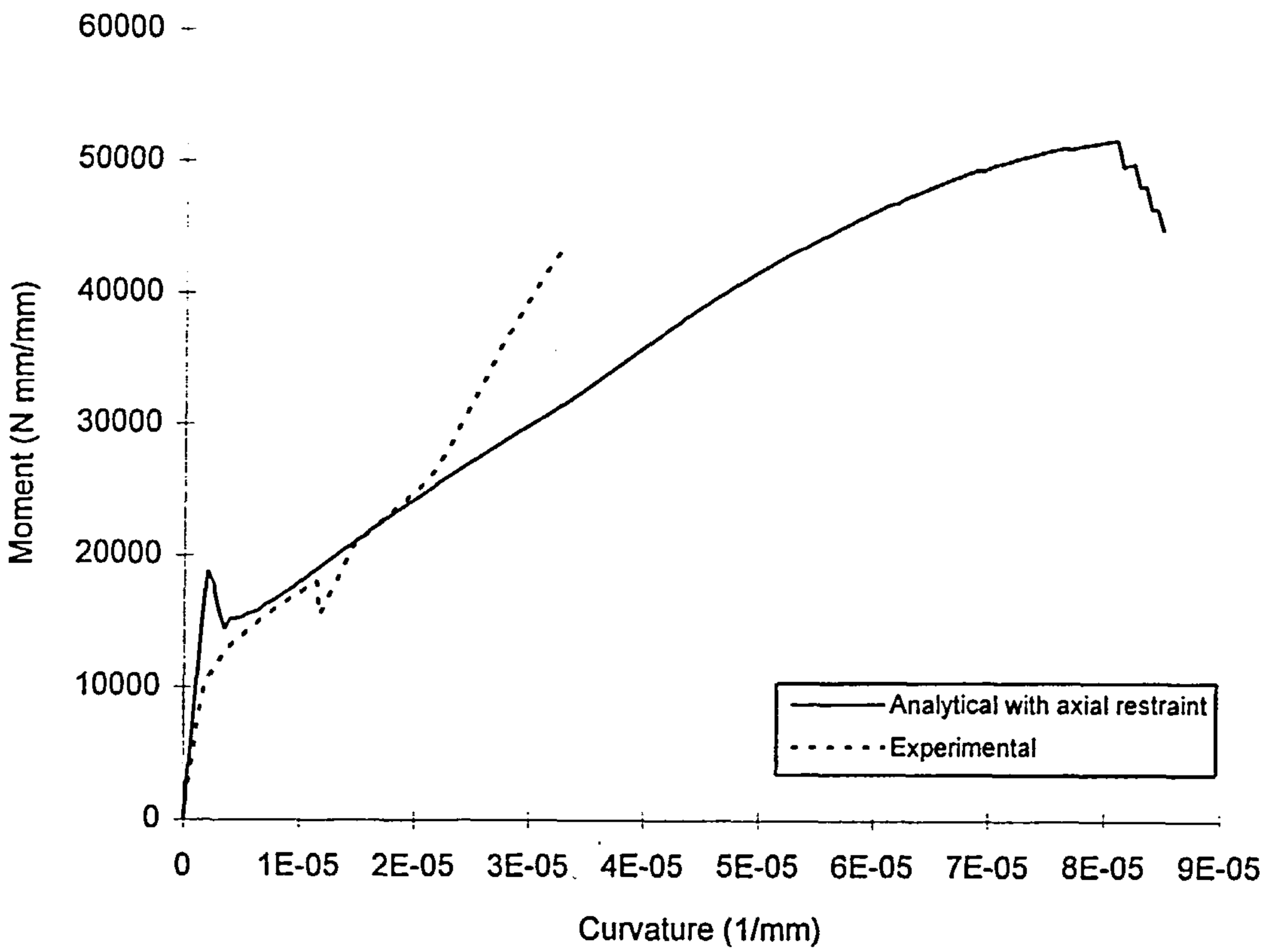

Figure 5.21: Comparison of experimental and analytical results of Samad's slab 12 with axial restraint

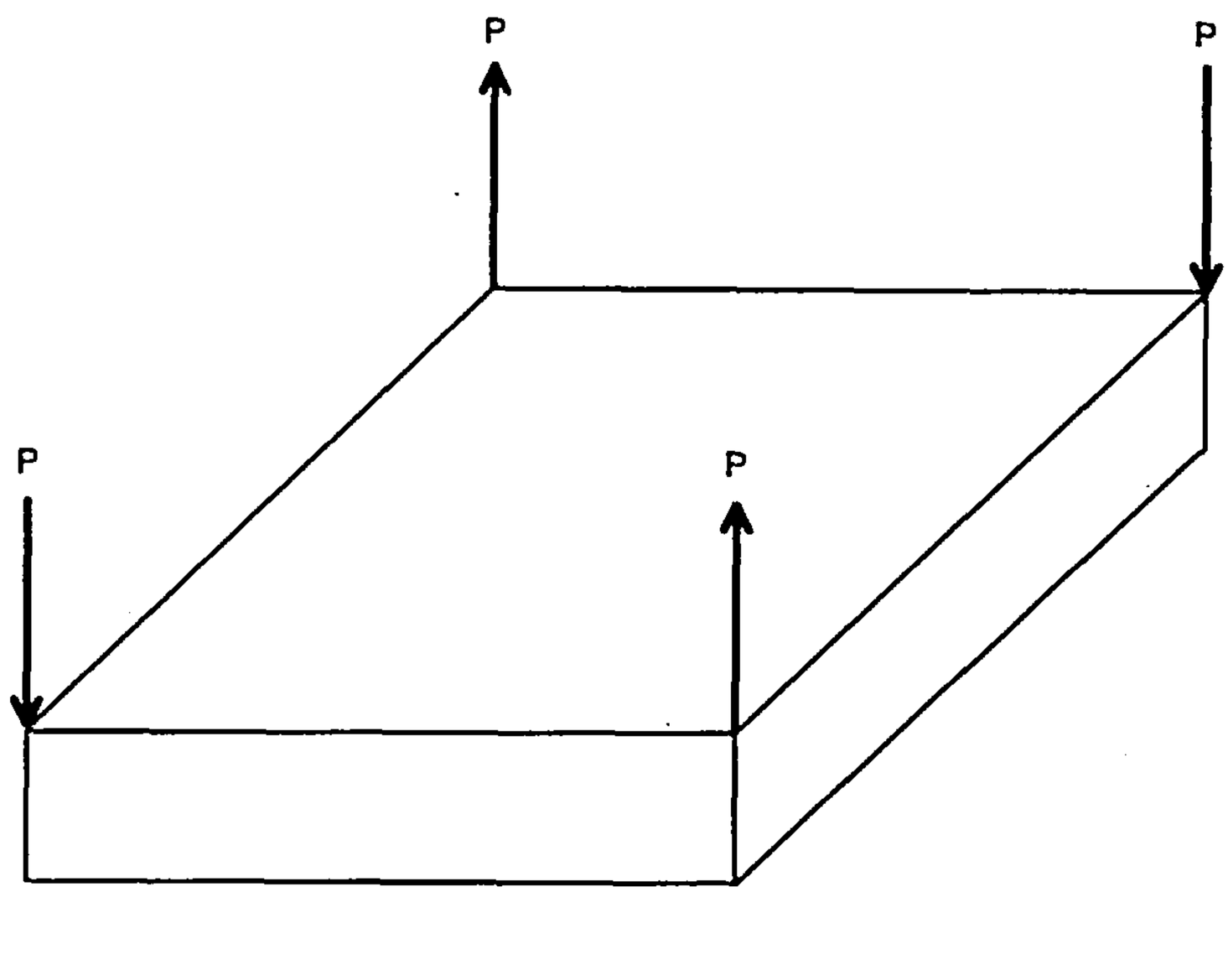

Figure 5.22: Loading arrangement for element under pure twisting

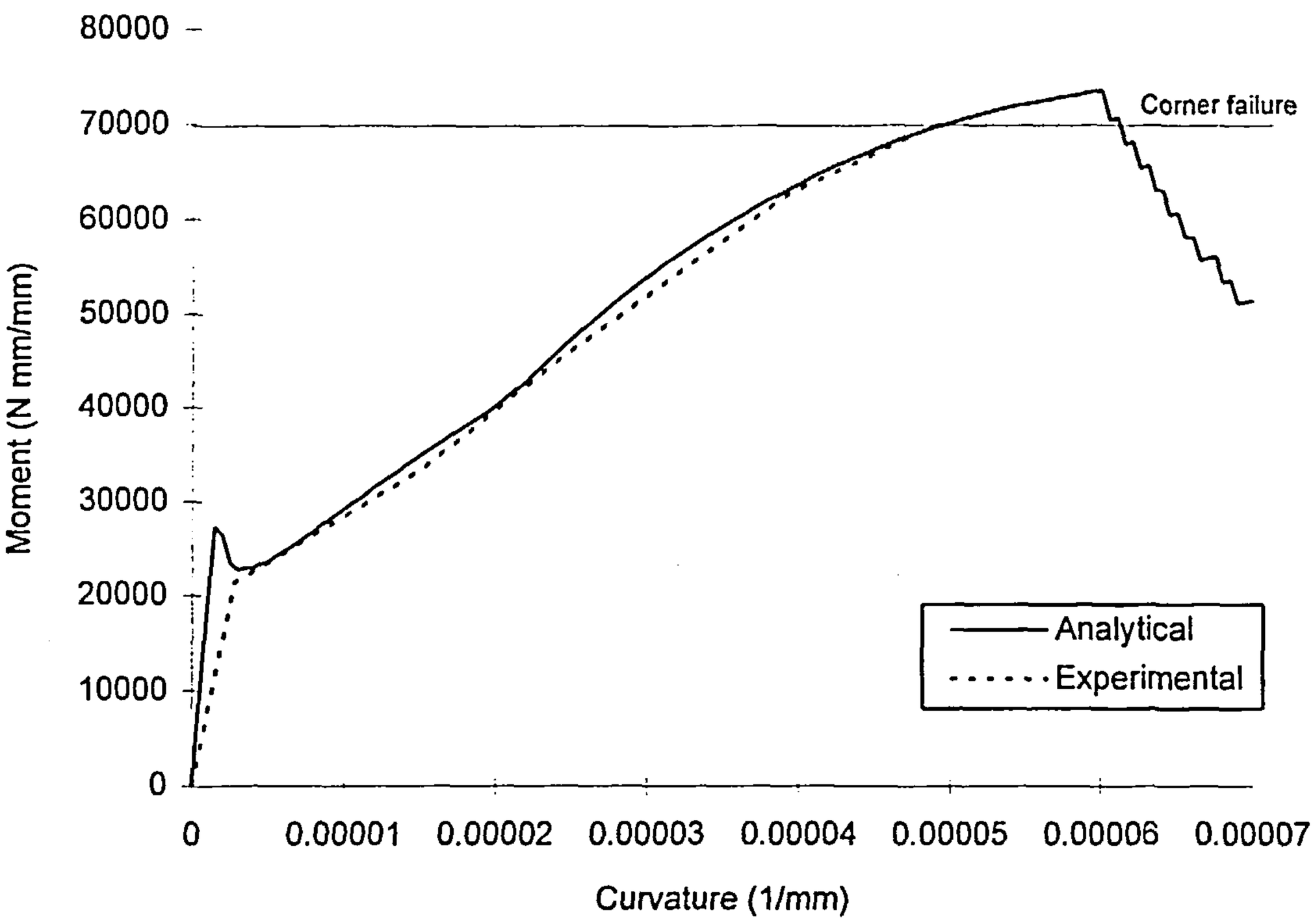

Figure 5.23: Comparison of experimental and analytical results of Marti et al's slab 2

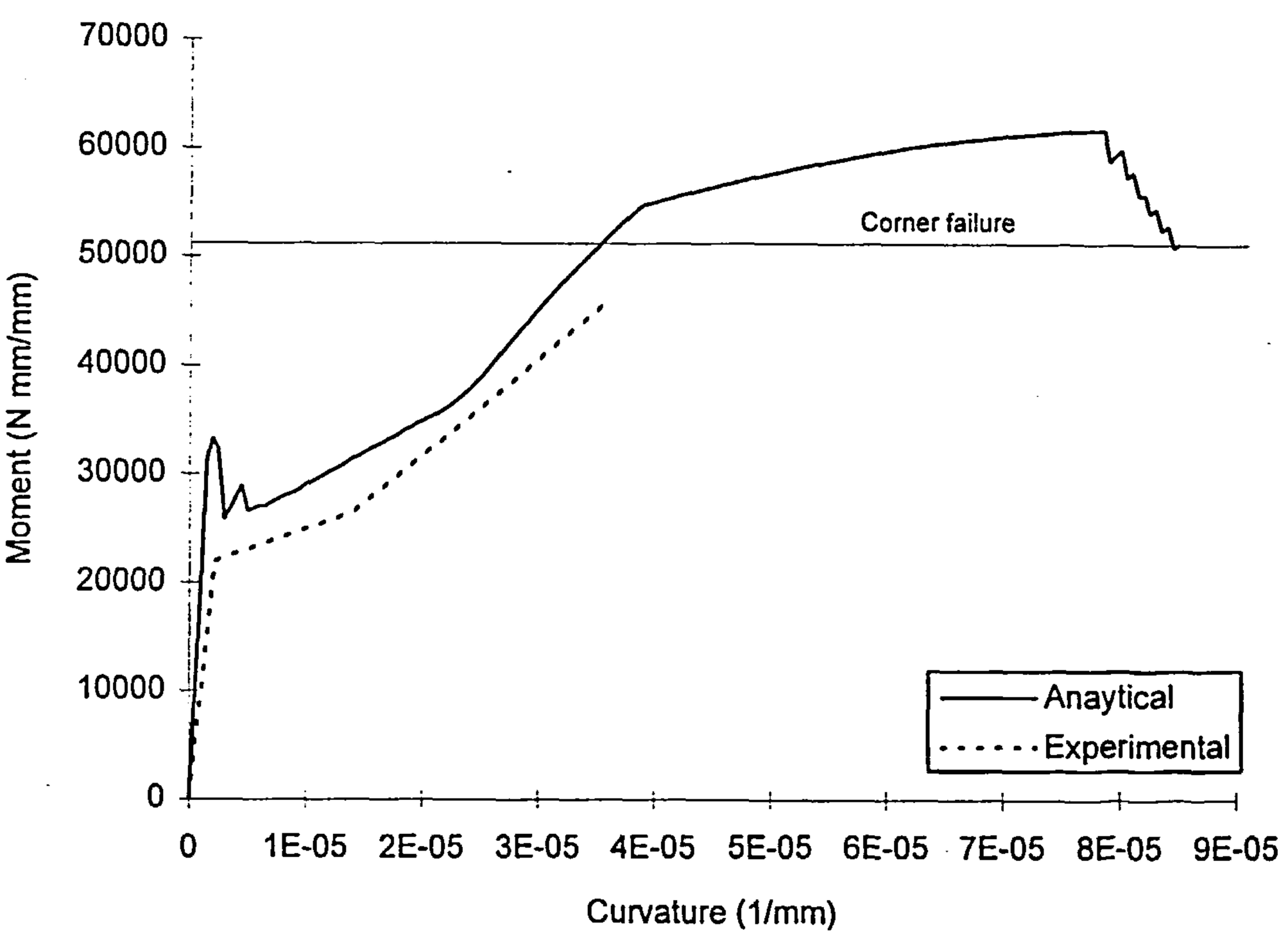

Figure 5.24: Comparison of experimental and analytical results of Marti et al's slab 4

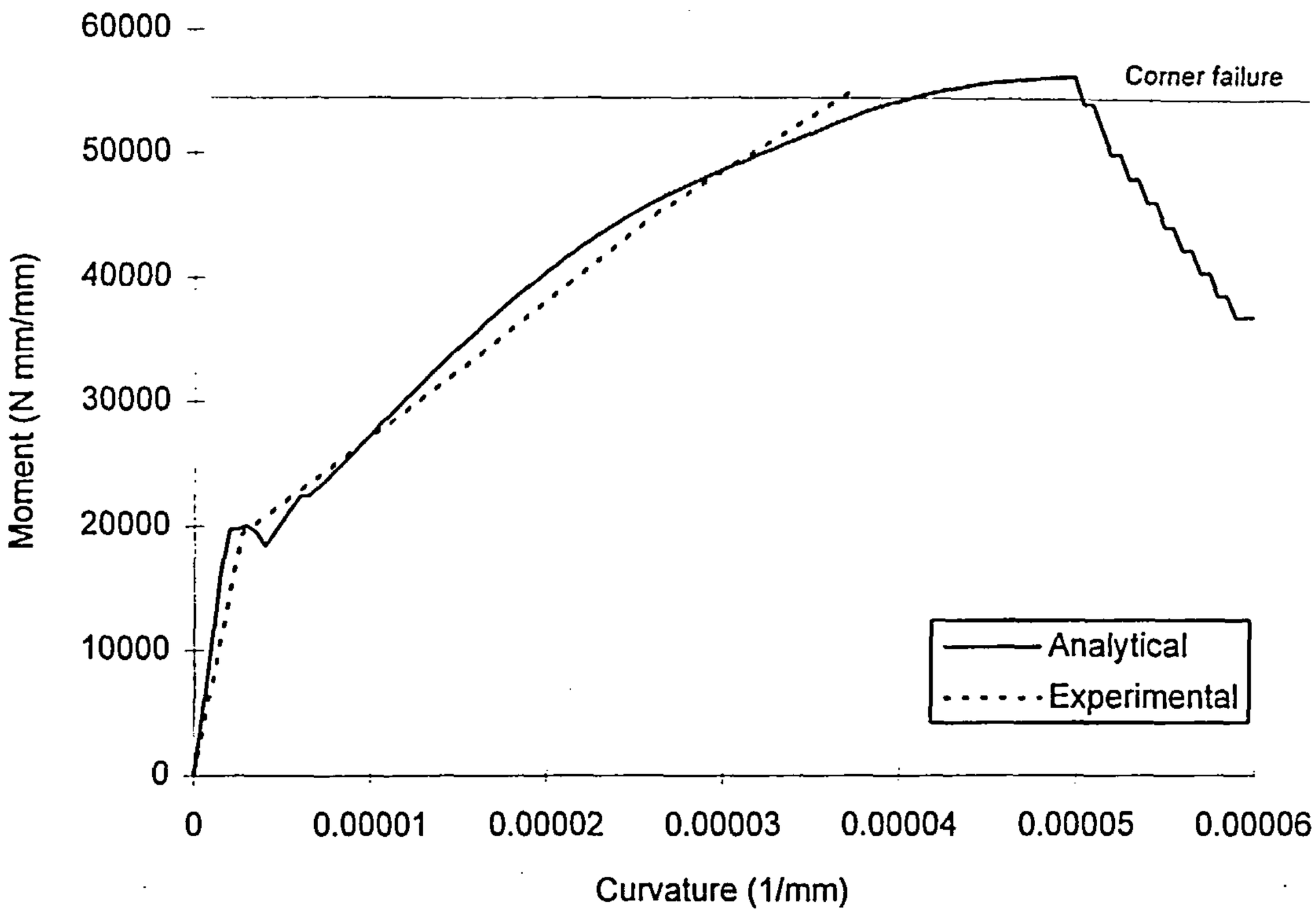

Figure 5.25: Comparison of experimental and analytical results of Marti' et al's slab 6

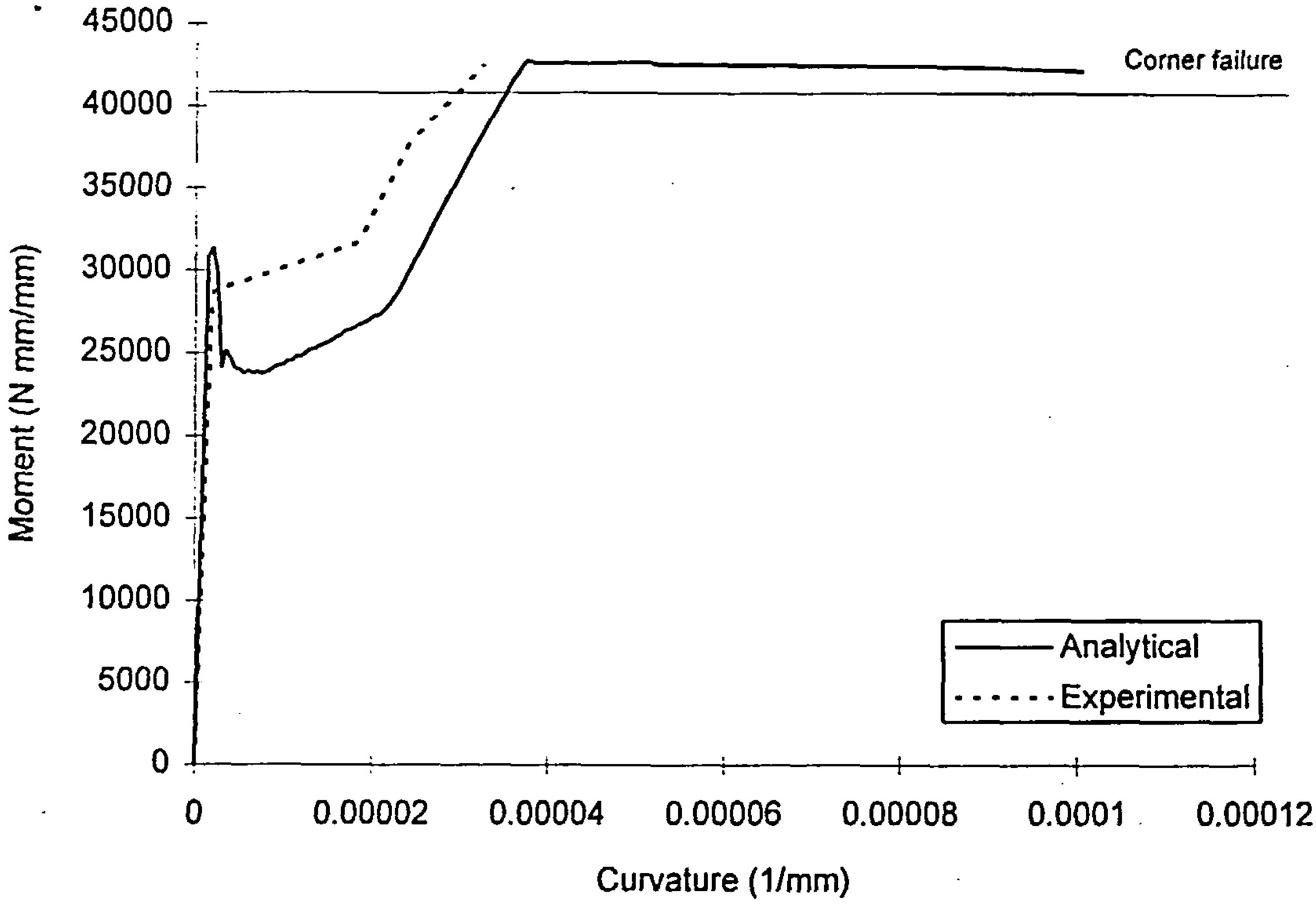

Figure 5.26: Comparison of experimental and analytical results of Marti et al's slab 7

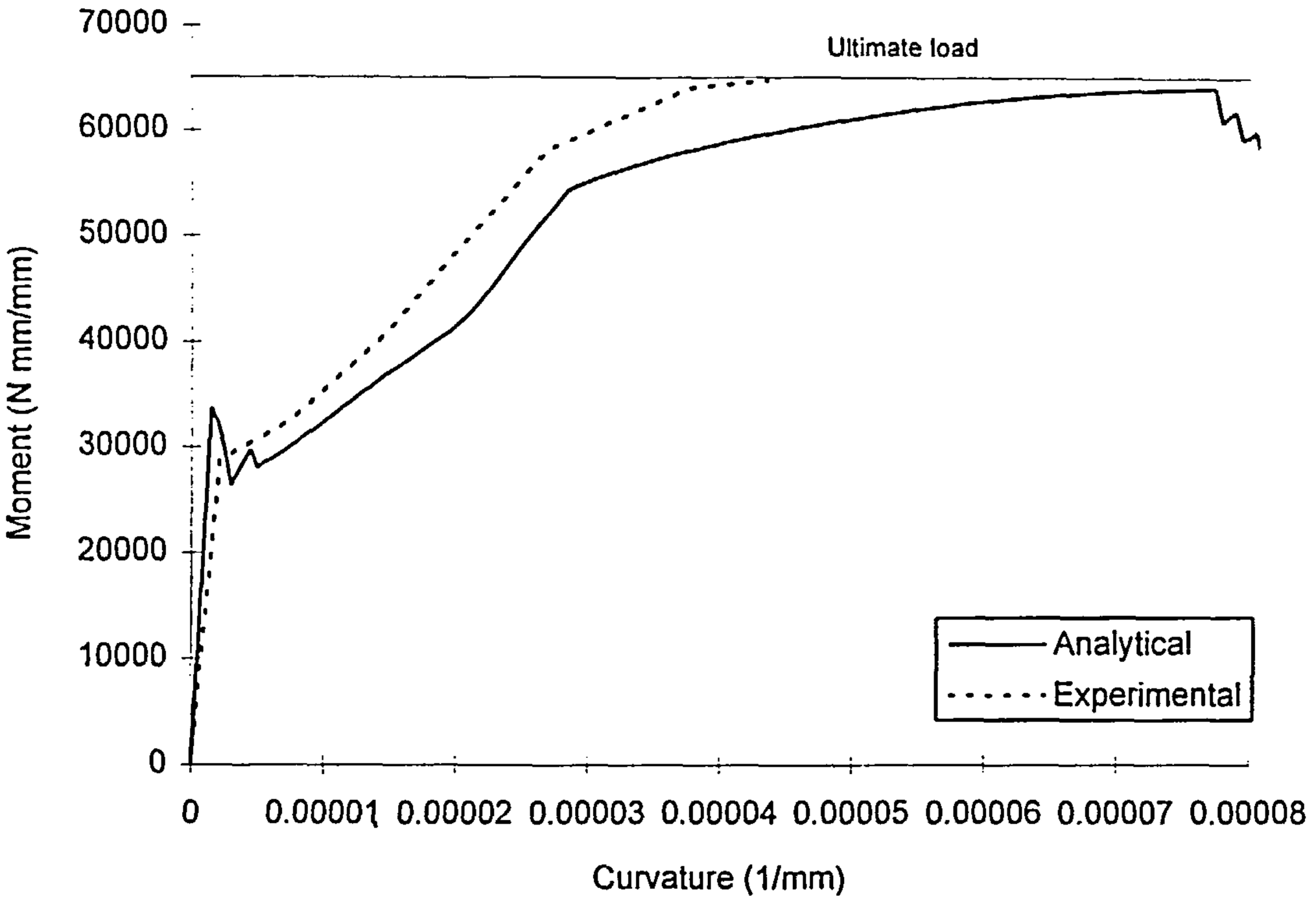

Figure 5.27: Comparison of experimental and analytical results of Marti et al's slab 8

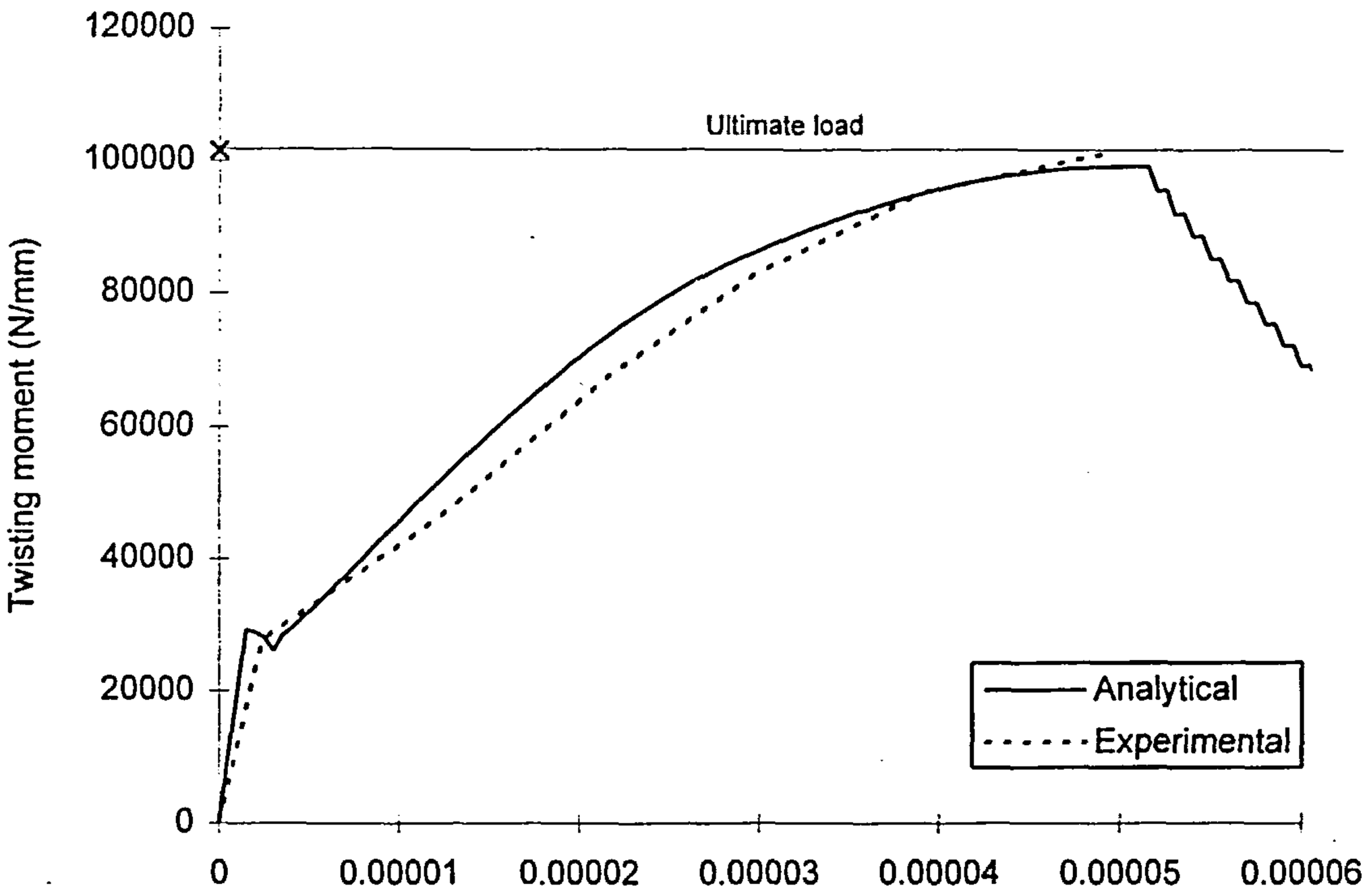

Figure 5.28: Comparison of experimental and analytical results of Marti's et al's slab 9

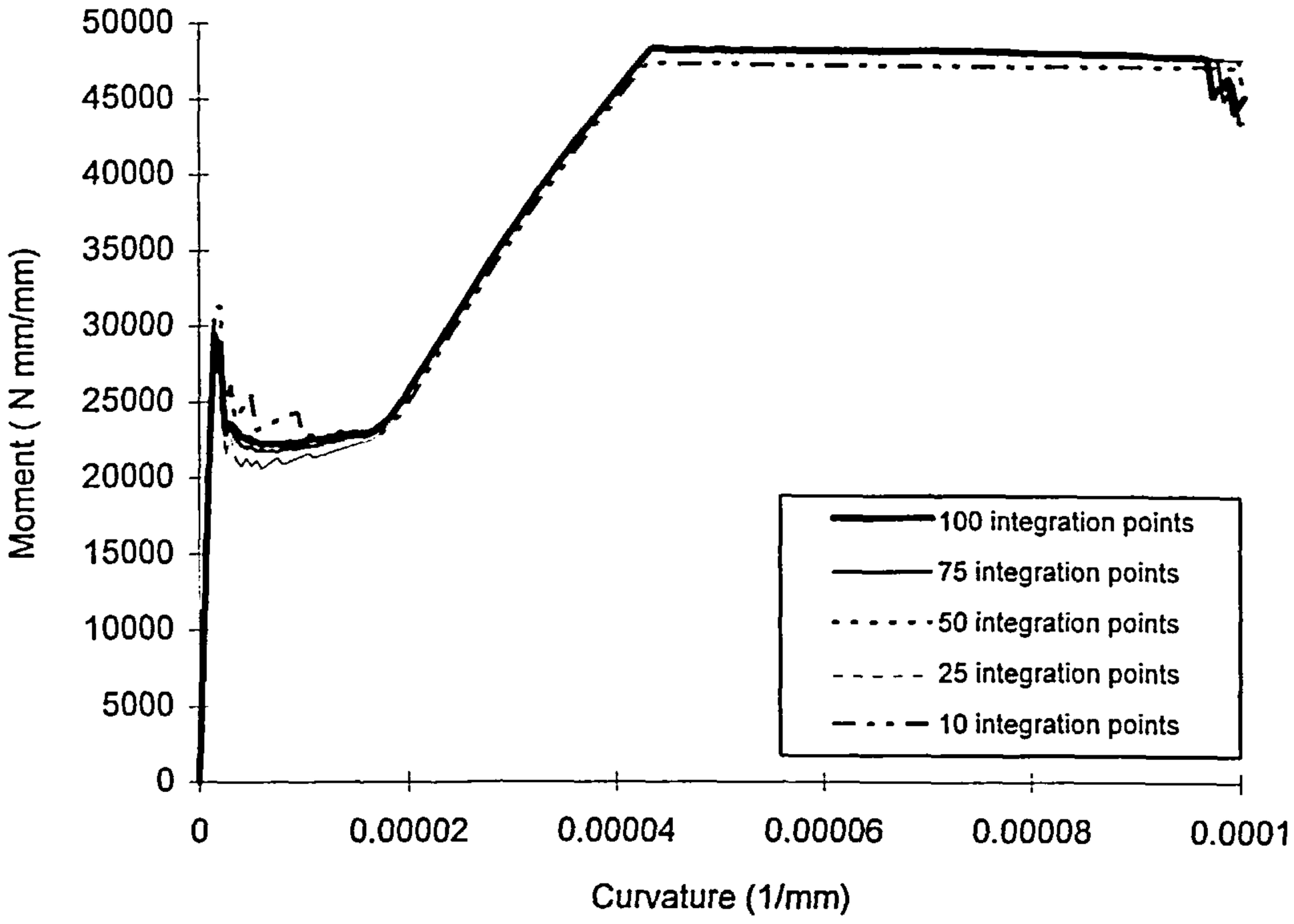

Figure 5.29: Response of an element subjected to pure twisting moment showing the effect of number of integration points through the depth

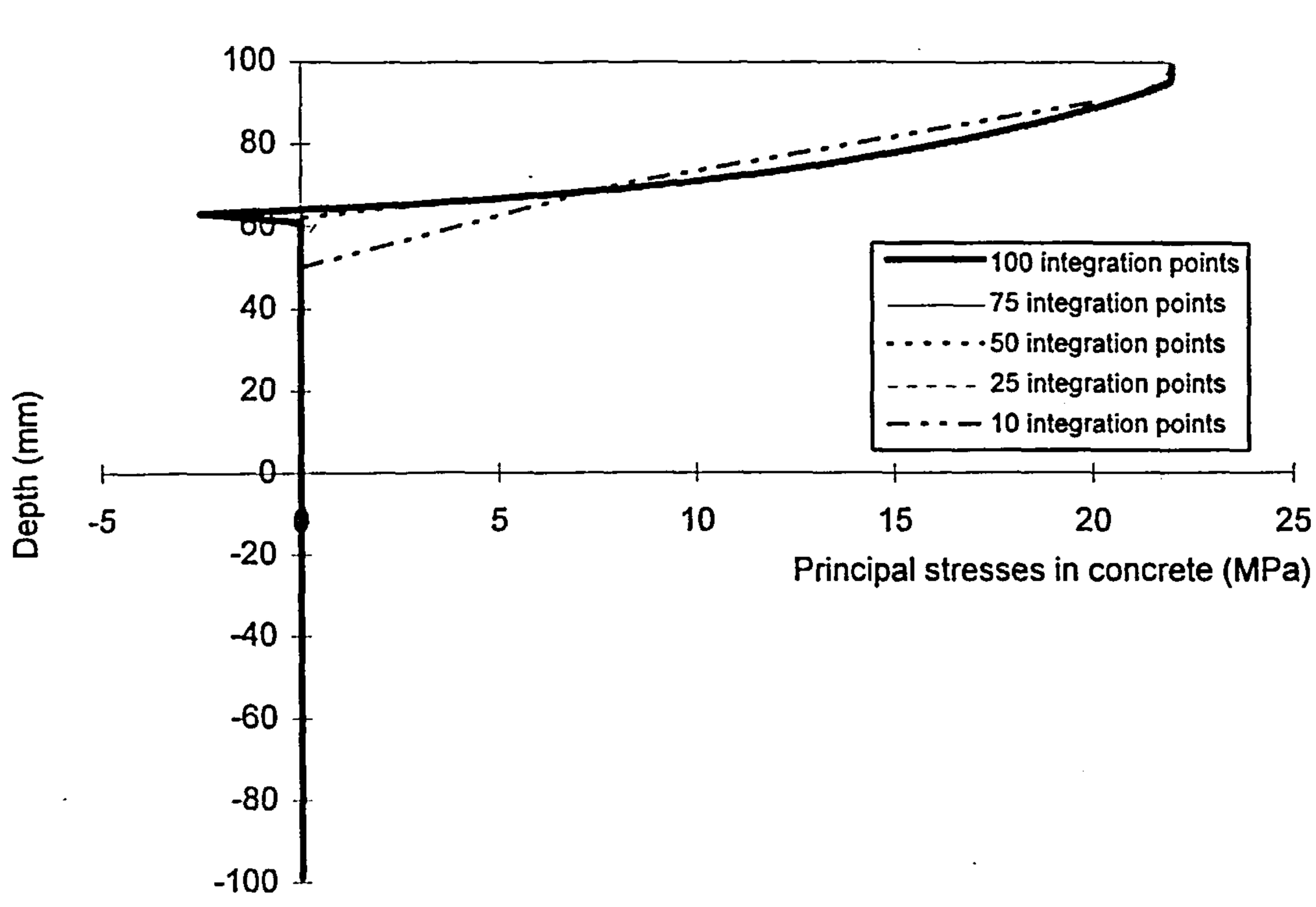

Figure 5.30: Principal stress distribution of concrete in direction 1-1 for an element subjected to pure twisting moment showing the effect of number of integration points through the depth

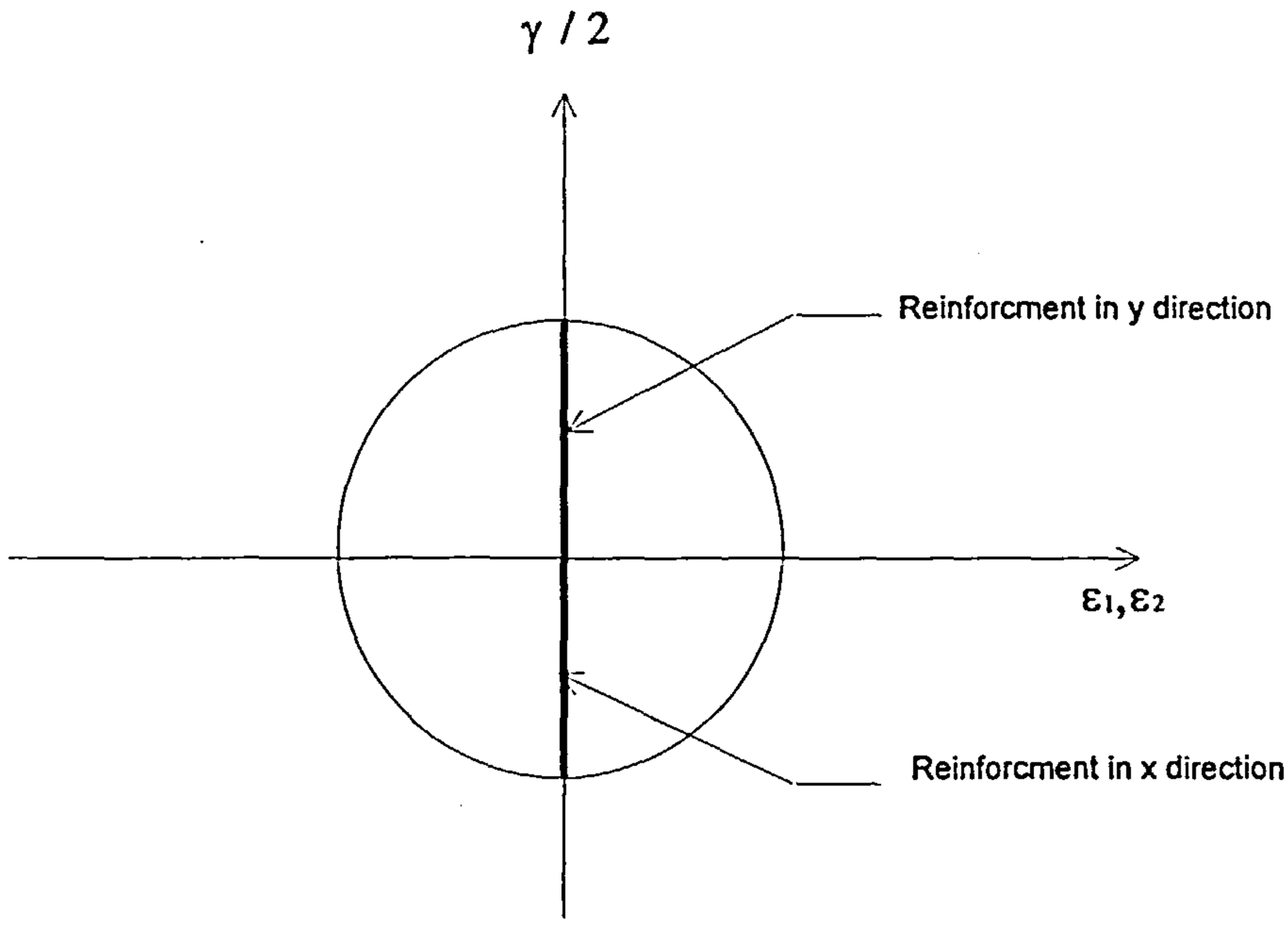

Figure 5.31: Strain state prior to cracking at the reinforcement level of an element either subjected to in-plane shear or pure twisting moment

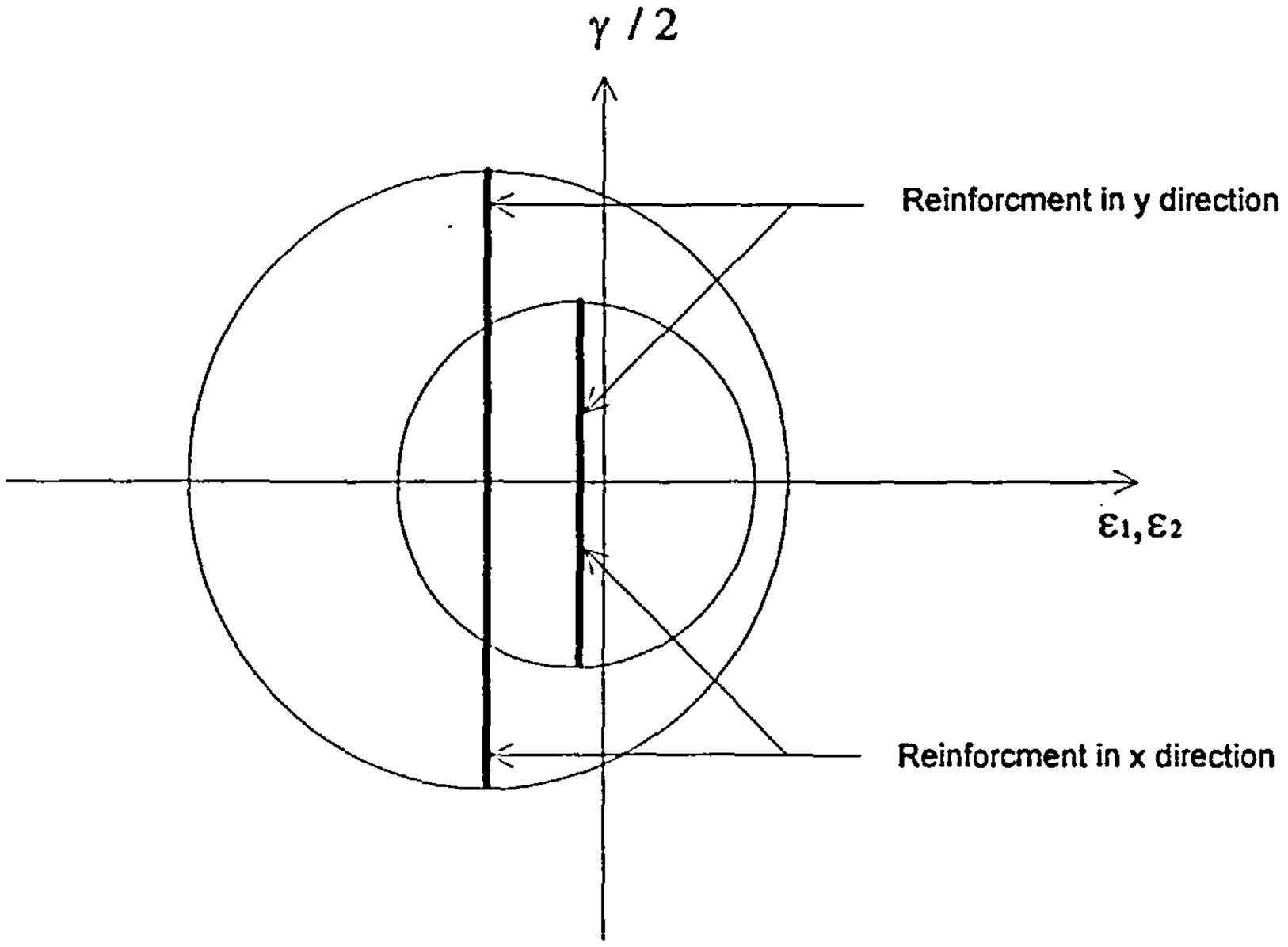

Figure 5.32: Strain state at the reinforcement level of an element subjected to progressively increasing in-plane shear or pure twisting moment

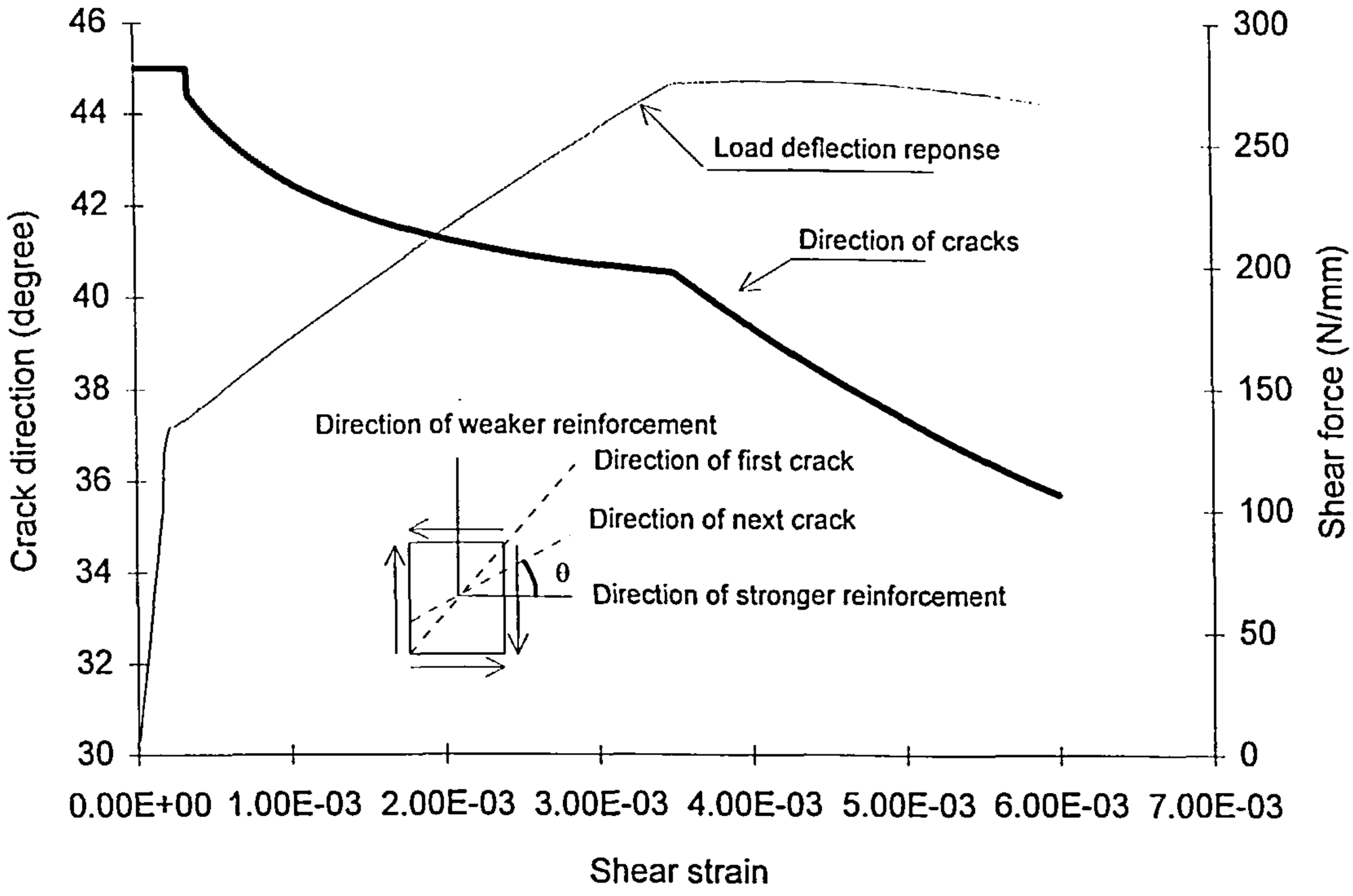

Figure 5.33: Analytical response of PV 19 along with the direction of cracks

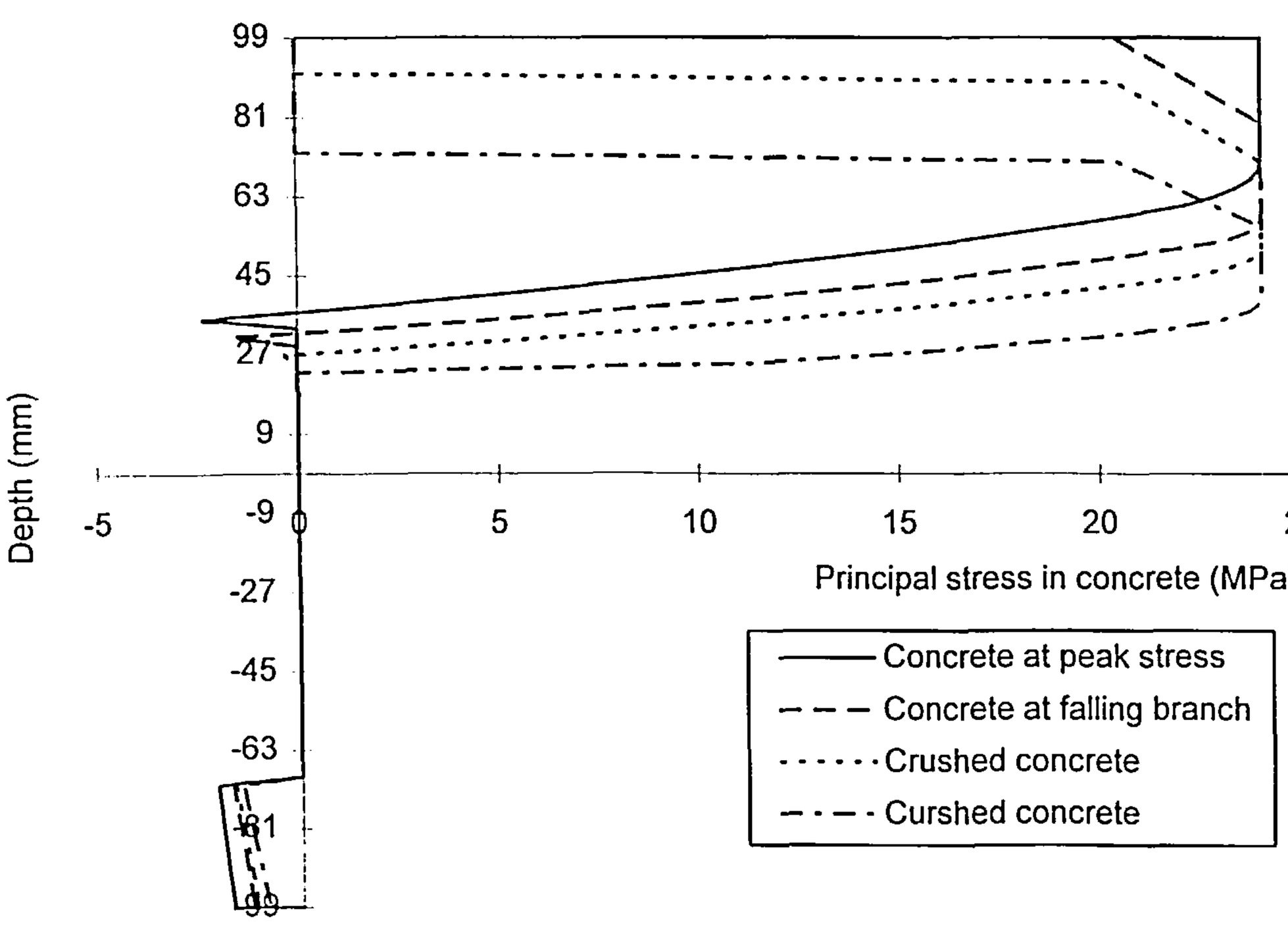

Figure 5.34: Stress distribution of concrete in principal stress direction 1-1 showing the post ultimate response of an element subjected to pure twisting

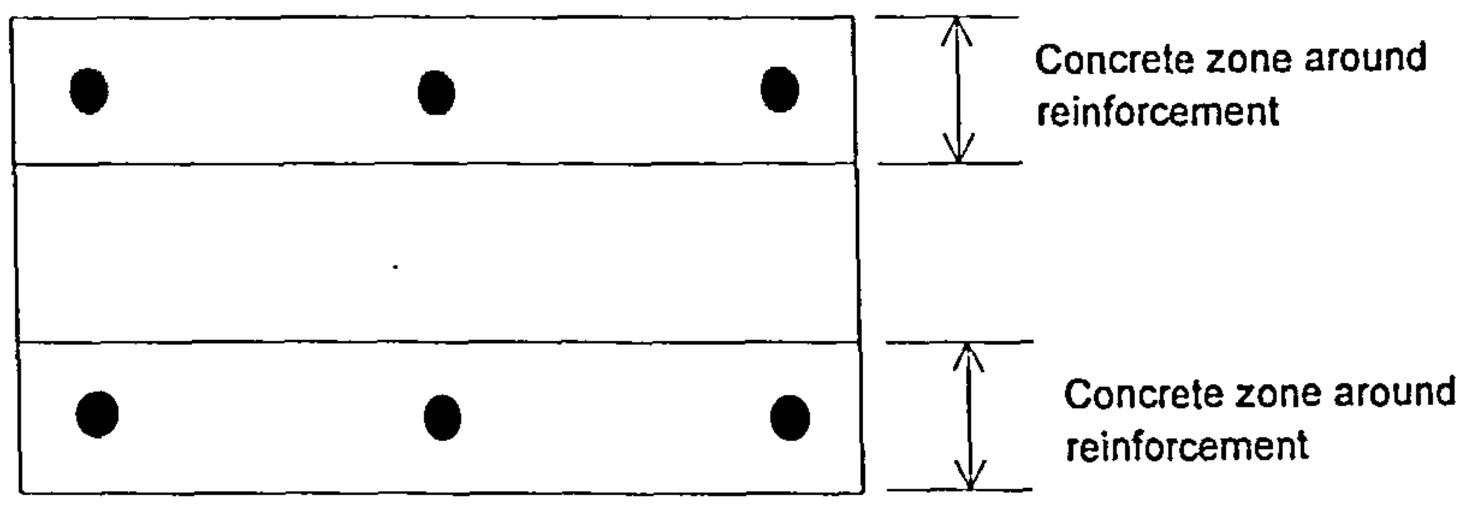

Figure 5.35: Zone of concrete around reinforcement to model tension stiffening

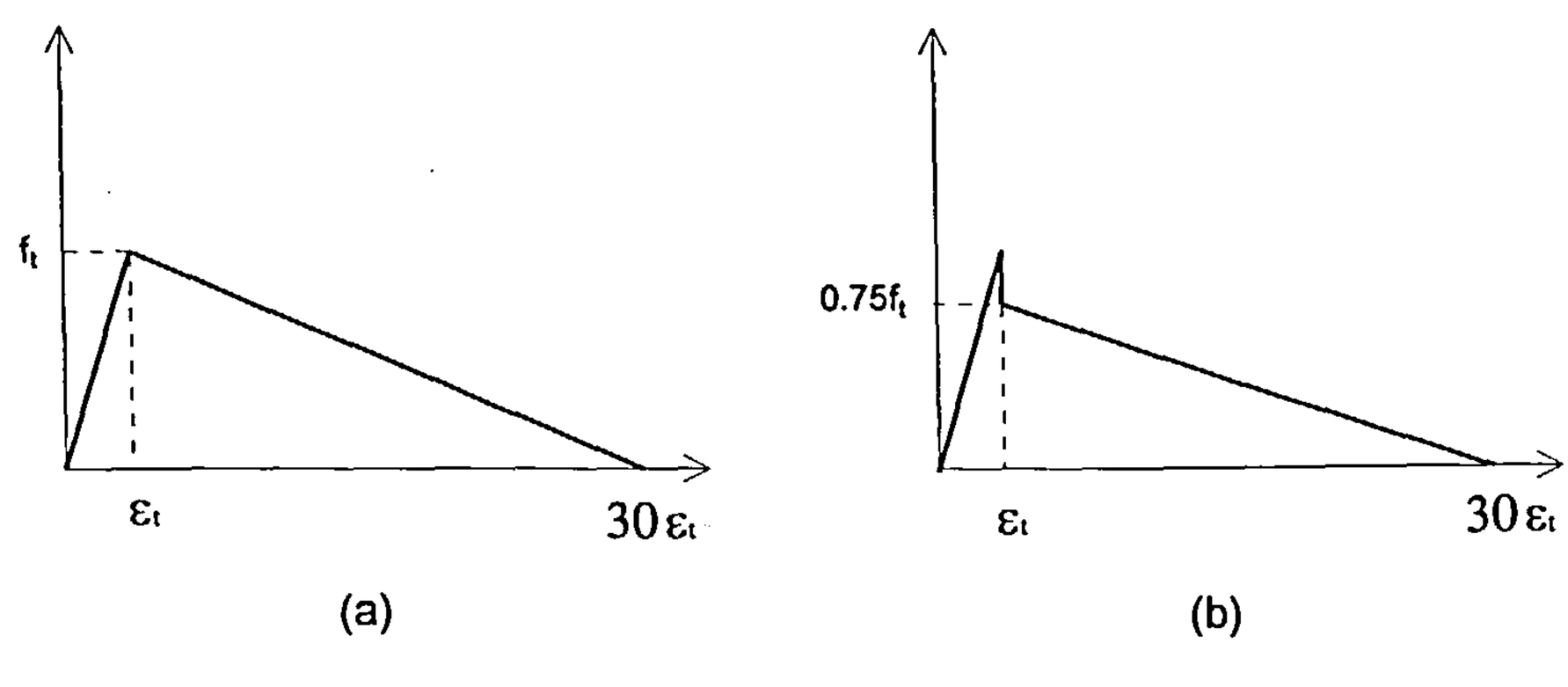

Figure 5.36: Tensile response of concrete to study the effect of discontiunity in tension stiffening model (a) Model 1 (b) Model 2 (c) Model 3 (d) Model 4

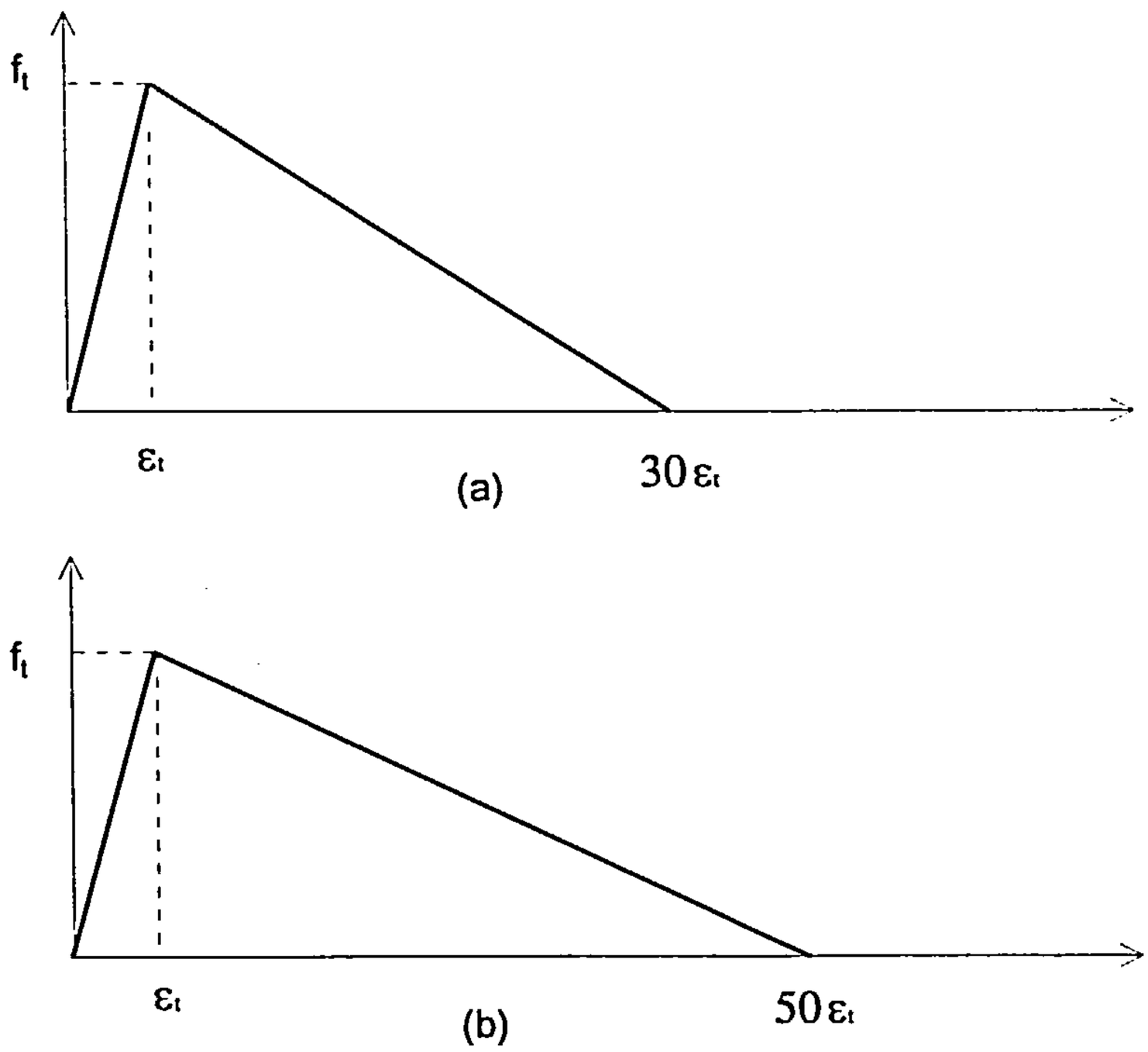

Figure 5.37: Tensile response of concrete to study the effect of length of falling branch of tensile stiffening (a) Model 5 (b) Model 6 (c) Model 7 (d) Model 8

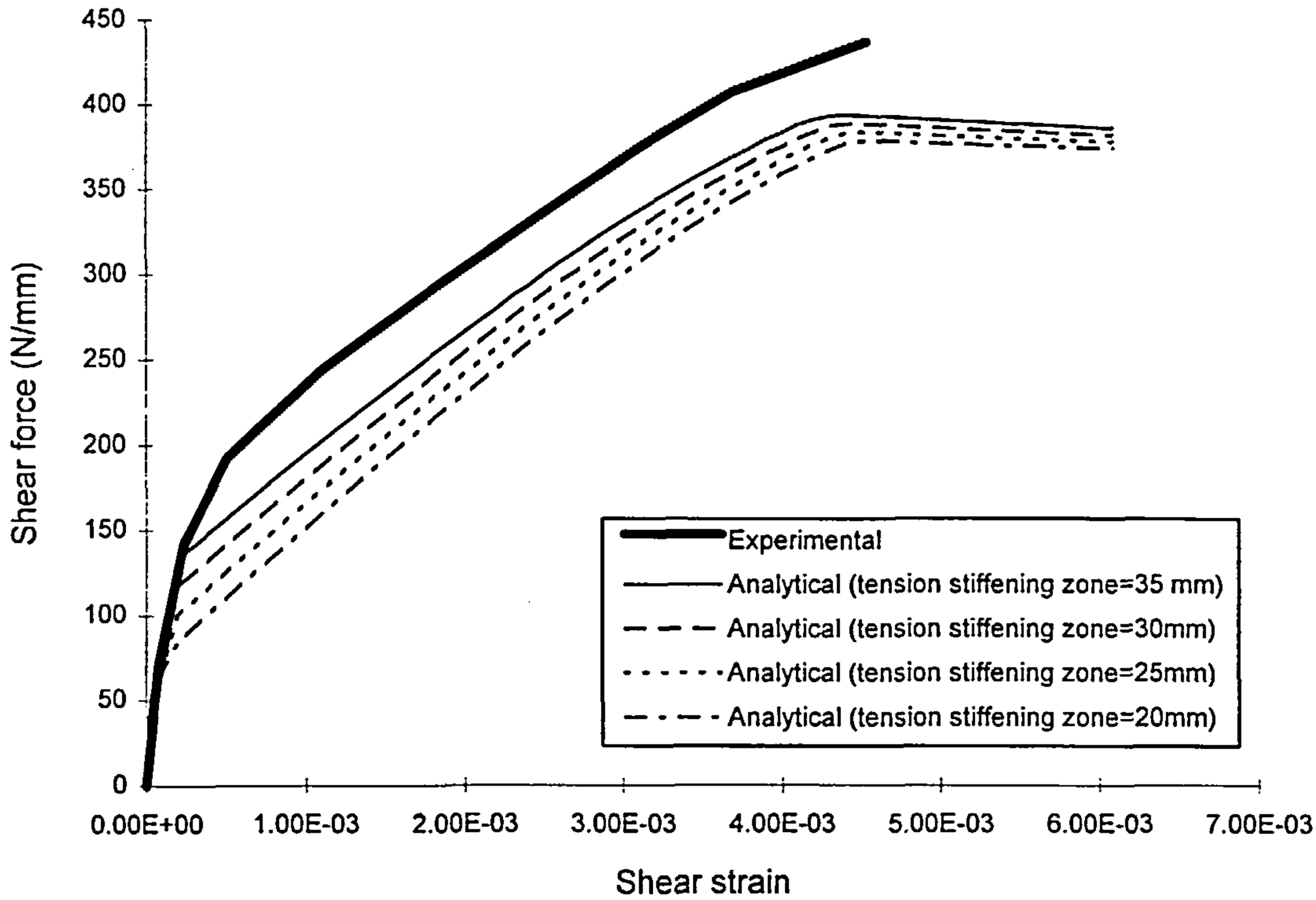

Figure 5.38: Effect of thickness of concrete zone around reinforcement in an element subjected to in-plane shear

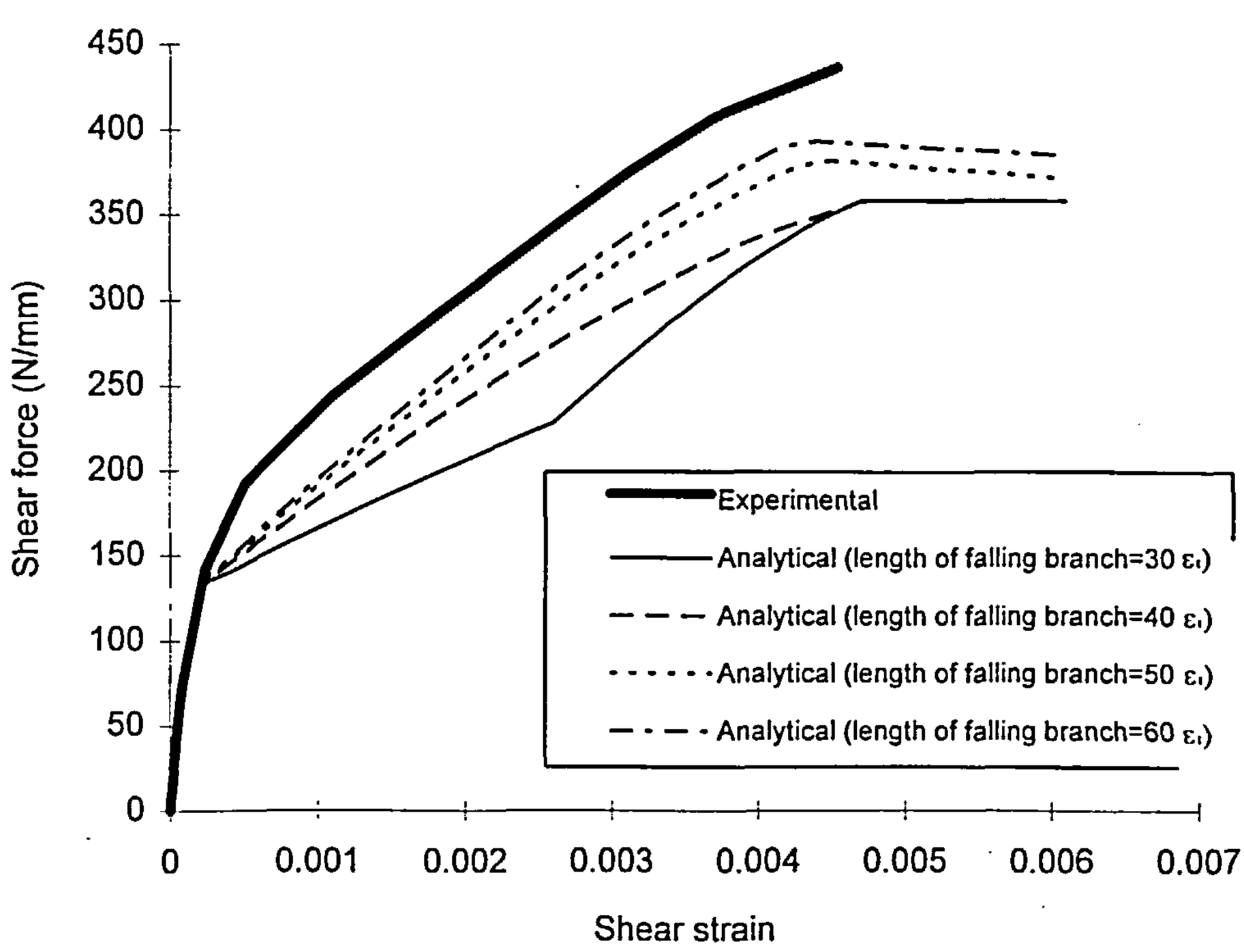

Figure 5.39: Effect of length of falling branch of tension stiffening response on element subjected to in-plane shear

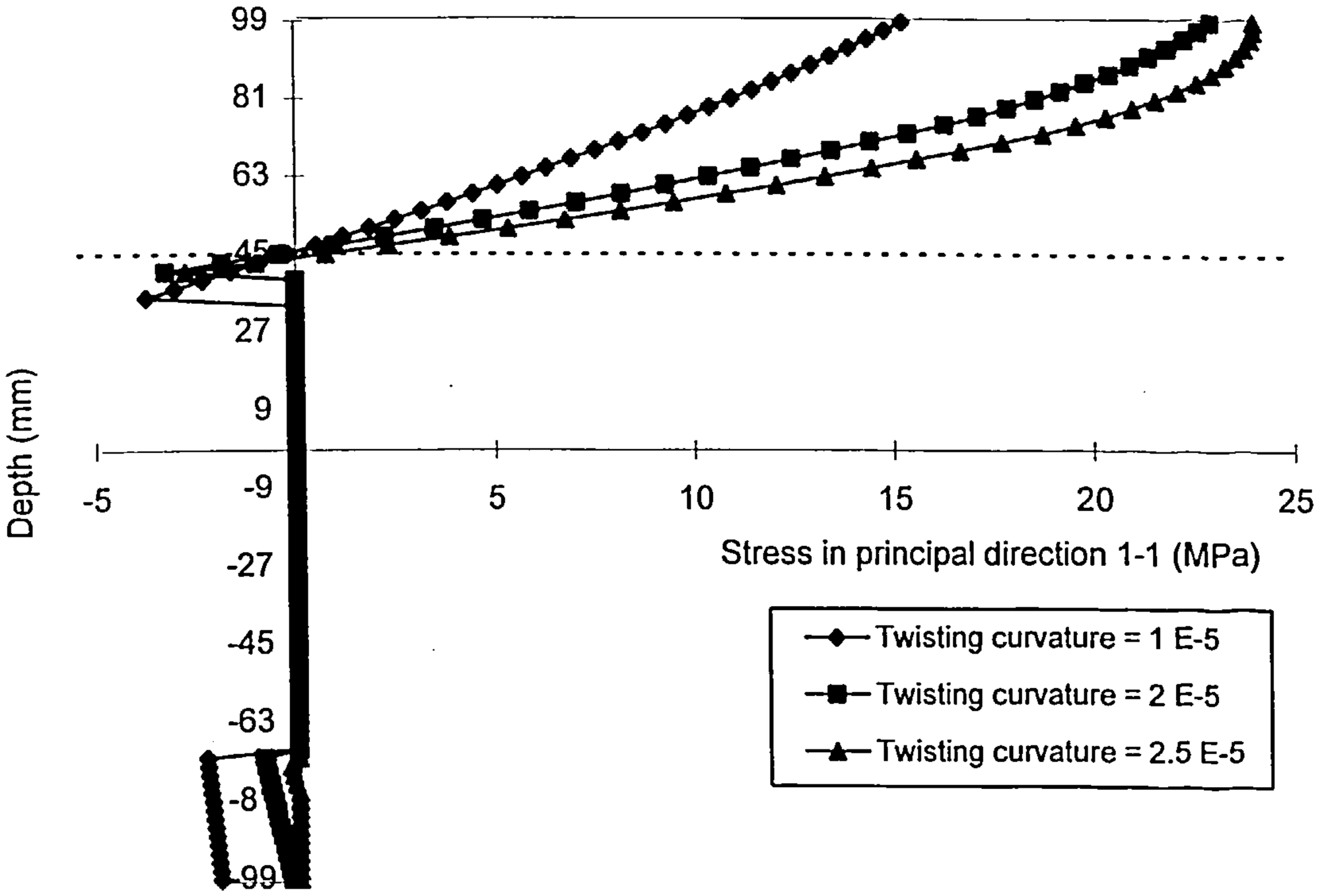

Figure 5.40: Stress distribution in concrete in principal stress direction 1-1 under progressively increasing pure twisting moment

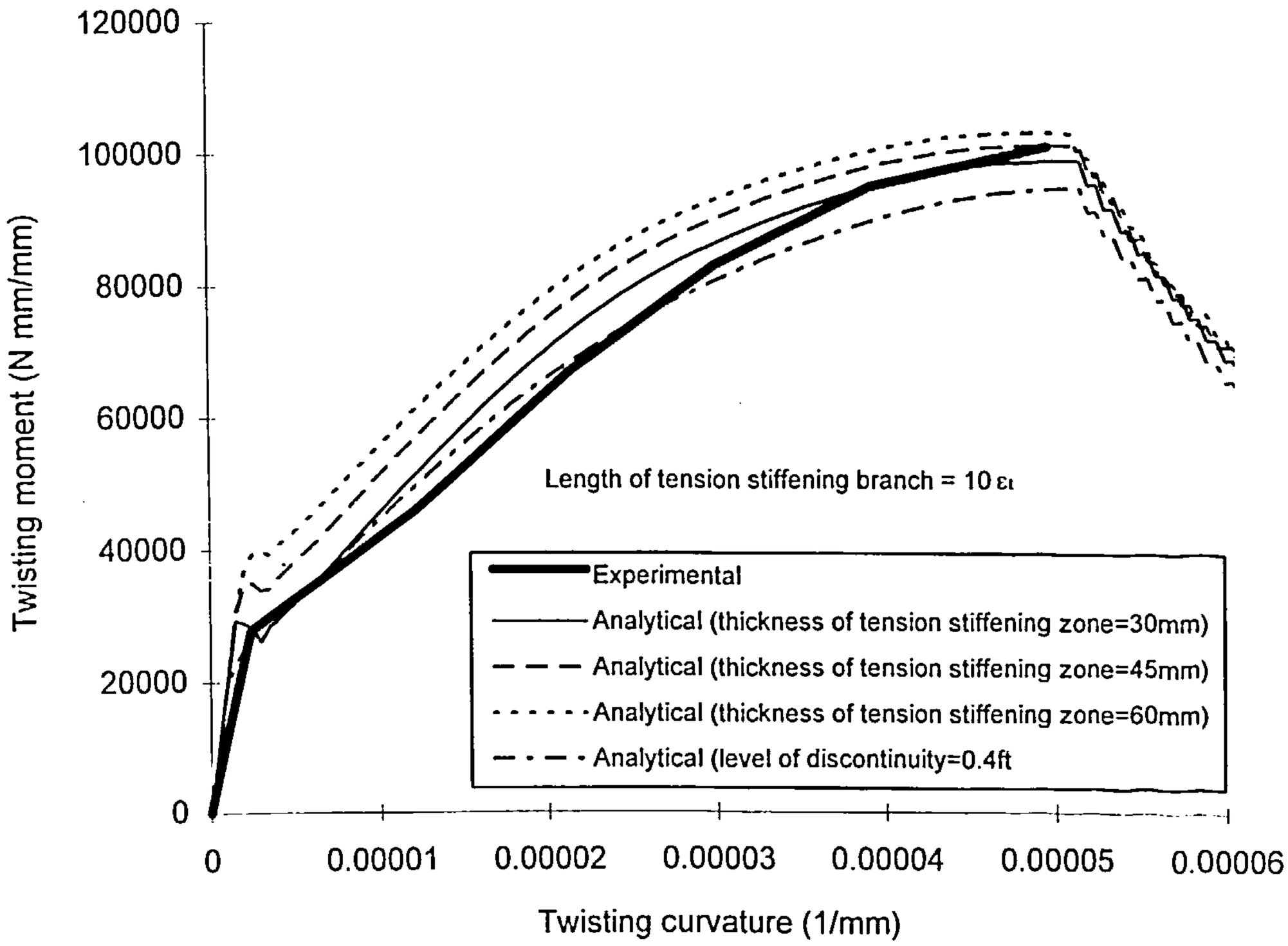

Figure 5.41: Response of an element under pure twisting moment with varying thickness of the zone of concrete around reinforcement

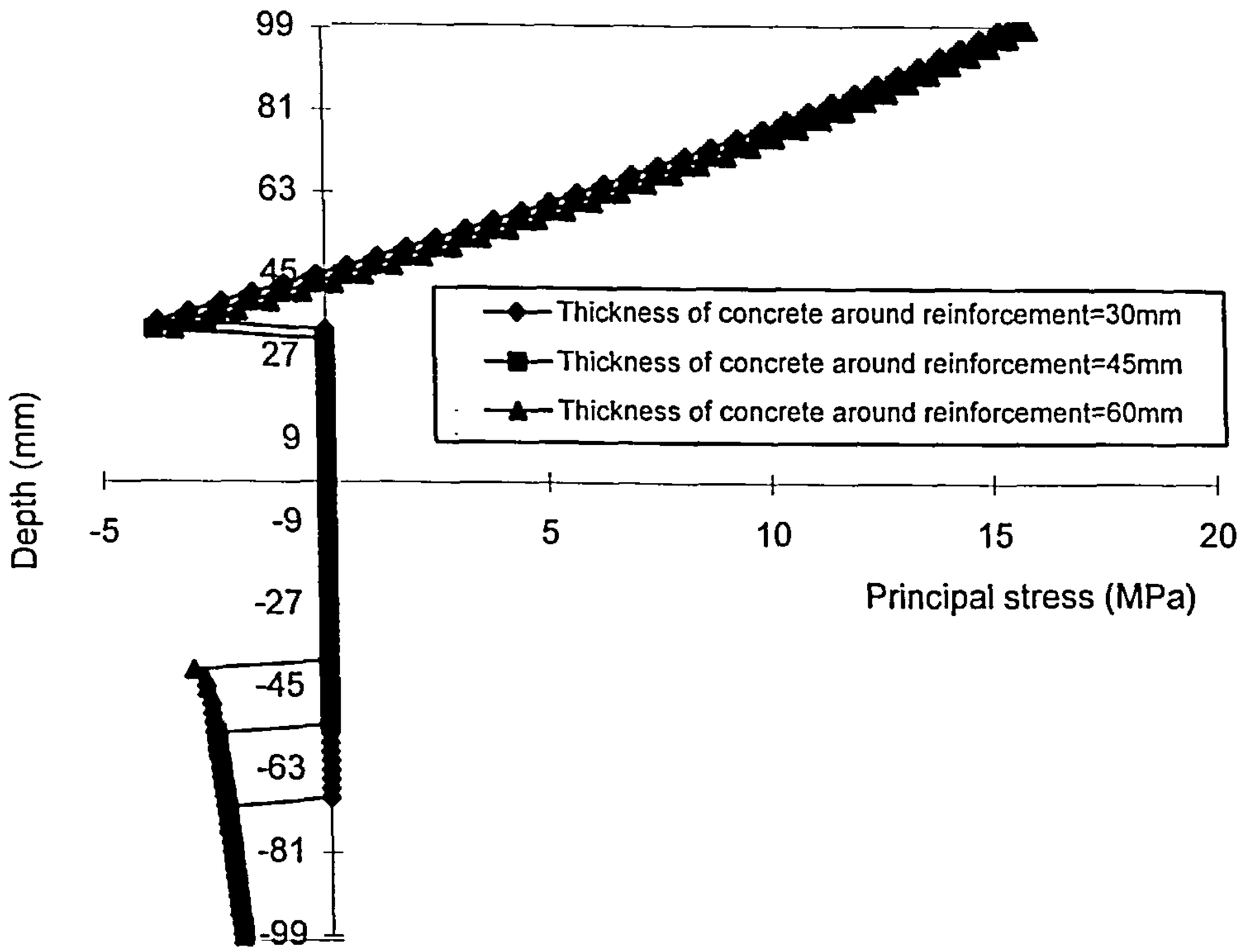

Figure 5.42: Principal stress distribution of concrete in direction 1-1 at 0.00001 1/mm curvature with different thickness of concrete zone around reinforcement under pure twisting moment

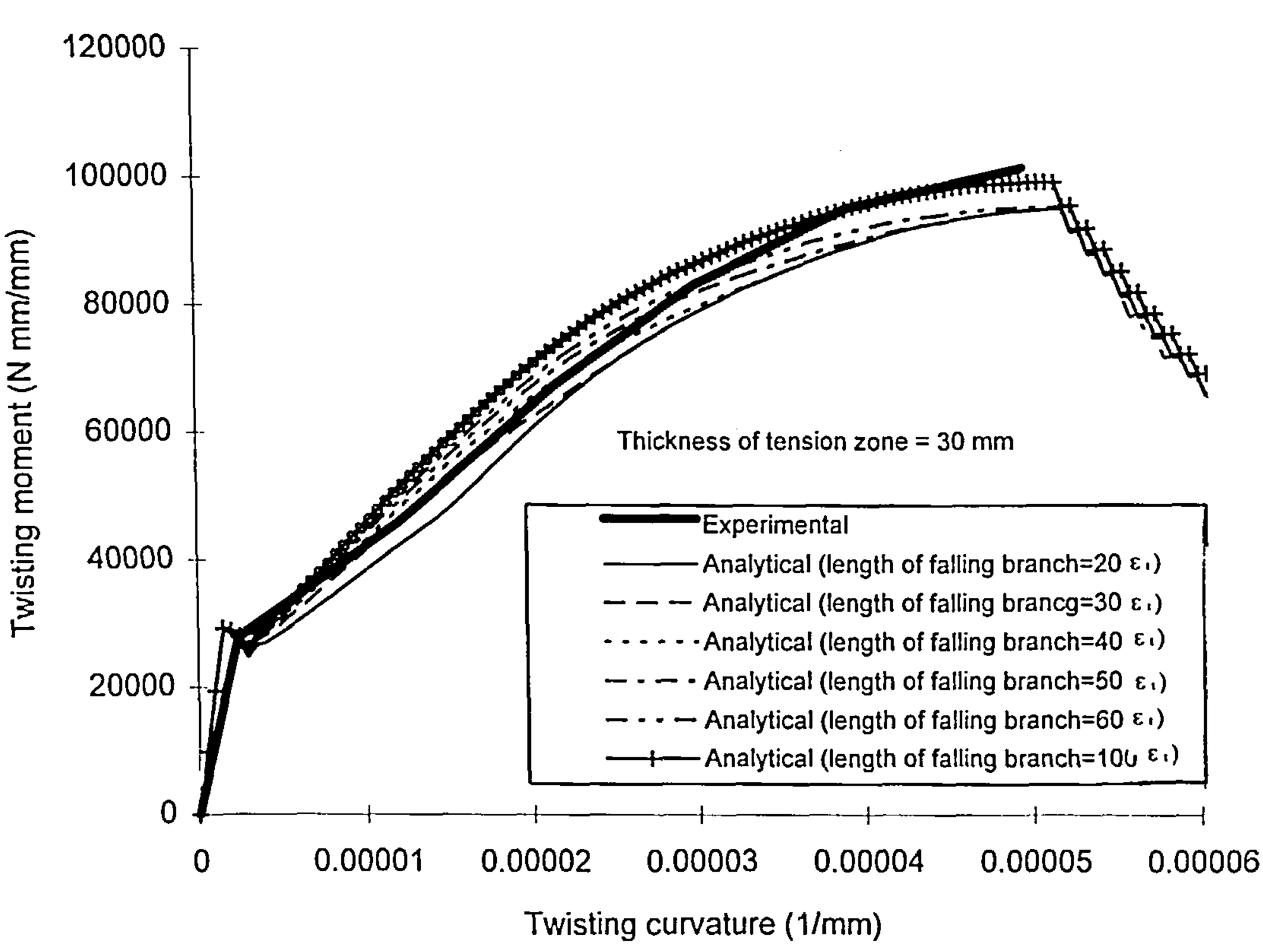

Figure 5.43: Response of an element subjected to pure twisting moment showing the effect of length of falling branch of tension stiffening

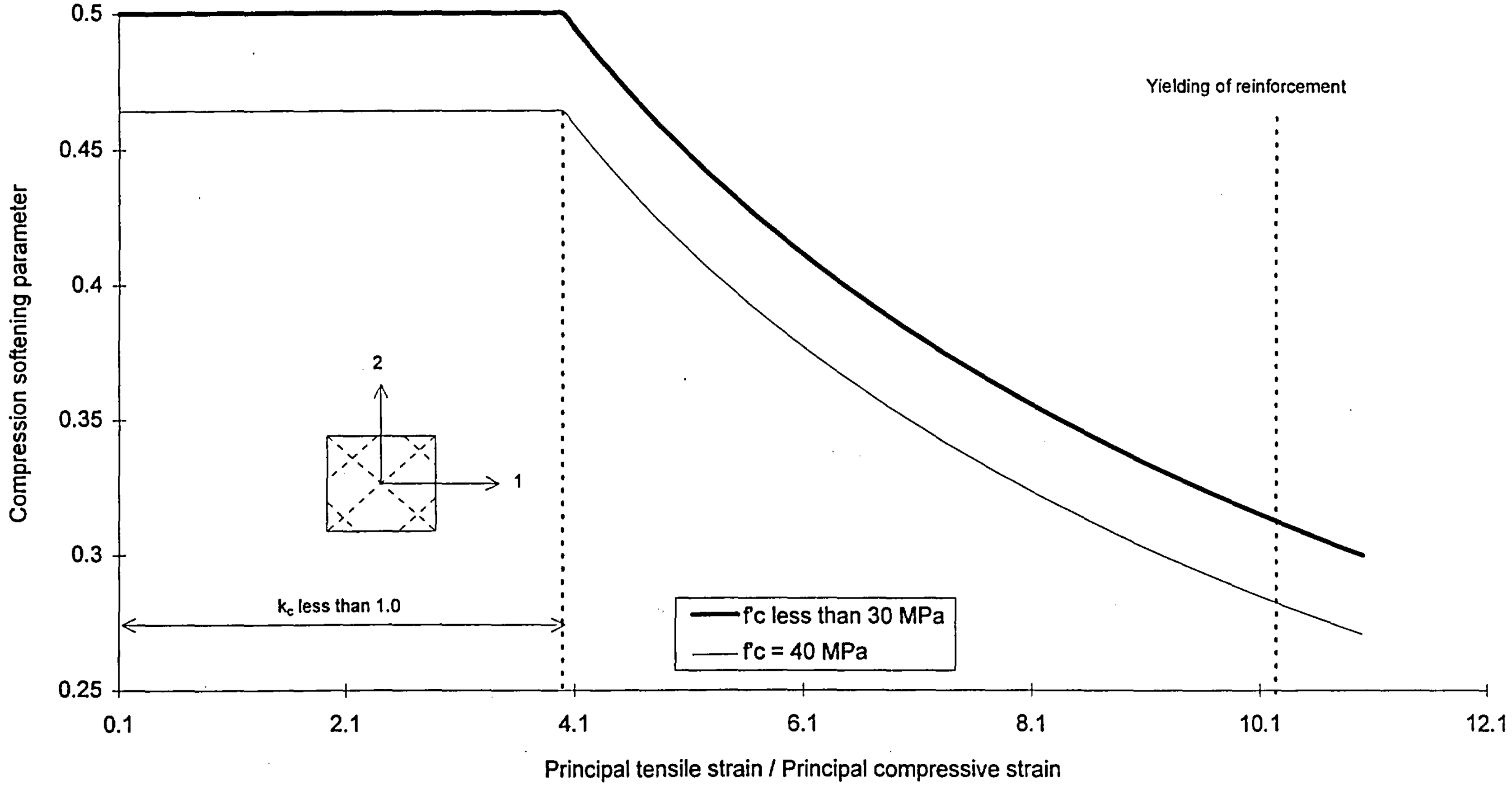

Figure 5.44: Variation of compression softening parameter

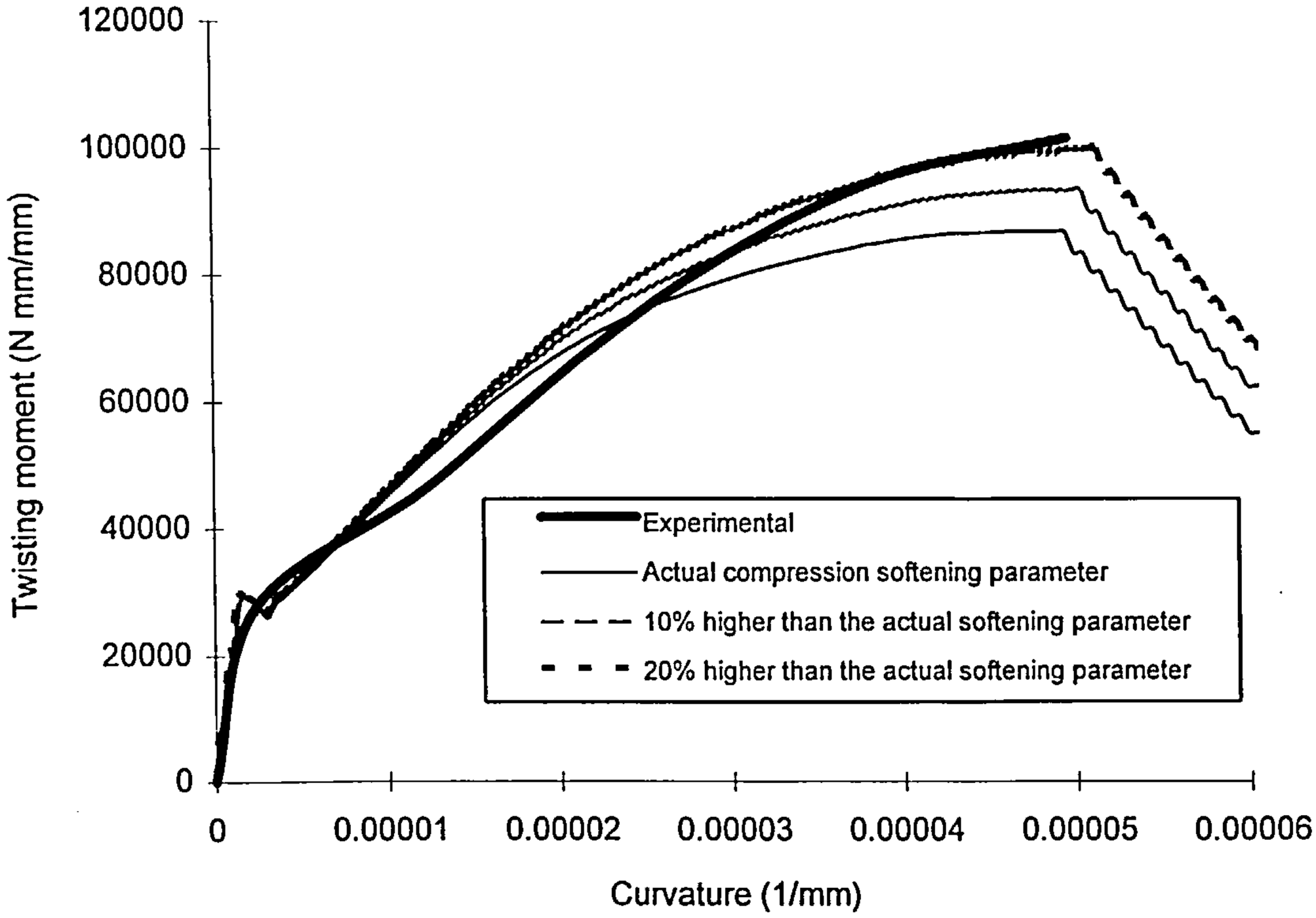

Figure 5.46: Response of an element subjected to pure twisting moment showing the effect of compression softening parameter

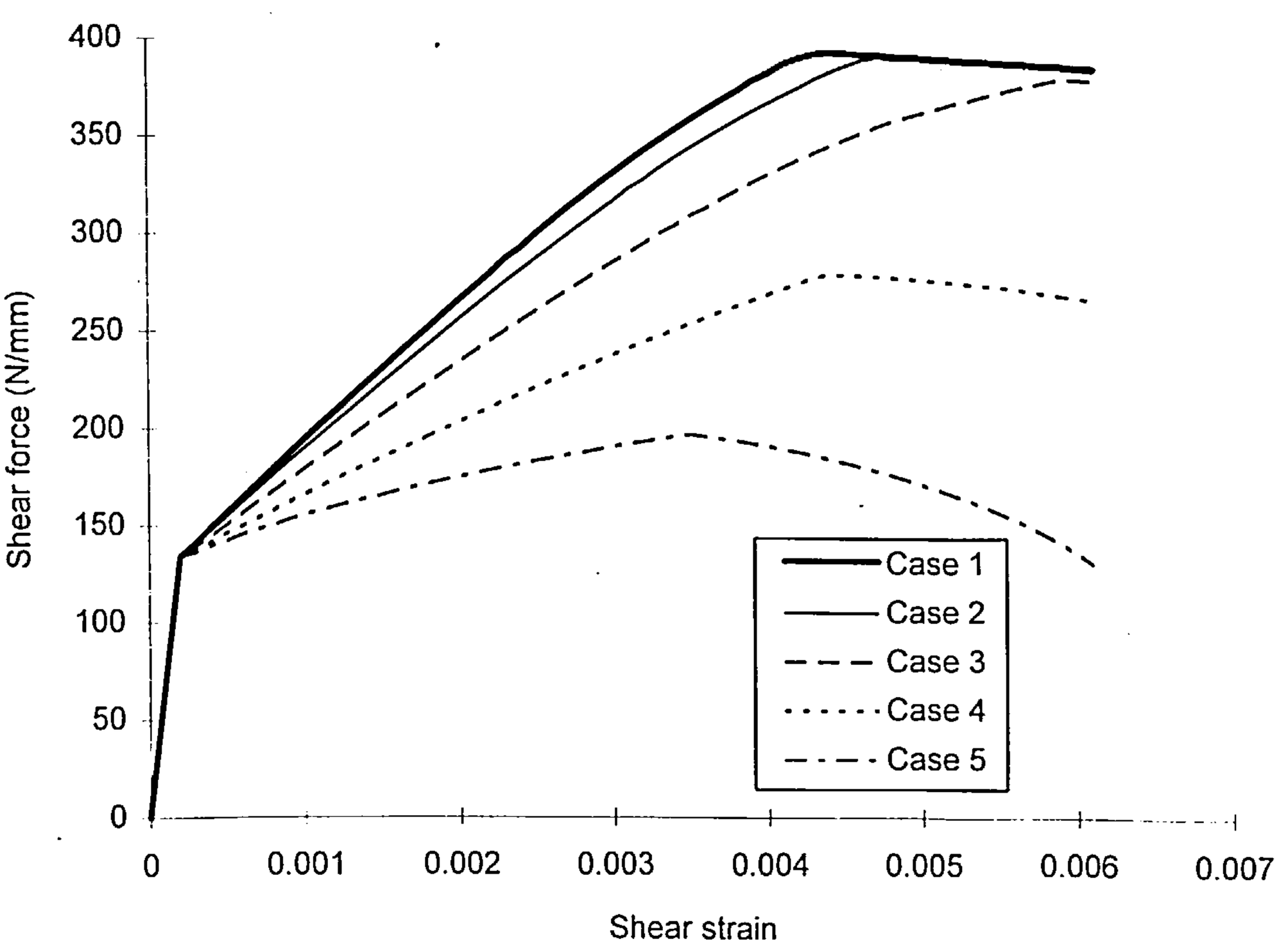

Figure 5.47: Effect of area of reinforcement when element is subjected to in-plane shear

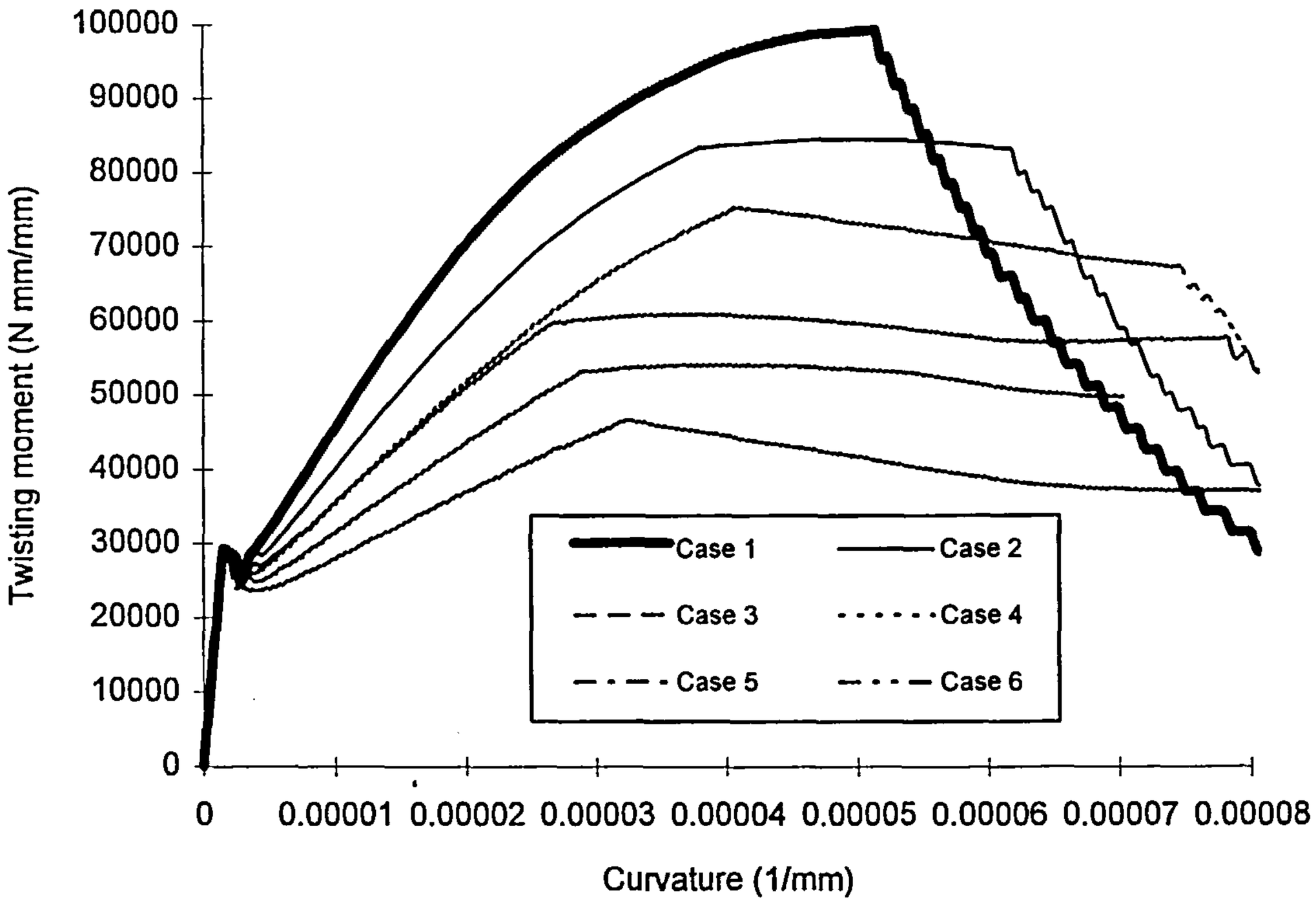

Figure 5.48: Effect of area of reinforcement when an element is subjected to pure twisting moment

CHAPTER 6

SLAB ELEMENTS AT ULTIMATE LOAD

6.1 INTRODUCTION

Reinforced concrete slabs can be designed for the ultimate state, for a generalised set of moments using the Wood-Armer rules[1,2]. These design rules provide optimum reinforcement for slabs. The rules use the normal moment yield criterion. The normal moment yield criterion uses Johansen's yield criterion[3] to define the strength of the slab. Johansen's yield criterion has some deficiencies and can provide increasingly unconservative strength predictions for certain load combinations. Several researchers[4,5,6,7] have pointed out the deficiencies in the normal moment yield criterion but the main cause, the use of Johansen's yield criterion, was not pointed out.

The software described in Chapter 4 has been used to determine the ultimate moment capacity of isotropic and orthotropic slab elements under different sets of moments with no in-plane forces. The deficiencies in the normal moment yield criterion have been confirmed which are due to the shortcomings in Johansen's yield criterion[3].

This Chapter presents failure surfaces calculated using the computer program for isotropic and orthotropic slab elements. Comparison between the failure surfaces developed numerically and using the normal moment yield criterion is made. The contribution of the concrete and the reinforcement at ultimate stress state under generalised loading condition are also shown.

6.2 YIELD CRITERION FOR ELEMENTS UNDER BENDING AND TWISTING MOMENTS

The ultimate stress state of an element is generally defined using a yield criterion. The yield criterion for a material can described as any combination of stresses which can cause the material to yield. It can be mathematically expressed as the relationship between the applied stresses and the material strength and can be expressed as follows,

$$F(\sigma_1,\sigma_2,\sigma_3,f_y)\geq 0 \qquad 6.1$$

where, σ_1, σ_2 and σ_3 are the principal stresses and f_y is the yield strength. When $F<0$, yield does not occur. But for $F \geq 0$ the material must yield.

For a reinforced concrete slab element subjected to moments only, with no in-plane forces, the yield criterion can be generally expressed as follows,

$$F(m_x, m_y, m_{xy}, m^*) \geq 0 \qquad 6.2$$

where, m_x, m_y and m_{xy} are the stress resultant and m^* is the yield strength of the slab element. The strength of an element depends on the section and the material properties.

In order to develop a yield criterion for a slab element, subjected to moments only, the following condition can be employed i.e. the strength of the member should be greater than or equal to applied moments. For slab elements with no in-plane forces a criterion can be used in terms of the normal moments such that,

$$m_{nu} \geq m_n \qquad 6.3$$

for any direction, n, in the plane of the slab,

where, m_n = normal moment in direction n due to the applied moments

and m_{nu} = capacity of the slab element in direction n.

The above expression only satisfies the condition for the moments acting normal to the direction of failure. Therefore, it is often termed as the Normal Moment Yield Criterion. It must be pointed out that on a slab element, in the failure direction apart from the normal moment, m_n, two further moments also exist, the tangential moment,

m_t, and the twisting moment, m_{nt}. The normal moment yield criterion neglects m_t and m_{nt}.

The normal moment yield criterion requires expressions defining the moment capacity of the slab element and the applied moments in the desired direction, n.

The ultimate moment capacity, m_{nu}, of a slab element in any direction can be defined by a yield criterion. The most widely and commonly used yield criterion is 'Johansen's Stepped Criterion[3]' which is mathematically expressed as,

$$m_{nu} = m_{xu} \cos^2\theta + m_{yu} \sin^2\theta \qquad 6.4$$

where, m_{xu} and m_{yu} are the ultimate moment capacities in the reinforcement directions x and y, and θ is the angle between the direction, n, and reinforcement in x direction, Figure 6.1. It is evident from equation 6.4 that the strength of a slab element in any direction, n, is a combination of the uniaxial bending strengths in the reinforcement directions x and y with a transformation in the required direction, n. This yield criterion has some deficiencies, Section 2.2.2, Chapter 2. One of the reasons for the criterion being popular is that it is easy to use and it provides a good estimation of strength of slab elements either with no twisting moment, or slabs with twisting moments but with low reinforcement ratios e.g. for isotropic slab elements

with $\rho\frac{f_y}{f_c}\leq\frac{1}{4}$ [7], ρ is the reinforcement ratio per layer in each direction, f_y is the yield strength of the reinforcement and f_c is the compressive strength of concrete.

In order to develop the expression for the normal applied moment, the applied moment components m_x, m_y and m_{xy} can be transformed to the direction, n, and can be expressed as

$$m_n = m_x \cos^2\theta + m_y \sin^2\theta - 2\, m_{xy} \sin\theta \cos\theta \qquad 6.5$$

To develop the yield criterion equation 6.3 can be rearranged and using equations 6.4 and 6.5 can be written as,

$$m_{xu} \cos^2\theta + m_{yu} \sin^2\theta - m_x \cos^2\theta - m_y \sin^2\theta + 2\, m_{xy} \sin\theta \cos\theta \geq 0 \qquad 6.6$$

To ensure that equation 6.6 is always satisfied when yield occurs in the failure direction, following condition must be fulfilled.

$$\frac{dm_{nu}}{d\theta} = \frac{dm_n}{d\theta} \qquad 6.7$$

Equations 6.4 and 6.5 are shown graphically in Figure 6.2 with point A representing the condition expressed in equation 6.7. Applying the above condition to equation 6.6, the failure direction, θ, is given by,

$$\tan\theta = \frac{(m_{xu} - m_x)}{m_{xy}} \qquad 6.8$$

substituting the value of θ from equation 6.8 in equation 6.6, the final form of the yield criterion can be obtained.

$$(m_{xu} - m_x)(m_{yu} - m_y) \geq m^2_{xy} \qquad 6.9a$$

The above yield criterion is based on positive moment capacities only. A similar expression can be obtained for the negative moment capacities m'_{xu} and m'_{yu}.

$$(m'_{xu} - m_x)(m'_{yu} - m_y) \geq m^2_{xy} \qquad 6.9b$$

Equations 6.9a and 6.9b completely define the normal moment yield criterion. In m_x, m_y, m_{xy} space, the normal moment yield criterion can be represented graphically by two elliptical cones lying back to back, Figure 6.3. The plane of intersection of the cones will be perpendicular to the m_x-m_y plane and the vertices of the two cones will lie in the positive-positive and the negative-negative quadrants of the m_x-m_y plane. In plan, a square or a rectangle will be formed depending, whether the element is isotropically or orthotropically reinforced, bounded by $m_x = m_{xu}$, $m_y = m_{yu}$, $m_x = m'_{xu}$ and $m_y = m'_{yu}$.

For a slab element with no twisting moment, the two sets of orthogonal reinforcement on either face will act independently with no interaction between them. With any

level of twisting moment the four sets of reinforcements will start to act interactively. The point of intersection of the two diagonals of square or rectangle, which is the projection of a point on the cone, represents the yielding of all four sets of reinforcement and the maximum twisting capacity of the element.

6.2.1 YIELD CRITERION FOR ISOTROPIC SLAB ELEMENTS

For an isotropically reinforced slab element where $m_{xu} = m_{yu} = m'_{xu} = m'_{yu} = m$ (if the slight difference between the moment capacities due to the different lever arms is neglected), the graphical representation of the normal moment yield criterion will be two circular cones as shown in Figure 6.4. Therefore, the pure twisting capacity of the element will be same as the uniaxial moment capacity, m.

The plane of intersection of the two cones will be at an angle of 45^{o} from the m_x and m_y axes. This plane will pass through the origin. The two vertices will have co-ordinates (m, m, 0) and (-m,-m, 0). In principal moment, m_1 and m_2, and θ space, the failure surface is represented by a cube.

6.2.2 YIELD CRITERION FOR ORTHOTROPIC SLAB ELEMENTS WITH DIRECTIONAL ISOTROPY

For an orthotropically reinforced element where $m_{xu} = -m'_{xu} = m$ and $m_{yu} = -m'_{yu} = \mu m$, the normal moment yield criterion will form two elliptical cones, Figure 6.5.

The pure twisting capacity will be the maximum twisting moment capacity of the element. The pure twisting moment capacity is given by the following expression.

$$m_{xyu} = \sqrt{\mu}\, m \qquad 6.10$$

The plane of intersection of the two cones will be at an angle, ϕ, from m_x axis and can be expressed as follows.

$$\tan\phi = \mu \qquad 6.11$$

This plane will pass through the origin. The two vertices will have co-ordinates $(m, \mu m, 0)$ and $(-m, -\mu m, 0)$.

6.2.3 YIELD CRITERION FOR COMPLETELY ORTHOTROPIC SLAB ELEMENTS

For a completely orthotropically reinforced slab element where the moment capacities are m_{xu} ,m_{yu} , m'_{xu} , m'_{yu}, the normal moment yield criterion is still represented by the two elliptical cones lying back to back, Figure 6.6. The plane of intersection of the two cones will be at an angle, ϕ, from the m_x axis which can be expressed as follows.

$$\tan\phi = \frac{m_{yu} - m'_{yu}}{m_{xu} - m'_{xu}} \qquad 6.12$$

The pure twisting capacity of the slab element will be the lesser of the two geometric means $\sqrt{(m_{xu})(m_{yu})}$ or $\sqrt{(m'_{xu})(m'_{yu})}$. As the plane of intersection of the two cones will not pass through the origin, the pure twisting capacity of the element will not be the maximum twisting capacity. The maximum twisting moment that such an element can resist will, however, be at the point intersection of the two diagonals, given by the following expression.

$$m_{xy} = \frac{1}{2}\sqrt{(m_{xu} - m'_{xu})(m_{yu} - m'_{yu})} \qquad 6.13a$$

The maximum twisting moment must be accompanied by the moments in x and y directions that are given by the following equations.

$$m_x = \frac{m_{xu} + m'_{xu}}{2} \qquad 6.13b$$

and,

$$m_y = \frac{m_{yu} + m'_{yu}}{2} \qquad 6.13c$$

The vertices of the two cones will still lie in the positive-positive and negative-negative quadrants of m_x-m_y plane with the co-ordinates (m_{xu}, m_{yu}, 0) and (m'_{xu}, m'_{yu},0) respectively.

6.2.4 EXTENSION OF THE YIELD CRITERION

Equations 6.12 and 6.13 give a general description of the normal moment yield criterion and can be used for any combination of moment capacities. Considering the case where the slab element has reinforcement on one face of the element only, in both the x and y directions with capacities m_{xu} and m_{yu} and $m'_{xu} = m'_{yu} = 0$. The normal moment yield criterion can still be represented by the two elliptical cones lying back to back. The two cones will lie in one quadrant, with one of the vertices at the origin and other at (m_{xu}, m_{yu}, 0), Figure 6.7. Such an element can not resist pure twisting moment as the intersection of the diagonals does not pass through the origin. In order to carry pure twisting moment the element must have reinforcement both at the top and bottom faces in x and y directions. However, the maximum twisting moment that such an element can resist is given below.

$$m_{xy} = \frac{1}{2}\sqrt{(m_{xu})(m_{yu})} \qquad 6.14a$$

The accompanying bending moments, Figure 6.8 in the reinforcement directions will be:

$$m_x = \frac{m_{xu}}{2} \qquad 6.14b$$

and,

$$m_y = \frac{m_{yu}}{2} \qquad 6.14c$$

6.3 DEFICIENCY IN THE NORMAL MOMENT YIELD CRITERION AND ITS CAUSES

The deficiency in the normal moment yield criterion, in its present form, is that it provides an over estimation of the strength with increasing reinforcement ratios as the angle between the reinforcement directions and the principal moment directions increases, to a limit of 45^{o}, Figure 6.1. The over estimation of strength becomes particularly significant when the principal moments are of opposite sign. This fact has been experimentally confirmed by Marti et al[6], Section 2.2.1, Chapter 2 but other researchers[4-8] have also pointed out the unconservatism of the normal moment yield criterion.

The normal moment yield criterion in its present form uses Johansen's yield criterion[3], equation 6.4, as explained in Section 6.2 earlier. Johansen's yield criterion determines the uniaxial bending moment capacities and then uses transformation to determine the strength for an orthogonally reinforced element in the desired direction. However, as the twisting moment increases in the reinforcement direction, the angles between the principal moment and the reinforcement directions increases. This forces the principal strain directions to change from the reinforcement directions. Thus it can be concluded that the increase in the twisting moment in the reinforcement direction increases the angles between the reinforcement and the principal strain directions. The reinforcement will have strains less than the maximum strain because it is not in the principal strain direction. Johansen's yield criterion can not predict the angle between

the reinforcement and the principal strain directions and consequently under estimates the neutral axis depth or over estimates the lever arm, therefore, over estimates the moment capacity of the slab element.

A comparison of the ultimate experimental moments obtained by Marti et al[6], for slabs subjected to pure twisting moment, and the ultimate moments obtained from equation 6.4 is shown in Table 6.1. It can be observed from Table 6.1 that the ultimate moment capacities using Johansen's yield criterion[3] becomes less accurate as the amount of reinforcement increases. Johansen's yield criterion has over estimated the capacity by upto 81%. Figure 6.9 shows the graphical representation of equation 6.4 and 6.5 along with the experimental ultimate moment for slab 3. The ultimate experimental moment capacity was 93.8 kN-m/m, whereas, the theoretical moment capacity predicted by equation 6.4 was 148.14 kN-m/m. The angle between the principal moments and the reinforcement direction 45^{o} and the deficiencies in Johansen's yield criterion[3] becomes more noticeable. The reasons for such an over estimation are explained below.

Consider an orthogonally reinforced slab element with isotropic reinforcement subjected to pure twisting moment $m_{xy} = m$. This is equivalent to being subjected to principal moments $\pm m$ acting at $\pm 45^{o}$ with respect to the reinforcement direction x as shown in Figure 6.10a. In case of pure twisting all four layers of reinforcement will be in tension as discussed in Section 5.4.2, Chapter 5 and it is assumed that at the ultimate load level all the four layers of reinforcement will be yielding.

Figure 6.10b shows the simplified stress distribution for faces 1 and 2 of the slab element. From equilibrium the expressions for the depth of the neutral axis and the moment capacity in the principal moment direction 1-1 can be calculated as:

$$a = \frac{2 A_s f_y}{\sigma_c} \qquad 6.15$$

$$m_{1\text{-}1} = \sigma_c a \left(\frac{h}{2} - \frac{a}{2}\right) = A_s f_y (h\text{-}a) \qquad 6.16a$$

where a = depth of the neutral axis

A_s = area of the reinforcement per layer in each direction

f_y = yield strength of reinforcement

σ_c = compressive strength of concrete

h = overall depth of the element

Similarly, the moment capacity of the element in principal direction 2-2 will be,

$$m_{2\text{-}2} = -\sigma_c a \left(\frac{h}{2} - \frac{a}{2}\right) = -A_s f_y (h\text{-}a) \qquad 6.16b$$

Using Johansen's yield criterion[3], the pure twisting moment capacity of the element is determined by calculating the uniaxial moment capacities in the reinforcement directions first. The uniaxial moment capacities are then transformed into the desired direction using transformation, equation 6.4. The following assumptions have been made in order to determine the uniaxial bending capacities,

- Tensile strength of concrete is neglected.

- Contribution of the reinforcement in compression is neglected.

- Both the sets of reinforcements in x and y direction are placed at the same level.

The depth of the neutral axis of the element under uniaxial bending will be,

$$a = \frac{A_s f_y}{\sigma_c} \qquad 6.17$$

The expression for the moment capacity of the element is,

$$m_{xu} = m_{yu} = A_s f_y (h - d_c - \frac{a}{2}) \qquad 6.18$$

where d_c is the distance to the centroid of the reinforcement from the nearest edge of the element, Figure 6.10. The transformation of the moment capacities into principal moment direction at 45° will yield,

$$m_{1\text{-}1} = m_{xu}\cos^2\theta + m_{yu}\sin^2\theta = A_s f_y (h - d_c - \frac{a}{2}) \qquad 6.19$$

as the depth of the cover is normally small as compared to the overall depth of the element and for simplicity, let $d_c = 0$, therefore,

$$m_{1\text{-}1} = A_s f_y (h - \frac{a}{2}) \qquad 6.20$$

The depth of the concrete stress block predicted for the pure twisting moment using equation 6.15 is twice that predicted by Johansen's yield criterion[3], equation 6.17. This is because of the fact that in the twisting analysis that both top and bottom reinforcement yield in tension. In Johansen's yield criterion only one layer is assumed to yield in tension. This in turn leads to an over estimation of the lever arm using Johansen's yield criterion and hence an over estimation of the ultimate twisting moment. It can be seen from equation 6.15 that this effect is worse with high area of steel and low concrete strength. Figure 6.11 shows the comparison between the ratio of the moment capacities calculated from twisting analysis, M_{twist}, and Johansen's yield criterion, M_{JYC}, and reinforcement ratios with and with out the effect of compression softening[9-11]. It is evident from Figure 6.11 that as the reinforcement ratio increases, M_{twist}/M_{JYC} decreases. The decreases M_{twist}/M_{JYC} in is due to the fact that as the reinforcement ratio increases, the difference between the neutral axis depth calculated using both the approaches increases, equations 6.15 and 6.17. This eventually increases the difference between the moment capacities using both the approaches.

Furthermore, in the case of pure twisting moment the concrete in the principal stress directions will be in the state of compression-tension. The tensile strain in one of the

principal stress direction will cause a significant reduction in the compressive strength of the concrete[9,10,11]. The reduction the strength of concrete will increase the depth of the neutral axis further as can be seen from equation 6.15. Thus compression softening will further reduce the overall lever arm in case of pure twisting and thus reduces the moment capacity, Figure 6.11. Johansen's yield criterion[3] does not account for compression softening and hence can grossly over estimate the moment capacity of the element with higher reinforcement ratios.

It is worth mentioning here that if there is no twisting moment present in the reinforcement directions and equal and opposite moments are applied in the reinforcement directions, the concrete will then be in compression-tension state and the compressive strength of concrete will reduce substantially. The reinforcement embedded in the compressive stress region of concrete will, however, remain in compression and thus the increase in the neutral axis depth will not be very significant. The increase in the depth of neutral axis due to compression softening alone does not significantly reduce the moment capacity as it is evident from slab 7 from the work carried out at the University of Manchester[12] discussed in Section 5.2.3, Chapter 5.

As the angle between the reinforcement and the principal strain or stress direction increases the depth of the neutral axis also increases. The increase in the depth of neutral axis not only reduces the moment capacity drastically but in some cases the mode of failure can change from an under reinforced failure, as predicted by Johansen's yield criterion[3], to an over reinforced failure. This is especially true for

higher reinforcement ratios, e.g. for isotropic elements under pure twisting with $(\frac{\rho f_y}{f_c} > \frac{1}{4})^7$ where, ρ is the reinforcement ratio, f_y is the yield strength of reinforcement and f_c is the softened compressive strength of concrete. The depth of the neutral axis given by equation 6.15 has been calculated on the assumption that the reinforcement is yielding. Elements with a high reinforcement ratio already have a larger depth of the neutral axis and any reduction in the compressive strength of concrete may increase the depth further. This slight increase in the depth of the neutral axis may be such that it may change the mode of failure, thus the assumption that reinforcement yields may not necessarily be valid for element with higher reinforcement ratios under twisting moment. The change of mode of failure has been observed for slabs 3 and 9[6], Table 6.1. The change in the mode of failure from the desired under reinforced to an over reinforced failure, nullifies the chances of moment redistribution.

6.3.1 SUMMARY

On the basis of the above, the causes for over estimation of moment capacity using normal moment criterion can be given. The prime cause of over estimation of moment capacity in the normal moment yield criterion is the use of Johansen's yield criterion[3]. The approach adopted in Johansen's yield criterion is that the uniaxial moment capacities are first determined and then the uniaxial moment capacities are transformed into the desired direction. The depth of the neutral axis is assumed to be the constant or the state of stress in concrete and reinforcement is assumed to be the same as that of uniaxial bending while applying transformation. Whereas, in fact as

the direction of the principal moments changes with respect to the reinforcement directions, the stress state of the element changes, altering the depth of the neutral axis. Johansen's yield criterion can not predict such changes. Consequently it can be concluded that the ordinary moment transformation can not predict the actual stress state of the concrete and the reinforcement.

The change in the depth of the neutral axis becomes more significant for when the ratio of the principal moments is negative because the reinforcement lying within the compressive stress block will be in tension due to its orientation from the principal stress direction. When the ratio of principal moments is positive, even though a significant amount of twisting moment is present in the reinforcement direction, the tensile stress in the reinforcement lying within the compressive stress block of concrete, but oriented at angle from the principal stress direction, does not significantly alter the depth of neutral axis and thus the moment capacity does not change significantly.

6.4 NUMERICALLY DEVELOPED FAILURE SURFACES FOR ISOTROPIC SLAB ELEMENTS

In order to confirm the deficiencies in the existing form of the normal moment yield criterion using Johansen's yield criterion[3], numerical experiments have been conducted to calculate the ultimate strength of slabs subjected to combinations of bending and twisting moments without in-plane forces, using the program described

in Chapter 4. Isotropically and orthotropically reinforced concrete slabs elements with varying reinforcement ratios were tested under different loading combinations.

Isotropic slab elements with varying reinforcement ratios (0.25%, 0.5% and 1% per layer in each direction) have been tested numerically. The section and material properties for the slab element tested are given in Table 6.2. The moments m_x, m_y and m_{xy} were applied in such a way that the directions of the principal moments were 0^o, 10^o, 30^o, and 45^o with respect to the reinforcement in direction x. The combination of the applied moments, m_x, m_y and m_{xy}, have been set such that for a given orientation of the principal moments a range of principal moment ratios were analysed ranging from +1 to -1. The reinforcement has been assumed to be placed at the same level in the x and the y directions at the top and the bottom faces of the slab element.

6.4.1 FAILURE SURFACES FOR 0.25% REINFORCEMENT

Figure 6.12 shows the failure surfaces in principal moment directions for an isotropically reinforced slab element with the reinforcement ratio of 0.25%. It is evident from Figure 6.12 that the difference between the ultimate moment capacities is not significant when compared with Johansen's yield criterion[3]. For the case of pure twisting, when the principal moments are $\pm m$, the numerically obtained moment capacity was only 5.3% lower than that using Johansen's yield criterion. This observation is in accordance with the fact that for low reinforcement ratios, although all the steel has yielded in tension and the depth of the neutral axis may have

increased, the difference between the two lever arms determined from equations 6.16 and 6.20 will not be significant.

The stress distribution in the concrete in the principal stress directions is shown in Figure 6.13 when the element is subjected to equal and opposite principal moments as the angle between the principal moment direction and the reinforcement changes from 0^{o} to 45^{o}. It can be observed from Figure 6.13 that the increase of the depth of the neutral axis can be significant as the twisting moment in the reinforcement directions increases from zero at 0^{o} to a maximum at 45^{o}, but because the neutral axis depth is small, the effect on the lever arm is not significant and the changes to the moment capacity are small. The reduction in the compressive strength of concrete due to compression softening can also be observed from Figure 6.13.

Figure 6.14 show the stresses in the reinforcement for the same loading combinations as shown in Figure 6.13. It can be seen that yielding in tension of two or more sets of reinforcement occur, as expected for all the load combinations. It can also be seen that when the angle between the principal moment and the reinforcement directions is less than about 30^{o} only two sets of reinforcement have yielded. They are orthogonal to each other, thus forming two hinge lines, one at the top and other at the bottom face of the slab. The two hinge lines will be perpendicular to each other. The only exception is the case of pure twisting where all the four sets of reinforcement have yielded in tension. The type of hinge line formation is in accordance with Johansen's yield criterion[3] and has been discussed in Section 6.2. It can also be observed from Figure 6.14 that as the orientation of principal moment changes, the stress in the

reinforcement lying within the compressive stress block of concrete but oriented at an angle from the principal stress direction, changes from compression to tension, thus forcing the neutral axis depth to increase.

6.4.2 FAILURE SURFACES FOR 0.5% REINFORCEMENT

The failure surfaces for isotropically reinforced slab element with 0.5% reinforcement are shown in Figure 6.15. Here again it can be concluded that the difference between the moment capacity predicted by the numerical analysis and Johansen's yield criterion[3] is not very large. In the case of pure twisting where the maximum difference in the capacities occur, the reduction is 12.7%. However, due to the low reinforcement ratio, all the four sets of the reinforcement yield in tension. The moment capacity depends on the lever arm which is not significantly different in this case when calculated using either the numerical technique or Johansen's yield criterion.

6.4.3 FAILURE SURFACES FOR 1% REINFORCEMENT

For the case of an isotropically reinforced slab element with 1% reinforcement, the failure surfaces for principal moment directions varying from 0^o to 45^o are shown in Figure 6.16. The difference in the analytical moment capacity and the capacity using Johansen's yield criterion[3] increases as the twisting moment in the reinforcement directions increases. The difference between the ultimate moment capacities using both the approaches is not very significant when the two principal moments are of the

same sign. But as the ratio of the principal moments becomes negative, the difference between the two capacities also increases significantly. For equal and opposite principal moments with principal moment directions of 0^{o}, 10^{o}, 20^{o}, 30^{o} and 45^{o} with respect to the reinforcement direction the reduction in the moment capacities are 2.2%, 10.3%, 25.4%, 40.5% and 47.9% respectively with respect to the capacities calculated using Johansen's yield criterion. For the principal moment directions of 30^{o} and 45^{o} the increase in the depth of the neutral axis is such that the mode of failure changes from under reinforced to over reinforced for the reasons discussed in Section 6.3.

The stress distribution in the concrete in the principal stress direction is shown in Figure 6.17 when the element is subjected to equal and opposite principal moments as the angle between the principal moment direction and the reinforcement changes from 0^{o} to 45^{o}. It can be observed from Figure 6.17 that the depth of the neutral axis is greater than that for similarly loaded elements but with a lower percentage of reinforcement, Figure 6.13, and the difference is significant as the twisting moment in the reinforcement directions increases from zero at 0^{o} to a maximum at 45^{o}. The change in the depth of neutral axis depth can significantly reduce the lever arm, hence the moment capacity.

Figure 6.18 shows the stresses in the reinforcement for the above cases and have shown yielding of the reinforcement as expected upto 20^{o}. Once again only two sets of reinforcement are yielding, thus forming two orthogonal hinge lines at the top and the bottom face of the slab respectively. But as the principal moment and the

reinforcement direction further deviate from each other, the increase in the depth of neutral axis is such that the reinforcement does not yield and the moment capacity thus reduces drastically. Furthermore, the stresses in the top reinforcement changes from compression to tension. The tension in the top reinforcement and compression in the surrounding concrete are the prime reason for the increase in the depth of neutral axis.

6.5 NUMERICALLY DEVELOPED FAILURE SURFACE FOR ORTHOTROPIC SLAB ELEMENT

An orthotropically reinforced slab element with 1% and 0.25% reinforcement in x and y directions respectively has been tested numerically upto and beyond failure. The reason for using such reinforcement ratios was to provide a reasonable difference in the reinforcement areas in the two directions and to retain practical reinforcement ratios. An isotropic slab element with 0.25% reinforcement showed minimal differences with respect to Johansen's yield criterion[3], Section 6.4.1. On the other hand the isotropic slab element with 1% reinforcement under large twisting moment exhibited an over reinforced failure, Section 6.4.3, therefore, reinforcement ratios higher than 1% will not substantially increase the moment capacity of the element. The intention of using such a reinforcement ratio was to check the validity of Johansen's yield criterion for a combination of the minimum and maximum reinforcement ratios. The section and material properties of the tested slab are given in Table 6.2. The moments, m_x, m_y and m_{xy}, were applied in such a combination that the principal moments were at angles of 0^o, 10^o, 30^o and 45^o to the reinforcement

directions. The combinations of the applied moments have been chosen such that for a given orientation of the principal moments a range of principal moment ratios from +1 to -1 were analysed. The reinforcement was assumed to placed at the same level in the x and y directions at the top and the bottom faces of the slab.

Figure 6.19 shows the numerically obtained ultimate strengths compared with the strengths from Johansen's yield criterion[3], plotted in principal moment space. The results show that for all principal moment directions Johansen's yield criterion[3] predicts too high a strength, but where the principal moments ratio is positive Johansen's yield criterion is safe. For positive principal moment ratios the maximum difference between the numerically obtained moment capacity and that from Johansen's yield criterion was 11.2%. This difference was for the loading condition when the principal moment directions were at $\pm 45^{o}$ with respect to the reinforcement directions and when the principal moment in one of the direction was zero.

In the case of a loading where the principal moments were at an angle of 0^{o} to the reinforcement directions and the principal moment ratio is positive, the difference in the strengths calculated from both the approaches is insignificant. There is, however, a slight increase in the strength in the numerically calculated ultimate strength and this is due to the fact that the concrete strength will increase because it will be in a state of compression-compression. The maximum increase in the strength was found to be 0.75% when the principal moment ratio was +1.

For a loading combination where the principal moment ratio is -1, but the reinforcement and the principal moment directions coincide, the reduction in the strength was found to be 2.25%. This reduction in the strength is due to compression softening[9-11]. It has been shown earlier, Section 6.3, that compression softening on its own can not reduce the moment capacity markedly. A similar response has been obtained for the loading combination when the principal moment ratio was -1 but the reinforcement was at 10^{o} principal moment direction.

For the loading combinations when the principal moments were at $\pm 30^{o}$ and $\pm 45^{o}$ from the reinforcement directions, Johansen's yield criterion[3] significantly over estimates the strength when the principal moment ratio was negative. For a load case when principal moment ratio was -1 and the reinforcements were at $\pm 30^{o}$, Johansen's yield criterion over estimated the moment capacity by 29.54% with respect to the numerically obtained moment capacity. Similarly for a loading combination when the principal moment ratio is -1 and the reinforcement is at $\pm 45^{o}$ from the principal moment directions i.e. pure twisting, the over estimation in strength is 30.24%. The over estimation in the strength is due to the facts discussed in Section 6.3.

Figure 6.20 shows the distribution of the stresses in the principal stress direction through the depth of the element for principal moment direction of 0^{o}, 10^{o}, 30^{o} to 45^{o} to the x reinforcement when the principal moment ratio is -1. It is evident from Figure 6.20 that as the twisting moment increases in the reinforcement direction i.e. as the angle between the principal moment and the reinforcement directions increases the depth of the neutral axis also increases. The concrete stress in the principal stress

direction 1-1 changes from compression to tension and then back to compression. This is due to the fact that the strain through the depth in the principal direction 1-1 varies in a similar fashion, Figure 6.21. The non-linear distribution of strain through the depth is due to the variation of the principal strain directions, Figure 6.22. The basic assumption that plane sections remain plane after bending, however, remains valid in numerical analysis. The stresses in the principal stress direction 2-2 are zero as the curvatures are so large that the tensile strains fall beyond the falling branch of the tension stiffening curve.

Figure 6.23 shows the stress in the reinforcement for the same loading combinations as for Figures 6.20 to 6.22. As the principal moment direction increases with respect to the reinforcement directions, Figure 6.1, the stress in the x direction reinforcement at the bottom face and the y direction reinforcement at the top changes from compression to continuously increasing tension. The increase in this tensile stress in the reinforcement, increases the depth of the neutral axis and eventually reduces the moment capacity, Section 6.3. For all the principal moment directions at least one hinge line have been observed as at least one set of reinforcement is yielding in tension except for the case of pure twisting where two sets of reinforcements are yielding. The two hinge lines in this case of loading will not be orthogonal to each other but will be formed to the top and bottom faces of the slab element.

Figure 6.24 shows the direct strains in the reinforcement directions and the shear strain through the depth of the element and Figure 6.25 shows the corresponding stresses for a case of pure twisting when the reinforcements are at $\pm 45^{o}$ to the

principal moment directions. The strain in all the four sets of the reinforcement are tensile and as the reinforcement has been modelled to carry only axial forces, all the sets of reinforcement will be in tension. The concrete stresses has been calculated for principal strains. Since the reinforcement and the principal strain directions do not coincide the stresses in concrete in one of the principal strain directions is in compression but the reinforcement will always be tension.

Figure 6.26 shows the stress distribution in the principal stress direction through the depth as the principal moment direction varies from 10^{o} to 45^{o} from the x direction reinforcement for the loading combination where principal moment produce uniaxial bending. The principal moment in direction 2-2 is zero. It can be once again observed that the principal moment changes from compression at the top to tension and back to compression. It is once again due to the non-linear strain distribution through the depth as shown in Figure 6.27.

The stresses in the reinforcement for the above mentioned principal moment uniaxial bending are shown in Figure 6.28. Once again it can be observed that the stress in the reinforcement lying within the compressive stress block of concrete but oriented at an angle from the principal stress direction, are tensile which causes the depth of the neutral axis to increase, Section 6.3. Only one hinge line have been produced as only one set of reinforcement is yielding, however, all four sets of reinforcement are interacting with each other because of the presence of the twisting moment.

Figure 6.29 and Figure 6.30 shows the direct and the shear strain and stress distribution through the depth of the element for uniaxial bending in principal moment directions with reinforcement at $\pm 45^{o}$. It can be observed from Figure 6.29 that the strain in the reinforcement directions are tensile but as the stresses in concrete are principal stresses they can be either compression or tension. Thus the reinforcement can be in tension even if lying within the compressive stress block of concrete since it is oriented at an angle from the principal stress direction.

6.6 EFFECT OF TWISTING MOMENT ON DUCTILITY

A reinforced concrete member is considered to be efficiently designed if apart from having a load capacity greater than the applied loads, it exhibits under reinforced behaviour. In an under reinforced member the reinforcement yields first followed by the crushing of concrete. The ratio of the deformation at the ultimate load to the deformation at the yield of the reinforcement is usually used to express the ductility of the member.

It has been established that the ductility of a reinforced concrete element depends on the following factors[13].

- An increase in the area of tension reinforcement reduces the ductility.

- A decrease in the concrete strength reduces the ductility.

- An increase in the area of compression reinforcement increases the ductility.

- An increase in the yield strength of the tension reinforcement reduces the ductility.

Apart from the factors mentioned above, it has been observed in this study that the ductility of a reinforced concrete slab element reduces with the increases in the twisting moment in the reinforcement directions. The effect of twisting moment on ductility of an element can be substantial. The increase in the twisting moment can change the mode of failure of an element from an under-reinforced when subjected to bending moments to an over reinforced under twisting moment. This fact has been discussed in Section 5.4.2, Chapter 5, Section 6.3 and can be observed in Figures 5.23, 5.25 and 5.28.

The effect of twisting moment on ductility is evident from Figure 6.31, which shows the moment-curvature response of an isotropic slab element with 1% reinforcement. The section and the material properties of the element are given in Table 6.2. The element was subjected to increasing twisting moments. This was accomplished by applying equal and opposite principal moments with the angle between the reinforcement and the principal moment directions as 0°, 10°, 20°, 30° and 45°. It can be observed from Figure 6.31 that as the twisting moment increases in the reinforcement directions, ductility decreases significantly. The ductility is usually

defined as the ratio of the curvature at ultimate moment, φ_u, to the curvature at the yield of the reinforcement, φ_y, Figure 6.32[13], i.e.

$$\text{Ductility index} = \frac{\varphi_u}{\varphi_y} \qquad 6.21$$

The ductility index of an isotropically reinforced element with 1% reinforcement ratio has reduced from 5.35 with no twisting moment to 2.66, 1.21, 1, 1 when the twisting moment is increased such that the angle between the reinforcement and the principal moment directions were 0^o, 10^o, 20^o, 30^o and 45^o respectively as shown in Figure 6.33. For 30^o and 45^o angles the element showed an over reinforced response in which the concrete crushes prior to the yielding of the reinforcement, thus has a ductility index of 1.

The reasons for the reduction in ductility are same as the causes of deficiencies in Johansen's yield criterion[3] which have been discussed in Section 6.3. However, the reasons have once again been summarised here. The increase of twisting moment in the reinforcement direction, increases the angle between the principal strain and the reinforcement directions. The reinforced concrete element consists of concrete which is a continuum and reinforcing bars which are discrete. Thus the concrete will be stressed at maximum direct strain i.e. principal strain. On the other hand the reinforcement can only have axial stress. The strain in the reinforcement direction will be less than the maximum direct strain on the element because the principal strain and reinforcement directions do not coincide. Therefore, as the twisting moment increases, so does the angle between the reinforcement and the principal strain

direction, consequently the stress in the reinforcement reduces. But as the concrete is still stressed in the principal strain direction it will have similar compressive stress as that of an element with lesser twisting moment. Hence the concrete is relatively more stressed as compared with the reinforcement with the increase in the twisting moment. Therefore, the ductility reduces with the increase of twisting moment in the reinforcement directions. Hence it is the balance between the principal compressive strain and the tensile strain in the reinforcement direction that defines the ductility of the element.

The other factor that effects the ductility with increase in the twisting moment is the reduction in the concrete strength due to compression softening[9-11]. With the increase in the twisting moment effect of compression softening increases, therefore, the strength of concrete reduces, decreasing the ductility.

The effect of area of reinforcement on ductility with the increase in the twisting moment can be observed in Figure 6.33. The variation of the ductility index with respect to the twisting moment is shown in Figure 6.33 for isotropic slab elements with 0.25%, 0.5% and 1% reinforcement ratios. It is evident from Figure 6.33 that the ductility is significantly reduced with the increase in the area of the reinforcement for a given angle between the principal moment and the reinforcement directions. The reduction in ductility with the increase in the reinforcement is due to the fact the at ultimate load, an element with lesser amount of reinforcement will have a shallower neutral axis depth as compared with an element with larger amount of reinforcement. Thus the principal tensile strain will be larger and subsequently the tensile strain and

stress the in the reinforcement will also be large. Therefore, in the elements with lesser amount of area of steel, the reinforcement will yield prior to the crushing of concrete, hence will be more ductile. For element with 0.25% reinforcement the ductility reduces significantly with the increase in the twisting moment, Figure 6.33, but it has exhibited an under reinforced response even under pure twisting i.e. at 45^{o} angle. The slab element with 0.5% reinforcement showed an over reinforced behaviour at pure twisting.

References

1 Wood, RH, The reinforcement of slabs in accordance with a predetermined field of moments, Concrete, London, vol. 2, February 1968, pp 69-76.

2 Armer GST, Discussion on 'The reinforcement of slabs in accordance with a predetermined field of moments', Concrete, London, vol. 8, August 1968, pp 319-321.

3 Johansen, KW, Brudlinieteorier, Gjellerup, Copenhagen, Denmark 1943, English edition: Yield line theory, Cement and Concrete Association, London 1962, 181p.

4 Nielsen, MP, Limit analysis of reinforced concrete slabs, Acta Polytechnica Scandinavica, Ci 26, Copenhagen, Denmark, 1964, 167 p.

5 Khalifa, JU, Limit analysis of reinforced concrete shell elements, PhD Thesis, Department of Civil Engineering, University of Toronto, May 1986, 222 p.

6 Marti, P, Leesti, P, Khalifa, WU, Torsion tests on reinforced concrete slab elements, Jnl. of St Eng., ASCE, vol. 113, no 5, May 1987, pp 994-1010.

7 Marti, P and Kong, K, Response of reinforced concrete slab elements to torsion, Jnl. of St Eng., ASCE, vol. 113, no 5, May 1987, pp 976-993.

8 Clark, LA, Tests on slab elements and skew slab bridges designed in accordance with the factored elastic moment field, Technical Report No. 42.474, Cement and Concrete Association, London, September 1972, 47 p.

9 Vecchio, FJ and Collins, MP, The modified compression field theory for reinforced concrete elements subjected to shear, ACI St. Jnl., vol. 82, no. 2, Mar-Apr. 1986, pp 219-231.

10 Vecchio, FJ and Collins, MP, Compression response of cracked reinforced concrete, Jnl. of St. Eng., ASCE, vol. 119, no. 12, December 1993, pp 3590-3610.

11 Belarbi, A and Hsu, TTC, Constitutive laws of softened concrete in biaxial tension-compression, ACI St. Jnl., vol. 92, no. 5, September 1995, pp 562-573.

12 Samad, AAA, The response of reinforced concrete slabs subjected to biaxial bending and twisting moments, PhD Thesis, University of Manchester, June 1994, 354 p.

13 Park, R and Pauly, T, Reinforced concrete structures, John Wiley and Sons, 1980, 618 p.

Table 6.1: Comparison of ultimate experimental moments of Marti et al[Error! Bookmark not defined.] slabs with ultimate moment capacities using Johansen's yield criterion[Error! Bookmark not defined.]

Slab no	ρ_{sx} (%)	ρ'_{sx} (%)	ρ_{sy} (%)	ρ'_{sy} (%)	m_{xu} (kN-m/m)	m_{yu} (kN-m/m)	m_{xyu} (equation 6.4) (kN-m/m)	m_{xyu} (experimental) (kN-m/m)	$\frac{m_{xyu}\text{ (equation 6.4)}}{m_{xyu}\text{ (experimental)}}$
1	0.25	0.25	0.25	0.25	49.0	46.8	47.9	44.4*	1.08
2	0.5	0.5	0.5	0.5	97.2	91.1	94.1	69.5*	1.35
3	1	1	1	1	155.5	141.1	148.1	93.8*[a]	1.58
4	0.5	0.5	0.25	0.25	98.0	46.8	67.7	50.8*	1.33
5	1	1	0.25	0.25	162.1	45.2	85.6	60.6*	1.41
6	1	1	0.5	0.5	155.2	85.0	114.8	63.6	1.80
7	0.25	0.25	0.25	0.25	43.4	40.8	42.1	42.5**	0.99
8	1	1	0.25	0.25	143.1	39.6	75.3	64.8	1.16
9	1	1	1	1	142.3	129.1	135.5	101.5[a]	1.33

* Corner failed prior to reaching ultimate load

** Corner failed after reaching ultimate load

[a] Over reinforced failure

Table 6.2: Section and material properties of the numerically tested slab.

Overall depth of the element	200 mm
Distance of r/f centroid to the nearest edge of element	18 mm
Reinforcement ratio	0.25% - 1% (varies-isotropic slab) 1% (x direction - orthotropic slab) 0.25% (y direction - orthotropic slab)
Compressive strength of concrete	37.5 N/mm^2
Strain corresponding to compressive strength	2.5×10^{-3}
Tensile strength of concrete	3.35 N/mm^2
Cracking strain of concrete	1.12×10^{-4}
Modulus of elasticity of steel	200×10^3 N/mm^2
Yield strength of steel	481 N/mm^2

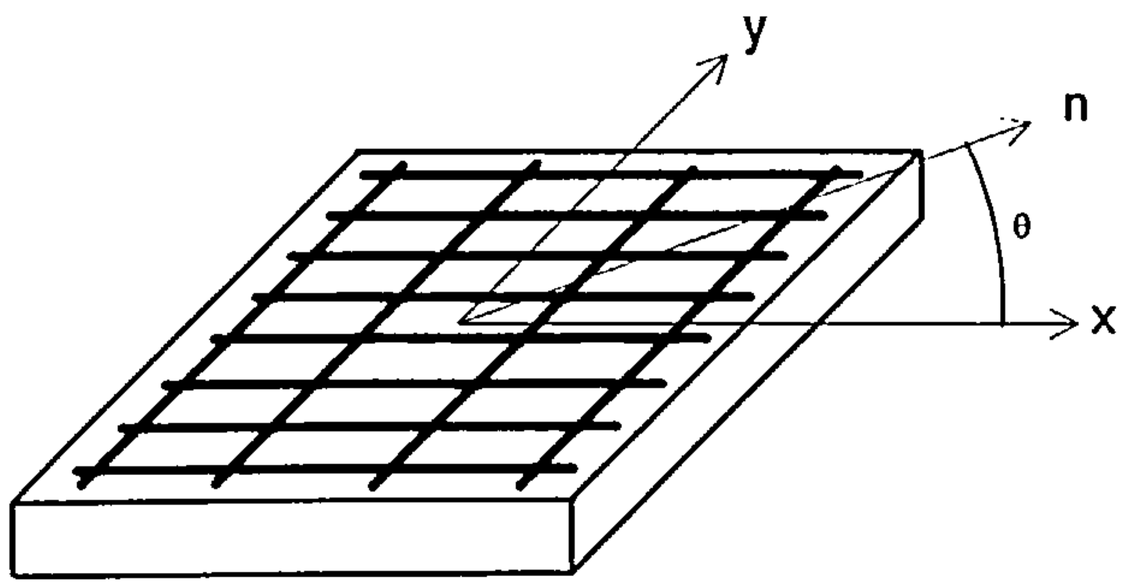

Figure 6.1: Reinforced concrete slab element

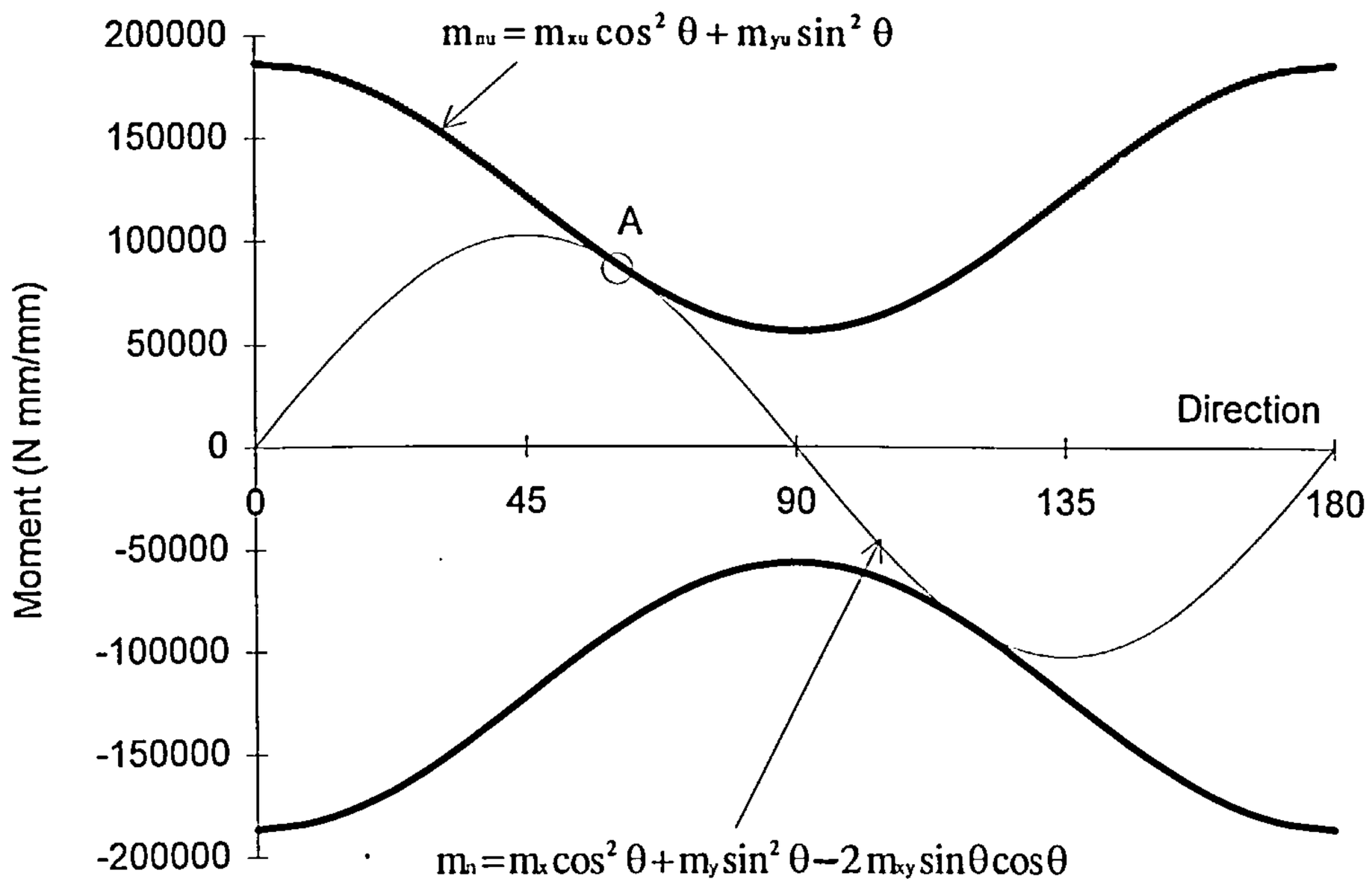

Figure 6.2: Graphical representation of the normal moment yield criterion

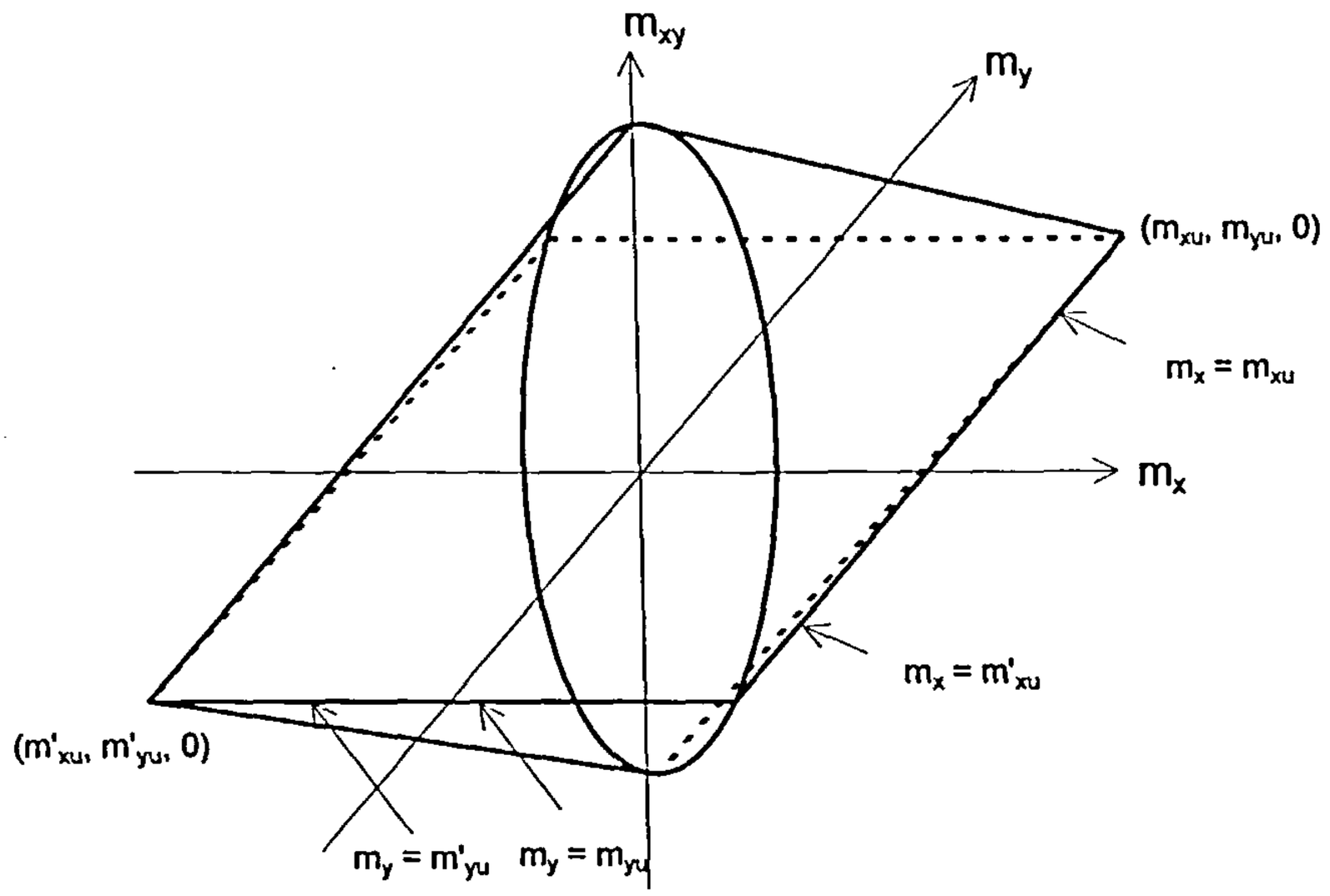

Figure 6.3: Normal moment yield criterion in m_x, m_y and m_{xy} space

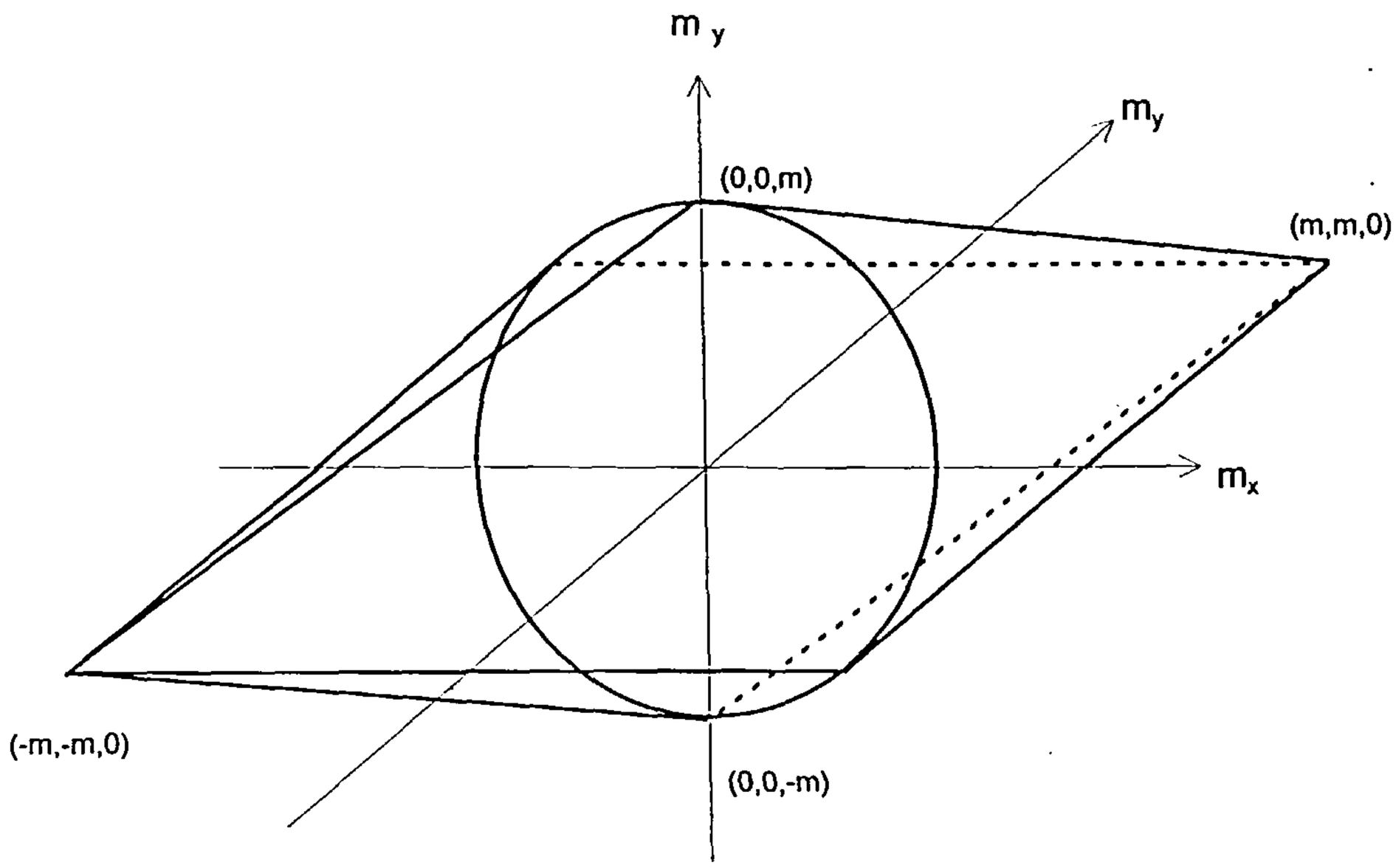

Figure 6.4: Normal moment yield criterion for isotropic slabs in m_x, m_y and m_{xy} space

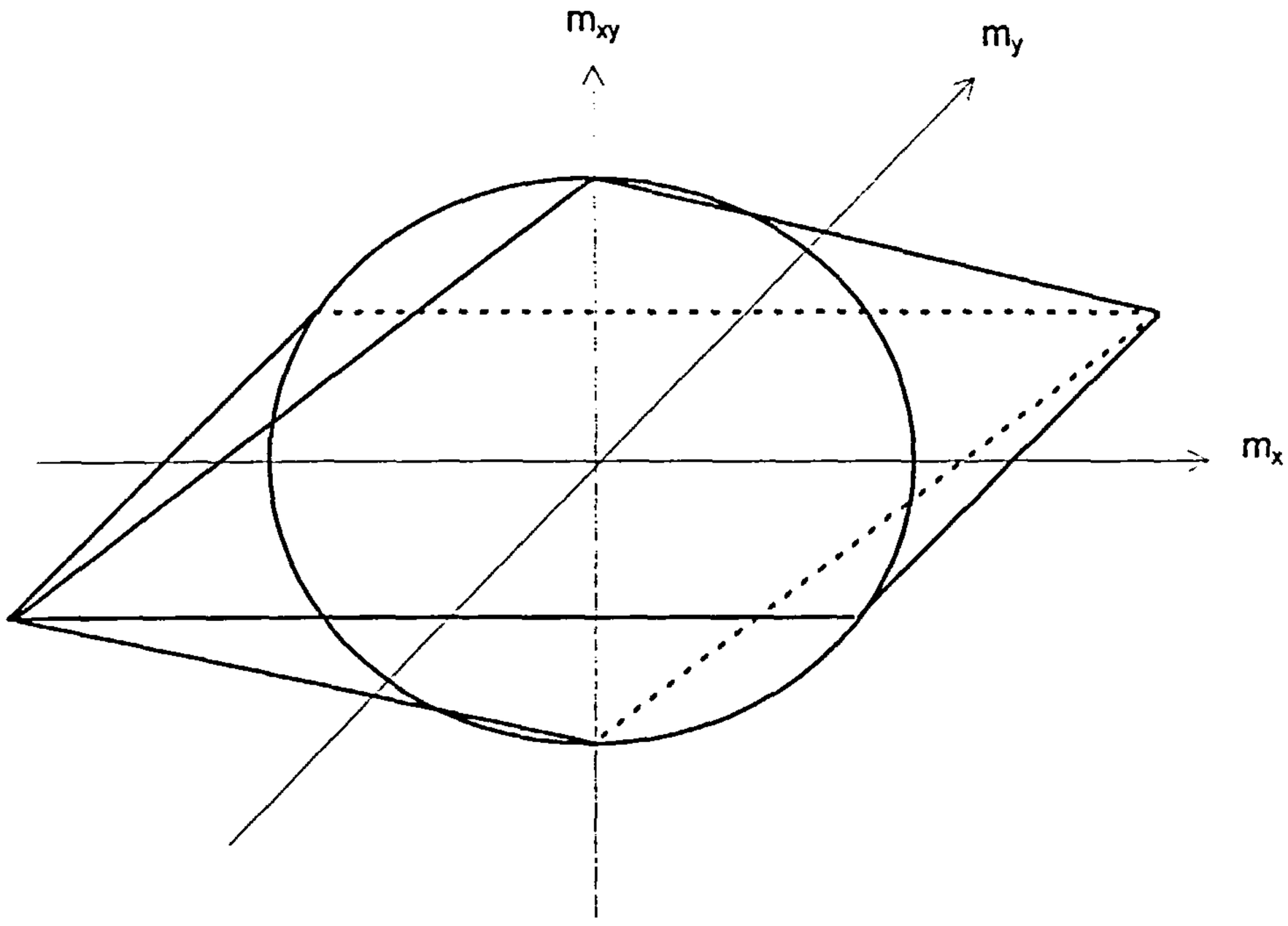

(a)

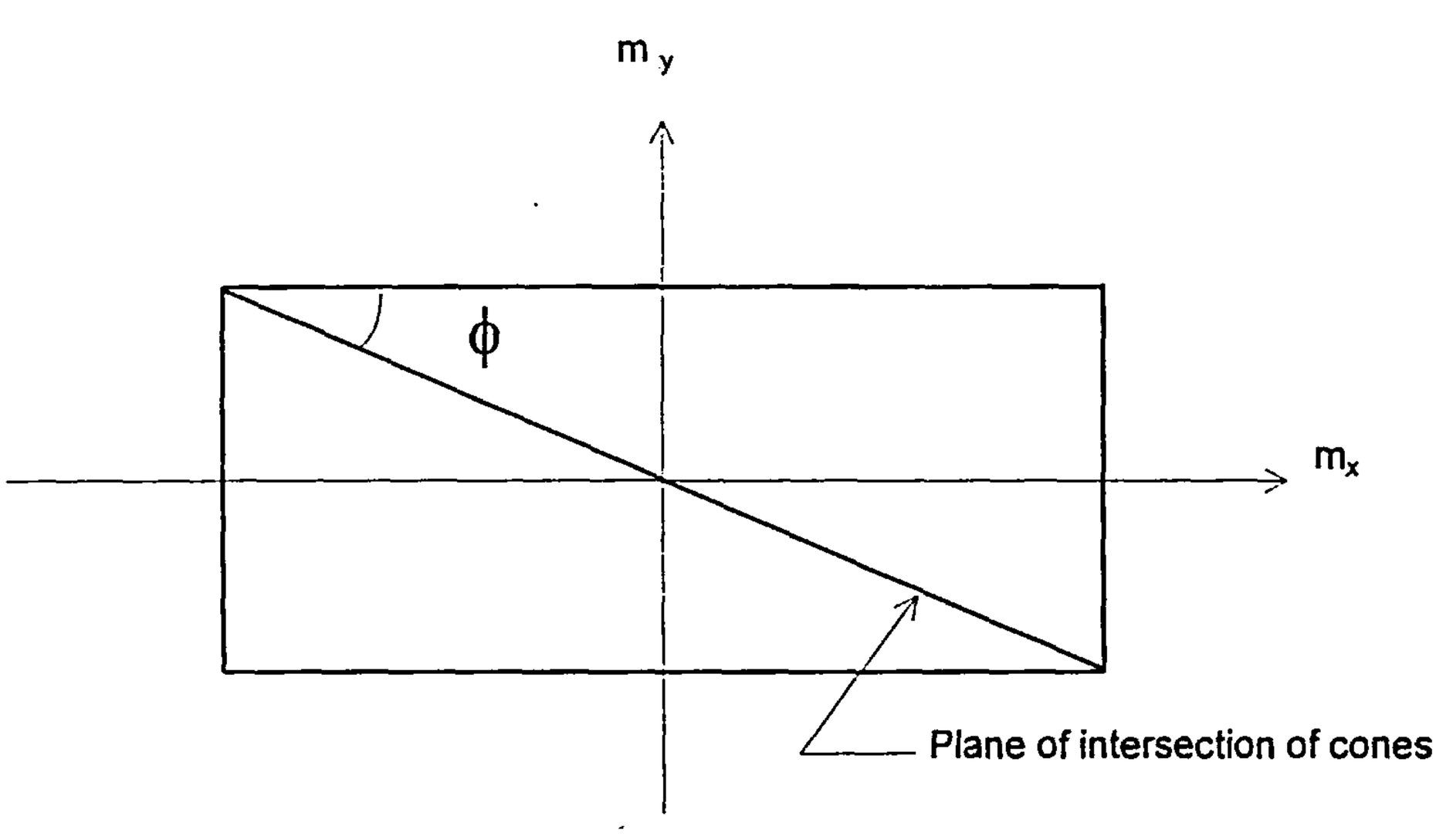

(b)

Figure 6.5: Normal moment yield criterion for orthotropic slabs with directional isotropy (a) in m_x, m_y and m_{xy} space (b) plan

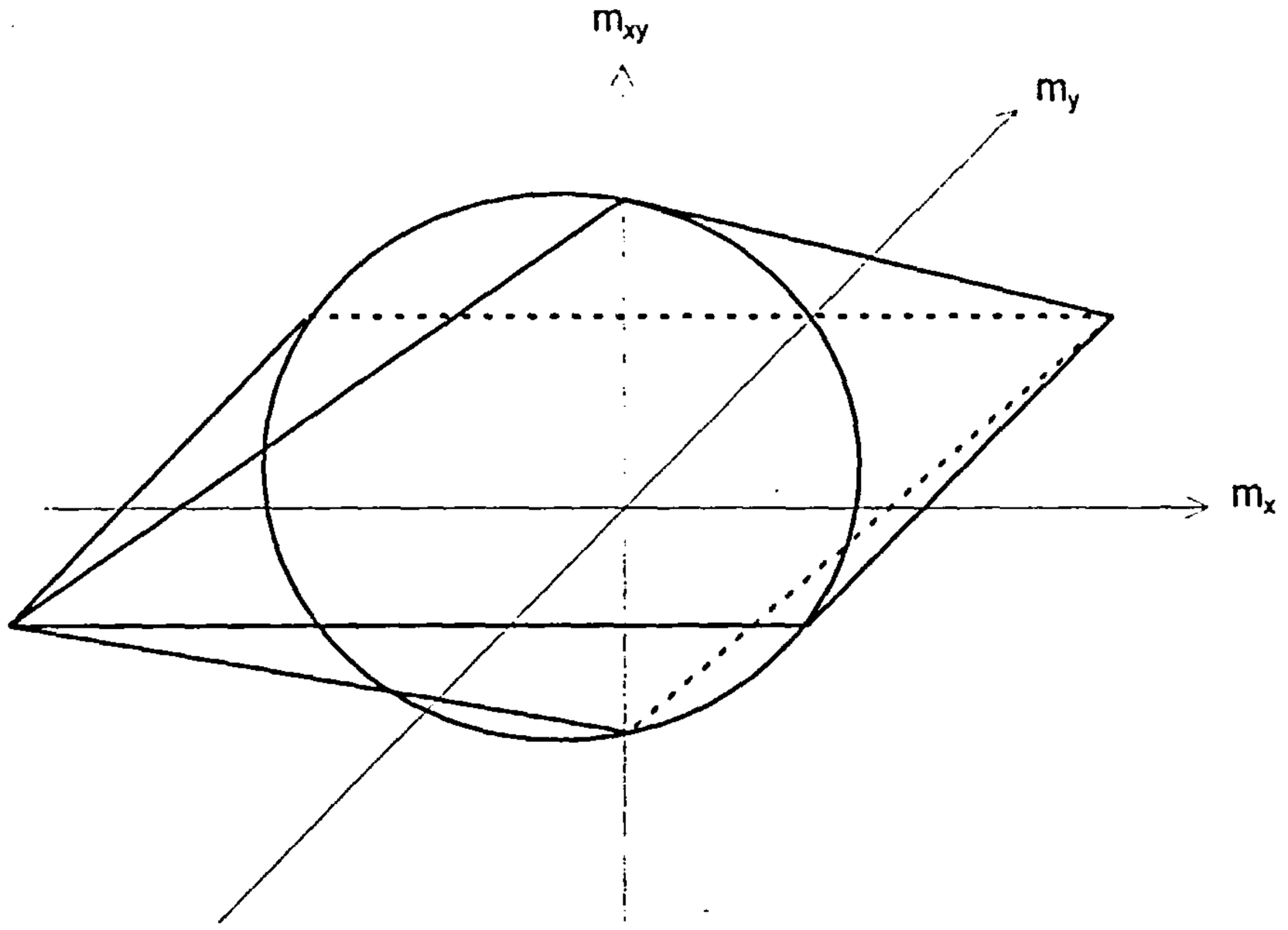

(a)

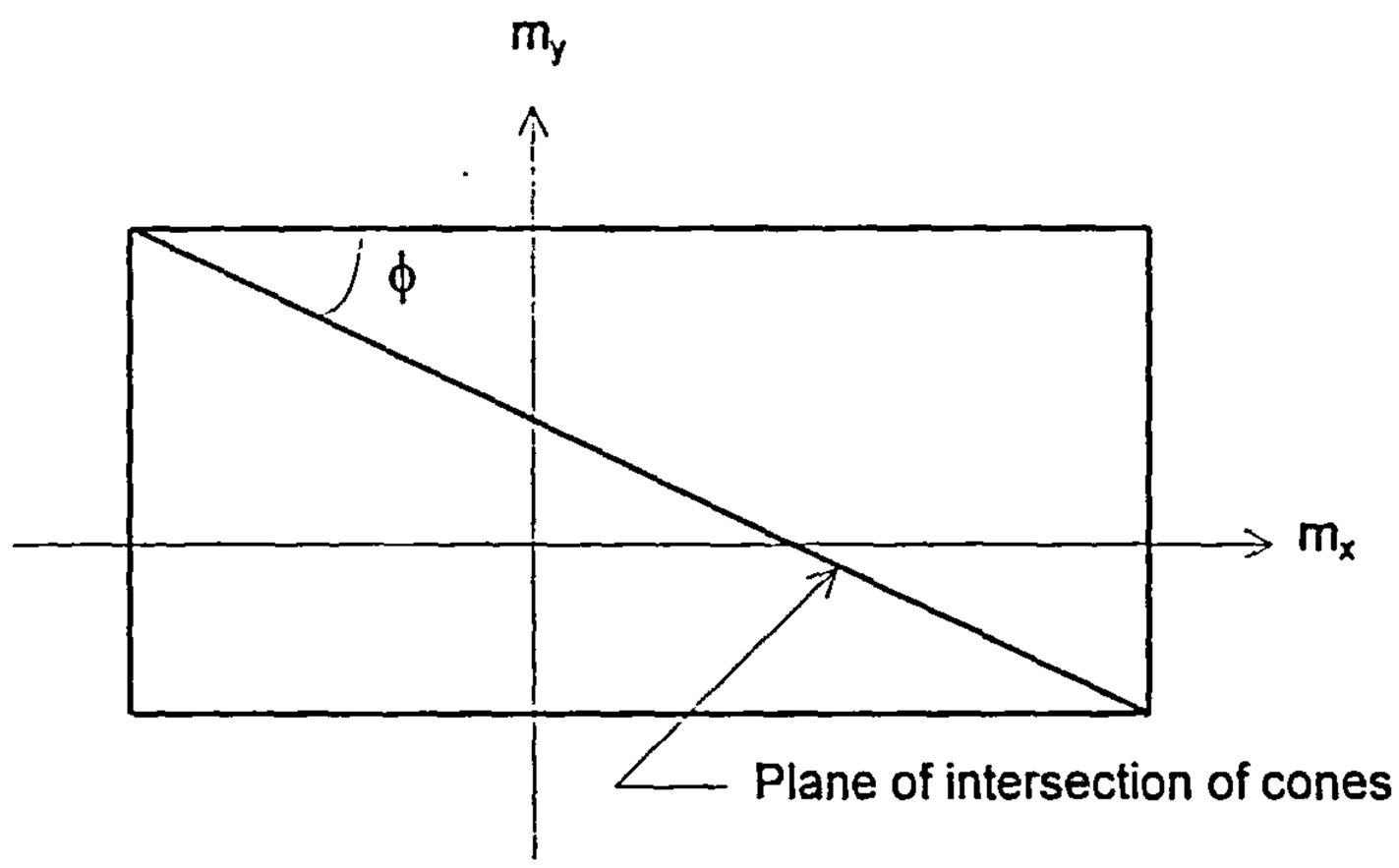

(b)

Figure 6.6: Normal moment yield criterion for orthotropic slab (a) in m_x, m_y and m_{xy} space (b) plan

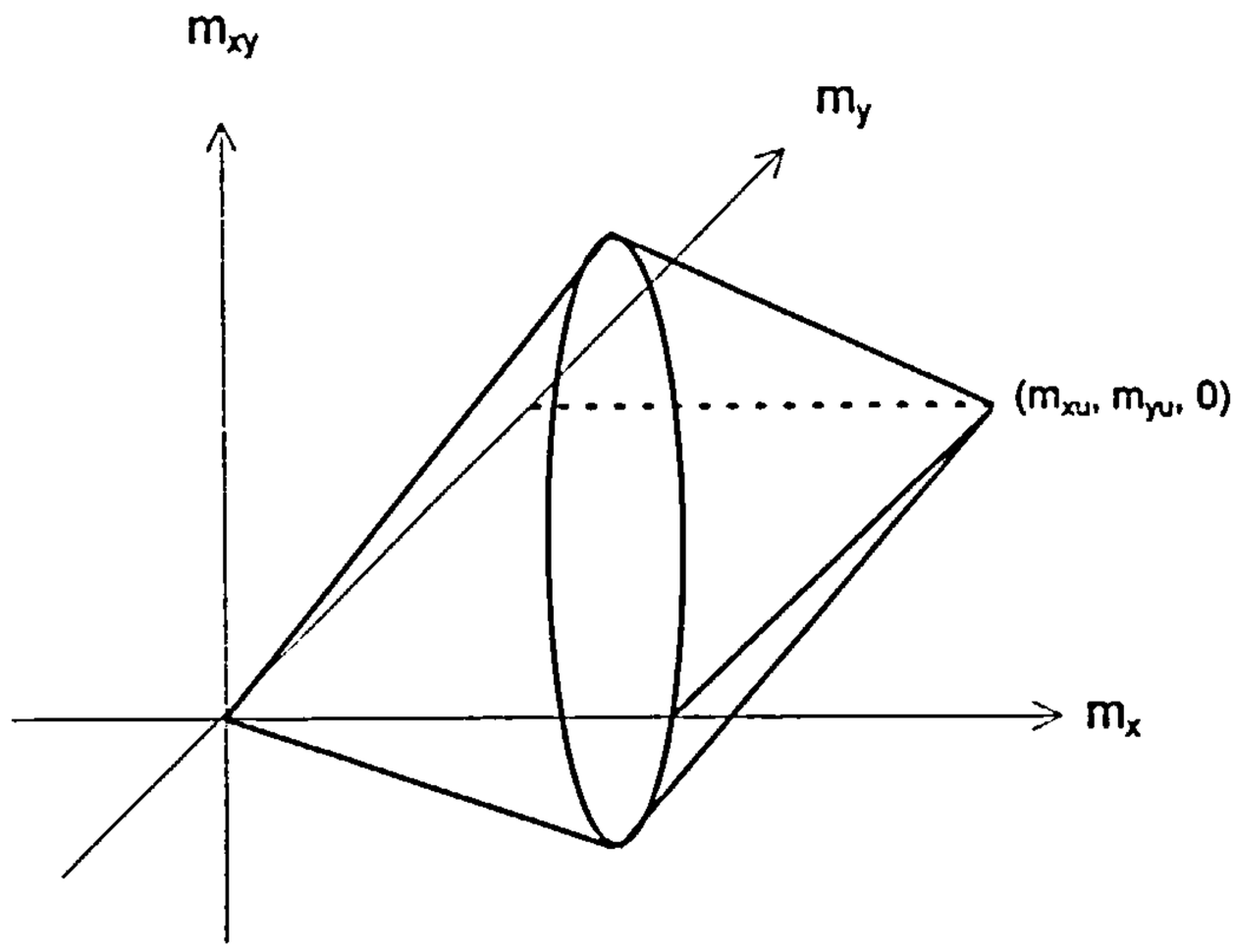

Figure 6.7: Normal moment yield criterion in m_x, m_y and m_{xy} space for slab with reinforcement at one face only

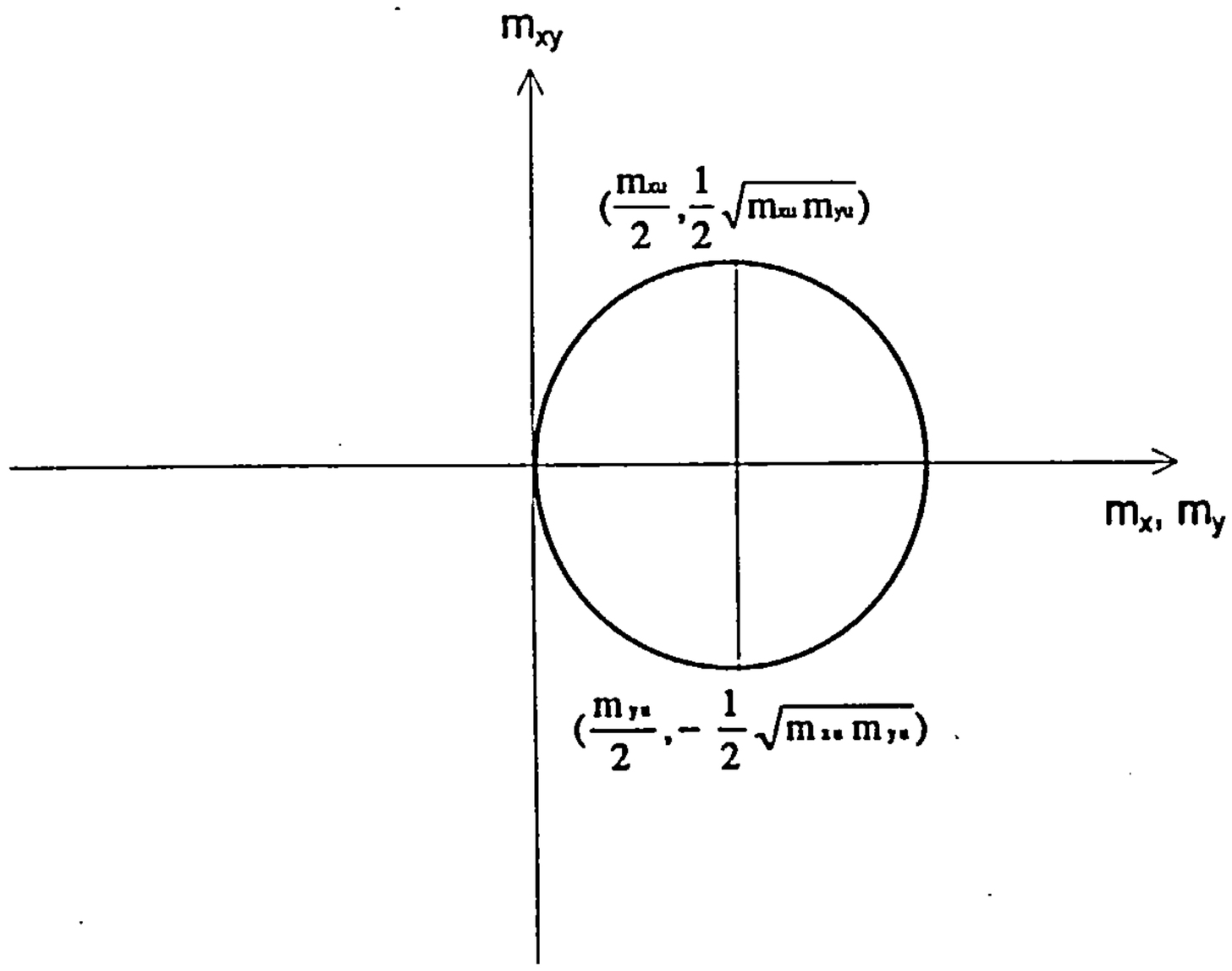

Figure 6.8: Mohr's circle of moment capacities for slab element with reinforcement on one face only

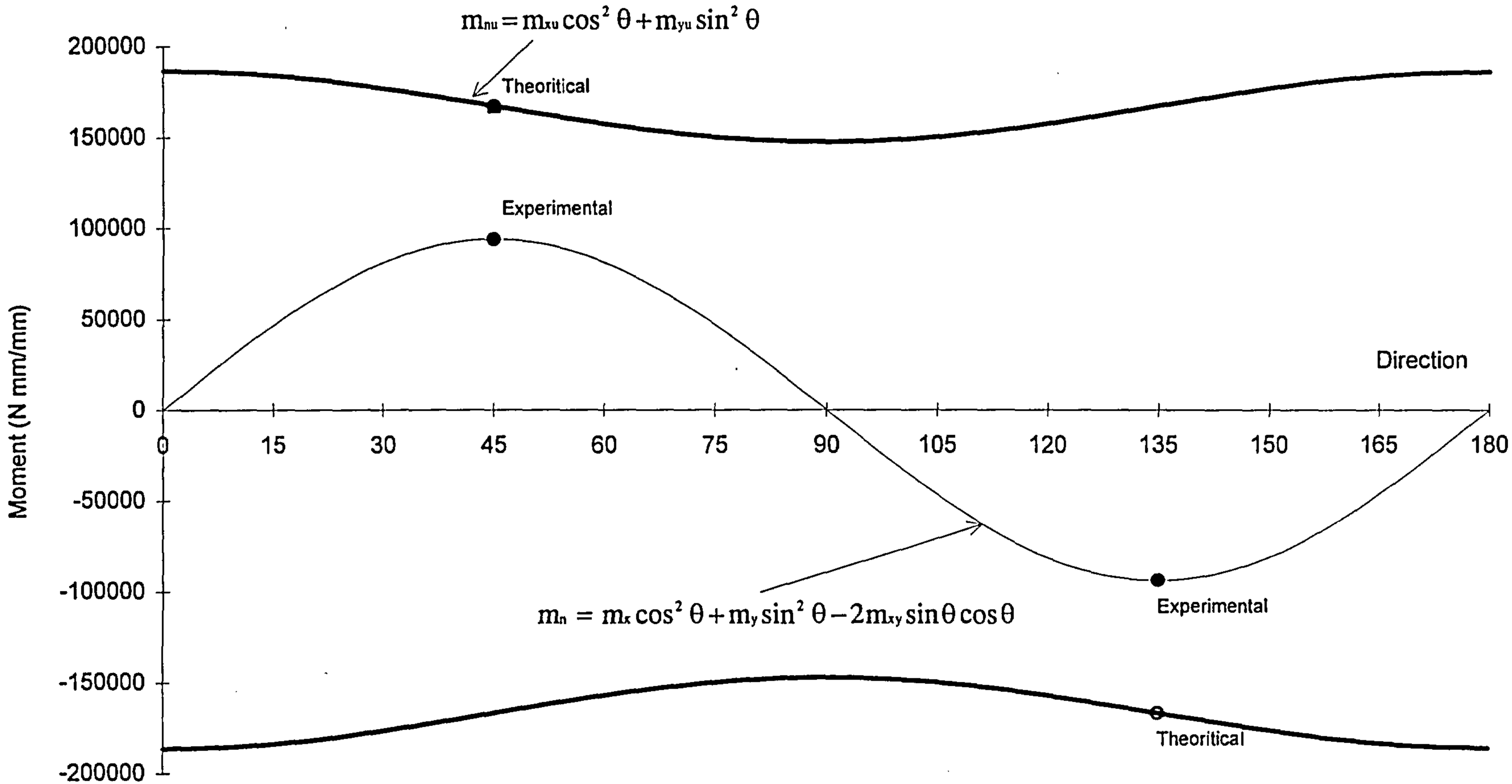

Figure 6.9: Graphical representation of the normal moment yield criterion with the experimental moment capacity of slab 3^6

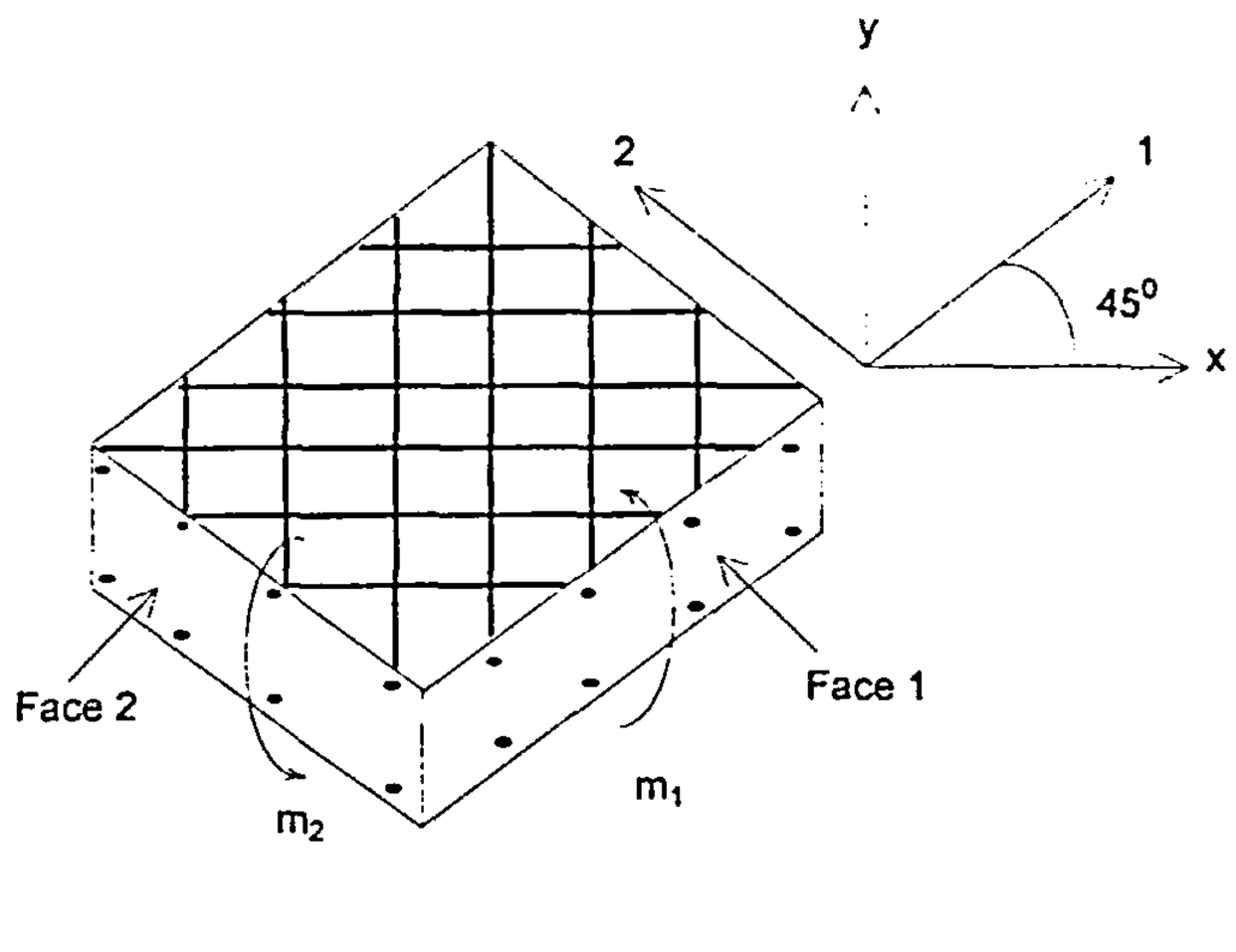

(a)

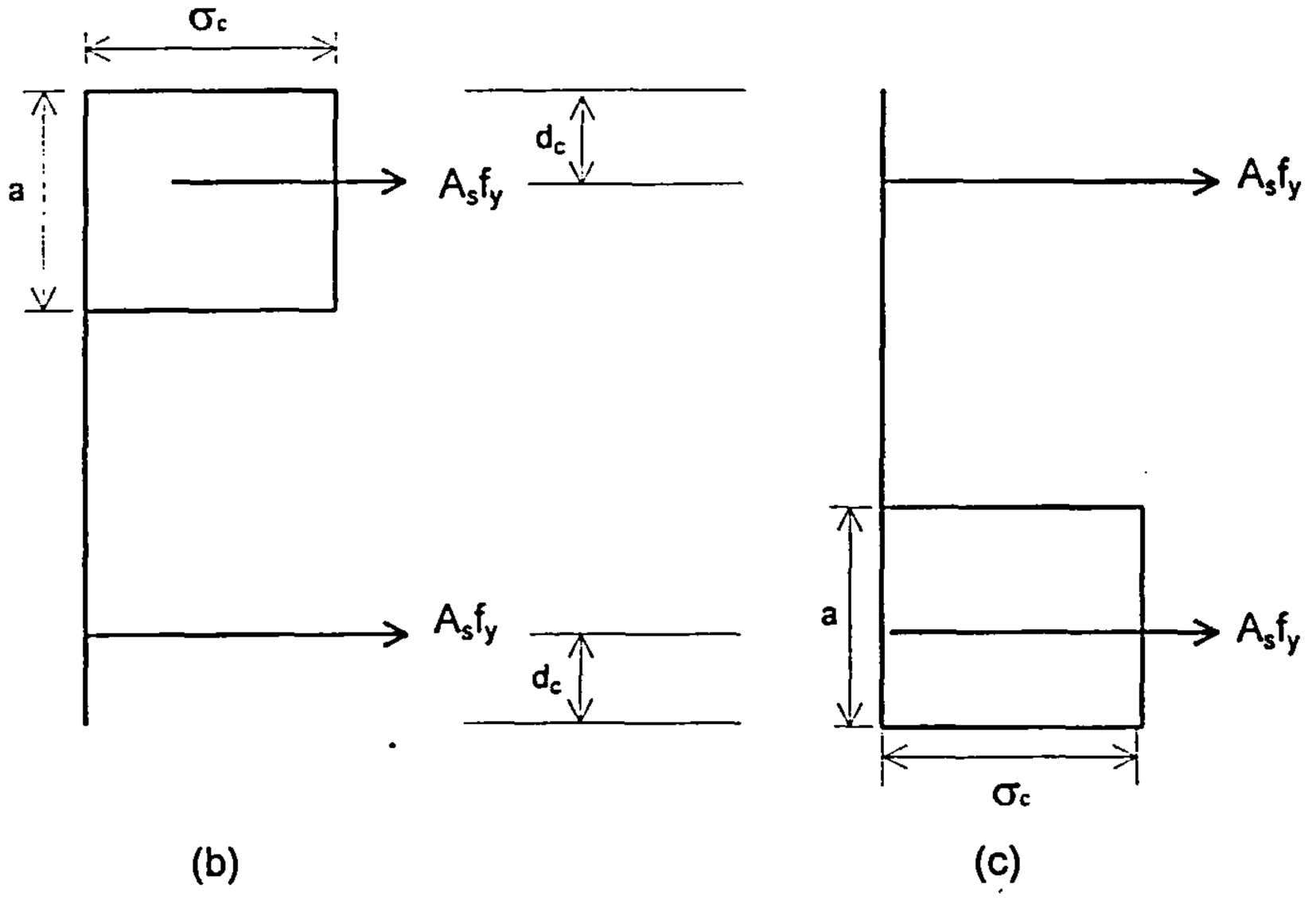

(b) (c)

Figure 6.10: Reinforced concrete slab element (a) subjected to pure twisting in principal moment directions (b) Stress distribution in principal direction 1-1on face 1 (c) Stress distribution in principal direction 2-2 on face 2

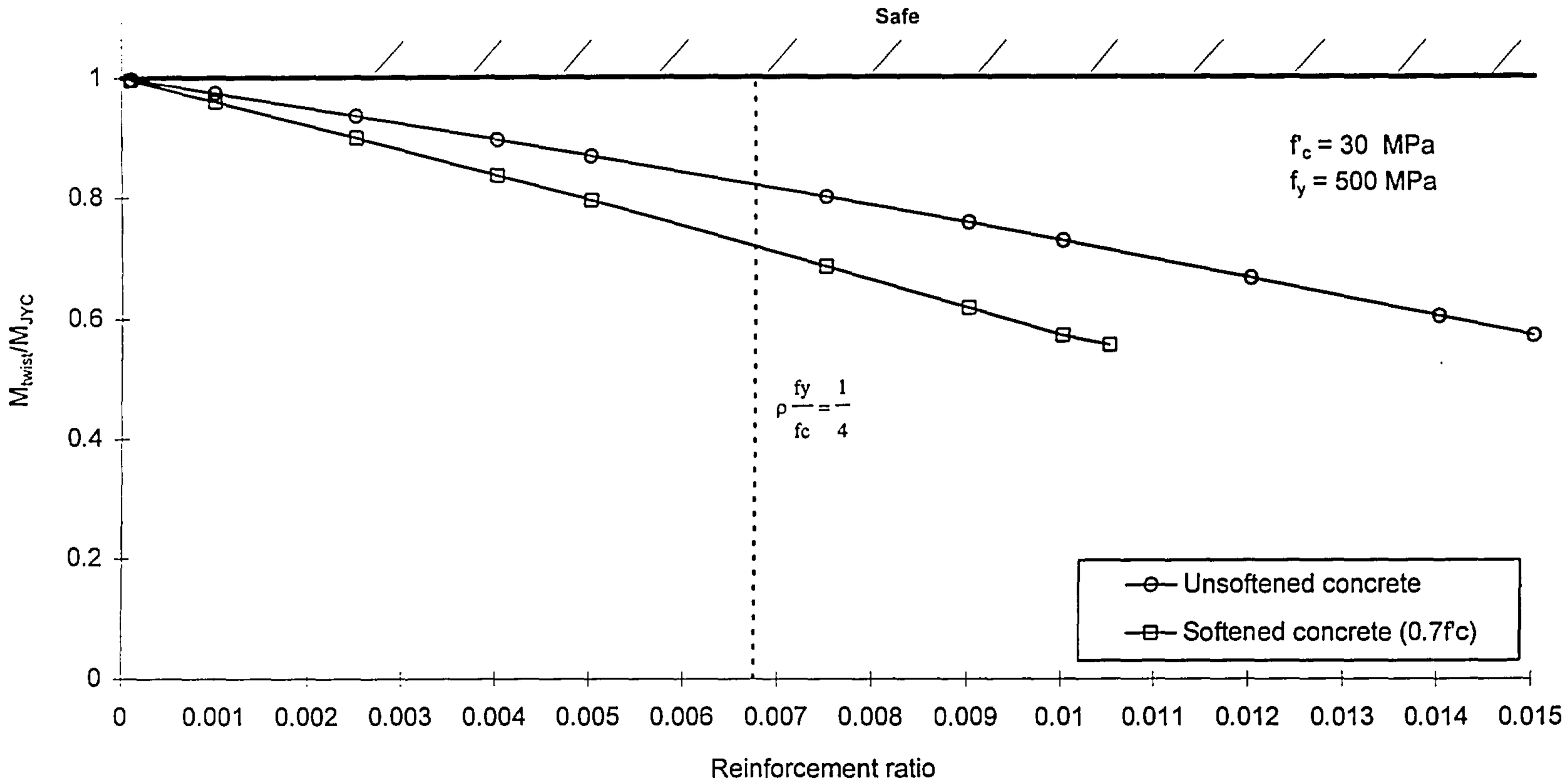

Figure 6.11: Comparison of twisting moment capacity of reinforced concrete slab element with Johansen's yield criterion[3]

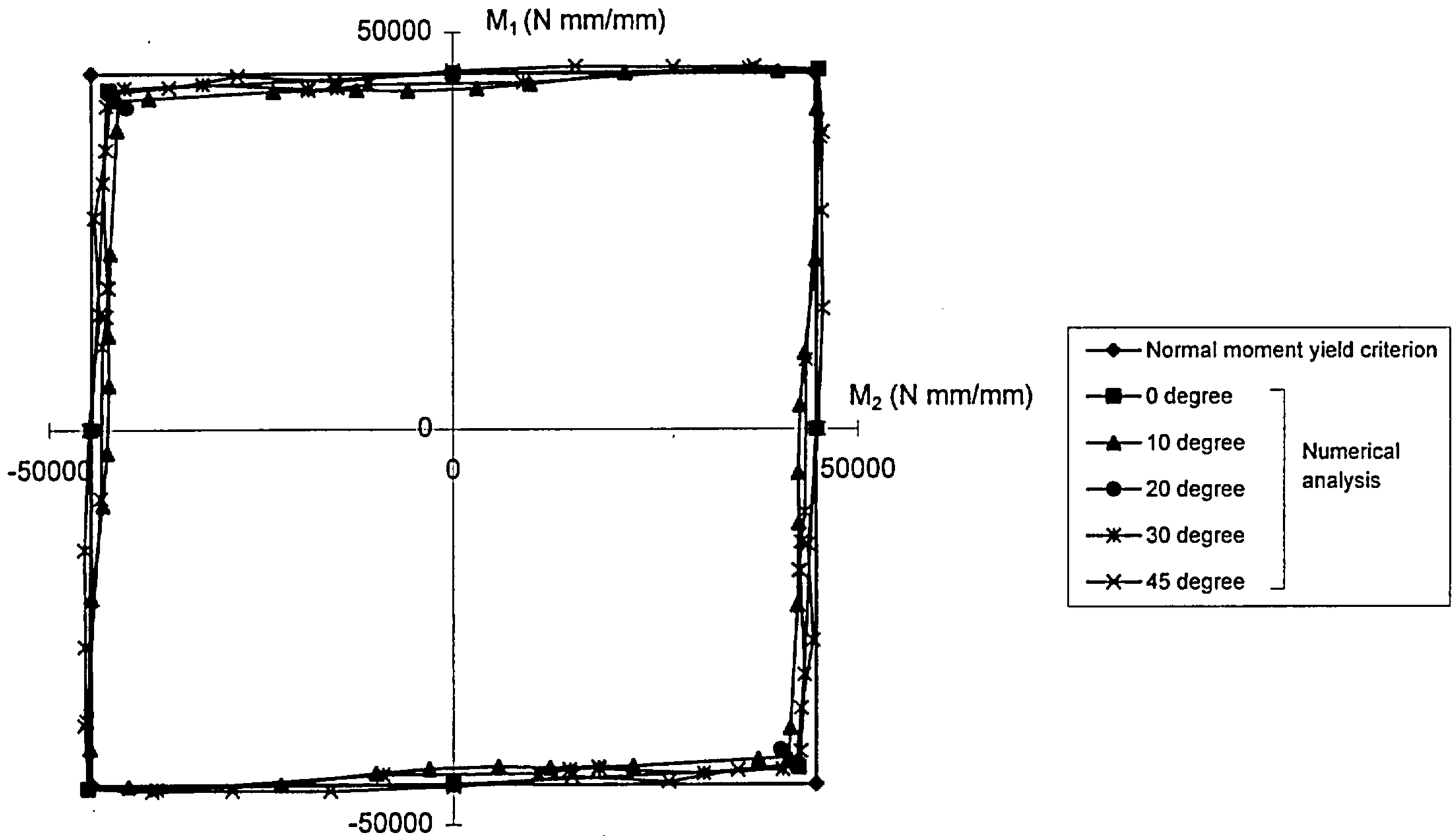

Figure 6.12: Comparison of numerically obtained yield surfaces for an isotropic slab element with 0.25% reinforcement with the normal moment yield criterion in principal moment field

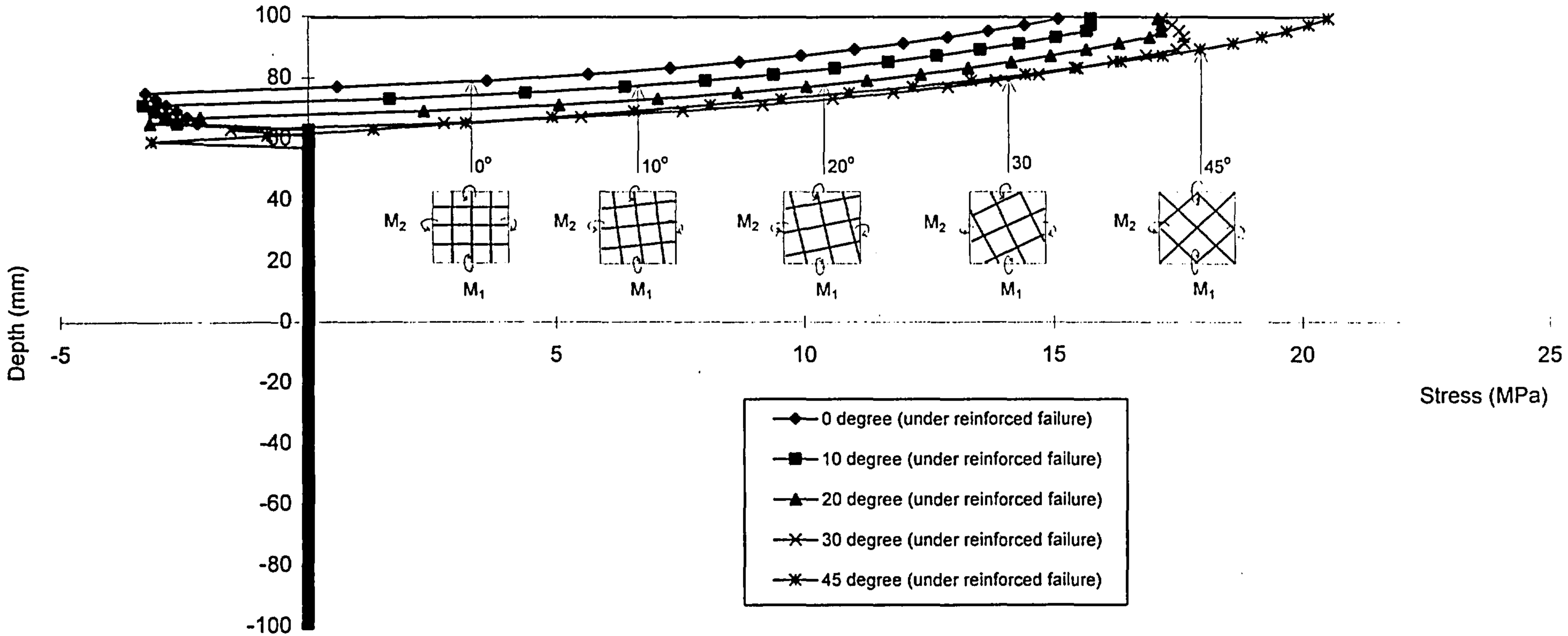

Figure 6.13: Principal stress distribution in concrete at ultimate load for isotropic slab element with 0.25% reinforcement when principal moment ratio is -1 with varying angle between the principal moment and reinforcement directions

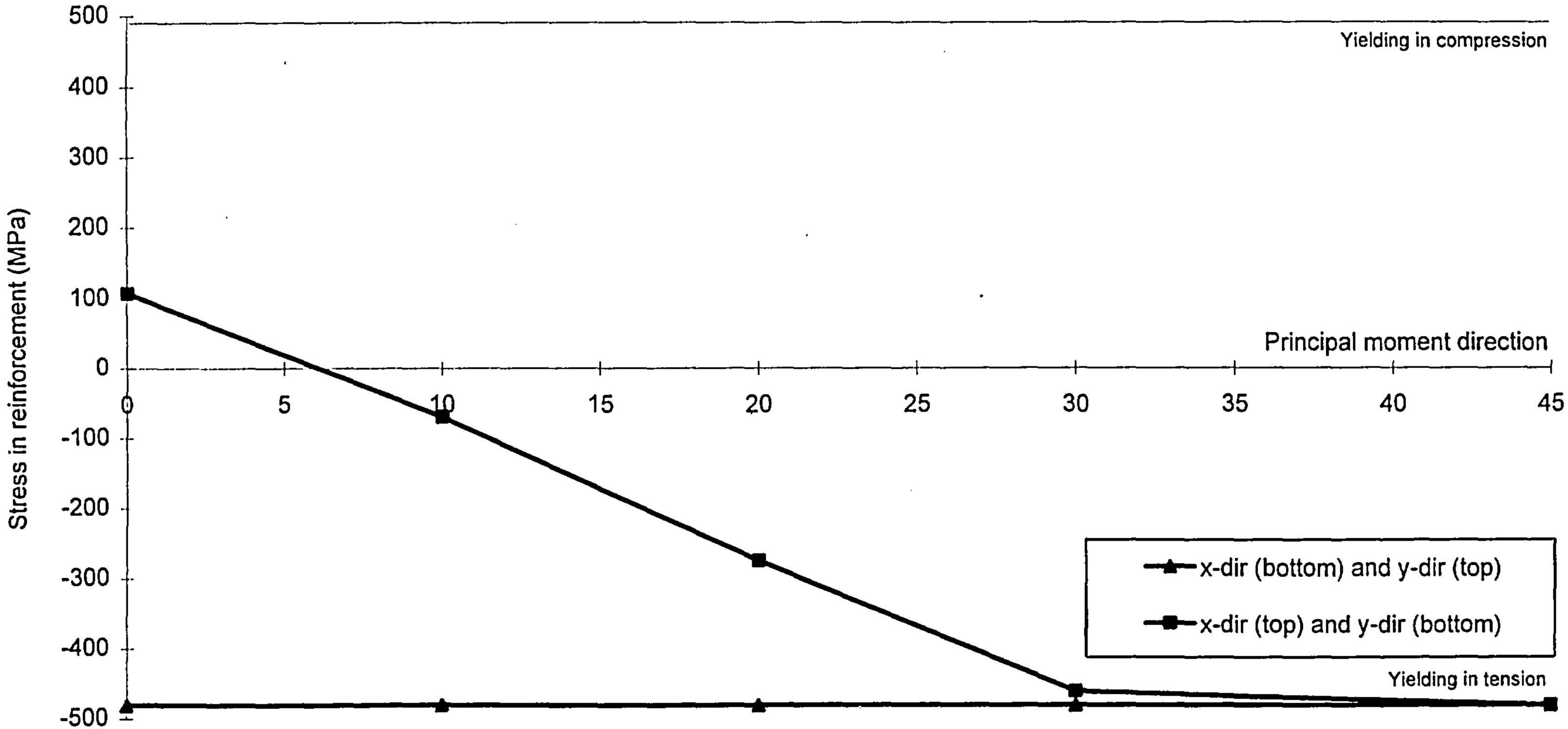

Figure 6.14: Variation of reinforcement stress at ultimate load for isotropic slab element with 0.25% reinforcement when principal moment ratio is -1 with varying angle between the principal moment and reinforcement directions

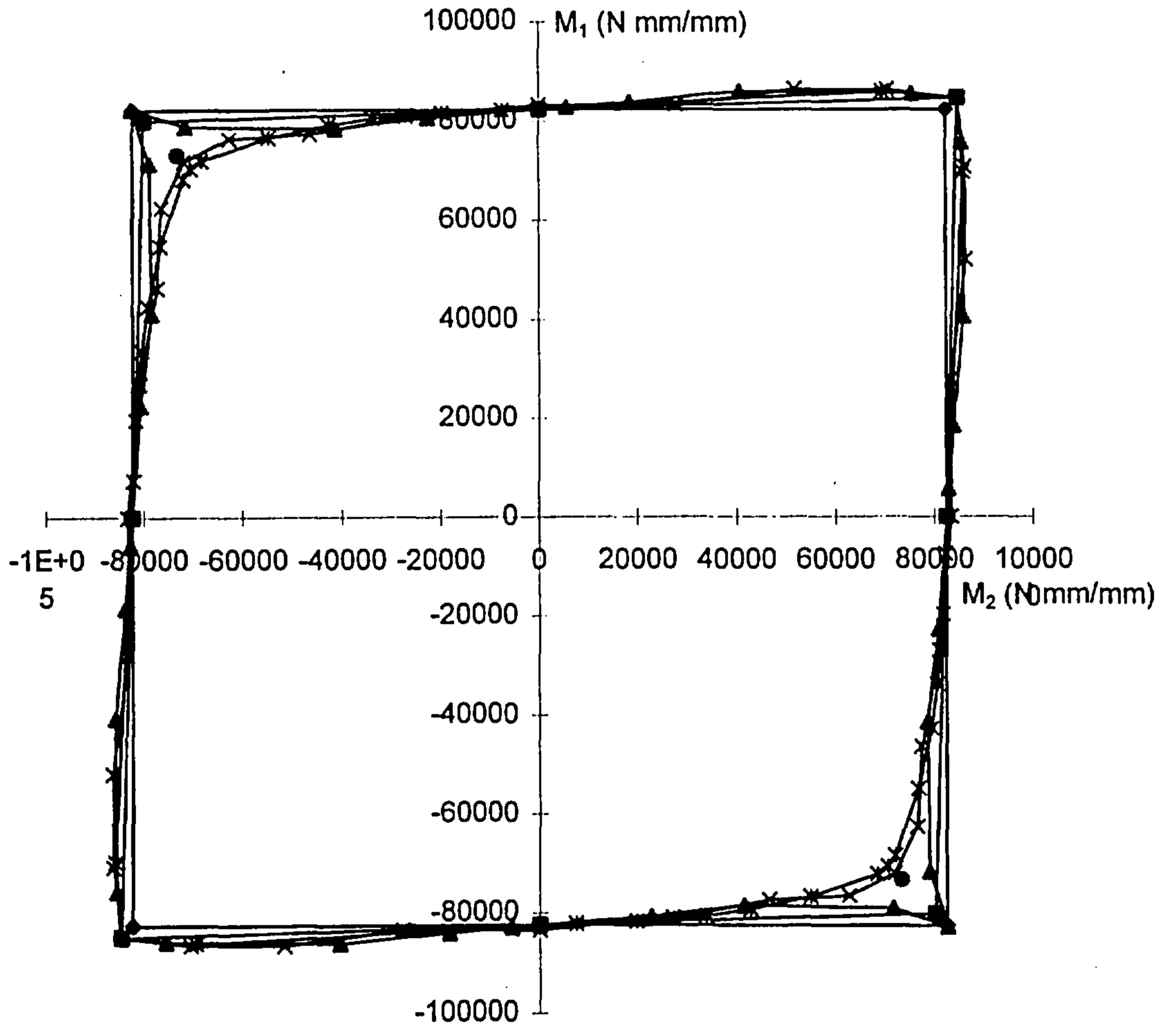

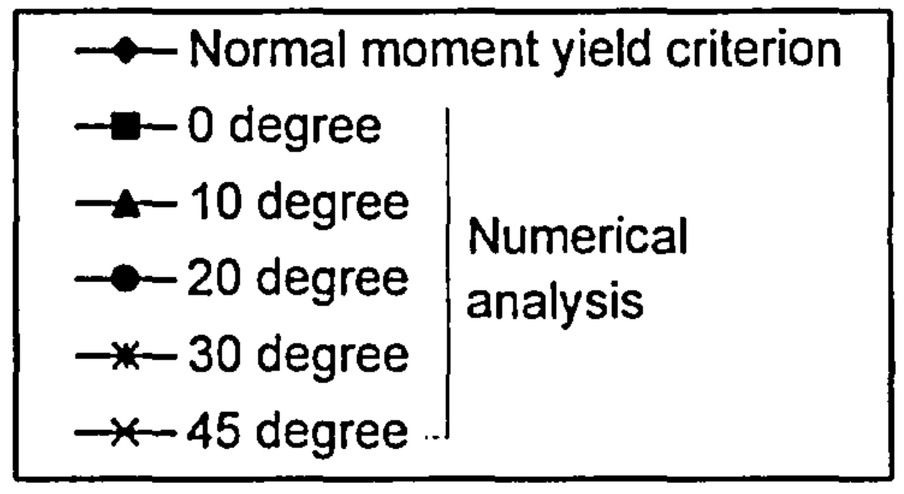

Figure 6.15: Comparison of numerically obtained failure surfaces for isotropic slab element with 0.5% reinforcement with the normal moment yield criterion in principal moment field

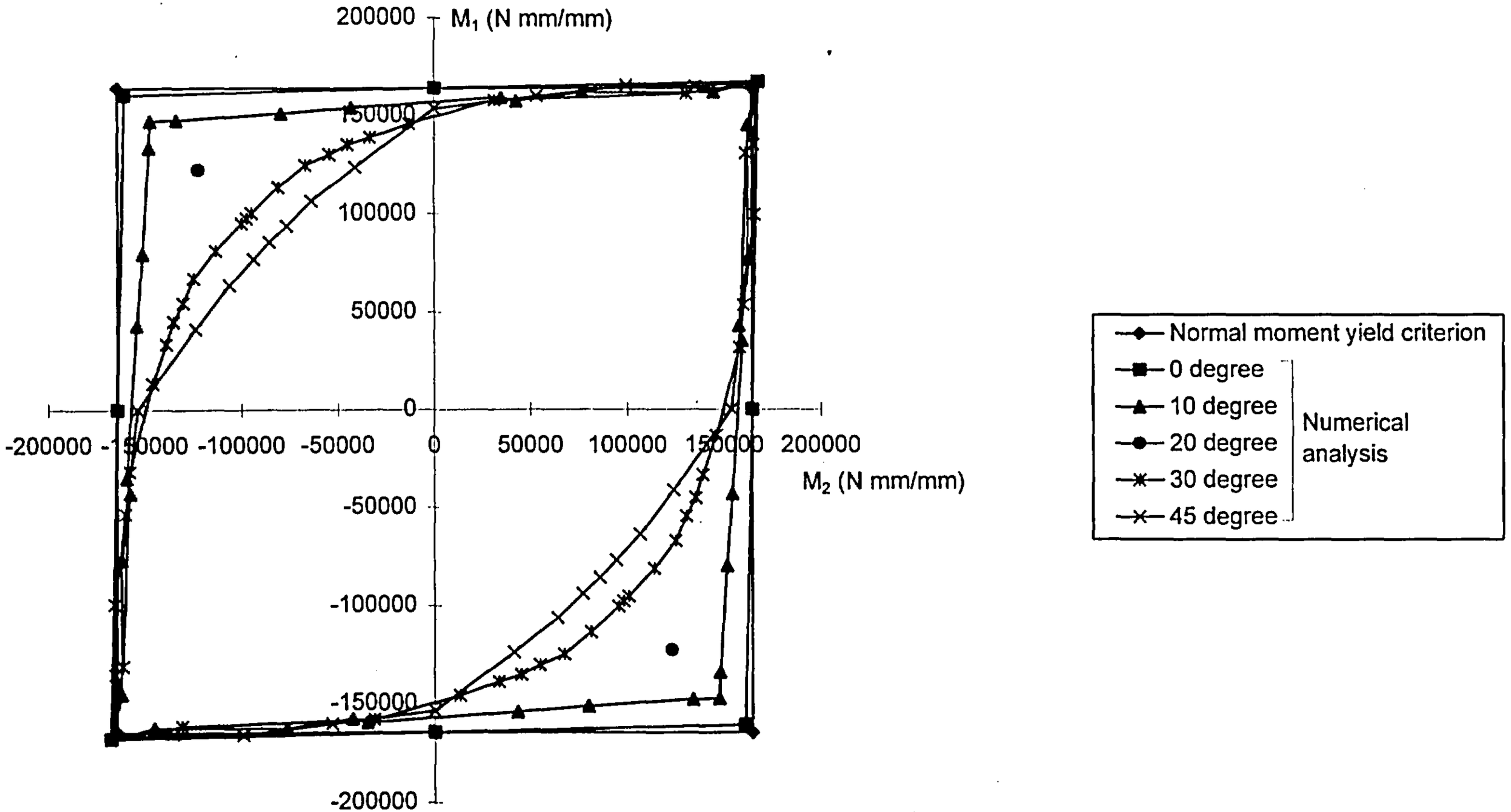

Figure 6.16: Comparison of numerically obtained failure surfaces for isotropic slab element with 1.0% reinforcement with the normal moment yield criterion in principal moment field

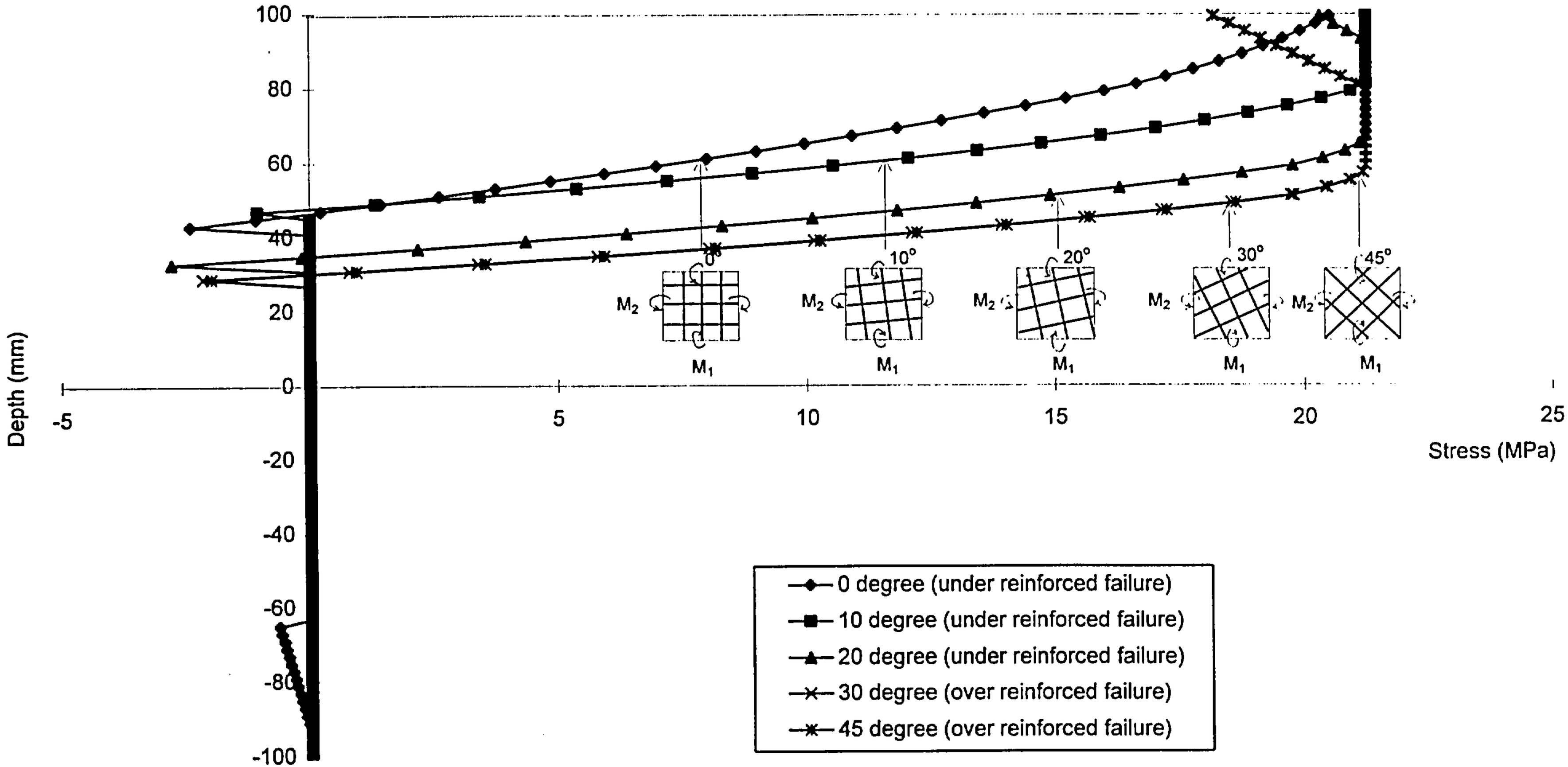

Figure 6.17: Principal stress distribution in concrete at ultimate for isotropic slab element with 1.0% reinforcement when principal moment ratio is -1 with varying angle between the principal moment and reinforcement directions

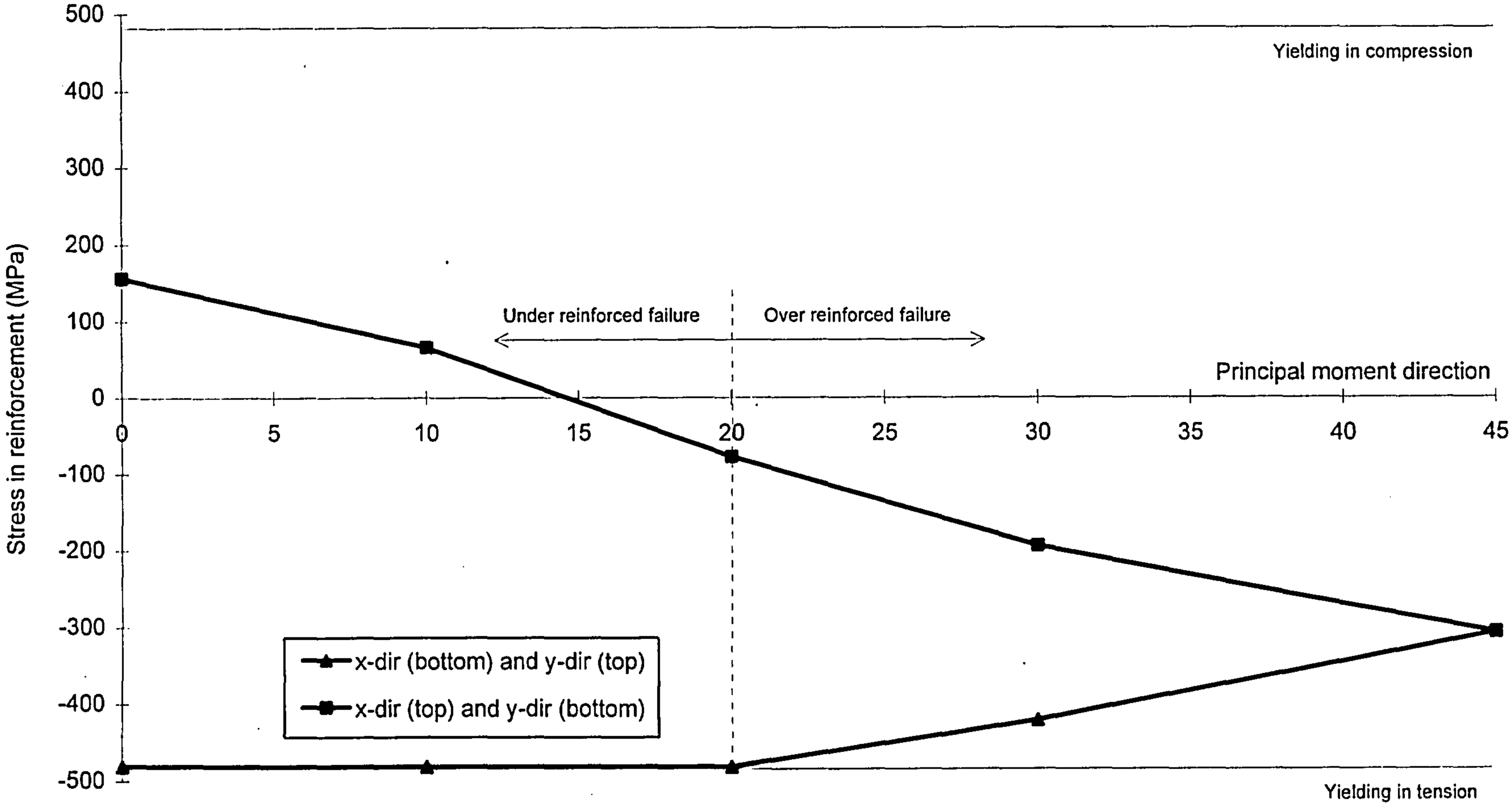

Figure 6.18: Variation of reinforcement stress at ultimate load for isotropic slab element with 1.0% reinforcement when principal moment ratio is -1 with varying angle between the principal moment and reinforcement directions

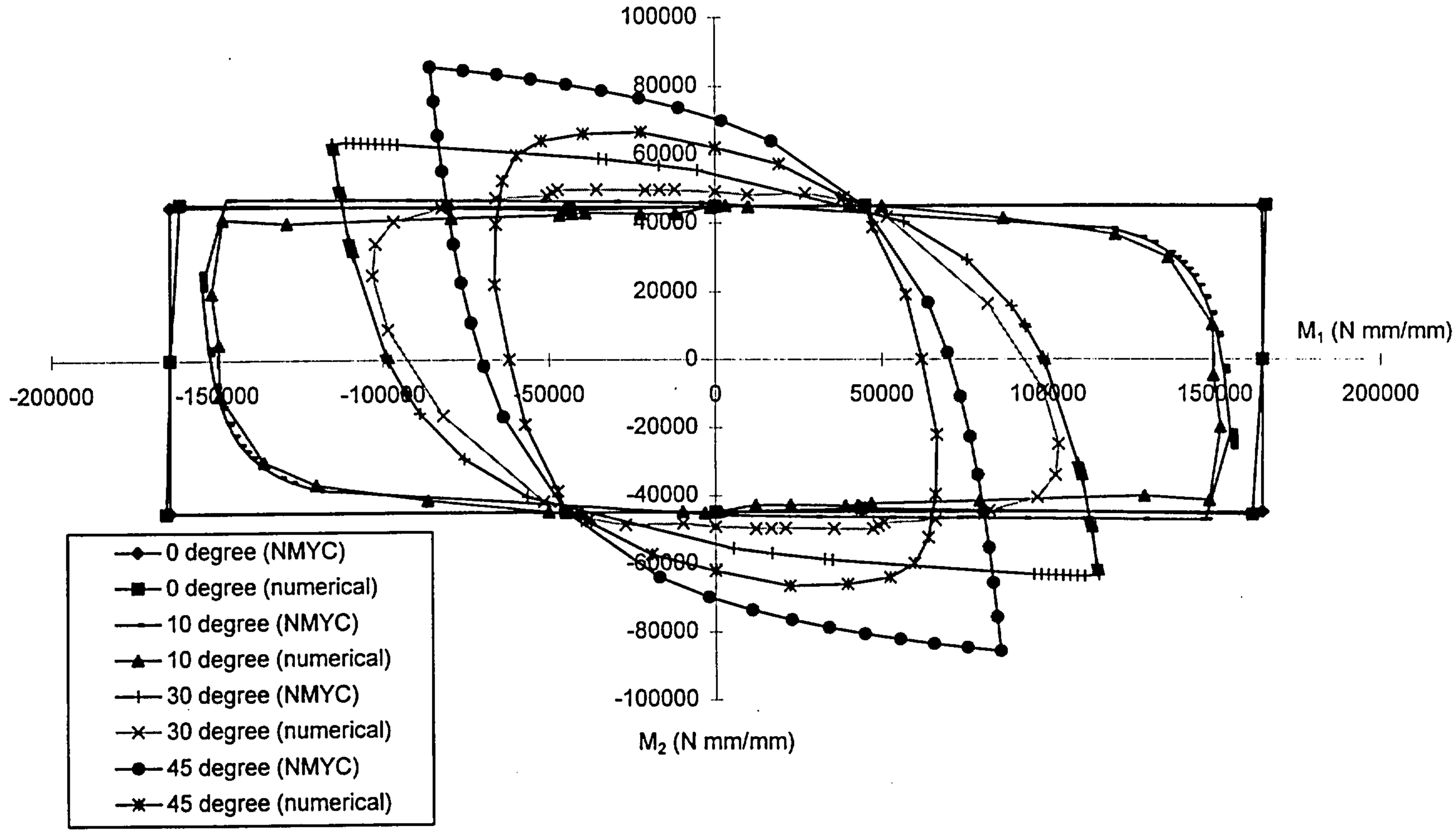

Figure 6.19: Comparison of numerically obtained failure surfaces for orthotropic slab element with 0.25% and 1.0% reinforcement with the normal moment yield criterion in principal moment field

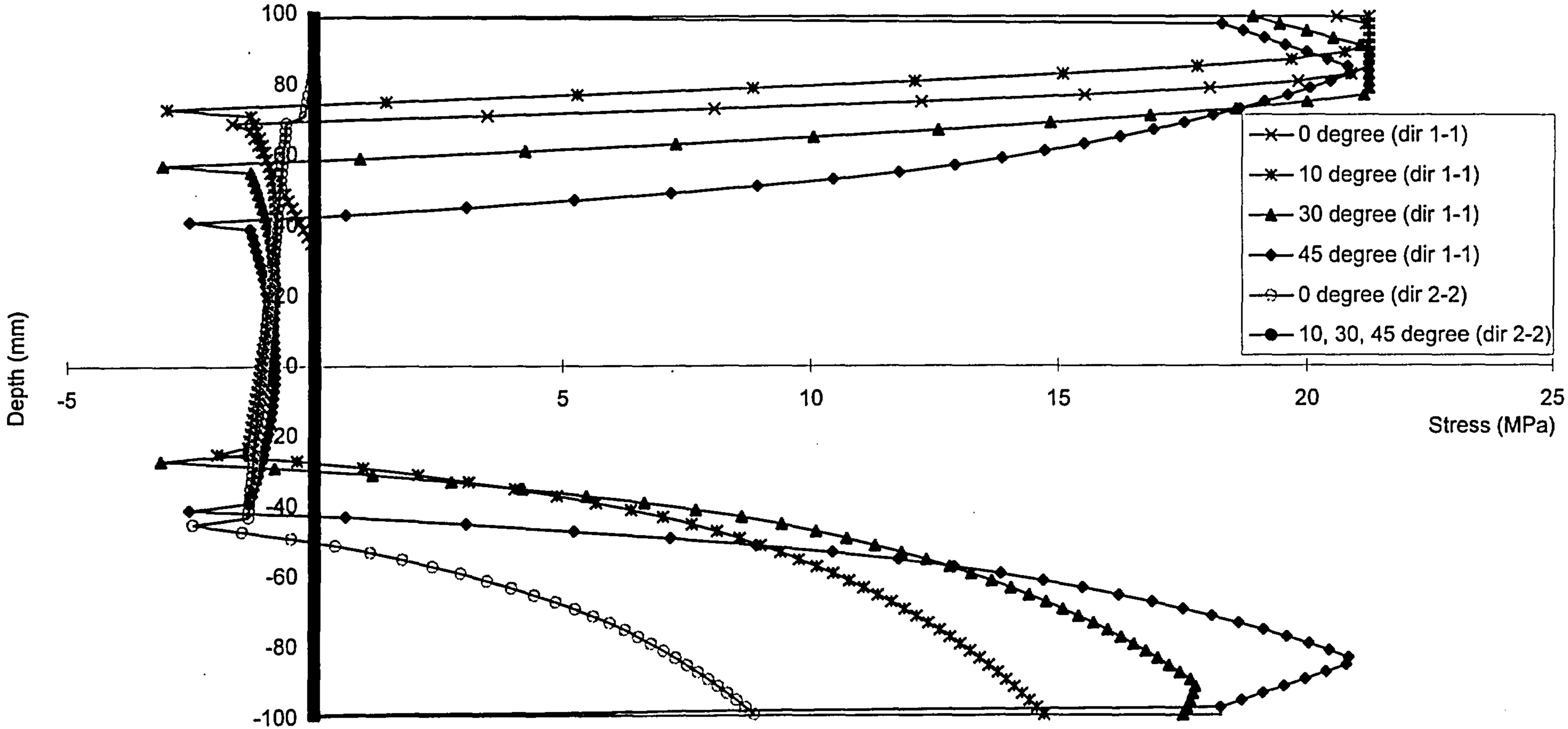

Figure 6.20: Principal stress distribution in concrete at ultimate load for orthotropic slab element with 0.25% and 1% reinforcement when principal moment ratio is -1 with varying angle between the principal moment and reinforcement directions

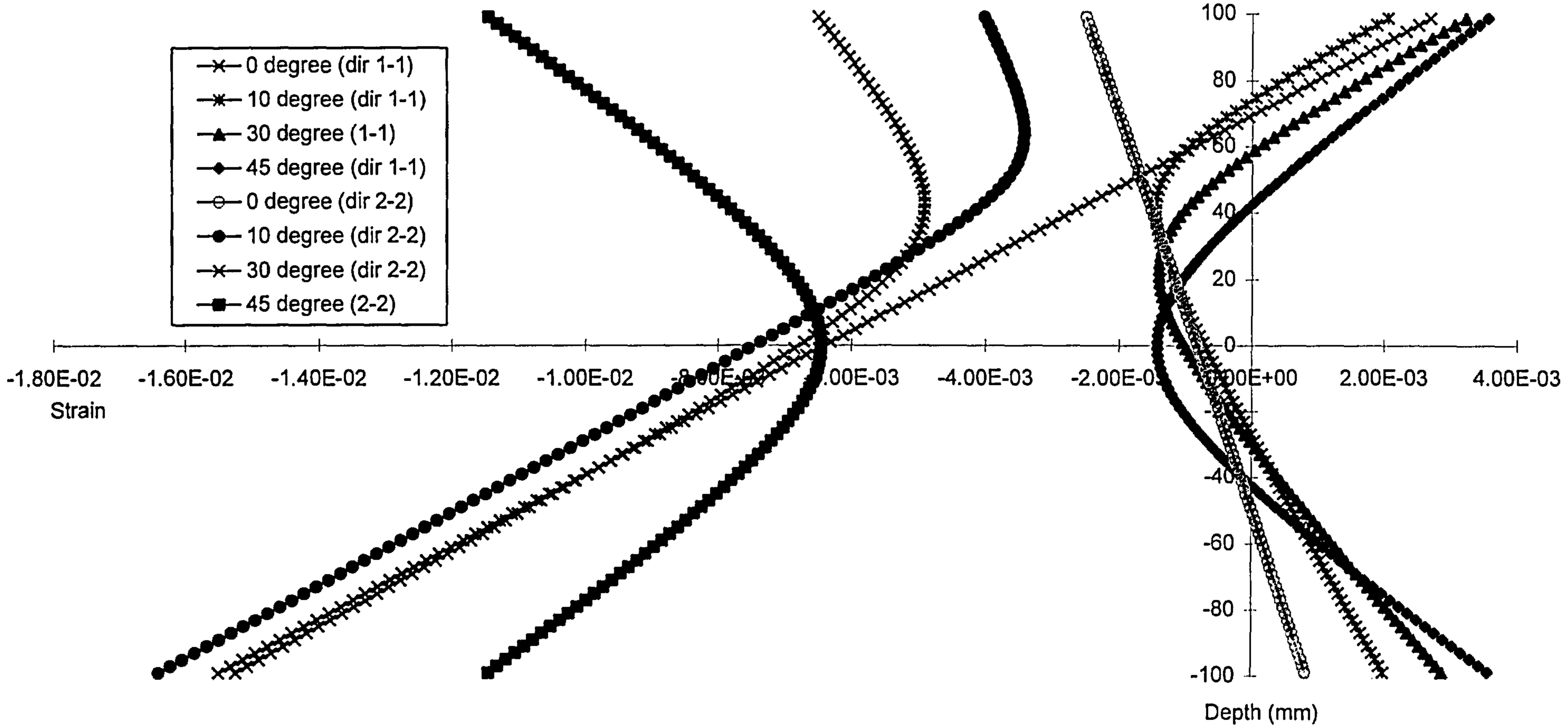

Figure 6.21: Principal strain distribution in concrete at ultimate load for orthotropic slab element with 0.25% and 1% reinforcement when principal moment ratio is -1 with varying angle between the principal moment and reinforcement directions

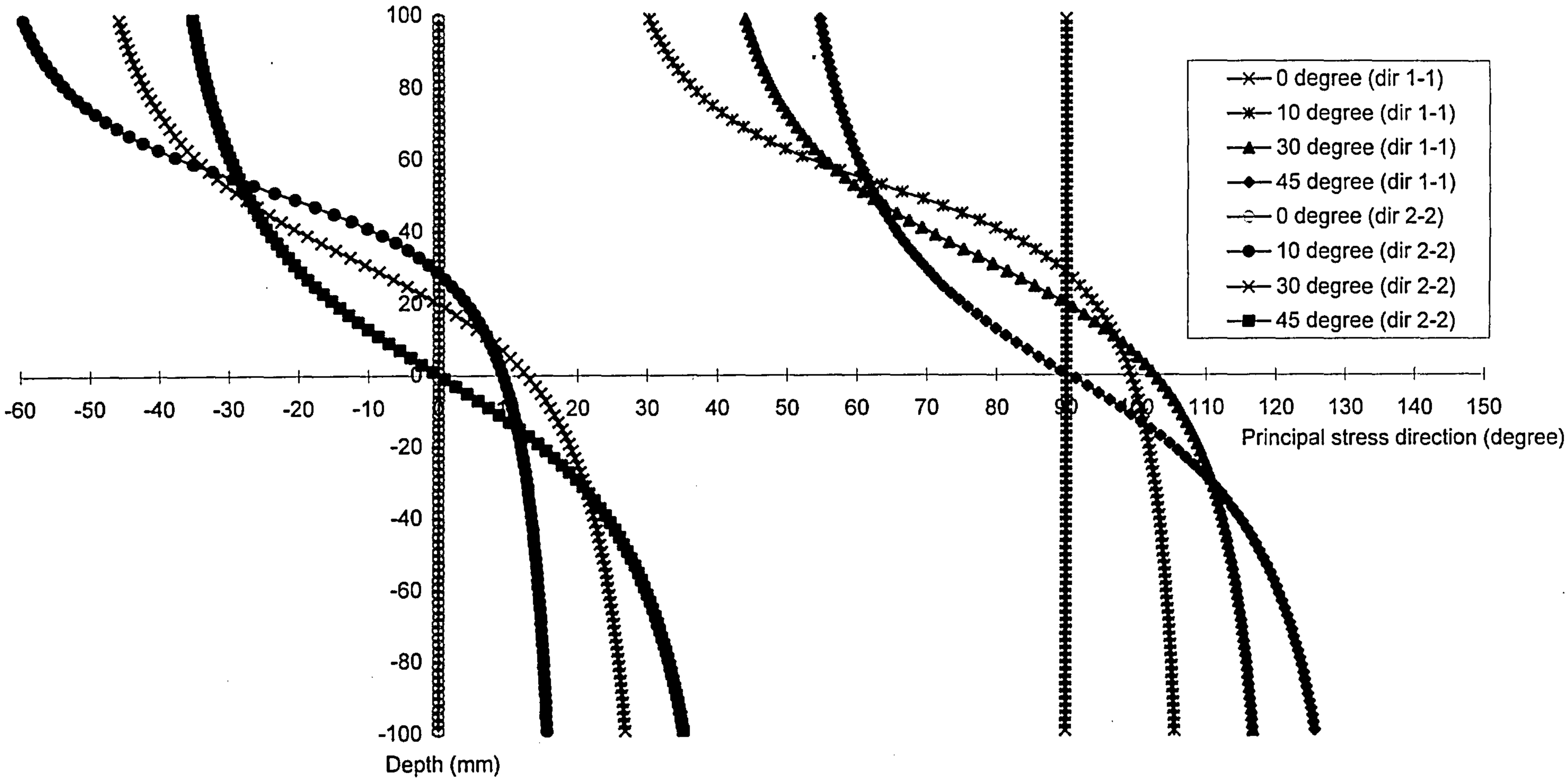

Figure 6.22: Principal stress directions at ultimate load for orthotropic slab element with 0.25% and 1% reinforcement when principal moment ratio is -1 with varying angle between the principal moment and reinforcement directions

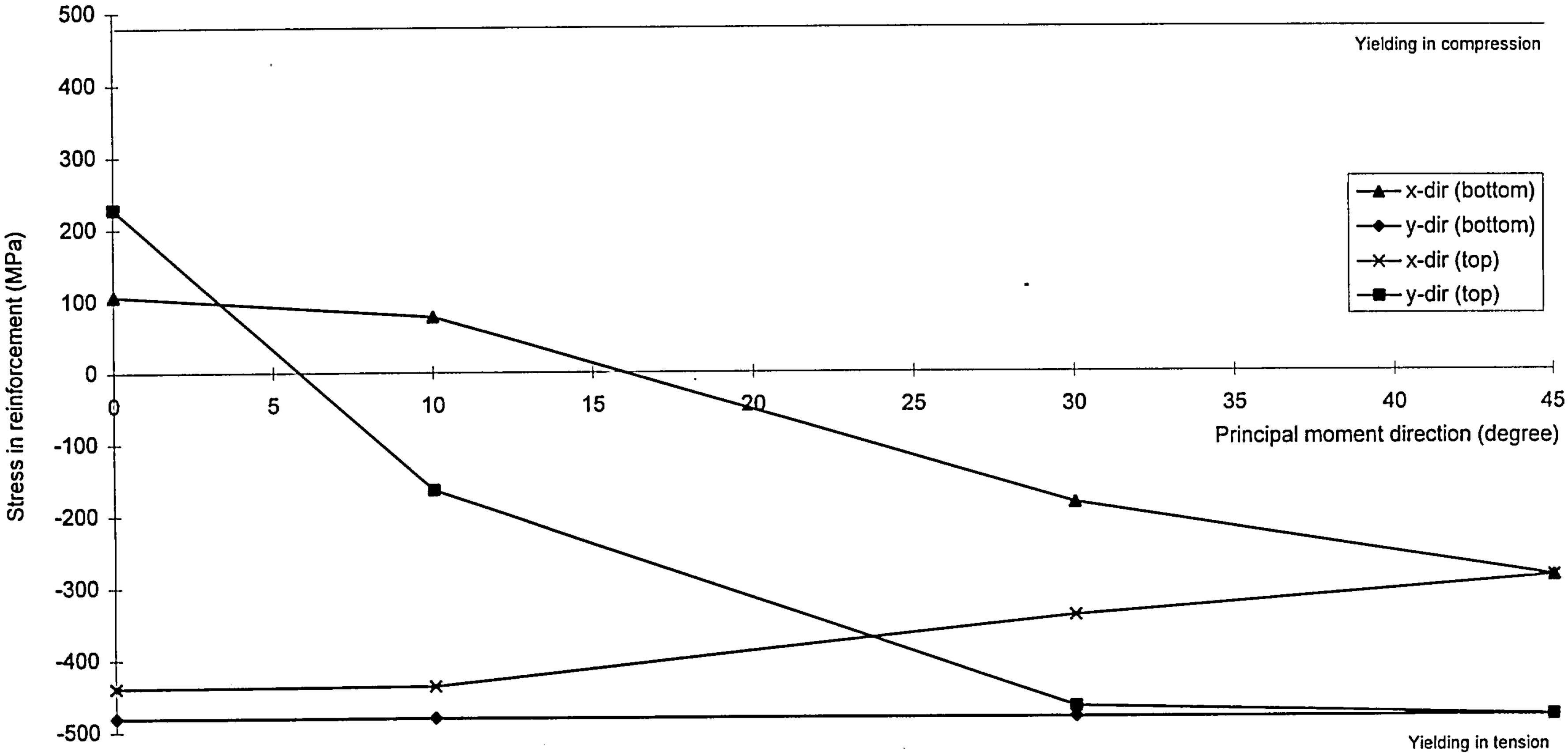

Figure 6.23: Variation of reinforcement stress at ultimate load for orthotropic slab element with 0.25% and 1% reinforcement when principal moment ratio is -1 with varying angle between the principal moment and reinforcement directions

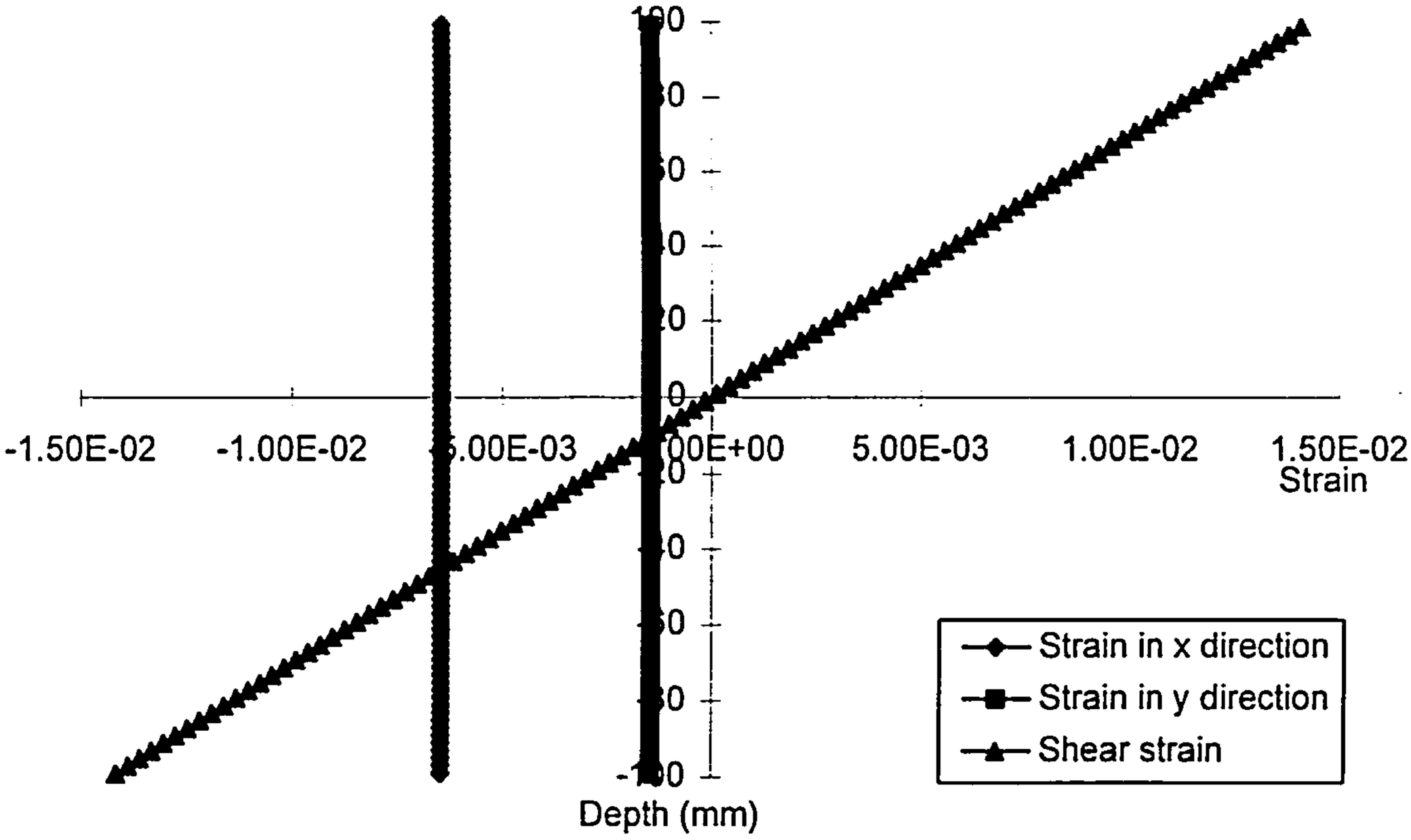

Figure 6.24: Strain state at ultimate load of orthotropically reinforced slab element in the reinforcement direction when subjected to pure twisting

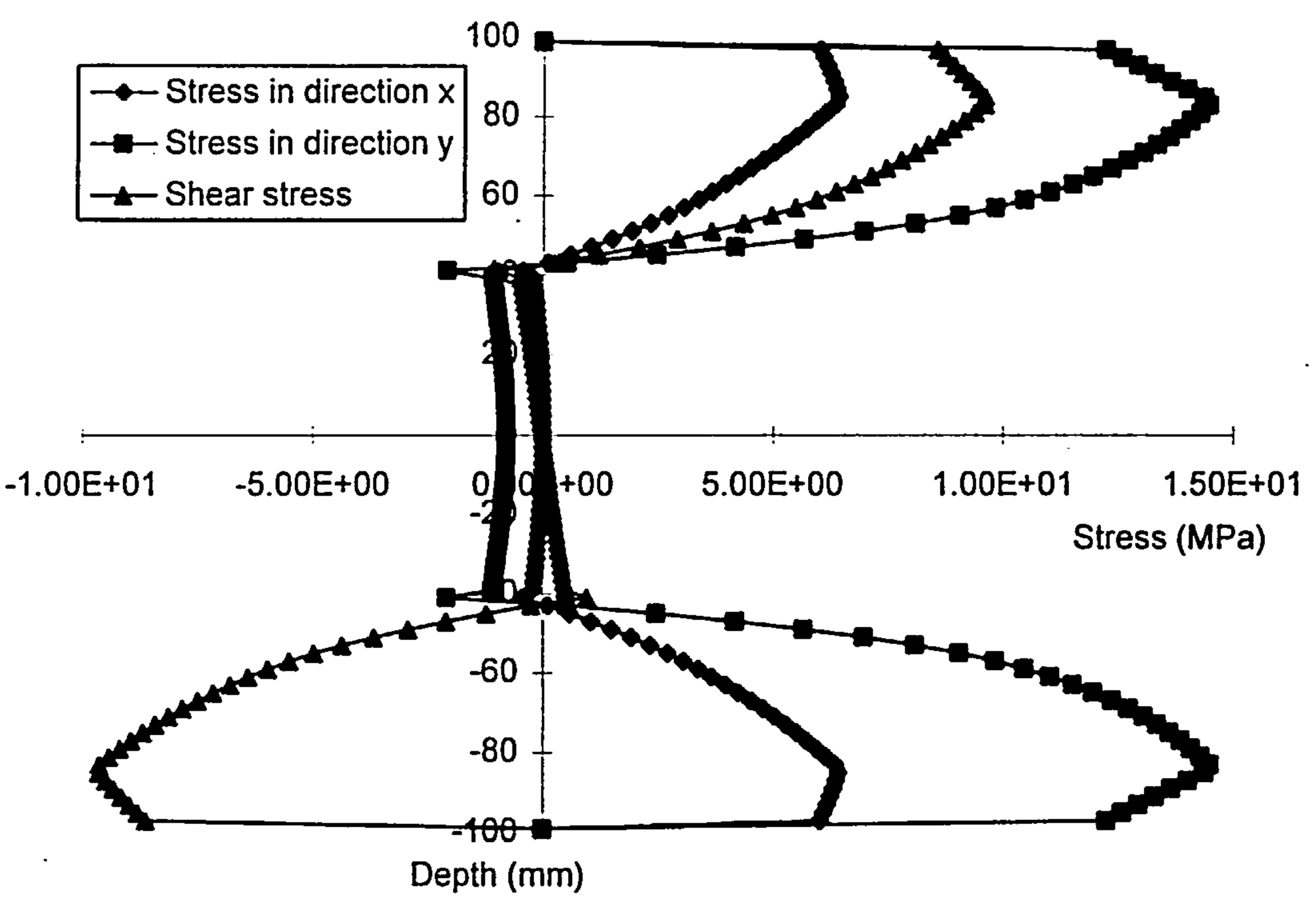

Figure 6.25: Stress state at ultimate load of orthotropically reinforced slab element in the reinforcement direction when subjected to pure twisting

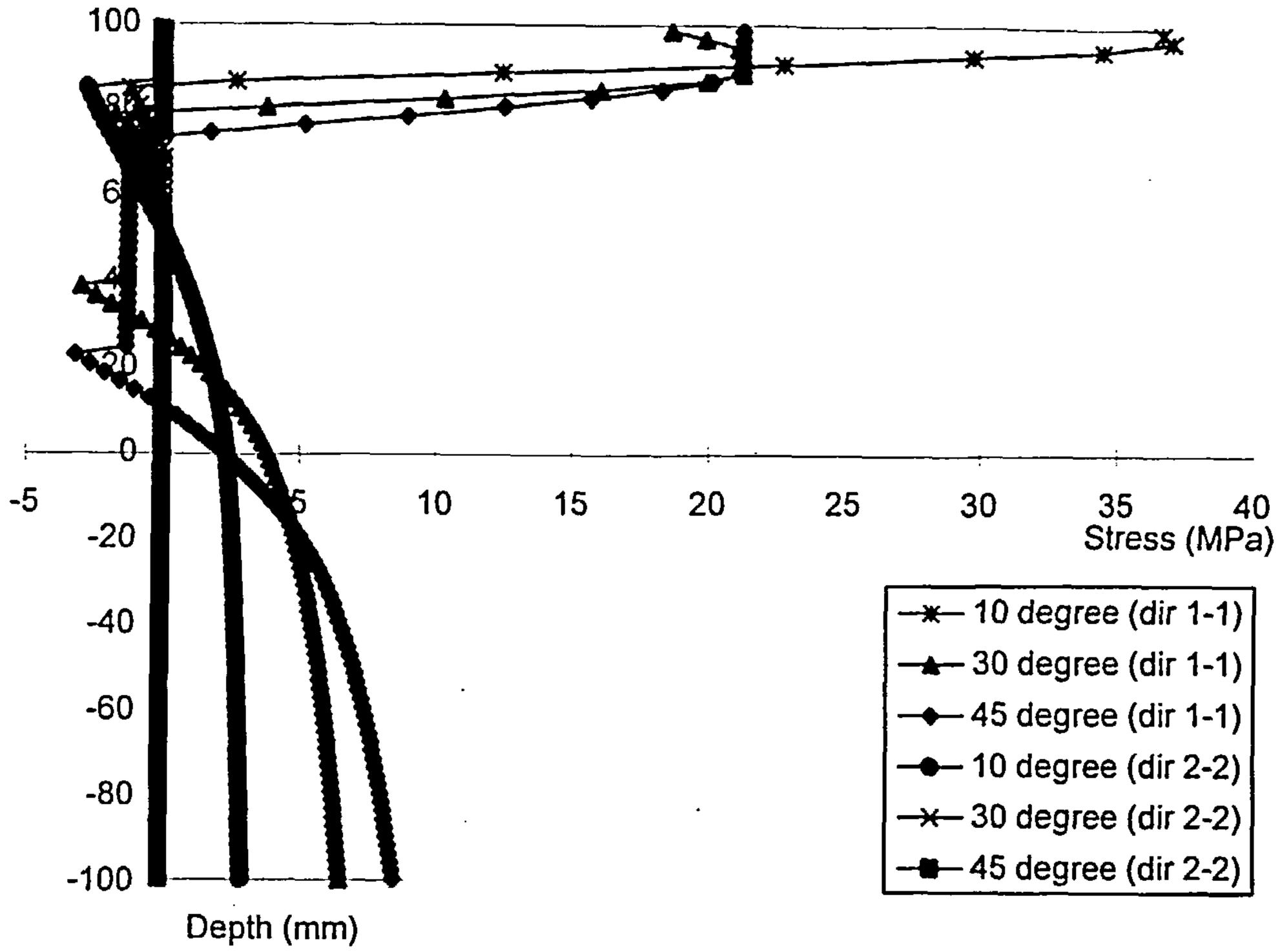

Figure 6.26: Principal stress state at ultimate load of orthotropically reinforced slab element when subjected to uniaxial bending in principal moment direction

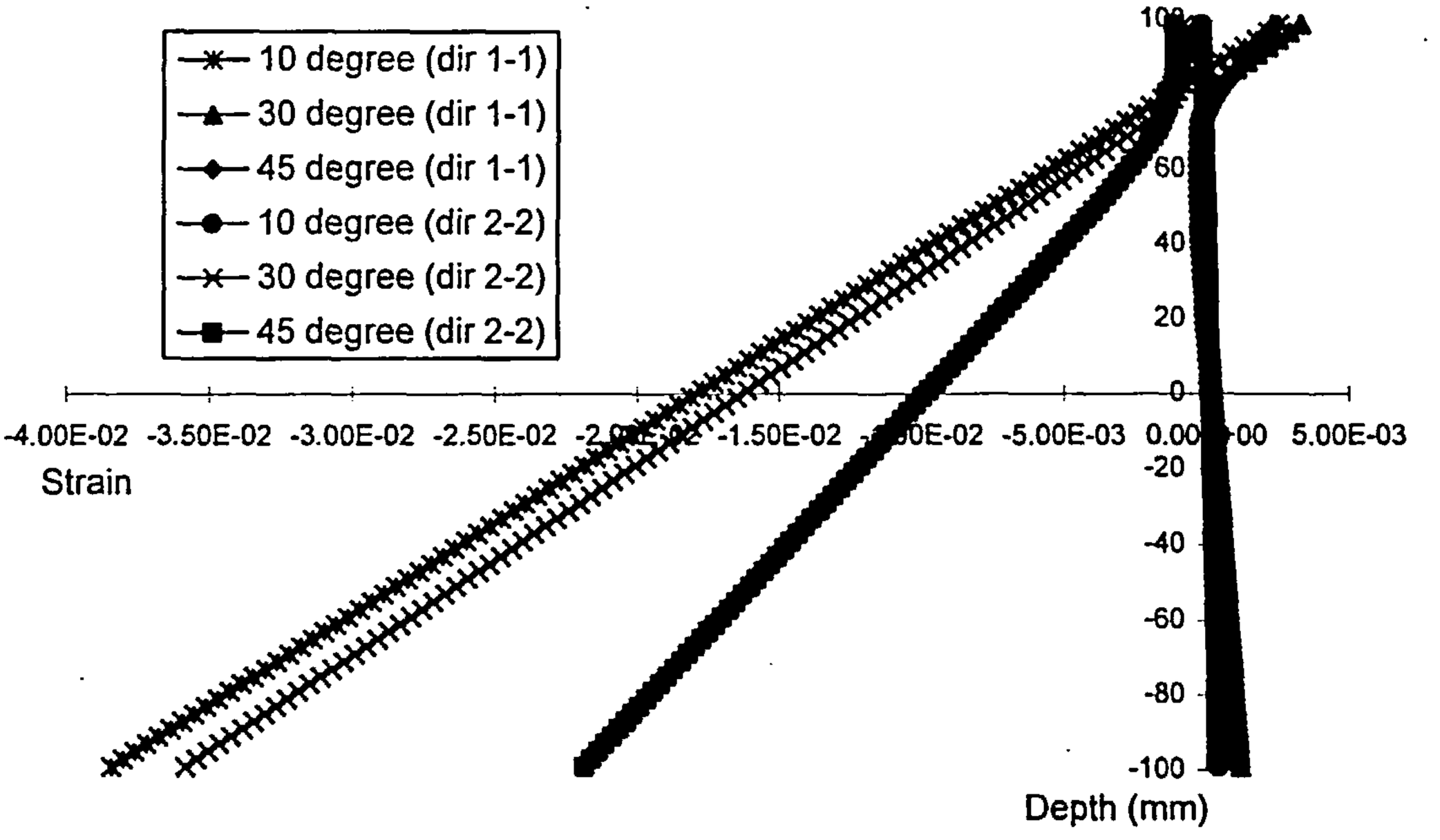

Figure 6.27: Principal strain state at ultimate load of orthotropically reinforced slab element when subjected to uniaxial bending in principal moment direction

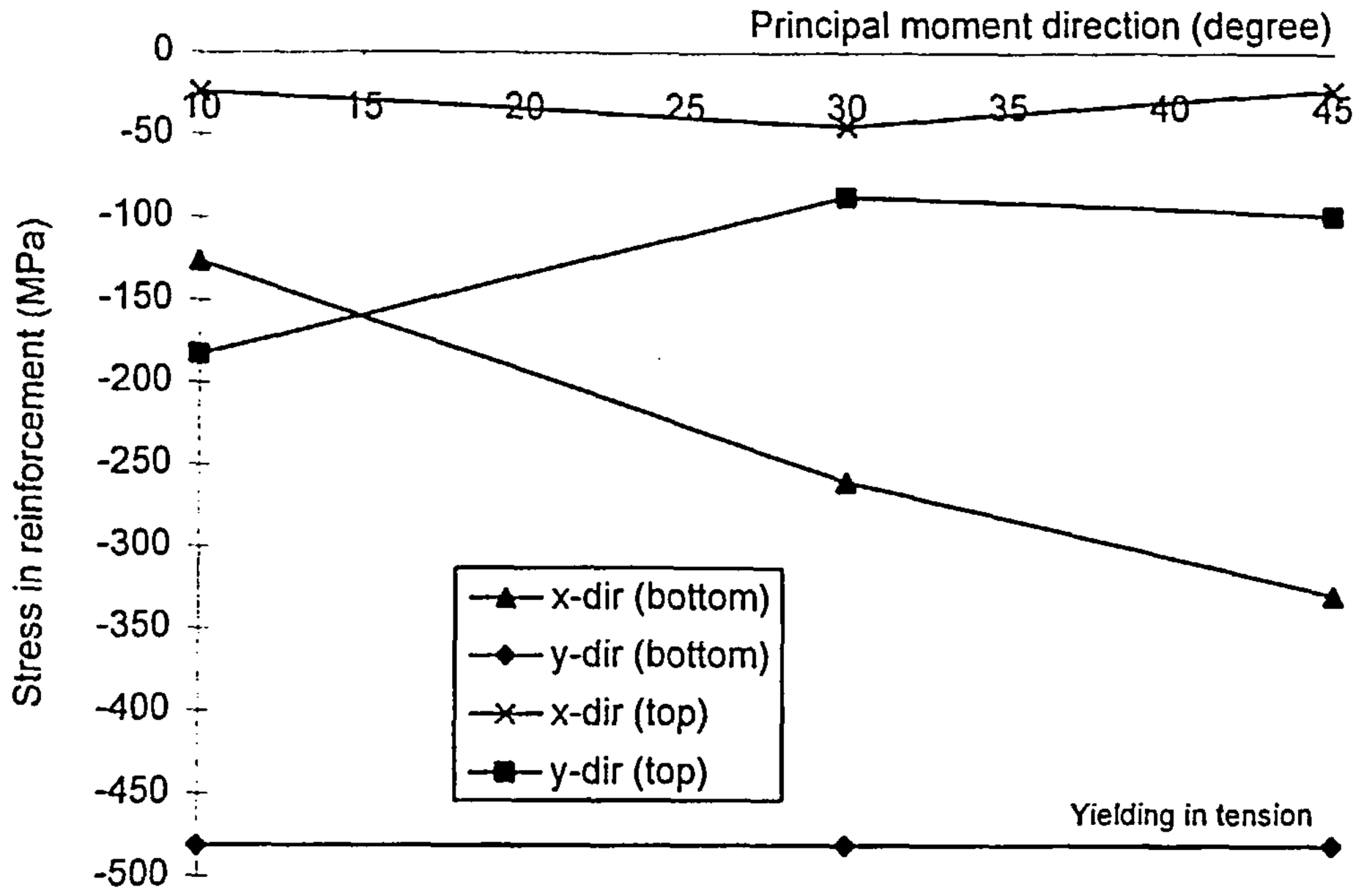

Figure 6.28: Variation of reinforcement stress at ultimate load for orthotropic slab element when subjected to uniaxial bending in principal moment direction

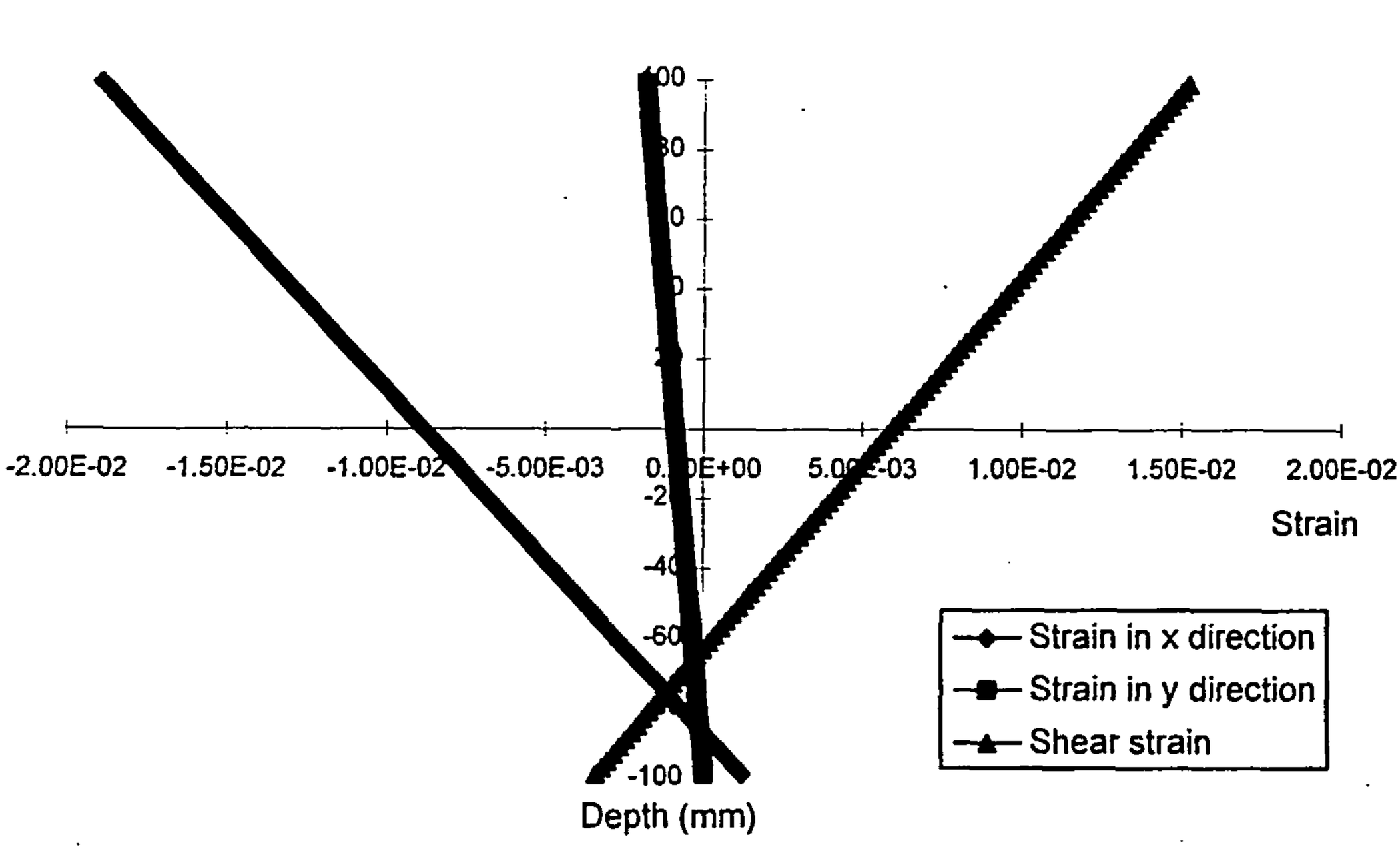

Figure 6.29: Strain state at ultimate load of orthotropically reinforced slab element in the reinforcement directions when subjected to uniaxial bending in principal moment direction with reinforcement at 45° from principal moment direction

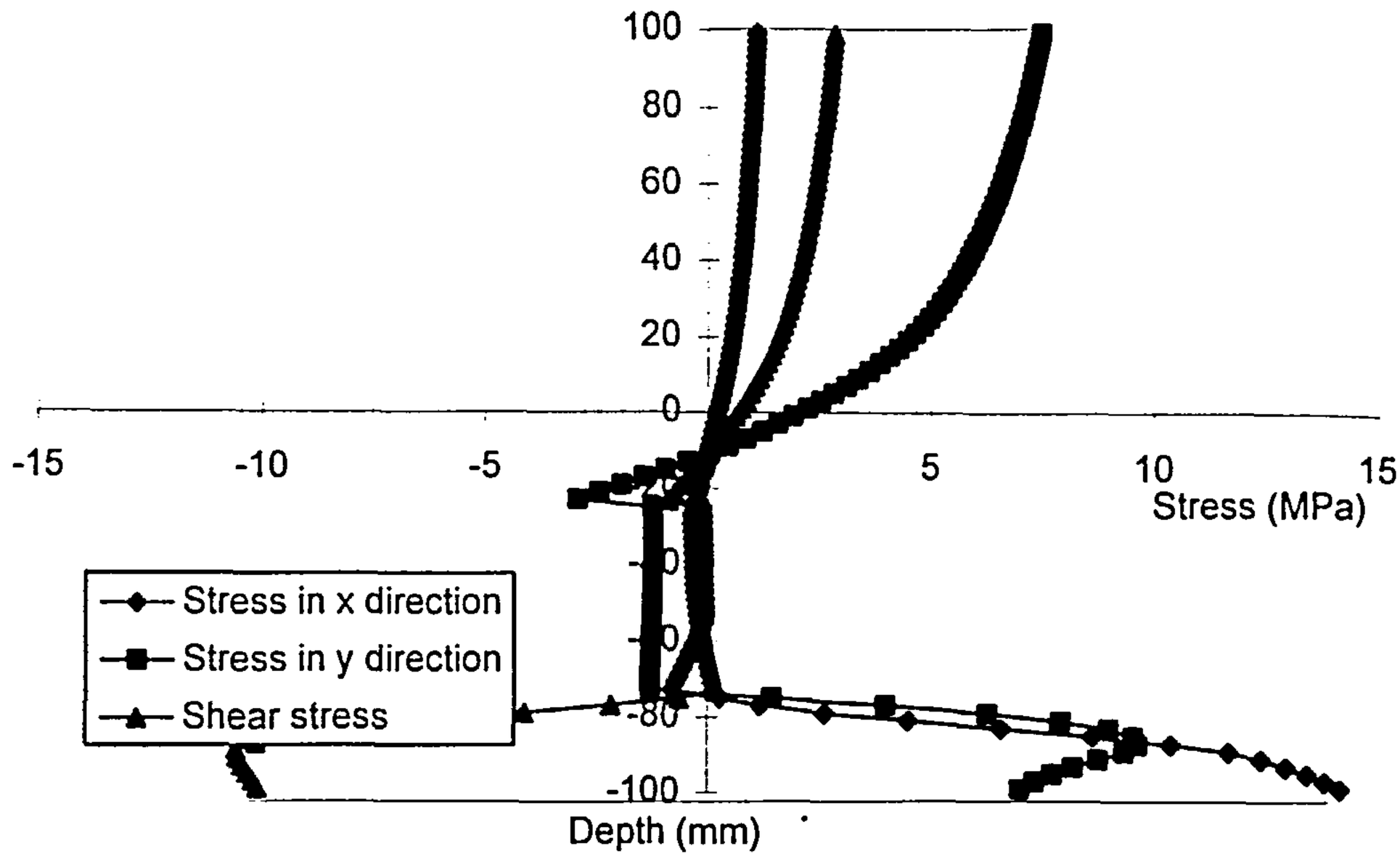

Figure 6.30: Stress state at ultimate load of orthotropically reinforced slab element in the reinforcement directions when subjected to uniaxial bending in principal moment direction with reinforcement at 45^0 from principal moment direction

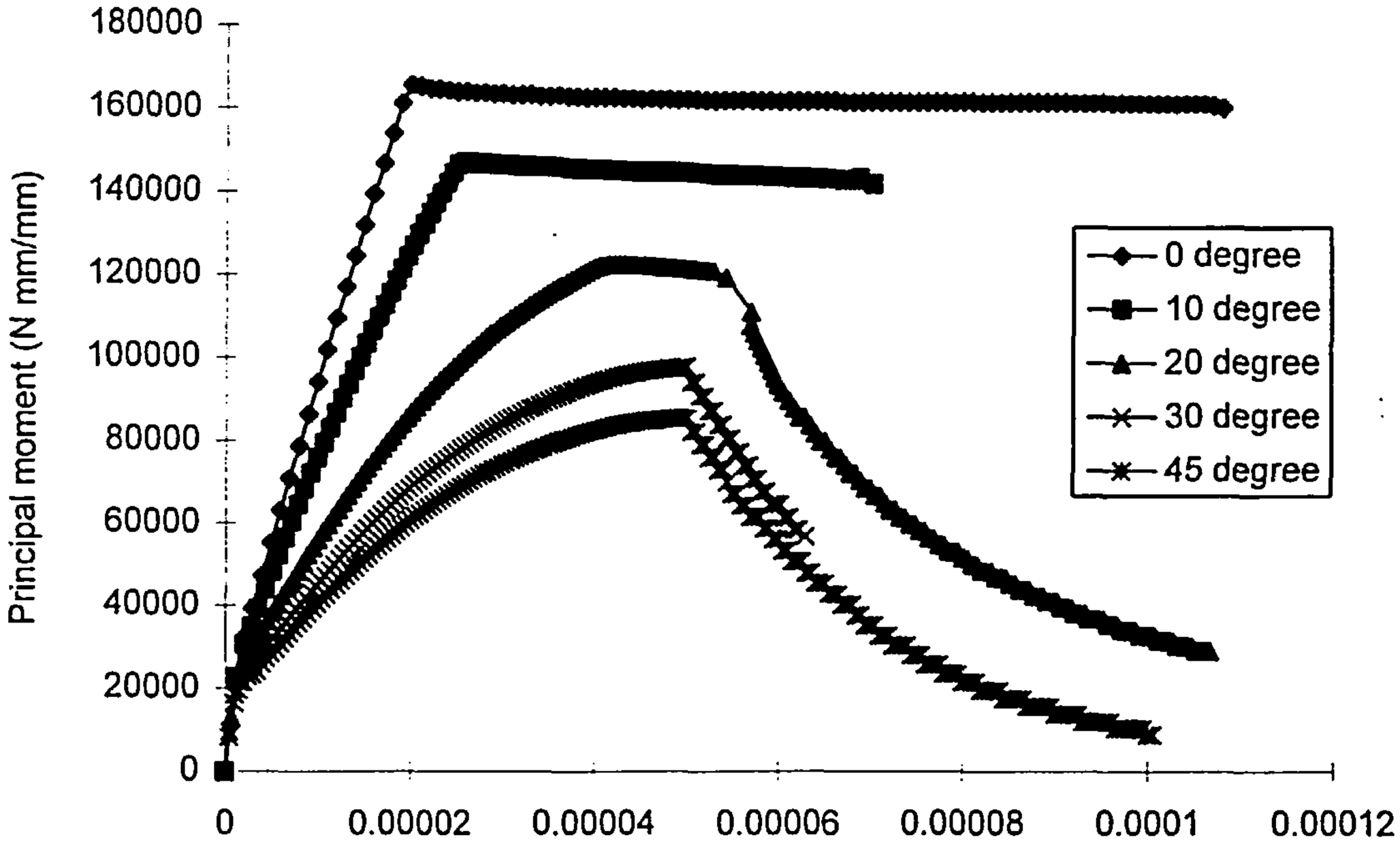

Figure 6.31: Moment curvature response of isotropic slab element with 1% reinforcement when subjected to principal moment ratio of -1 with varying angle between the principal moment and reinforcement direction

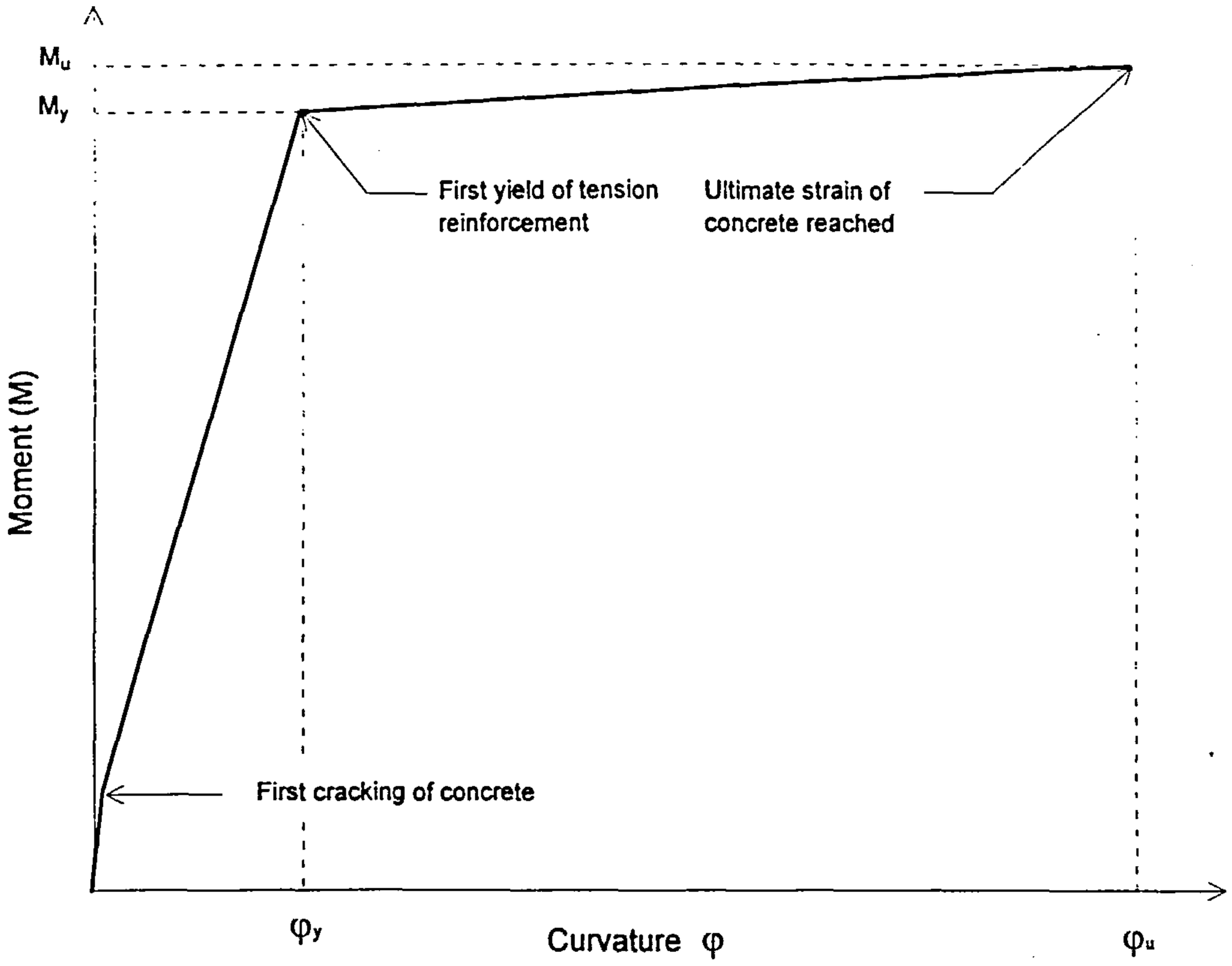

Figure 6.32: Idealized moment curvature response of reinforced concrete slab element

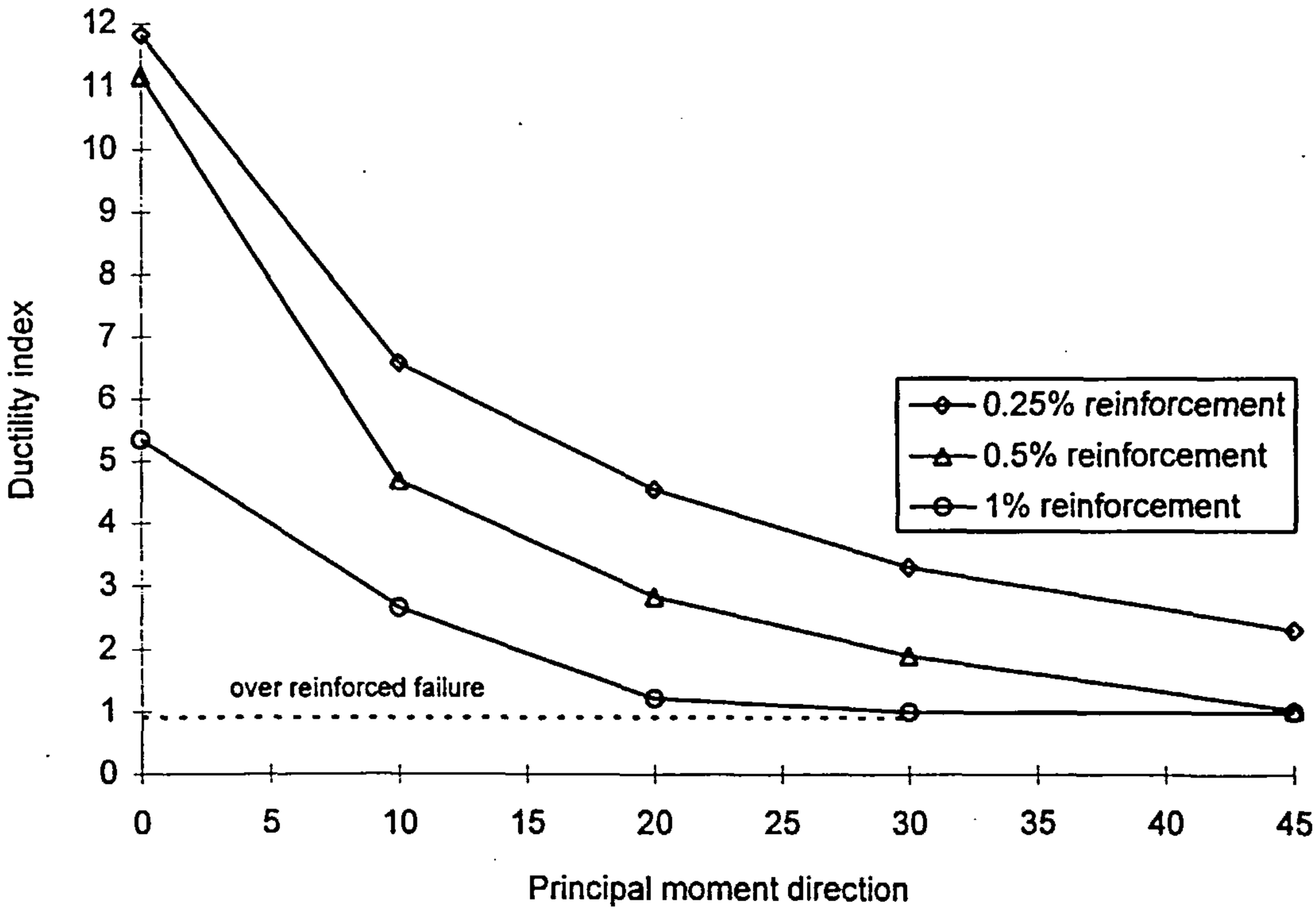

Figure 6.33: Variation of ductility for isotropic slab elements when subjected to principal moment ratio of -1

CHAPTER 7

DESIGN OF REINFORCED CONCRETE SLAB ELEMENTS

7.1 INTRODUCTION.

Over recent decades researchers[1,2,3,4,5] have developed many design techniques for reinforced concrete slabs subjected to mixed moment fields. One of the most popular design techniques make use of the Wood-Armer[3,4] rules, especially in the UK. However, these rules are also used in other countries[6]. These design rules are easy to use and are being used especially for the design of reinforcement for bridge decks. These design rules can produce unsafe results under certain loading conditions i.e. an element designed using these rules may have a lower capacity than it is designed for. This over estimation of strength is due to the fact that the design rules use the normal moment yield criterion which uses Johansen's yield criterion[7]. Johansen's yield criterion has some serious deficiencies which have been discussed in Section 6.3, Chapter 6.

In order to use any design procedure, that uses the normal moment yield criterion, safely either the criterion defining the strength of the slab element i.e. Johansen's

yield criterion[7] must be modified or some limit must be imposed on the maximum area of reinforcement to ensure an under reinforced failure under given loading conditions. Modifying Johansen's yield criterion for a generalised set of loading where the failure direction does not coincide with the reinforcement directions is not easy and may be impossible. Imposing an upper limit on the area of reinforcement that can be provided in the element may be more practical. It has been shown in Section 6.4, Chapter 6, that for low areas of reinforcement the strength predictions using Johansen's yield criterion are reasonably accurate.

This Chapter deals with the design and analysis of reinforced concrete slab elements subjected to moments only i.e. with no in-plane forces. This Chapter provides a hand calculation method that can be used for the design and analysis of slab elements subjected to pure twisting moment. A procedure to design and analyse slab elements in mixed moment field has also been discussed. However, it was not possible to provide simple calculation method for design and analysis for slab elements due to certain difficulties. Instead a numerical procedure, based on the computer program discussed in Chapter 4, has been proposed to design slab elements in mixed moment field.

7.2 DESIGN PHILOSOPHY FOR REINFORCED CONCRETE ELEMENTS

The design of a reinforced concrete element in flexure is considered to be safe if the capacity of the element is greater than the required design moment and the element is under reinforced i.e. the failure is initiated by yielding of the reinforcement. In order

to ensure yielding of the reinforcement either the depth of the neutral axis is restricted or the area of reinforcement to be provided is limited. The area of reinforcement at which the concrete crushes and the reinforcement yields simultaneously is termed as the balanced area of reinforcement. The balanced area of reinforcement is the upper limit on the amount of reinforcement that can be provided to ensure yielding of the reinforcement. It is usually expressed as a proportion of the overall depth of the element and termed as balanced reinforcement ratio.

The balanced reinforcement ratio is dependent on the type of loading i.e. the strain profile through the depth of the slab element. Therefore, expressions for the balanced reinforcement ratio for different strain states have been developed in the following Sections. The following assumptions have been made in order to determine the expressions for the balanced reinforcement ratio.

1. Plane section remains plane after bending.
2. A rectangular stress block for concrete in compression has been used, Figure 7.2.
3. The strength of concrete in tension has been neglected.
4. The reinforcement can carry stress axial stress only.
5. The reinforcement has been assumed to be placed at the same level, at the top and bottom faces, in the two orthogonal directions.

7.2.1 BALANCED REINFORCEMENT RATIO FOR AN ELEMENT UNDER UNIAXIAL BENDING

Consider a reinforced concrete slab element of overall depth, h, with the balanced area of reinforcement provided at the bottom face in the direction of bending, Figure 7.2a and 7.2b. The strain profile at ultimate load in the principal direction 1-1 is shown in Figure 7.2c. The stress distribution through the depth in the principal direction 1-1 is shown in Figure 7.2d. Figure 7.3 shows the Mohr's circle of strain at the reinforcement level. It is important to point out that the principal strain, the principal moment and the reinforcement directions coincide the failure direction is at right angles.

The following expression can be obtained, Figure 7.2c,

$$\frac{x^{B}_{bal}}{d - x^{B}_{bal}} = \frac{0.0035}{f_y / E_s} \qquad 7.1$$

where, x^{B}_{bal} = depth of neutral axis in uniaxial bending for a balanced section

d = effective depth of the element

f_y = yield strength of the reinforcement

E_s = modulus of elasticity of the reinforcement

If E_s is taken as 200×10^3 MPa then equation 7.1 can be rewritten as,

$$x^{B}_{bal} = \frac{700\,d}{700 + f_y} \qquad 7.2$$

From Figure 7.2d,

$$A^{B}_{bal}\, f_y = k_1\, f'_c\, x^{B}_{bal} \qquad 7.3$$

where A^{B}_{bal} = balanced area of reinforcement in uniaxial bending

k_1 = factor related to width of simplified compressive stress block

f'_c = compressive strength of concrete

or,
$$\rho^{B}_{bal} = k_1 \frac{f'_c}{f_y} \frac{x^{B}_{bal}}{h} \qquad 7.4$$

where, ρ^{B}_{bal} = balanced reinforcement ratio in uniaxial bending = A^{B}_{bal} / h

h = overall depth of the element

substituting the value of x^{B}_{bal} from equation 7.2 into equation 7.4,

$$\rho^{B}_{bal} = k_1 \frac{f'_c}{f_y} \left(\frac{700}{700 + fy}\right) \frac{d}{h} \qquad 7.5$$

From equations 7.1 and 7.4 it is evident that the balanced area of reinforcement depends on the compressive strength and crushing strain of concrete, the yield strength and modulus of elasticity of the reinforcement.

For practical range of f'_c/f_y the value of ρ^B_{bal} varies from 1.9% to 3.8% if d/h is assumed to be 0.9, Figure 7.4.

7.2.2 BALANCED REINFORCEMENT RATIO FOR AN ELEMENT UNDER BIAXIAL EQUAL AND OPPOSITE BENDING MOMENTS

Consider now an element subjected to biaxial equal and opposite moments in the reinforcement directions. The balanced amount of reinforcement is provided at the bottom face of the element in the x direction and at the top face in the y direction to resist bending moments, Figure 7.5a. The strain profiles at ultimate load in the principal strain directions are shown in Figures 7.5b and 7.5c. The stress distribution in the principal stress direction 1-1 is shown in Figure 7.5d. In this case the principal strain directions and the reinforcement directions coincide. The concrete will be in a state of compression-tension throughout the depth and the compressive strength of the concrete will, therefore, be reduced[8,9,10]. The ratio of the principal moments is -1 and the principal moment directions, the reinforcement and the failure directions will coincide.

The depths of the neutral axes will be the same in two principal strain directions, Figures 7.5b and 7.5c, and are given by equation 7.2. In order to obtain the expressions for the balanced reinforcement ratio in the two reinforcement directions a similar procedure can be employed as that used for uniaxial bending. However, the

balanced reinforcement ratio will be the same in both the directions. The following expression will be obtained.

$$\rho^{B}_{bal} = k_1 \frac{f'_c}{f_y} \left(\frac{700}{700 + fy}\right) \frac{d}{h} \qquad 7.6$$

The above expression is similar to equation 7.5 but due to compression softening[8,9,10], the compressive strength of the concrete will be substantially reduced and the factor k_1 will also be reduced. This will result in a smaller value for the balanced reinforcement ratio compared with that for uniaxial bending but the depths of the neutral axes will be the same as that for uniaxial bending. A comparison of the depths of the neutral axes and balanced reinforcement ratio have be carried out in Section 7.2.5. However, for pratical range of f'_c/f_y the value of ρ^{B}_{bal} varies from 1.6% to 3.25% if d/h is assumed to be 0.9, Figure 7.4.

7.2.3 BALANCED REINFORCEMENT RATIO FOR AN ELEMENT UNDER PURE TWISTING

An element subjected to pure twisting moments require similar areas of reinforcement in the x and y directions in both top and bottom faces. All four sets of reinforcement will be in tension. The concrete will be in a state of compression-tension in the principal stress directions throughout the depth, therefore, the compressive strength of the concrete will be reduced due to compression softening[8-10].

The principal strain directions, principal moment directions and the failure directions will be at $\pm 45^{o}$ with respect to the reinforcement directions. The ratio of the principal moments will be -1.

Consider an element of depth, h, subjected to pure twisting moments has a balanced area of reinforcement, A^{T}_{bal}, in the x and y directions, at both the top and bottom faces. Figures 7.6b and 7.6c show the strain profiles at ultimate load through the depth of the element in the principal strain directions 1-1 and 2-2 respectively. Figures 7.6d and 7.6e show the stress distribution in the principal stress directions 1-1 and 2-2 respectively. The Mohr's circle of strains at ultimate load, Figure 7.7, indicates the strain both in the principal strain and the reinforcement directions. ε_t is the principal tensile strain at the bottom reinforcement level in direction 1-1 and ε_c is the principal compressive strain at the bottom reinforcement level in direction 2-2. All the sets of the reinforcement will yield in tension and the strain in the reinforcement directions will be f_y/E_s. Since the reinforcement is at 45^{o} from the principal strain direction, the principal tensile strain will be obviously greater than the yield strain of the reinforcement. Hence, Figure 7.7, the principal tensile strain direction 1-1, ε_t, is,

$$\varepsilon_t = \varepsilon_c + 2\, f_y / E_s \qquad 7.7$$

and from Figure 7.6c,

$$\varepsilon_c = \frac{0.0035\,(x^{T}_{bal} - c)}{x^{T}_{bal}} \qquad 7.8$$

where, ε_c = compressive strain in principal direction 2-2 at the level of the reinforcement

x^T_{bal} = depth of the neutral axis for a balanced section under pure twisting

c = distance between the centroid of the reinforcement and the nearest concrete edge

and from Figure 7.6b,

$$\frac{x^T_{bal}}{d - x^T_{bal}} = \frac{0.0035}{\varepsilon_t} \qquad 7.9$$

substituting the value ε_t from equation 7.7 and ε_c from equation 7.8 into equation 7.9 and assuming E_s = 200 MPa and simplifying, the depth of the neutral axis is given by.

$$x^T_{bal} = \frac{700\,h}{1400 + 2f_y} \qquad 7.10$$

Figure 7.6d shows the simplified stress block for the concrete in compression and the tensile forces in the reinforcement in the principal stress direction 1-1. From equilibrium of forces,

$$2A^T_{bal}\, f_y = k_1\, f'_c\, x^T_{bal} \qquad 7.11a$$

where k_1 is the factor related to the width of simplified compressive stress block. The numerical value of k_1 will be different from that used in equation 7.3 since the concrete will be in state of compression-tension.

Thus,
$$\rho^T_{bal} = \frac{k_1}{2}\frac{f'_c}{f_y}\frac{x^T_{bal}}{h} \qquad 7.11b$$

where, ρ^T_{bal} = balanced reinforcement ratio for a section under pure twisting

$= A^T_{bal}/h$

Substituting the value x^T_{bal} from equation 7.10 in equation 7.11b gives the following expression.

$$\rho^T_{bal} = \frac{k_1}{2}\frac{f'_c}{f_y}\left(\frac{700}{1400+2f_y}\right) \qquad 7.12a$$

or,
$$\rho^T_{bal} = 0.284\frac{f'_c}{f_y}\left(\frac{700}{1400+2f_y}\right) \qquad 7.12b$$

For pratical range of f'_c/f_y the value of ρ^T_{bal} varies from 0.45% to 0.9%, Figure 7.4.

The moment capacity of the balanced section in pure twisting can be derived using Figure 7.6d and applying moment equilibrium.

$$M^{T}_{bal} = k_1 f'_c x^{T}_{bal} (\frac{h}{2} - k_2 x^{T}_{bal}) \qquad 7.13a$$

or, $$M^{T}_{bal} = 0.568 f'_c x^{T}_{bal} (\frac{h}{2} - 0.55 x^{T}_{bal}) \qquad 7.13b$$

where k_2 = factor associated with the centroid of the rectangular compressive stress block of concrete

The compressive response of concrete is different in the compression-tension stress state from the uniaxial compressive response, Section 3.2.1.2, Chapter 3. The determination of the values of k_1 and k_2 in equations 7.12b and 7.13b using the model adopted for the compressive response of concrete in the numerical analysis for the state of compression-tension is given in Appendix B.

7.2.4 BALANCED REINFORCEMENT RATIO FOR AN ELEMENT UNDER MIXED MOMENT FIELD

Slab elements are commonly subjected to a combination of bending moments in the reinforcement directions accompanied by twisting moments. When an element is designed for such a moment field, orthotropic sets of reinforcement are required. Orthotropically reinforced slabs are thus the most common type of slabs in use. Such slabs are difficult to analyse and design since the reinforcement directions, principal moment directions, principal strain and stress directions and the failure directions do not coincide with each other. The design or the strength assessment of

an orthotropic slab element is complicated further because the principal strain and stress directions vary throughout the depth. An attempt has been made in the following Sections to provide a possible line of action for the design and strength assessment of orthotropic slabs elements using hand calculations but the complete solution to the problem has not been achieved. However, numerical techniques such as that described in Chapter 4 can be used in strength assessment and design such slab elements and has been discussed in Section 7.4.

7.2.4.1 Balanced Reinforcement Ratio for an Element under Biaxial Equal and Opposite Bending and Twisting Moments

An element subjected to biaxial equal and opposite bending moments in the reinforcement directions accompanied by a twisting moment when designed using the Wood-Armer[3,4] rules, will have an area of reinforcement in the x direction in the bottom face equal to that the y direction in the top face. It will have an area of reinforcement in the y direction in the bottom face and that the same in x direction in the top face but different to that in the other directions.

The orientation of the principal strain and stress directions through out the depth will be constant. However, the principal strain direction will not coincide with the reinforcement directions or the principal moment direction but the failure directions, according to the normal moment yield criterion, will be at $\pm 45^{o}$ from the reinforcement directions if the optimum amount of reinforcement is provided. The ratio of the principal moments will be -1.

Consider an element of overall depth h and the area of reinforcement in the x direction in the bottom face and the area of reinforcement in the y reinforcement in the top face A and that in the y direction bottom face and the x reinforcement top face A'. Assumed that $A > A'$, Figure 7.8. Assume that the loading ratio is such that all the four sets of reinforcement are in tension.

In order to have a balanced failure the smaller area of reinforcement, A', will yield first followed by the yielding of the larger area of reinforcement, A, and the crushing of concrete simultaneously. The principal strain profiles, principal stress distributions are shown in Figure 7.9. The Mohr's circles of strain at the top and bottom reinforcement levels are shown in Figure 7.10. It is evident for Figure 7.10 that the strain in the larger area of reinforcement, A, will be at yield strain, f_y/E_s, but the tensile strain in the smaller area of reinforcement, A', will be larger than the yield strain of the reinforcement.

If ε_t and ε_c are the principal tensile and compressive strain at the level of the reinforcement then from Figure 7.9,

$$\varepsilon_c = \frac{0.0035\,(x_{bal} - c)}{x_{bal}} \qquad 7.14$$

$$\varepsilon_t = \frac{0.0035\,(d - x_{bal})}{x_{bal}} \qquad 7.15$$

and from Figure 7.10a,

$$\varepsilon_t = \varepsilon_c + (\lambda + 1)\, f_y / E_s \qquad 7.16$$

where, λ = ratio of tensile strain in the smaller area of reinforcement direction to the yield strain.

From Figure 7.9a

$$\frac{X_{bal}}{d - X_{bal}} = \frac{0.0035}{\varepsilon_t} \qquad 7.17$$

Substituting the values of ε_t and ε_c from equation 7.16 and 7.14 into equation 7.17 and using E_s =200 MPa and simplifying,

$$X_{bal} = \frac{700\, h}{1400 + (\lambda + 1)\, f_y} \qquad 7.18$$

From Δ ABC in Figure 7.10a

$$AB = AC \cos 2\theta \qquad 7.19$$

where, θ = angle between the larger area of reinforcement, A, and principal strain direction 1-1

and AC = Diameter of circle = $\varepsilon_t + \varepsilon_c$ 7.20

Substituting the values of ε_t and ε_c from equations 7.14 and 7.15 into the above expression to obtain

$$AC = \frac{0.0035(d - x_{bal})}{x_{bal}} \qquad 7.21$$

and

$$AB = \frac{f_y}{E_s}(\lambda - 1) \qquad 7.22$$

Now substituting the values of AC and AB from equation 7.21 and 7.22 into 7.19 and simplifying to obtain the following.

$$\lambda = \frac{x_{bal} + 700(d - c)\cos 2\theta}{x_{bal} f_y} \qquad 7.23$$

using Es = 200 MPa

Now by putting the value of λ from equation 7.23 into 7.18 to obtain,

$$x_{bal} = \frac{700h - 700(d - c)\cos 2\theta}{1400 + 2f_y} \qquad 7.24$$

The above expression is valid for principal moment ratio of -1 where $45^\circ \leq \theta \leq 90^\circ$.

From Figure 7.9c,

$$(A + A')f_y = k_1 f'_c x_{bal} \qquad 7.25a$$

or,
$$\rho_{bal} + \rho' = k_1 \frac{f'_c}{f_y} \frac{x_{bal}}{h} \qquad 7.25b$$

where, $\rho' = A'/h$

Substituting the value of x_{bal} from equation 7.18 into above equation to get the following expression.

$$\rho_{bal} + \rho' = k_1 \frac{f'_c}{f_y} \frac{x_{bal}}{h} \qquad 7.26a$$

or,
$$\rho_{bal} + \rho' = 0.568 \frac{f'_c}{f_y} \frac{x_{bal}}{h} \qquad 7.26b$$

or,
$$\rho_{bal} = 0.568 \frac{f'_c}{f_y} \frac{x_{bal}}{h} - \rho' \qquad 7.26c$$

The value of x_{bal} can be obtained using equation 7.24 if the angle between the larger area of reinforcement and principal strain direction, θ, is known. It not possible to predict the value of θ in most of the loading cases. However, it is also difficult to proportion the reinforcement using the above described procedure. The calculation of the value of k_1 in equation 7.19c is given in Appendix B.

7.2.4.2 Balanced Reinforcement Ratio for an Element under Generalised Set of Moments

For a more generalised set of loading in which bending moments of different magnitudes are applied in the reinforcement directions accompanied by twisting moment, the design will produce a completely orthotropically reinforced element i.e. all the four sets of reinforcement will have different areas to each other. The orthotropically element with generalised set of loading will be difficult to analyse. In the element the reinforcement directions will not coincide with principal moment directions, principal strain and stress directions and failure directions.

It is evident from Sections 7.2.1, 7.2.3 and 7.2.4.1 that the balanced reinforcement ratio depends on the principal strain profile through the depth of the element. If the reinforcement is at an angle from the principal strain directions then the principal strain at the reinforcement level can not be estimated unless the angle between the reinforcement and principal strain directions is known. However, expressions for depth of the neutral axis for balanced section and balanced reinforcement ratio can be developed provided the strain distribution remains linear as shown in Section 7.2.4.1. Such expressions, however, remain indeterminate as the angle between the principal strain and reinforcement directions is not known. For a completely orthotropic element the principal strain distribution through the depth is not linear since the principal strain directions continuously change. The varying principal strain directions further complicates the interpolation of strains at any level through the depth and thus

the analytical expression for the depth of neutral axis for a balanced section and balanced reinforcement ratio may not be developed easily.

However, numerical procedures such as described in Chapter 4 can be used to design the slab elements in mixed moment field which has been discussed later in Section 7.4.

7.2.5 DISCUSSION

From an inspection of the analytical expressions for the balanced reinforcement ratio and the depth of neutral axis in the preceding Sections, it can be concluded that both the balanced reinforcement ratio and the depth of neutral axis are dependent on the strain profile through the depth of the element i.e. the type of loading and varies significantly with it. The reason is that as the angle between the principal moment directions and the reinforcement directions increases or as the twisting moment in the reinforcement directions increases, the angle between the principal strain directions and the reinforcement directions also increases. The balanced reinforcement ratio mainly depends on the depth of neutral axis which in turn depends on the principal tensile strain at the reinforcement level. As the angle between the reinforcement directions and the principal strain direction increases, the principal tensile strain at the level of the reinforcement also increases. An increase in the principal tensile strain at the level of the reinforcement not only increases the principal curvature but also reduces the depth of the neutral axis, because the principal compressive strain is the crushing strain of concrete which is fixed, Figure 7.11. The reduction in the depth of the neutral axis depth reduces the balanced area of reinforcement. Thus an element

under pure twisting requires significantly lesser area of reinforcement to be over reinforced as compared to an element under uniaxial bending, Section 6.6, Chapter 6.

Figure 7.12 shows the moment capacities of an isotropically reinforced element for different reinforcement ratios when subjected to uniaxial bending and pure twisting moments. It is evident from Figure 7.12 that the balanced reinforcement ratio is significantly lower for the case of pure twisting moment. For an isotropically reinforced slab element under pure twisting the angle between the principal strain and reinforcement directions is a maximum i.e. $\pm 45^{o}$, thus the principal tensile strain at the level of reinforcement must be larger than the corresponding tensile strain under uniaxial strain. Under uniaxial bending for a balanced section the maximum tensile strain at the level of the reinforcement is the same as the yield strain since the reinforcement directions and the principal strain directions coincide. Figure 7.11 shows the strain profiles for isotropic slab element under pure twisting and uniaxial bending whereas, Figure 7.13 shows the Mohr's circles for strain at the bottom reinforcement level. It is evident from Figures 7.11 and 7.13 that as the angle between the principal strain and reinforcement directions increases, the maximum principal tensile strain at the reinforcement level also increases, forcing the depth of the neutral axis to reduce because the maximum compressive strain is fixed, eventually reducing the balanced reinforcement ratio.

The balanced reinforcement ratio also depends on the compressive strength of concrete and the yield strength of the reinforcement. The balanced reinforcement ratio varies in direct proportion with f'_c/f_y where f'_c is the compressive strength of the

concrete and f_y is the yield strength of the reinforcement. When the concrete is in the state of compression-tension the compressive strength of concrete is significantly reduced[8-10] due to the orthogonal tensile strain. Thus in case of pure twisting, the compressive strength is reduced due to compression softening and this affects the balanced reinforcement ratio. This effect may not be as significant as the effect due to the angle between the principal strain and reinforcement directions but when the two effects are combined, the effect on the balanced amount of reinforcement ratio is compounded. Figure 7.4 shows the variation of balanced reinforcement ratio with f'_c/f_y for different type of loading. The balanced reinforcement ratio for the case when biaxial equal and opposite moments are applied is 15% lower than the balanced reinforcement ratio for uniaxial bending but it is 76.5% lower in case of pure twisting. A similar comparison is shown in Table 7.1 in order to quantify the effects of the reduction of the compressive strength of the concrete due to compression softening and the effect of the angle between the principal strain and the reinforcement directions separately. A slab element of overall depth 200 mm, f'_c = 40 MPa and f_y = 500 MPa, subjected to uniaxial bending, biaxial equal and opposite bending and pure twisting separately is considered. The depth of the neutral axis for a balanced section and balanced reinforcement ratio can be calculated from equations 7.2, 7.4, 7.10 and 7.12b respectively, for each case. As expected the depth of the neutral axis for uniaxial bending and biaxial bending with equal and opposite moments does not change. In the case of pure twisting the depth of neutral axis reduces by 45% as compared to the neutral axis depth for uniaxial bending. The effect of reduction of the compressive strength[8-10] due to compression softening on the balanced reinforcement ratio can be observed by comparing it with the balanced

reinforcement ratio for uniaxial bending. The reduction in the balanced reinforcement ratios was similar as mention earlier.

From the above discussion it can be concluded that the moment capacity of an element is dependent on the type of loading. An element may be safe and efficient for one set of moments but may not be adequate for another set. Therefore, it is necessary to develop guidelines for the analysis and design of slab elements in which the principal moment and the reinforcement directions do not coincide.

7.3 GUIDELINES FOR ANALYSIS AND DESIGN OF ELEMENTS UNDER PURE TWISTING

A reinforced concrete slab element subjected to pure twisting moment requires four sets of isotropic reinforcement if designed using the Wood-Armer[3,4] rules. Such an element can be rendered safe for all loading conditions if the area of reinforcement is low i.e. $\rho\frac{f_y}{f_c}\leq 0.11$, Section 7.3.1.1 and Table 7.2.

If the above condition is satisfied then the failure of the element is by yielding of the reinforcement and thus the strength prediction is fairly accurate, Section 6.4, Chapter 6. But if $\rho\frac{f_y}{f_c}>0.11$ the element is an over reinforced element and the reinforcement does not yield, making the strength prediction using Johansen's yield criterion inaccurate and unsafe. Figure 7.14 shows the variation of the strength index,

M_{twist}/M_{JYC}, with the reinforcement ratio, where M_{twist} is the moment capacity of the element under pure twisting moment using equation 7.13b and M_{JYC} is the pure twisting moment capacity using Johansen's yield criterion. It can be observed from Figure 7.14 that for a reinforcement ratio less than the balanced reinforcement ratio, the pure twisting capacity of the element is not very different from the capacity using Johansen's yield criterion. But for a reinforcement ratio greater than the balanced reinforcement ratio, the difference between the capacities increases significantly. It is due to the fact that for the reinforcement ratios greater than the balanced reinforcement ratio, the reinforcement does not yield and this can not be predicted using Johansen's yield criterion.

Since the analytical expressions for the balanced reinforcement ratio and the depth of the neutral axis for a balanced section under pure twisting have been obtained, therefore, the discussion in this Section is limited to the analysis and design of elements under pure twisting moment only. The procedure to be adopted for the design of the slab elements in mixed moment field is given in Section 7.4.

7.3.1 ANALYSIS OF AN ELEMENT UNDER PURE TWISTING

For an element subjected to pure twisting moment, the angle between the principal strain and the reinforcement direction is a maximum i.e. $\pm 45^{o}$. A hand calculation procedure is proposed in this Section to evaluate the pure twisting moment capacity of an isotropically reinforced element with given reinforcement. The procedure is

1. Determine ρ^T_{bal} from equation 7.12b and check whether the provided steel ratio, $\rho_{pro} \leq \rho^T_{bal}$, where, $\rho_{pro} = A_{pro}/h$ and A_{pro} is the area of reinforcement provided per layer per direction

2. If $\rho_{pro} \leq \rho^T_{bal}$, the moment capacity of the element will be,

$$M^T = 0.568 f'_c x^T \left(\frac{h}{2} - 0.55 x^T\right) \qquad 7.27$$

where,

$$x^T = \frac{\rho_{pro} h f_y}{0.284 f'_c} \qquad 7.28$$

3. If $\rho_{pro} > \rho^T_{bal}$, the moment capacity of the element can still be calculated using equation 7.27 but x^T has to be obtained by solving the following quadratic equation.

$$0.568 \frac{f'_c (x^T)^2}{\rho^T_{pro} h} + 1400 x^T - 700 h = 0 \qquad 7.29a$$

or,

$$x^T = \frac{\rho_{pro} h}{1.136 f'_c} \left[-1400 + \sqrt{(1400)^2 + 1590.4 f'_c / \rho_{pro}}\right] \qquad 7.29b$$

The moment capacity obtained from equations 7.27 and 7.29 assumes a partial safety factor of 1, associated with the material properties as suggested by British Codes of Practice[11].

Examples are given in Appendix C.

7.3.1.1 Validation of Model for Moment Capacity

In order to validate the procedure to calculate the moment capacity of the element, comparisons have been made with four experimental studies[12,13,14,15] on isotropically reinforced slab under pure twisting. The results and details of the material and section properties of the specimens have been tabulated in Table 7.2. The balanced reinforcement ratio, actual depth of the neutral axis and the twisting moment capacity of the elements have been calculated using equations 7.11b, 7.10 and 7.13b respectively. The comparison of the moment capacities is found to be good and on an average the moment capacity is under estimated by 2% with respect to the experimental results with a standard deviation of 6.7%. The model also accurately predicts the mode of failure. It can be concluded from Table 7.2 that if $\rho\frac{f_y}{f_c}\leq 0.11$, the element behaves as an under reinforced element, hence Johansen's yield criterion can be used to determine the pure twisting capacity, Figure 7.14, under such a condition. In order to determine the softened strength of concrete, f_c, a softening factor of 0.7 has been used. An incorrect mode of failure has been predicted for Lenshow and Sozen's[14] slab B16. This is due to the support system employed in the test to apply the twisting moment as discussed in Section 2.2.1, Chapter 2.

7.3.1.2 Comparison with the Theory of Plasticity Approach

Nielsen[2] proposed a technique to predict the twisting moment capacity of the element using the theory of plasticity and by modelling the reinforcement as elastic-plastic material.

In the reinforcement directions i.e. at $\pm 45^{o}$ from the principal stress directions, the maximum stress in the concrete, τ_{xy}, will be $f_c/2$, where f_c is the maximum compressive stress resisted by concrete. f_c will be less than the uniaxial compressive strength of concrete due to compression softening[8-10]. The effect of compression softening, to Nielsen's analysis, was introduced by Marti and Kong[16]. The expression for the pure twisting capacity of the element based on perfect plastic models for the constituents is

$$m_{xyu} = h^2 \rho \ f_y(1-2\rho f_y/f_c) \qquad 7.30$$

where, m_{xyu} = twisting capacity of the element

ρ = reinforcement ratio per layer per direction

It has stated by Nielsen[2] that for low reinforcement ratios equation 7.30 predicts the twisting capacity accurately. It was further stated that the elements with low reinforcement ratio will have smaller neutral axis depth and it was found that when the depth of the neutral axis $\leq$ 10% of the overall depth, the predictions of equation

7.30 were accurate. The reason is that the reinforcement yields at ultimate moment as assumed in the adopted model.

Equation 7.30 gives the moment capacity of an element assuming that the mode of failure is under reinforced which is not true always. If the area of reinforcement is larger than the balanced area of reinforcement, then the strain in the reinforcement will never be as high as the yield strain and thus the reinforcement does not yield.

Nielsen[2] also pointed out that the maximum depth of the neutral axis can be h/2. Marti and Kong[16] explained that when $\rho\frac{f_y}{f_c} > 1/4$, the twisting moment capacity approaches to $f_c h^2/8$ with the depth of the neutral axis equal to h/2. When the maximum twisting moment is applied to an element at ultimate concrete crushes, however, the reinforcement does not yield. Thus the maximum twisting capacity of an element is the capacity of over reinforced element.

Table 7.2 also compares the moment capacity of the slab elements using the theory of plasticity approach with the experimental results. The plasticity approach over estimated the capacity with an average of 9% and a standard deviation of 12%. It can be observed from Table 7.2 that the greater the value of $\rho\frac{f_y}{f_c}$, the higher the estimation. This is due to the fact that in these specimens the reinforcement does not yield as assumed in plasticity approach.

7.3.2 DESIGN GUIDELINES FOR ELEMENTS UNDER PURE TWISTING

To design a reinforced concrete slab element under pure twisting the following procedure is proposed.

1. Determine the design moments in the reinforcement direction using the Wood-Armer[3,4] rules. The design moments in case of pure twisting in the reinforcement directions will be

$$m^{*}_{x} = m^{*}_{y} = m^{**}_{x} = m^{**}_{y} = |m_{xy}| \qquad 7.31$$

where; m^{*}_{x}, m^{*}_{y} = design moment for bottom reinforcement in x and y directions respectively

m^{**}_{x}, m^{**}_{y} = design moment for top reinforcement in x and y directions respectively

m_{xy} = applied twisting moment

2. Design the reinforcement but as the concrete will be in state of compression-tension, the compressive strength of concrete will be reduced and it is proposed to use a softening factor of 0.7 on the compressive strength of concrete.

3. Determine the ρ^T_{bal} from equation 7.12b and check whether the required reinforcement is less than or equal to ρ^T_{max} where,

$$\rho^T_{max} = 0.75\,\rho^T_{bal} \qquad 7.32$$

where, ρ^T_{max} = maximum amount of steel ratio that can be provided in an element to ensure ductile under reinforced failure

A factor of safety of 0.75 has been used with ρ^T_{max} to ensure ductile failure and has been adopted from American Code of Practice[17].

4. If the amount of reinforcement provided is less than the balanced amount of reinforcement, then the yielding of the reinforcement is assured and Johansen's yield criterion[7] or the Wood -Armer[3,4] rules can be safely used.

5. If the amount of reinforcement required is greater than the maximum amount of reinforcement allowed then the section properties must to changed in order to have a safe design.

Worked examples are given in Appendix C.

7.4 GUIDELINES FOR THE ANALYSIS AND DESIGN OF ELEMENTS UNDER A GENERALISED SET OF MOMENTS

Reinforced concrete slab elements are often subjected to a set of moments in which m_x, m_y and m_{xy} are all different. If such an element is designed using the Wood-Armer rules[3,4], different areas for the four sets of reinforcement are obtained. It has been pointed out in Section 7.3 that these rules do not necessarily produce a safe design. It is, therefore, the intention of this Section to provide guidelines for the design of such slab elements. It has also been pointed out in Sections 7.2.4.1 and 7.2.4.2 that the principal stress directions, failure direction and the principal moment directions do not coincide with each other for a completely orthotropically reinforced element. The principal stress direction varies through the depth in such an element, making the analysis and design more complicated. Numerical procedures such as that described in Chapter 4 can, however, be adopted for the analysis of orthotropically reinforced slab elements. However, if one of the following conditions are satisfied, the Wood-Armer rules can still be used for design.

- The reinforcement and the principal moment directions coincide.
- The strength ratio, $\frac{\rho f_y}{f_c} \leq 0.11$.
- The ratio of the principal moments is positive.

- The ratio of the principal moments is negative but the angle between the principal moment and the reinforcement directions is less than equal to 20^{o}.

If any of the above condition is not satisfied then the slab element can be designed using the following procedure.

1. Design the reinforcement using the Wood-Armer rules[3,4] for the given set of moments m_x, m_y and m_{xy}.

2. For the given areas of reinforcement and loading, determine the moment capacity of the slab element for a known material and section properties using the computer program described in Chapter 4.

3. If the moment capacity of the element is less than the required moment capacity, redesign the reinforcement for bending moments, m_x, m_y and twisting moment m_{xy} independently. Add the reinforcement required by bending and twisting moments. Since the concrete will be in state of compression-tension, the compressive strength of the concrete will be reduced. It is proposed that a softening factor of 0.7 should be used on the compressive strength of concrete.

4. Check the moment capacity of the slab element with new set of reinforcement using the computer program.

5. If the moment capacity is still less than the required moment capacity, increase the overall depth of the element using the following.

$$h_{new} = \frac{m_{req}}{m_{cap}} h \qquad 7.33$$

where, h_{new} = new overall depth of the slab element

h = original overall depth of the slab element

m_{req} = required moment

m_{cap} = moment capacity of the slab element using the computer program

6. Repeat steps 4 and 5 until the required moment capacity is obtained.

In order to demonstrate the procedure outlined above, assume a slab element 200 mm deep is subjected to a mixed moment field such that the applied moments are in a ratio $m_x : m_y : m_{xy} = 0.57735 : -0.57735 : 1$. The assumed loading ratio gives a principal moment ratio of -1 with the reinforcements at 30° from the principal moment directions. Assume that the required twisting moment capacity, m_{req}, is 40 kN-m/m and the compressive strength of the concrete is 40 MPa and the yield strength of the reinforcement is 500 MPa. The reinforcement required using the Wood-Armer rules[3,4] will be $A_{sx} = A'_{sy} = 0.7273$ mm^2/mm and $A_{sy} = A'_{sx} = 0.19$ mm^2/mm if the softened compressive strength of concrete is used i.e. $f_c = 0.7 f'_c$.

For the given moment ratio, section and material properties, the slab element was analysed using the computer program and the ultimate moments $m_x = -m_y = 11.3$ kN-m/m and $m_{xy} = 19.54$ kN-m/m were obtained. Since the moments are less than the required moments the reinforcements was redesigned separately for bending and twisting moments and added to obtain the following sets of reinforcements $A_{sx} = A'_{sy}$ $= 0.7273$ mm^2/mm and $A_{sy} = A'_{sx} = 0.4547$ mm^2/mm. Subsequently the moment capacities of $m_x = -m_y = 20.6$ kN-m/m and $m_{xy} = 35.87$ kN-m/m were obtained using the computer program for the new reinforcement areas. Once again the moments are less than the required moments, hence the overall depth of the slab element was then increased using equation 7.33 and $h_{new} \cong 225$ mm was obtained. The slab element was again analysed using h_{new} and moment capacities of $m_x = -m_y =$ 23.67 kN-m/m and $m_{xy} = 41$ kN-m/m were obtained. Hence $m_{cap} > m_{req}$.

Figure 7.15 shows the part of the yield surface using the normal moment yield criterion along with the numerical results for the above example. It can be observed that by increasing the reinforcement for twisting moment the failure surface expands and approaches towards the failure surface for an isotropically reinforced element. The computer program produced a moment capacity 52% lower that the normal moment yield criterion for the areas of reinforcement obtained from the Wood-Armer rules[3,4] whereas the capacity of the element was 27.4% lower than that predicted by the normal moment yield criterion with the new areas of reinforcement. By increasing the depth of the element the required moment capacity was achieved.

It was observed that for a given set of moments, the reinforcement with larger area did not yield, whereas the reinforcement with smaller area yielded, in both the cases i.e. when designed using the Wood-Armer rules and using the new design procedure. However, by adopting the new design procedure, the area of reinforcement in the y direction was increased as compared to the area of reinforcement obtained using the Wood-Armer rules while the area of reinforcement in the x direction remained unchanged. By increasing the area of reinforcement in the y direction, a significant increase in the moment capacity was achieved. The increase in the moment capacity is due to the fact that effectively more area of reinforcement is available in the failure direction. The increase in the effective area of reinforcement in the failure direction resulted in better efficiency of both the sets of reinforcement, Figure 7.16.

References

1 Hillerborg, A, Reinforcement for slabs and shells designed according to the theory of elasticity, Betong 1953, vol. 38, no. 2, pp 101-109. Translated by GN Gibson, Garston, Building Research Station, January 1962, 7 p, Library communication No. 1081.

2 Nielsen, MP, Limit analysis of reinforced concrete slabs, Acta Polytechnica Scandinavica, Ci 26, Copenhagen, Denmark, 1964, 167 p.

3 Wood, RH, The reinforcement of slabs in accordance with a predetermined field of moments, Concrete, London, vol. 2, February 1968, pp 69-76.

4 Armer GST, Discussion on 'The reinforcement of slabs in accordance with a predetermined field of moments', Concrete, London, vol. 8, August 1968, pp 319-321.

5 Morley, CT, The minimum reinforcement of concrete slabs, International Jnl. of Mechanical Sciences, vol. 8, no. 4, April 1966, pp 305-319.

6 Hillerborg, A, Discussion on 'A Yield criterion for Reinforced Concrete Slabs, ACI Jnl., Proceeding , vol. 64, no. 11, November 1967, pp 786-789.

7 Johansen, KW, Brudlinieteorier, Gjellerup, Copenhagen, Denmark 1943, English edition: Yield line theory, Cement and Concrete Association, London 1962, 181p.

8 Vecchio, FJ and Collins, MP, The modified compression field theory for reinforced concrete elements subjected to shear, ACI St. Jnl., vol. 82, no. 2, Mar-Apr. 1986, pp 219-231.

9 Vecchio, FJ and Collins, MP, Compression response of cracked reinforced concrete, Jnl. of St. Eng., ASCE, vol. 119, no. 12, December 1993, pp 3590-3610.

10 Belarbi, A and Hsu, TTC, Constitutive laws of softened concrete in biaxial tension-compression, ACI St. Jnl., vol. 92, no. 5, September 1995, pp 562-573.

11 Structural use of concrete - Part I, Code of practice for design and construction, BS 8110: 1985, British Standard Institution, London.

12 Marti, P, Leesti, P, Khalifa, WU, Torsion tests on reinforced concrete slab elements, Jnl. of St. Eng., ASCE, vol. 113, no. 5, May 1987, pp 994-1010.

13 Harder, NA, Strength of the concrete in the shear zone of a reinforced concrete cross section, Experiments with plates loaded in tension, Instituttet for Bygningsteknik, Aalborg, Report No. 7901, August 1979, 49 p.

14 Lenshow, R, Sozen, MA, A Yield Criterion for Reinforced Concrete Slabs, ACI Jnl., Proceedings vol. 64, no. 5, May 1967, pp 266-273.

15 Morley CT, The ultimate bending strength of reinforced concrete slabs, PhD Thesis, University of Cambridge, June 1965, 212 p.

16 Marti, P and Kong, K, Response of reinforced concrete slab elements to torsion, Jnl of Structural Engineering, ASCE, vol. 113, no. 5, May 1987, pp 976-993.

17 Building code requirements for reinforced concrete and commentary 1989, ACI 318-89/ ACI 318R-89, American Concrete Institute, Detroit, Mich.

Table 7.1: Effect of type of loading on balanced reinforcement ratio.

Type of Loading	**Depth of neutral axis** (mm)	**Balanced of reinforcement ratio** (%)	**Reduction in neutral depth axis with respect to uniaxial bending** (%)	**Reduction in balanced reinforcement ratio with respect to uniaxial bending** (%)
Uniaxial bending	105	2.814	0	0
Biaxial equal and opposite bending	105	2.386	0	15.2
Pure twisting	58.33	0.663	44.45	76.4

Table 7.2: Comparison of the model with the experimental data.

Researcher	Slab ref	Area of steel provided ρ_{pro}	Strength of concrete f'_c (MPa)	Yield strength of steel f_y (MPa)	Balanced reinforcement ratio ρ^T_{bal}	$\frac{\rho_{pro} f_y}{f_c}$	$\frac{\rho_{pro}}{\rho^T_{bal}}$	Actual depth of neutral axis (mm)	Twisting moment capacity of section M_{cap} (kN m/m)	Plastic twisting moment capacity M_{plas} (kN m/m)	Experimental twisting moment M_{exp} (kN m/m)	$\frac{M_{cap}}{M_{exp}}$	$\frac{M_{plas}}{M_{exp}}$	Mode of failure
Marti, Leesti & Khalifa[12]	1	0.0025	46.7	551	0.006734	0.0421	0.371	20.77	48.80	50.46	44.40*	-	-	UR
(h = 200 mm)	2	0.005	36.2	551	0.00522	0.1087	0.958	55.22	79.06	86.24	69.50*	-	-	UR
	3	0.01	37.5	481	0.006562	0.1832	1.524	66.43	89.80	121.89	93.80*	-	-	OR
	7	0.0025	44.4	479	0.007815	0.0385	0.32	18.99	42.90	44.21	42.50	1.01	1.04	UR
	9	0.01	44.4	412	0.009633	0.1326	1.038	63.58	104.28	121.11	101.50	1.03	1.19	OR
Harder[13]	1	0.005386	17.5	276	0.006441	0.1216	0.836	37.48	15.57	17.57	16.14	0.96	1.09	UR
(h = 125 mm)	3	0.005386	21.6	292	0.007404	0.1041	0.727	32.08	17.63	19.45	19.16	0.92	1.02	UR
	5	0.005386	43.5	292	0.014942	0.0516	0.360	15.90	21.13	22.04	22.38	0.94	0.98	UR
	7	0.005386	18.2	486	0.003146	0.2050	1.712	42.57	17.24	24.13	17.70	0.97	1.36	OR
	9	0.005386	25.0	486	0.004313	0.1495	1.249	39.26	22.81	28.67	24.69	0.92	1.16	OR
	11	0.005386	39.7	486	0.006849	0.0941	0.786	29.00	30.46	33.20	28.31	1.08	1.17	UR
	13	0.005386	24.4	270	0.009268	0.0851	0.581	26.21	17.48	18.85	17.60	0.99	1.07	UR
	15	0.005386	40.9	270	0.015521	0.0508	0.347	15.65	19.59	20.41	20.67	0.95	0.99	UR
	17	0.005386	46.1	270	0.017494	0.0451	0.308	13.89	19.94	20.67	21.02	0.95	0.98	UR
Lenshow & Sozen[14]	B16	0.008911	32.6	333	0.009422	0.130	0.9458	41.77	21.93	23.13	24.15	0.91	0.96	UR
(h = 102.616 mm)	B20	0.00408	37.9	357	0.009977	0.0550	0.409	13.90	13.05	13.65	15.21	0.86	0.90	UR
Morley[15]	10/45/4	0.0054	41.2	555	0.005878	0.1039	0.919	8.94	2.63	2.90	2.58	1.02	1.12	UR
(h = 34.925 mm)	6/45/1	0.0054	46.4	618	0.005658	0.1028	0.954	8.85	2.94	3.24	3.11	0.94	1.04	UR
	6/45/2	0.0054	44.3	593	0.005742	0.1032	0.940	8.89	2.81	3.10	2.88	0.98	1.08	UR
	2/45/1	0.0054	39.9	609	0.004965	0.1179	1.088	10.15	2.73	3.07	2.68	1.02	1.14	OR
	2/45/2	0.0054	43.0	617	0.00525	0.1109	1.028	9.54	2.84	3.17	2.47	1.15	1.28	OR
											Avg.	0.98	1.09	
											St dev	0.067	0.12	

* corner failed prior to reaching ultimate load : UR under reinforced failure : OR over reinforced failure

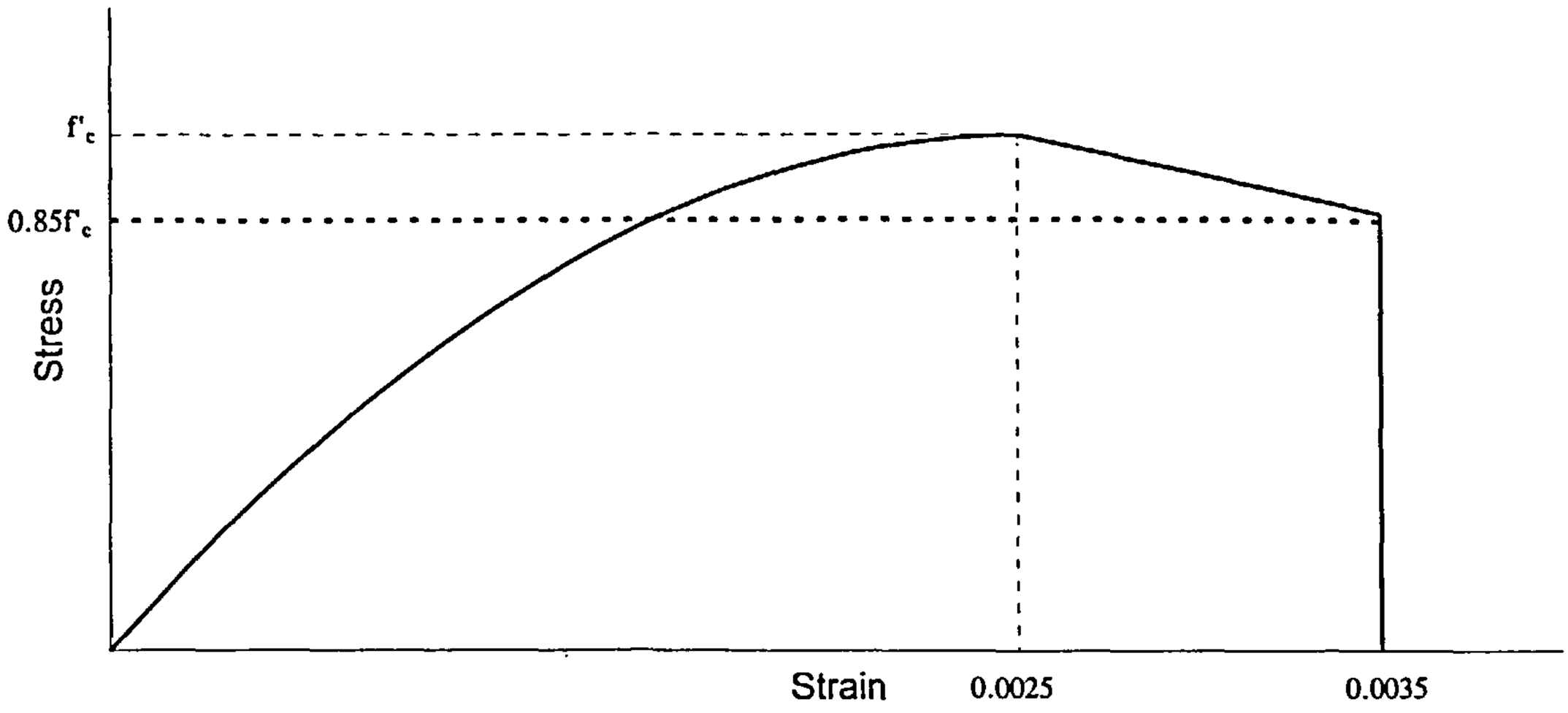

Figure 7.1: Simplified stress-strain response of concrete in compression

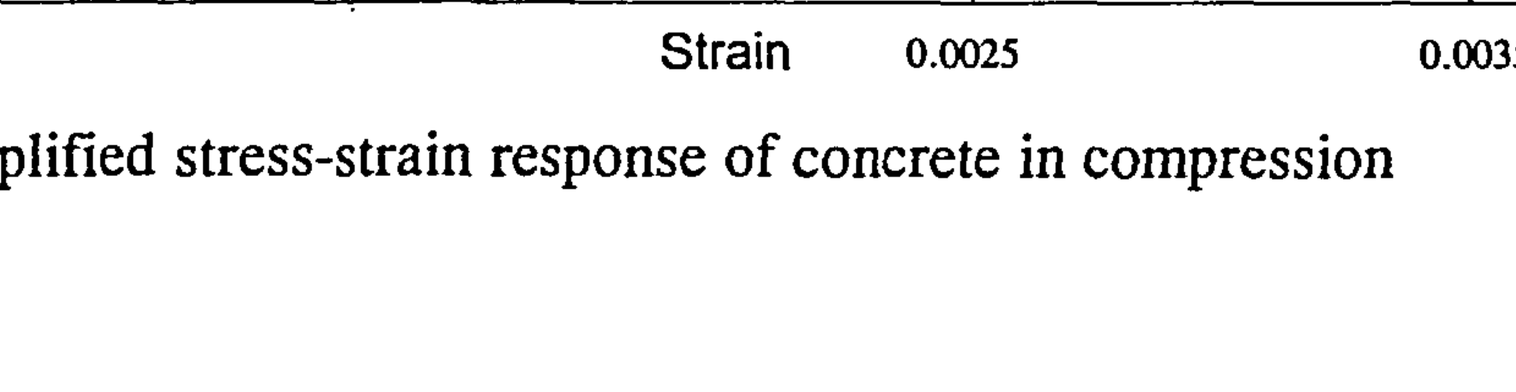

(a)

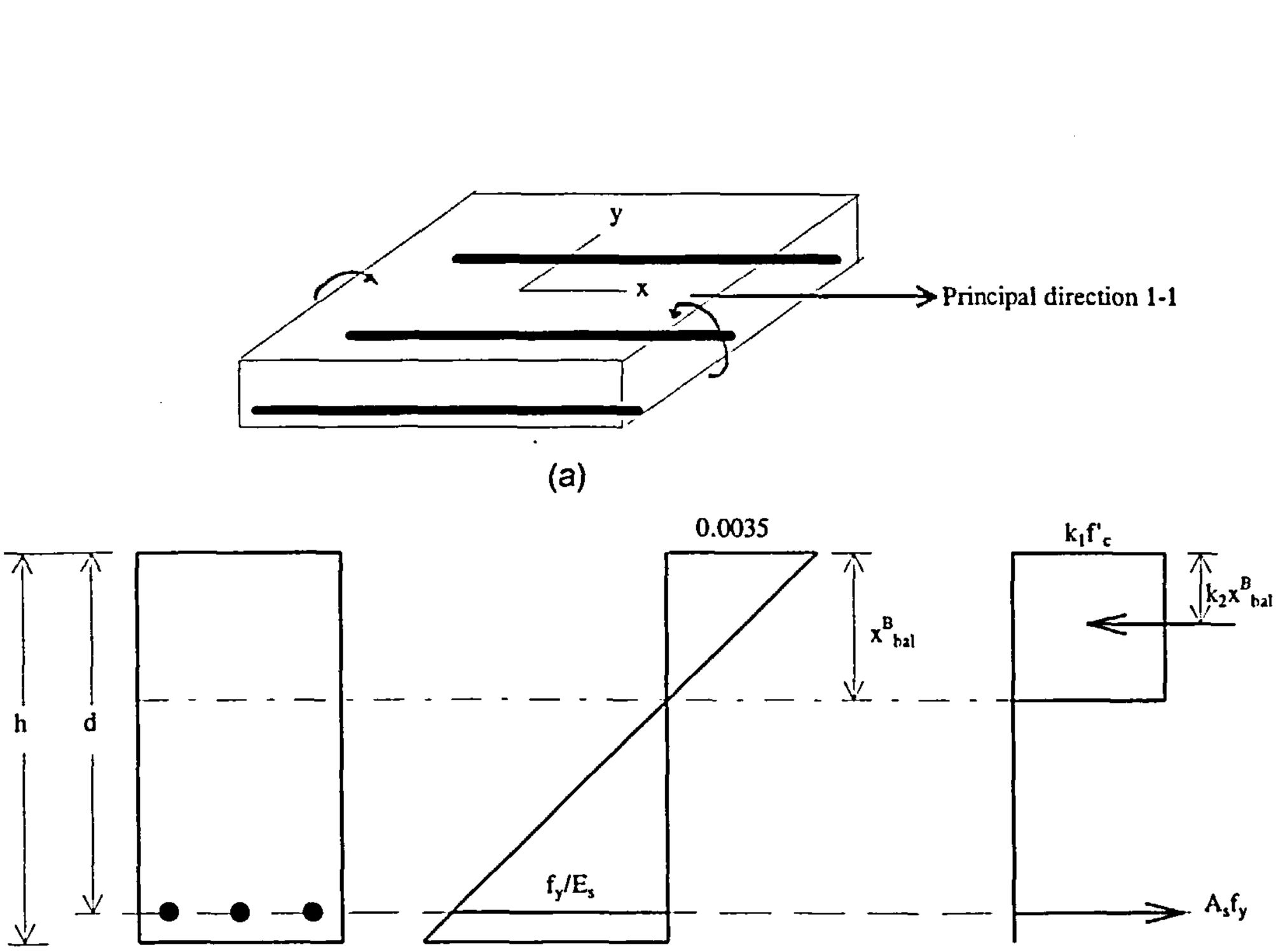

(b) (c) (d)

Figure 7.2: Reinforced concrete slab element under uniaxial bending (a) slab element (b)cross-section of the slab element (c) strain profile in principal strain direction 1-1 (d) simplified stress block in principal stress direction 1-1

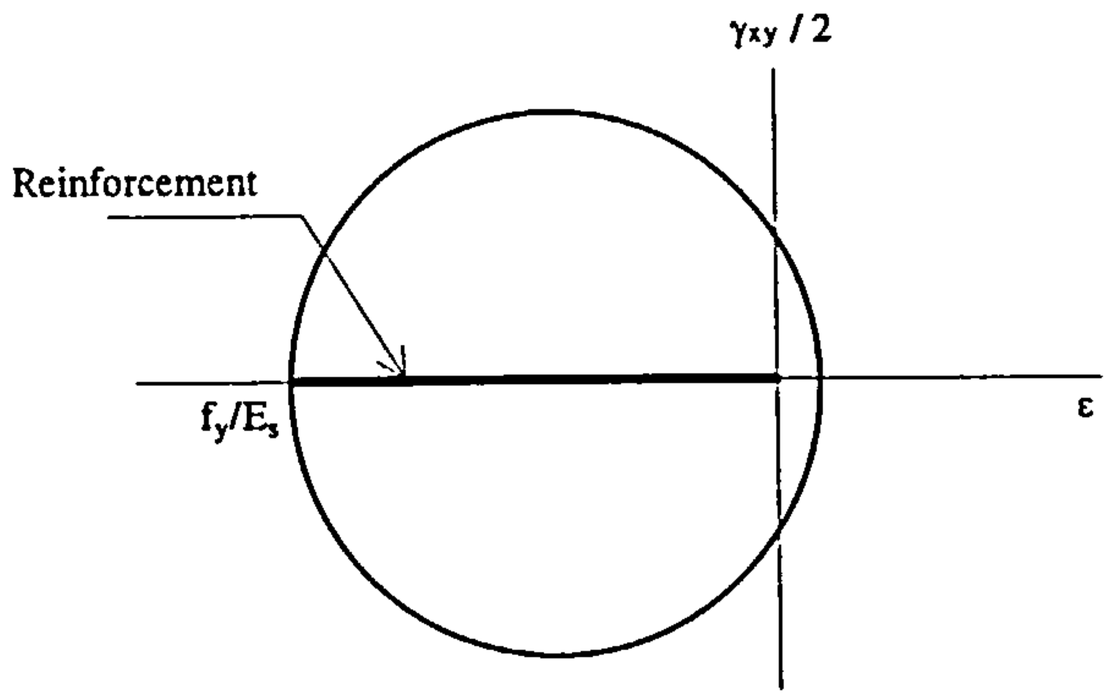

Figure 7.3: Mohr's circle of strain at the reinforcement level

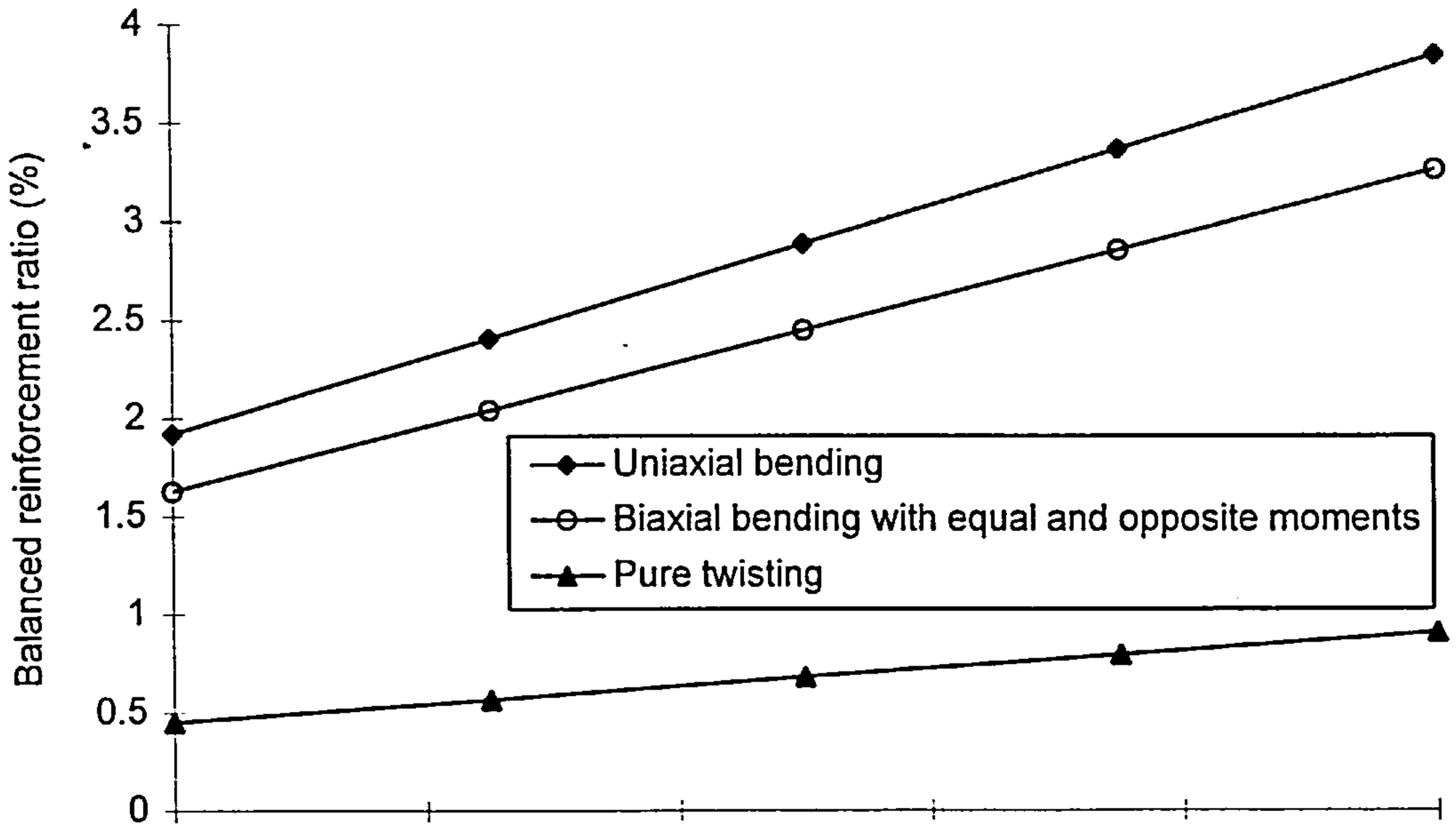

Figure 7.4: Variation of balanced reinforcement ratio

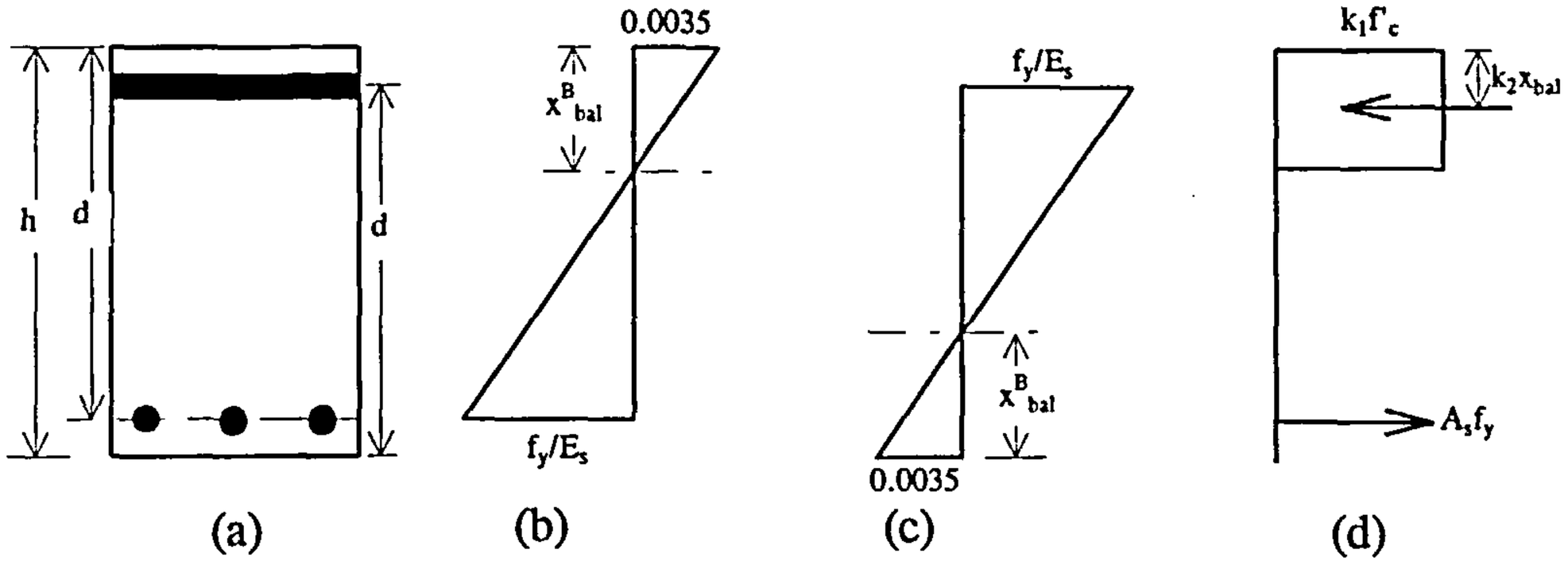

Figure 7.5: Slab element under biaxial equal and opposite bending (a) cross-section (b) strain profile in principal strain direction 1-1 (c) strain profile in principal strain direction 2-2 (d) stress distribution in principal stress direction 1-1

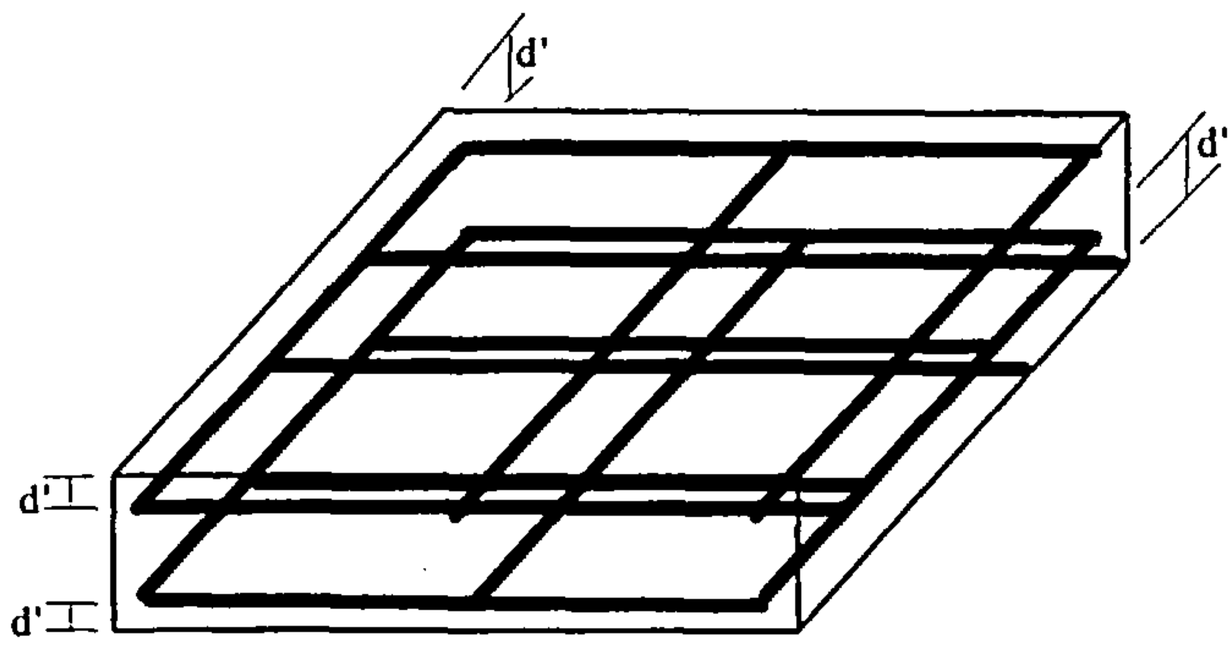

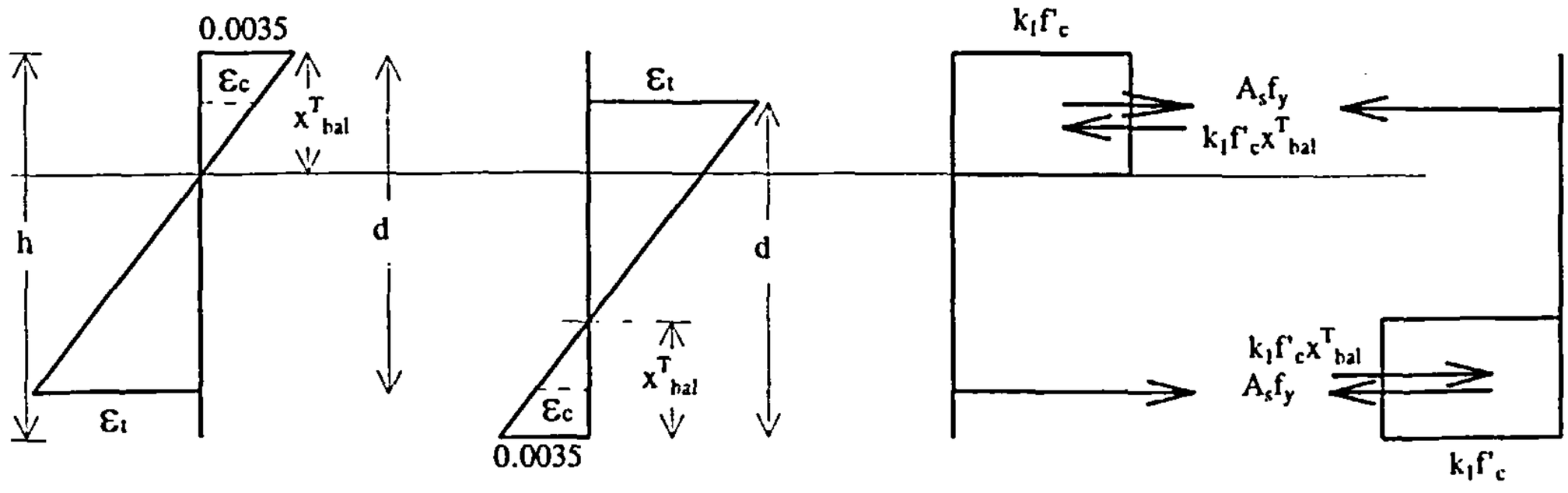

Figure 7.6: Slab element under pure twisting (a) the element (b) strain profile in direction 1-1 (c) strain profile in direction 2-2 (d) stress distribution in direction 1-1 (e) stress distribution in direction 2-2

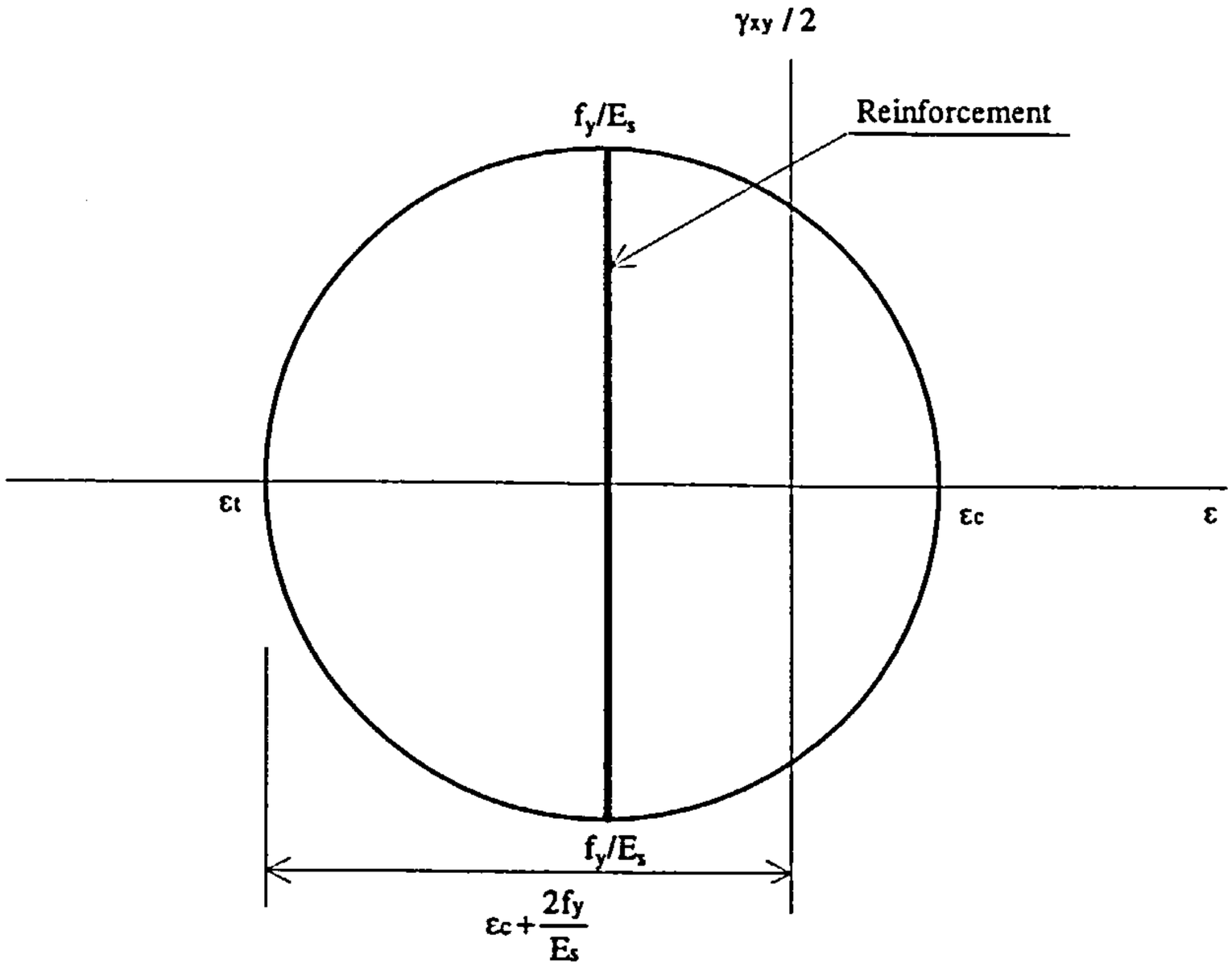

Figure 7.7: Mohr's circle of strain at the bottom reinforcement level for an element under pure twisting moment

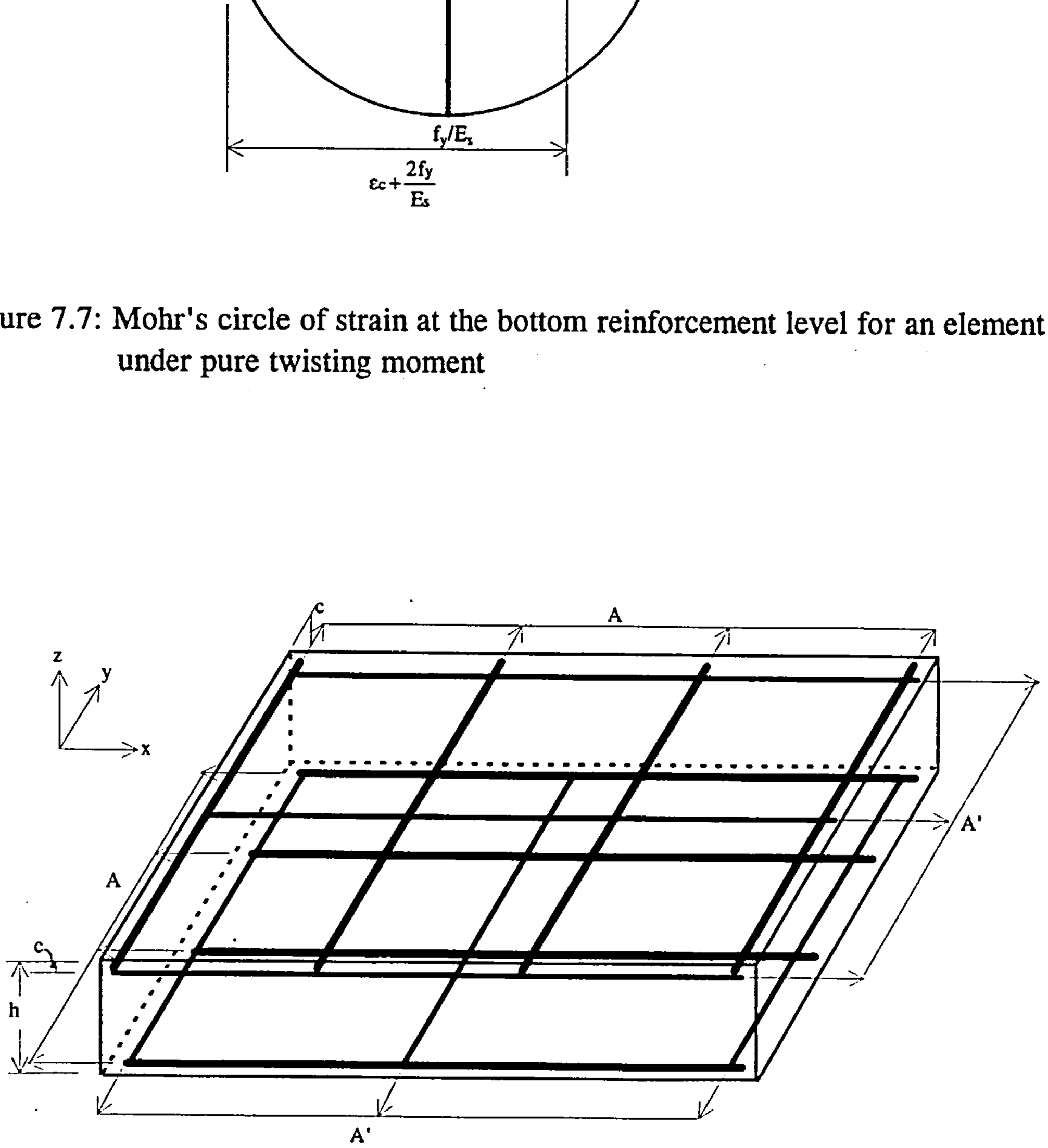

Figure 7.8: Slab element under biaxial equal and opposite bending and twisting moment

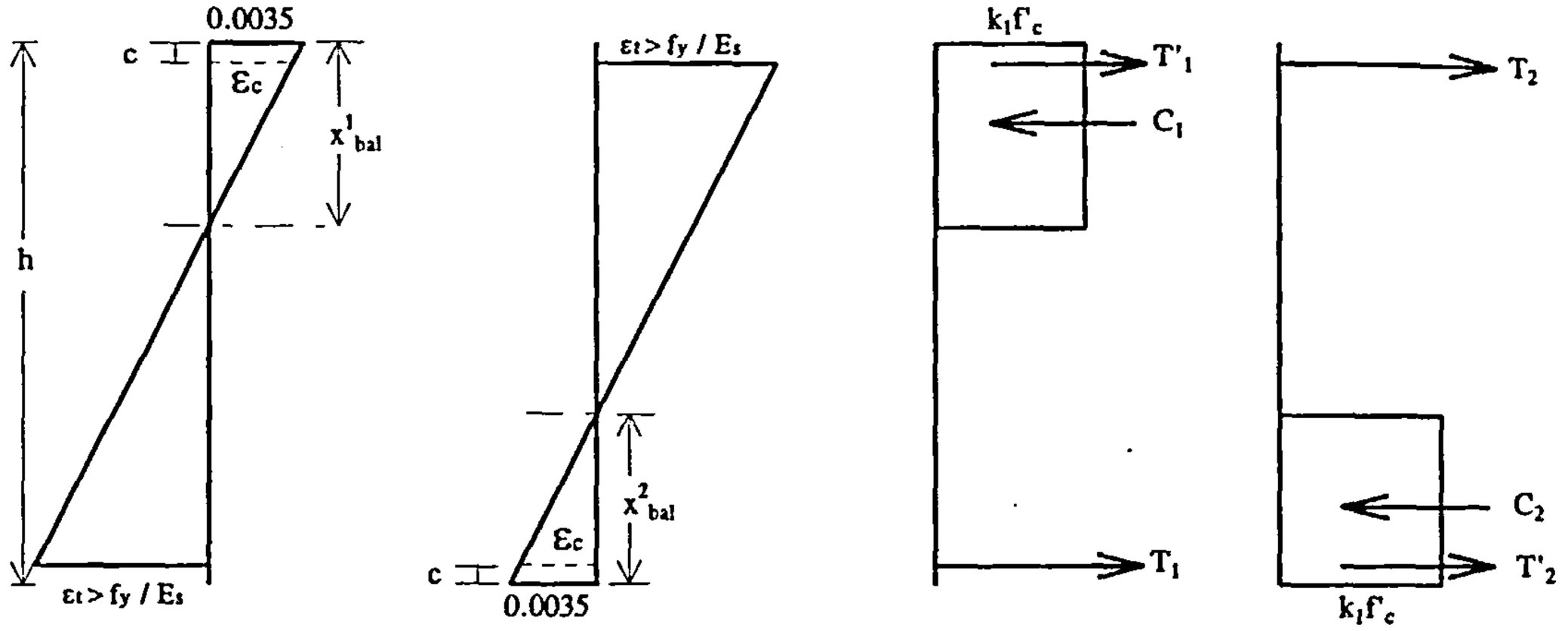

(a) (b) (c) (d)

Figure 7.9: Stress-strain distribution of an element subjected to biaxial equal and opposite bending with twisting moments (a) strain profile in principal strain direction 1-1 (b) strain profile in principal strain direction 2-2 (c) stress distribution in principal stress direction 1-1 (d) stress distribution in principal stress direction 2-2

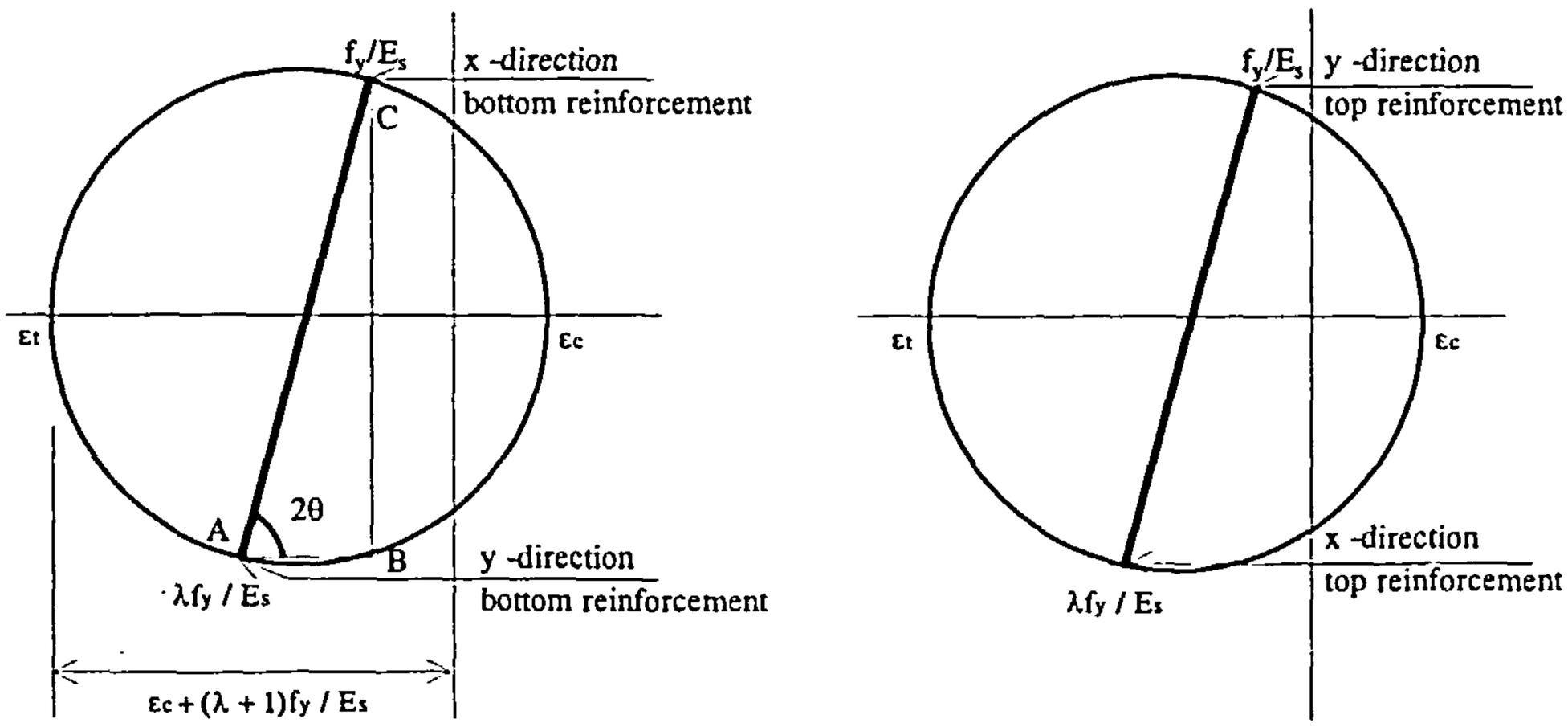

(a) (b)

Figure 7.10: Mohr's circle of strain (a) at the bottom reinforcement level (b) at the top reinforcement level

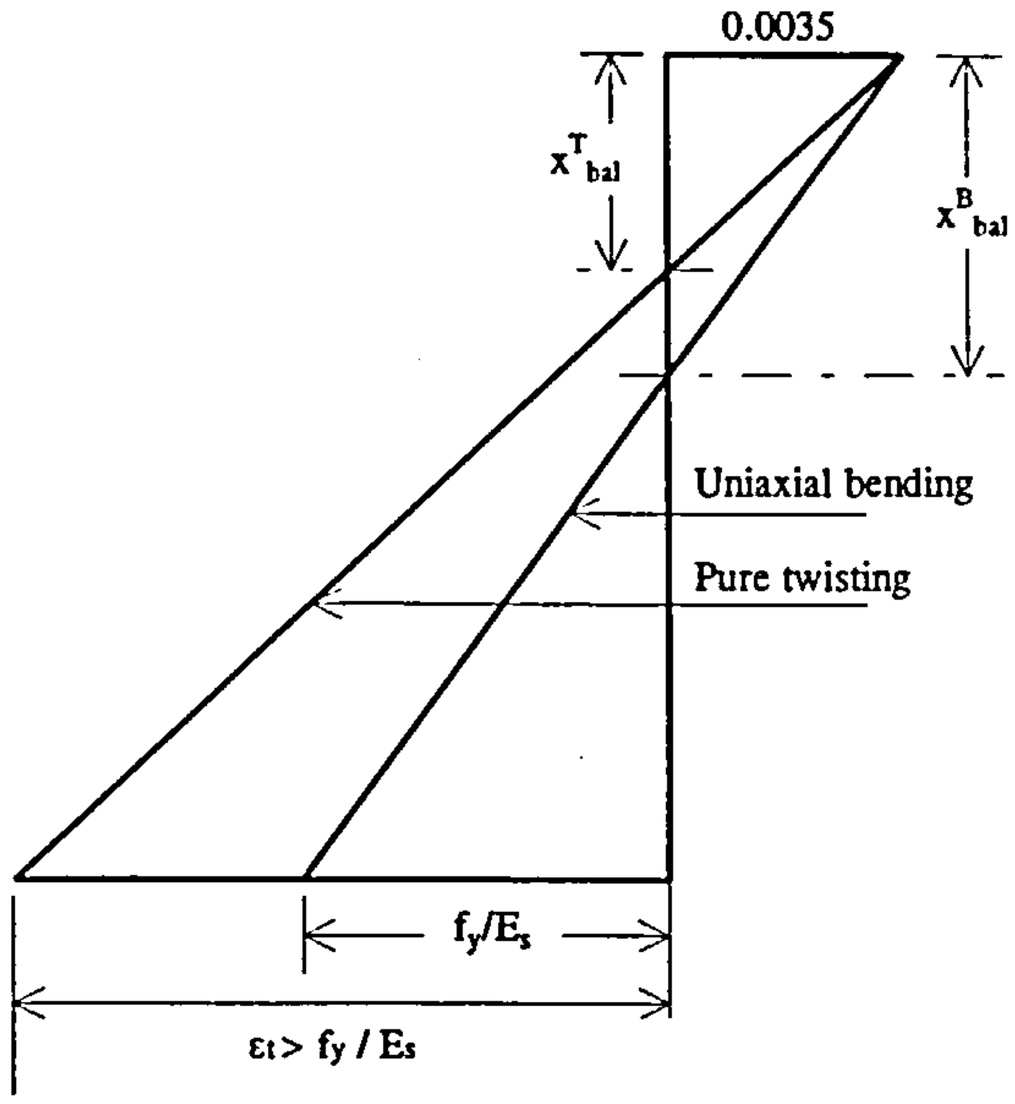

Figure 7.11: Strain profiles in principal strain direction 1-1 for an isotropically reinforced element subjected to uniaxial bending and pure twisting moments

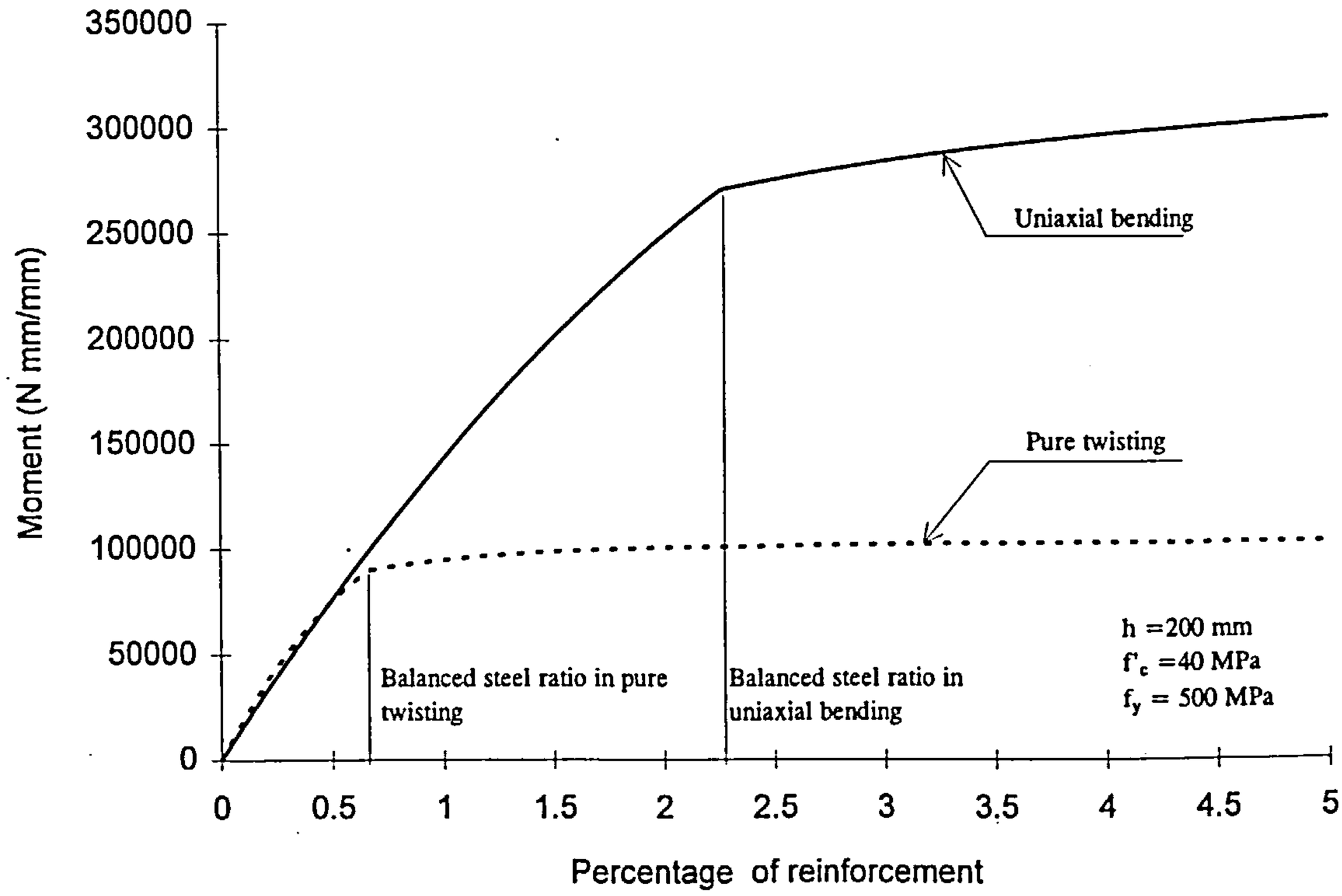

Figure 7.12: Moment capacity of an isotropically reinforced element

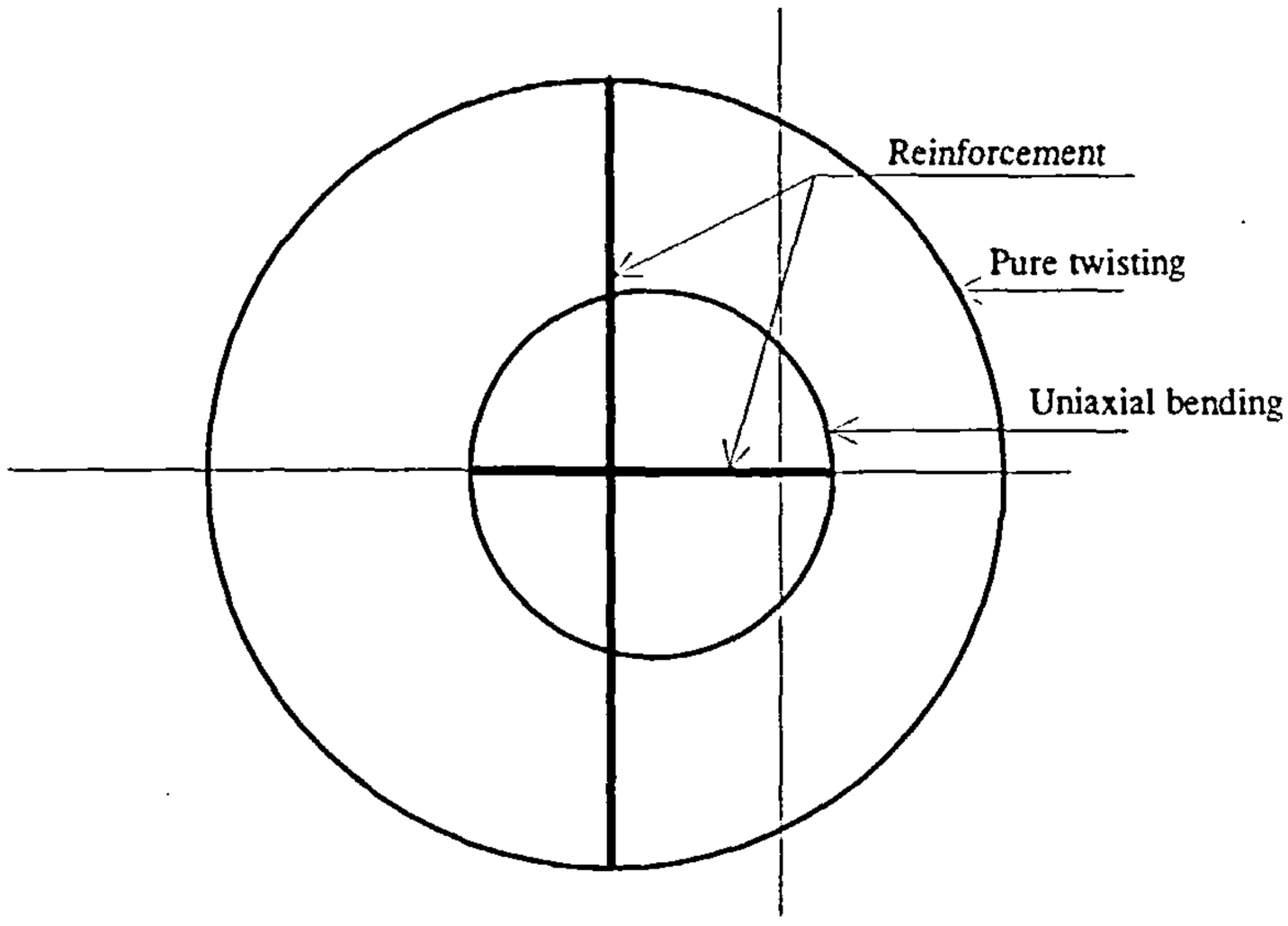

Figure 7.13: Mohr's circles of strain at the bottom reinforcement level for balanced section under pure twisting and uniaxial bending

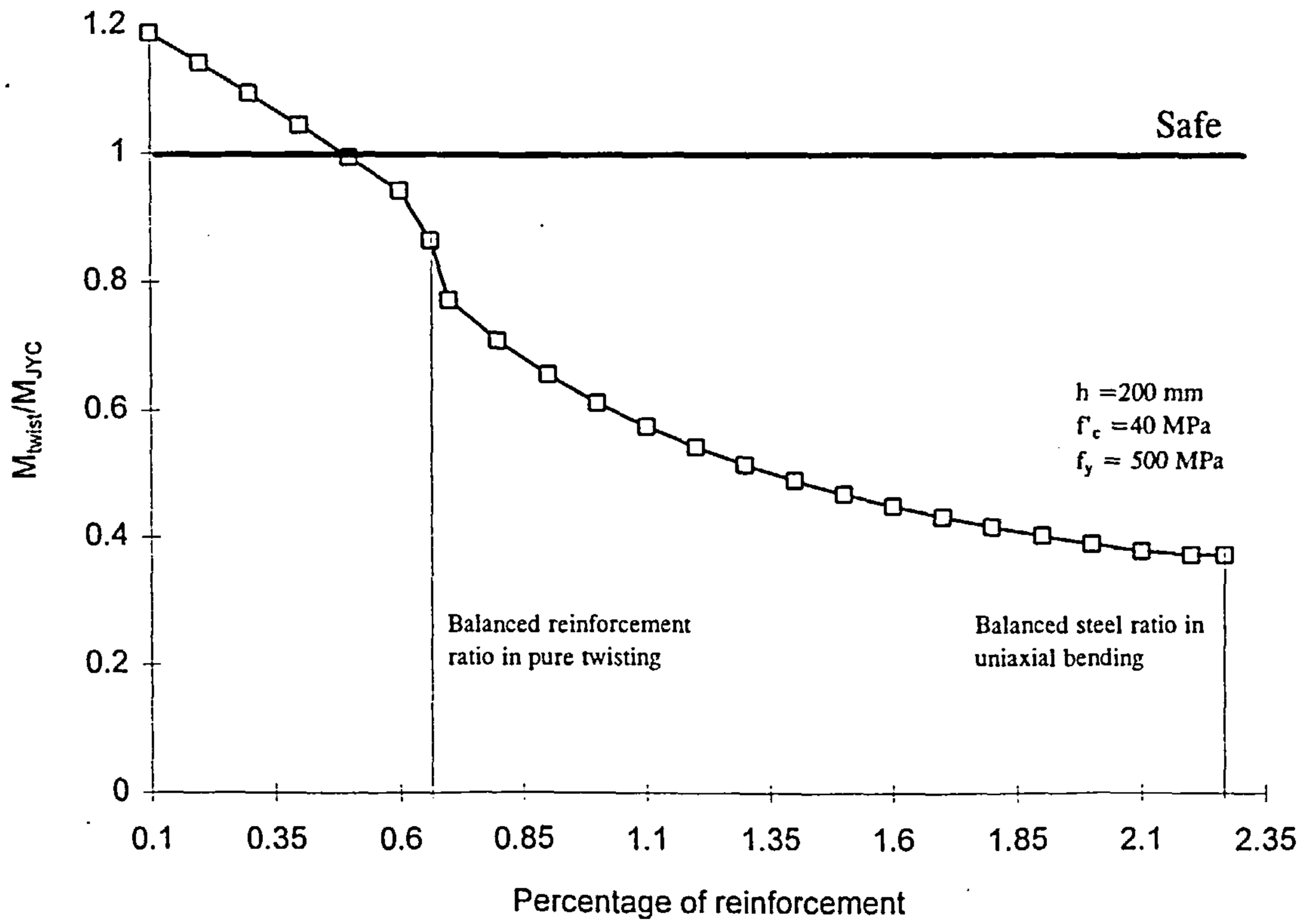

Figure 7.14: Comparison of pure twisting capacity of a isrotropically reinforced element using Johansen's[7] yield criterion and equation 7.13b

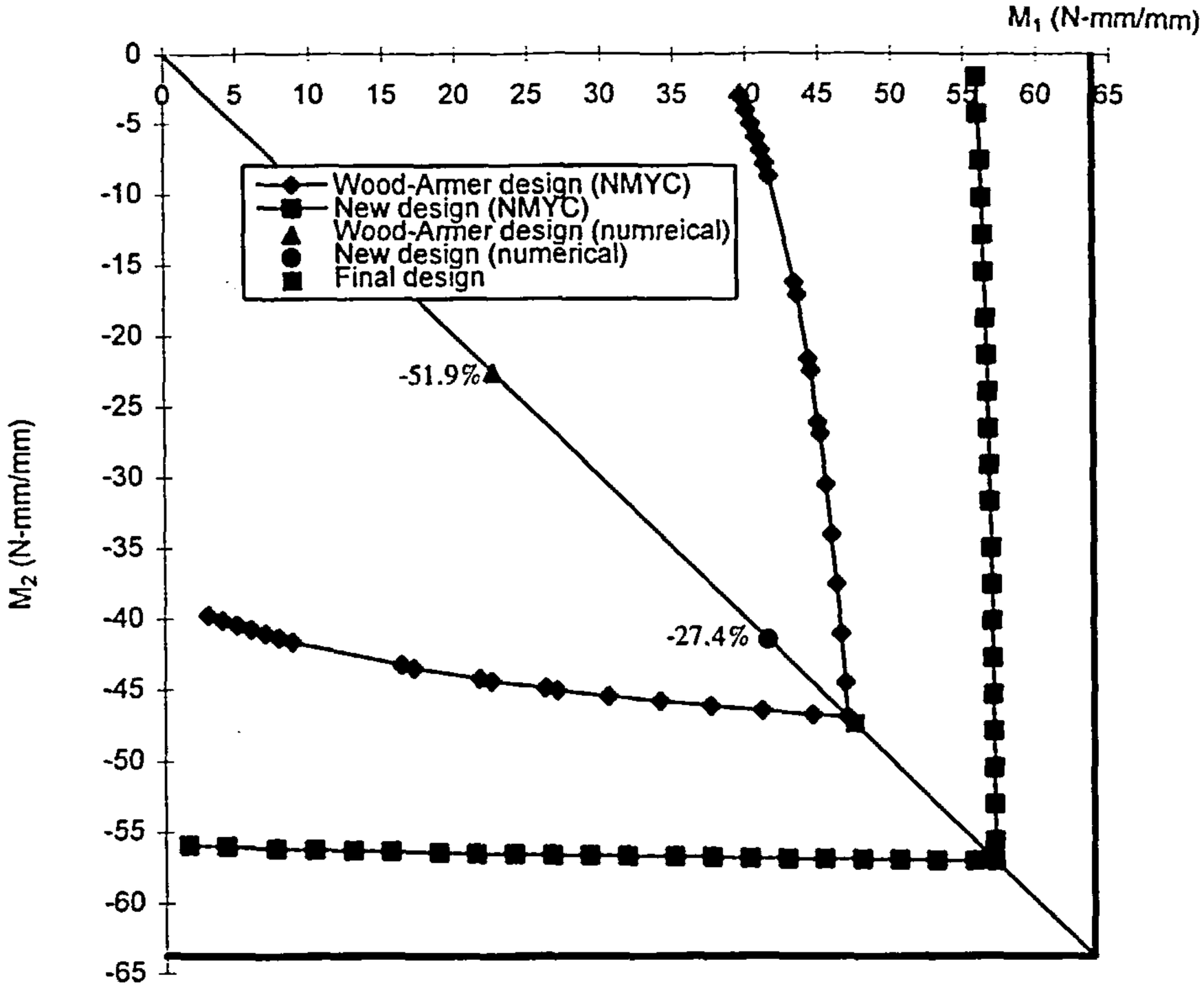

Figure 7.15: Failure surface using the normal moment yield criterion for slab element under mixed moment field with the numerical results

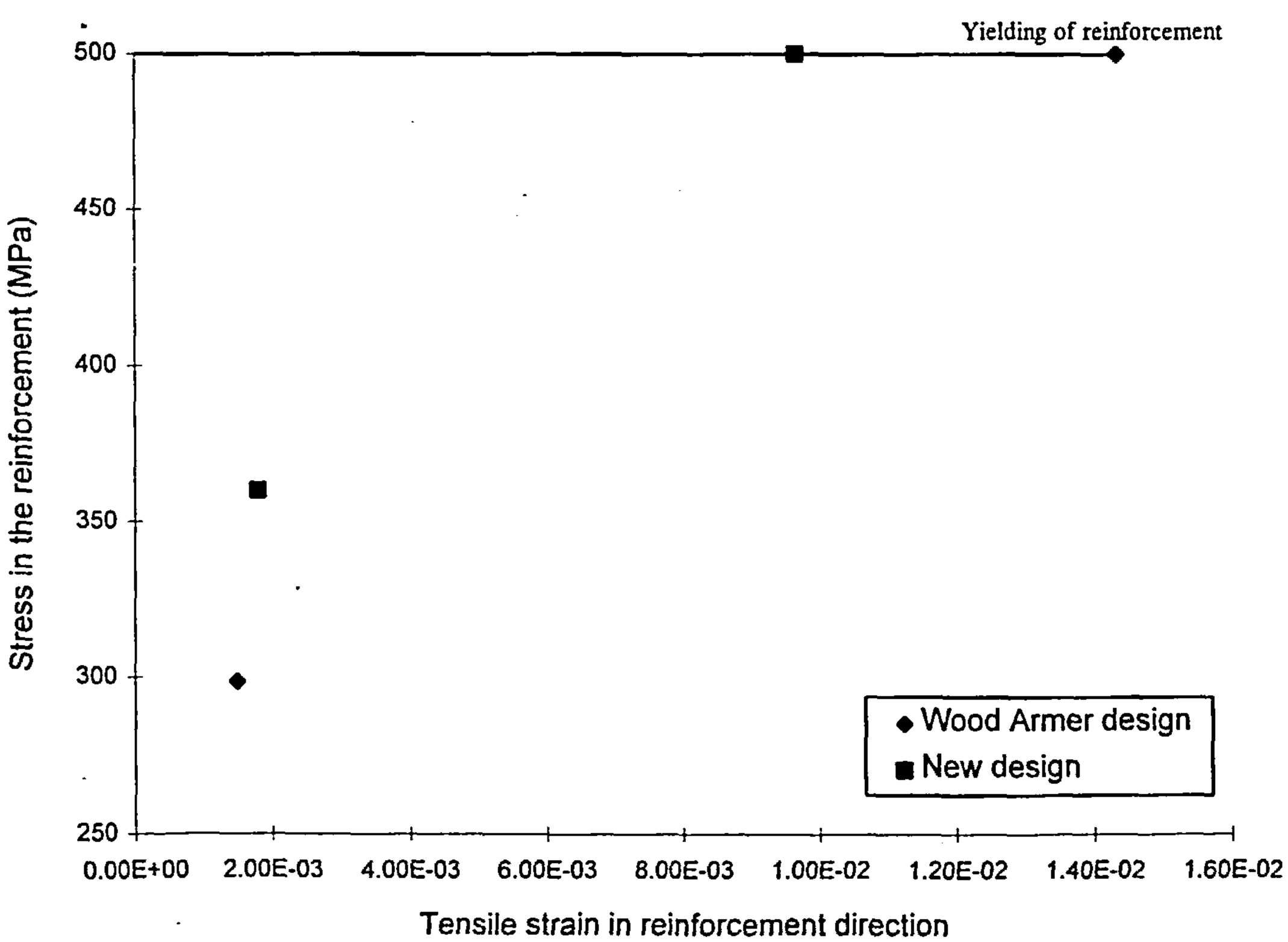

Figure 7.16: Reinforcement stresses and strain at ultimate moment

CHAPTER 8

CONCLUSIONS AND RECOMMENDATIONS

8.1 CONCLUSIONS

A computer program has been written that can predict the non-linear response of reinforced concrete shell elements up to and beyond failure. The computer program uses non-linear stress-strain models for the concrete and the reinforcement based on the theory of elasticity. The material models for concrete include phenomena such as tension stiffening and compression softening. The computer program has been validated against several experimental studies.

A study has been carried out to determine the optimum number of integration points that can be used for elements subjected to pure twisting moments and it was found that about 10 integration points adequately represent the response.

The analysis includes a non-linear isotropic model which has been developed to represent the ultimate stress and strain state of concrete under biaxial compression. A layered approach has been used successfully to model tension stiffening in which it

has been assumed that the stress state in concrete in the tension region will not the same. The stress state in the tension region is affected by the slip of bond between the reinforcement and the concrete and the tensile resistance offered by the cracked concrete decays away from the reinforcement. Hence the tension region was divided into two further zones and two different tensile responses were used for each zone. In the first zone, the concrete around the reinforcement, the tensile response of concrete was modelled by a linear ascending branch up to cracking followed by a linear descending branch. In the second zone the concrete was assumed to have tensile strength and was modelled by an ascending branch up to cracking but the post cracking response was assumed to be zero.

While carrying out the parameteric study it was found that the compression softening models developed for reinforced concrete elements loaded in plane stress over estimated the softening when an element is subjected to bending and twisting moments by as much as 20%.

The program has been validated against several experimental studies. The experimental studies chosen to validate the program had a variety of loading. Three studies had tested reinforced concrete elements under in-plane loading whereas in the remaining two studies tests were carried out under bending and twisting moments. The experimental results were compared with the analytical results and a good agreement was obtained.

The program was used to study the ultimate strength of reinforced concrete slab element subjected to bending and twisting moments. It was observed that the increase in the twisting moment in the reinforcement directions increases the angle between the principal strain and the reinforcement directions. It was found that the normal moment yield criterion can be used for the design of reinforced concrete slab elements provided that the appropriate modifications have been made in the criterion defining the strength to account for the angle between the principal strain and the reinforcement directions. Johansen's yield criterion which is used to define the strength of the slab elements in the normal moment yield criterion can not predict the strength of all loading conditions because it can not predict the actual stress state of the elements if the principal strain and the reinforcement directions do not coincide. It was found that for an element subjected to pure twisting moments, Johansen's yield criterion accurately predicts the moment capacity if $\frac{\rho f_y}{f_c} \leq 0.11$. But for elements with $\frac{\rho f_y}{f_c} > 0.11$, Johansen's yield criterion over estimates the pure twisting capacity of the slab. The over estimation increases with the increase in the reinforcement ratio.

However, Johansen's yield criterion can only be used to predict the strength of the slab elements if atleast one of the following conditions is satisfied.

i. The reinforcement and the principal moment directions coincide.

ii. The strength ratio, $\frac{\rho f_y}{f_c} \leq 0.11$.

iii. The principal moment ratio is positive.

iv. If the ratio of the principal moments is negative but the angle between the reinforcement and the principal moment directions is less than or equal to 20°.

It was also observed that with the increase of twisting moment in the reinforcement directions the ductility of the slab element also reduced. This reduction can not be predicted by the theory of plasticity.

An attempt has been made to develop a simple hand calculation procedure for the design of slab elements subjected to moments in mixed moment field. Expressions have been developed for the balanced reinforcement ratio for elements subjected to pure twisting moments. Simple hand calculation procedures have also been developed for the design and analysis reinforced concrete slab elements subjected to pure twisting moments. A numerical procedure has been proposed and tested which can be used to design the slab elements subjected to a mixed moment field.

8.2 RECOMMENDATIONS FOR FUTURE RESEARCH

In the light of the work carried out in this study and the conclusion drawn above the following recommendations are made for future research.

1. The effect of in-plane membrane forces be studied for slab elements subjected to a mixed moment field using the sectional analysis and a yield criterion or a failure surface be developed to include the effect of membrane forces on slab elements.

2. The material models developed for concrete and reinforced concrete should be included in a finite element program for the analysis of plates to study the effect of in-plane forces and moments on reinforced concrete slabs.

3. Effect of bond properties be included in the material models instead of tension stiffening to improve the modelling of reinforced concrete.

4. Experiments be carried out on reinforced concrete slab elements under bending to improve the modelling of compression softening effect.

APPENDIX A

Linear elastic stiffness matrix of a orthotropic reinforced concrete slab element

In order to use Modified Newton Raphson method to solve the non-linear system of equations, described in Chapter 4, the initial tangent stiffness matrix, [k], must be evaluated.

Procedure adopted for determining the initial tangent stiffness matrix, [k], for a reinforced element with reinforcement on the bottom face only has been described in detail in this Appendix. However, a similar procedure can be employed to determine the initial tangent stiffness matrix for a general slab cross-section which may or may not have top and bottom reinforcement in the two orthogonal directions. This generalised tangent stiffness matrix was then used in the analysis later.

For a reinforced concrete element, with reinforcement on the tension face only in one direction, the total internal resistance offered by the cross-section can be divided into two parts i.e. the resistance offered by the concrete and the resistance offered by the reinforcement. if the concrete is assumed to be a linear elastic material, then the internal resistance can be expressed as

$$\begin{Bmatrix} P_T \\ M_T \end{Bmatrix} = \begin{bmatrix} AE_c & 0 \\ 0 & E_cI \end{bmatrix} \begin{Bmatrix} \varepsilon_{CL} \\ \phi_{CL} \end{Bmatrix} + \text{contribution due to reinforcement} \qquad A.1$$

The contribution of the reinforcement easily determined as below.

The total internal axial force resistance offered by the section will be,

$$P_T = P_c + P_s \qquad \text{A.2}$$

From Figure A.1

$$P_c = AE_c\varepsilon_{CL} \qquad \text{A.3}$$

and
$$P_s = A_s\sigma_s = A_sE_s\varepsilon_s \qquad \text{A.4}$$

but
$$\varepsilon_s = \phi_a\frac{d}{2} - \varepsilon_a \qquad \text{A.5}$$

or,
$$P_s = -A_sE_s\varepsilon_a + A_sE_s\phi_a\frac{d}{2} \qquad \text{A.6}$$

Similarly, the total internal resistive moment of the section can be written as,

$$M_T = M_C + M_S \qquad \text{A.7}$$

where,
$$M_c = E_cI\phi_a \qquad \text{A.8}$$

From Figure A.1,

$$M_s = P_s\frac{d}{2} = (-E_sA_s\frac{d}{2})\varepsilon_{CL} + (A_sE_s\frac{d^2}{4})\phi_{CL} \qquad A.9$$

where, P_s, P_c = axial force carried by the concrete and the steel respectively

A = gross area of cross-section of concrete

A_s = area of steel

E_c, E_s = Young's modulus of elasticity of concrete and steel

σ_s = stress in the reinforcement

ε_s = strain in the reinforcement

ε_{CL} = strain at the centre line of the element

ϕ_{CL} = section curvature

d = effective depth of the element

M_c, M_s = moments of resistance offered by concrete and reinforcement respectively

I = second moment of area of the section

The governing equation A.1 can now be written as,

$$\begin{Bmatrix} P_T \\ M_T \end{Bmatrix} = \begin{bmatrix} AE_c + A_sE_s & -A_sE_s\frac{d}{2} \\ -A_sE_s\frac{d}{2} & E_cI + A_sE_s\frac{d^2}{4} \end{bmatrix} \begin{Bmatrix} \varepsilon_{CL} \\ \phi_{CL} \end{Bmatrix} \qquad A.10$$

The above expression includes the contribution both from the concrete and the reinforcement.

A similar expression for stiffness matrix can be obtained for an element with top and bottom reinforcement.

$$[k]=\begin{bmatrix} AE_c + A_sE_s + A'_sE_s & -A_sE_s\frac{d}{2} + A'_sE_s(\frac{d}{2}-d') \\ -A_sE_s\frac{d}{2} + A'_sE_s(\frac{d}{2}-d') & E_cI + A_sE_s\frac{d^2}{4} + A'_sE_s(\frac{d}{2}-d')^2 \end{bmatrix} \quad \text{A.11}$$

where, A'_s = area of top reinforcement

d' = distance of centroid of top reinforcement for the top of the element

A generalised expression for linear elastic stiffness matrix of a reinforced concrete slab can now be obtained on the basis of the procedure explained above.

For an isotropic plate element the governing equation can be expressed as follows,

$$\begin{Bmatrix} P_x \\ P_y \\ P_{xy} \\ M_x \\ M_y \\ M_{xy} \end{Bmatrix} = \frac{E_c h}{1-\nu^2} \begin{bmatrix} 1 & \nu & 0 & 0 & 0 & 0 \\ \nu & 1 & 0 & 0 & 0 & 0 \\ 0 & 0 & \frac{1-\nu}{2} & 0 & 0 & 0 \\ 0 & 0 & 0 & \frac{h^2}{12} & \frac{\nu h^2}{12} & 0 \\ 0 & 0 & 0 & \frac{\nu h^2}{12} & \frac{h^2}{12} & 0 \\ 0 & 0 & 0 & 0 & 0 & \frac{h^2(1-\nu)}{24} \end{bmatrix} \begin{Bmatrix} \varepsilon_x \\ \varepsilon_y \\ \gamma_{xy} \\ \phi_x \\ \phi_y \\ -2\phi_{xy} \end{Bmatrix} \quad \text{A.12}$$

where, h = overall depth of the element

$\varepsilon_x, \varepsilon_y$ = axial strain at centre of section in x & y directions respectively

γ_{xy} = shear strain at the centre of the element

ϕ_x, ϕ_y = curvature at centre of the element in x & y direction respectively

ϕ_{xy} = curvature of shear strain at the centre of the element

ν = Poisson's ratio

For a reinforced concrete slab element with both top and bottom reinforcement in the orthogonal directions, Figure A.2, the contribution of the reinforcement can be incorporated into the initial tangent stiffness matrix for an isotropic plate element using the procedure described above. The initial tangent stiffness matrix for an orthotropic slab element is shown in Figure A.3.

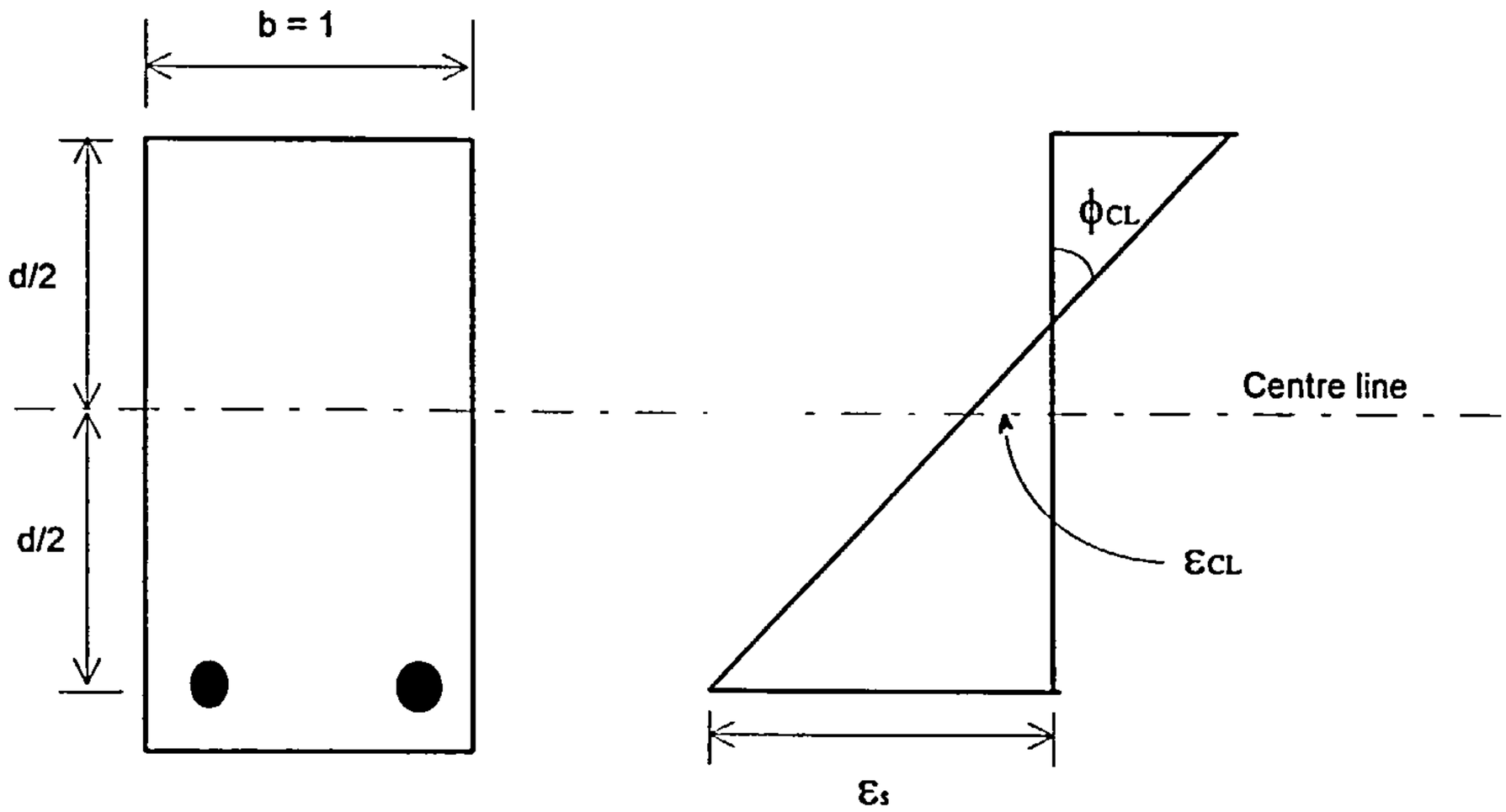

Figure A.1: Typical cross-section of an element with bottom reinforcement only with the strain profile through the depth

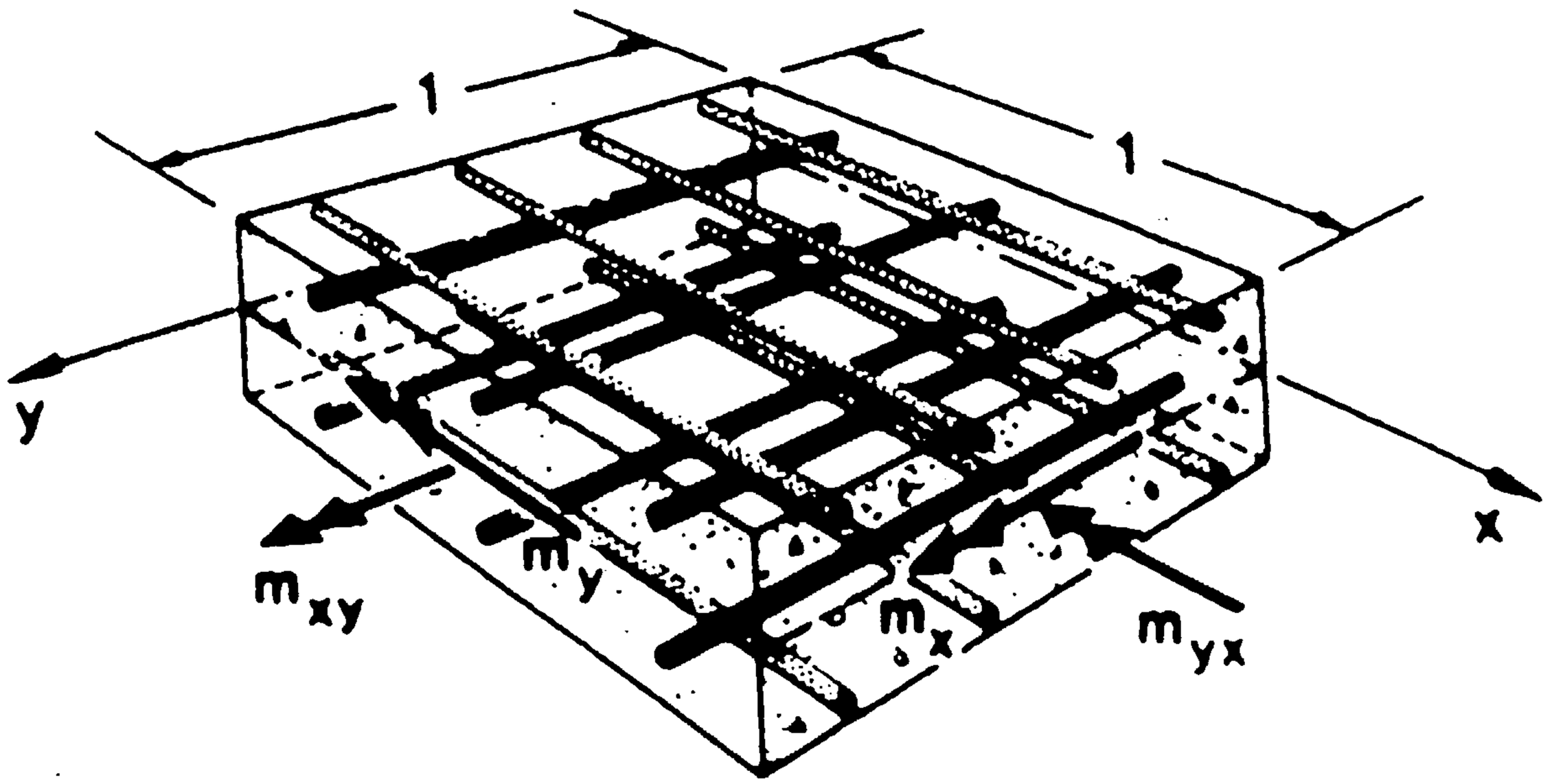

Figure A.2: Typical reinforced concrete slab element

$$
[k]=\begin{bmatrix}
\frac{Ec\,h}{1-\nu^2}+A_{sx}Es+A'_{sx}E_s & \frac{\nu E_c h}{1-\nu^2} & 0 & -A_{sx}E_s(\frac{h}{2}-d_x)+A'_{sx}Es(\frac{h}{2}-d'_x) & 0 & 0 \\
\frac{\nu E_c h}{1-\nu^2} & \frac{E_c h}{1-\nu^2}+A_{sy}E_s+A'_{sy}E_s & 0 & 0 & -A_{sy}E_s(\frac{h}{2}-dy)+A'_{sy}E_s(\frac{h}{2}-d'y) & 0 \\
0 & 0 & \frac{E_c h}{2(1-\nu)^2} & 0 & 0 & 0 \\
-A_{sx}E_s(\frac{h}{2}-d_x)+A'_{sx}Es(\frac{h}{2}-d'_x) & 0 & 0 & \frac{E_c h^3}{12(1-\nu^2)}+A_{sx}E_s(\frac{h}{2}-d_x)^2+A'_{sx}Es(\frac{h}{2}-d'_x)^2 & \frac{\nu Ec\,h^3}{12(1-\nu^2)} & 0 \\
0 & -A_{sy}E_s(\frac{h}{2}-d_y)+A'_{sy}E_s(\frac{h}{2}-d'_y) & 0 & \frac{\nu E_c h^3}{12(1-\nu^2)} & \frac{E_c h^3}{12(1-\nu^2)}+A_{sy}E_s(\frac{h}{2}-d_y)^2+A'_{sy}E_s(\frac{h}{2}-d'_y)^2 & 0 \\
0 & 0 & 0 & 0 & 0 & \frac{E_c h^3(1-\nu)}{24(1-\nu^2)}
\end{bmatrix}
$$

Figure A.3: Linear elastic stiffness matrix of a orthotropic reinforced concrete slab element

APPENDIX B

Evaluation of factors k_1 and k_2 for the state of compression-tension

For a slab element in the state of compression-tension, the actual stress distribution, strain distribution and simplified rectangular stress block along the depth are given in Figure B.1. The softening parameter $\beta = 0.7$ has been assumed. The factors k_1 and k_2 associated with the area and the centroid of the equivalent rectangular stress block can be calculated as follows.

$$A_1 = \frac{2}{3}(x_1)(0.7f'_c) = \frac{2}{3}(\frac{1.75}{3.5}x^T_{bal})(0.7f'_c) = 0.233f'_c x^T_{bal}$$

$$A_2 = (x_2-x_1)(0.7f'_c) = (\frac{2.5-1.75}{3.5}x^T_{bal})(0.7f'_c) = 0.150f'_c x^T_{bal}$$

$$A_3 = (x^T_{bal}-x_2)(0.595f'_c) = (\frac{3.5-2.5}{3.5}x^T_{bal})(0.595f'_c) = 0.170f'_c x^T_{bal}$$

$$A_4 = \frac{1}{2}(x^T_{bal}-x_2)(0.7f'_c-0.595f'_c) = \frac{1}{2}(\frac{3.5-2.5}{3.5}x^T_{bal})(0.105f'_c) = 0.015f'_c x^T_{bal}$$

$$\sum A_i = 0.568f'_c x^T_{bal}$$

Since the actual stress block has to be transformed to an equivalent rectangular stress block of similar depth, then

$$k_1 f'_c x^T_{bal} = 0.568 f'_c x^T_{bal}$$

or, $$k_1 = 0.568$$

Taking moment of area at the top of the element,

$$\bar{x}_1 = x^T_{bal} - \frac{2}{5}x_1 = x^T_{bal} - \frac{2}{5}\left(\frac{175}{3.5}x^T_{bal}\right) = 0.800x$$

$$\bar{x}_2 = x^T_{bal} - \frac{1}{2}x_2 = x^T_{bal} - \frac{1}{2}\left(\frac{25}{3.5}x^T_{bal}\right) = 0.643x$$

$$\bar{x}_3 = \frac{1}{2}(x^T_{bal} - x_2) = \frac{1}{2}x^T_{bal}\left(1 - \frac{25}{3.5}\right) = 0.143x^T_{bal}$$

$$\bar{x}_4 = \frac{2}{3}(x^T_{bal} - x_2) = \frac{2}{3}x^T_{bal}\left(1 - \frac{25}{3.5}\right) = 0.190x^T_{bal}$$

Now,

$$k_2 = \frac{\sum A_i \bar{x}^T_{bali}}{\sum A_i}$$

$$k_2 = 0.55$$

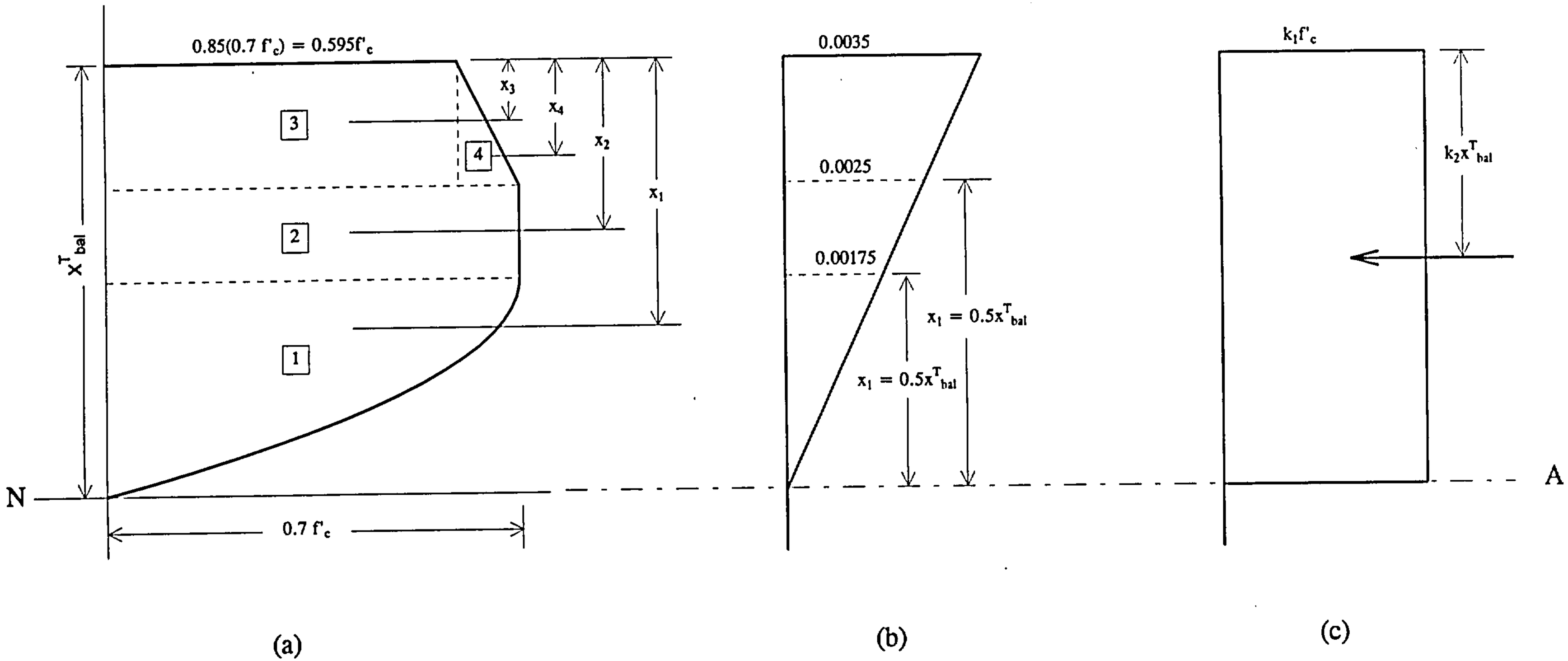

Figure B.1: Strain and strain profile through the depth (a) actual stress distribution (b) strain profile (c) simplified compressive stress block

APPENDIX C

Procedure the for analysis and design of slab elements under twisting moments

The following examples explain the procedure to be adopted in the analysis and design of slab elements under pure twisting.

EXAMPLE 1:

Determine the twisting moment capacity of an element with following section and material properties.

$h = 200$ mm $\quad f'_c = 30$ MPa $\quad f_y = 550$ MPa $\quad \rho_{pro} = 0.0025$

1. From equation 6.12b,

$$\rho^T{}_{bal} = 0.00434$$

2. Since $\rho_{pro} < \rho^{T}_{bal}$, element will be under reinforced, thus equations 6.21 and 6.20 can be used to determine the depth of neutral axis and moment capacity respectively.

$$x^{T} = 32.28 \text{ mm}$$

$$M^{T} = 45.24 \text{ kN-m/m}$$

EXAMPLE 2:

Determine the pure twisting capacity of an element with following section and material properties.

$$h = 150 \text{ mm} \quad f'_c = 25 \text{ MPa} \quad f_y = 550 \text{ MPa} \quad \rho_{pro} = 0.01$$

1. From equation 6.12b,

$$\rho^{T}_{bal} = 0.00565$$

2. Since $\rho_{pro} > \rho^{T}_{bal}$, section will be over reinforced, thus equations 6.22b and 6.20 are used to determine the depth of neutral axis and moment capacity respectively.

$$x^{T} = 54.74 \text{ mm}$$

$$M^T = 34.9 \text{ kN-m/m}$$

EXAMPLE 3:

Design a reinforced concrete element to carry twisting moment of 100 kN-m/m. Use $f'_c = 35$ MPa and $f_y = 500$ MPa.

Assume the overall thickness of the section h = 200 mm.

1. Using Wood-Armer rules to determine the design moment in the reinforcement directions.

$$m^*_x = m^*_y = m^{**}_x = m^{**}_y = |m_{xy}|$$

or, $$m^*_x = m^*_y = m^{**}_x = m^{**}_y = 100 \text{ kN-m/m}$$

2. The required area of steel per layer per direction will be,

$$A_{sx} = A'_{sx} = A_{sy} = A'_{sy} = 1.20 \text{ mm}^2/\text{mm}$$

or, $$\rho = 0.006$$

using the maximum compressive stress $f_c = 0.7 f'_c$ and an effective depth of 180 mm.

3. The balanced amount of steel ratio from equation 6.12b will be,

$$\rho^T_{bal} = 0.0058$$

thus the maximum amount of reinforcement allowed from equation 6.25, in the section will be,

$$\rho^T_{max} = 0.0044$$

4. Since the required amount of reinforcement is greater than the maximum allowed area of reinforcement, the depth of the section must be increased.

Now assume h = 225 mm and repeating steps 2 and 3.

2. $\rho = 0.0044$

3. Since the required amount of reinforcement is equal to the maximum allowed reinforced, the section can be rendered safe.

In the above procedure for the analysis or design of reinforced concrete slab elements the partial safety factors have been assumed to be 1.